

## University of Southampton Research Repository

Copyright © and Moral Rights for this thesis and, where applicable, any accompanying data are retained by the author and/or other copyright owners. A copy can be downloaded for personal non-commercial research or study, without prior permission or charge. This thesis and the accompanying data cannot be reproduced or quoted extensively from without first obtaining permission in writing from the copyright holder/s. The content of the thesis and accompanying research data (where applicable) must not be changed in any way or sold commercially in any format or medium without the formal permission of the copyright holder/s.

When referring to this thesis and any accompanying data, full bibliographic details must be given, e.g.

Thesis: Author (Year of Submission) "Full thesis title", University of Southampton, name of the University Faculty or School or Department, PhD Thesis, pagination.

Data: Author (Year) Title. URI [dataset]

ADAPTIVE APPROACHES TO SIGNAL ENHANCEMENT AND DECONVOLUTION  
(with Particular Reference to Reflection Seismology)

by

Peter Martin Clarkson

Institute of Sound and Vibration Research  
Faculty of Engineering and Applied Science  
University of Southampton

Thesis submitted for the degree of

Doctor of Philosophy

December 1983



to my wife Sophie

ABSTRACTFACULTY OF ENGINEERING AND APPLIED SCIENCE  
INSTITUTE OF SOUND AND VIBRATION RESEARCHDoctor of PhilosophyADAPTIVE APPROACHES TO SIGNAL ENHANCEMENT AND DECONVOLUTION  
(WITH PARTICULAR REFERENCE TO REFLECTION SEISMOLOGY)

by Peter Martin Clarkson

Deconvolution and signal enhancement are important aspects of digital signal processing. Many techniques have been developed to achieve these twin aims, the vast majority however were designed to deal with stationary signals. However, many practically occurring signals are significantly non-stationary and these techniques are rendered at least partially ineffective.

This thesis is devoted to the study of adaptive techniques, these form a class of methods which are specifically designed to give the flexibility to deal with non-stationarity. The thesis demonstrates the value of adaptive approaches to problems of deconvolution and signal enhancement, particularly in reflection seismology. Adaptive processes are divided into two classes - modelled and empirical. The power of both these approaches is demonstrated by concentrating primarily on one algorithm of each class. In the case of the modelled approach the technique chosen is a recent approach to deconvolution based on the methods of optimal control. The method is redeveloped in discrete-time, the theory is extended to include the important problem of noise reduction in deconvolution, and for the first time, the method is applied to physical problems. The principal application is to the deconvolution of seismic data incorporating both stationary and non-stationary models. A second application is to the deconvolution of data derived from a velocity meter.

The empirical approach to adaptive processing is illustrated by the so-called LMS (least mean-square) algorithm. The theory of this method is rationalised and extended both for broadband inputs, particularly for the important area of non-stationary random processes, and for narrowband inputs. Two new configurations of the LMS algorithm are introduced for signal enhancement. One, dubbed the generalised comb filter, is designed for the enhancement of signals which may be considered to consist of a series of slowly time-varying wavelets of unknown form, recurring at roughly constant intervals and embedded in random noise with unknown properties. The theory of this method is developed and the technique is applied to the enhancement of voiced speech and to the enhancement of seismic signals. This seismic enhancement has two forms - one for highly reverberant single-channel seismic data, and the other for enhancing multi-channel data. The second novel configuration of the LMS is in the form of a sparse adaptive filter, that is one with relatively few coefficients in relation to its length, with the objective of signal enhancement by cancellation of multiple interfering sinusoids. This technique is also applied to the problem of speech enhancement.

## ACKNOWLEDGEMENTS

---

I would like to thank my supervisor Dr. Joe Hammond, for all his help and advice during the course of this project. I also wish to thank the staff of Seismograph Service Limited, particularly Dr. Terry Hubbard (now of B.N.O.C.) and Mr. Derek March for their help with the seismic aspects of the work. Similarly thanks are due to the staff of the Data Analysis Centre for their assistance with computational matters, and to all who helped prepare the typescript. Finally, I wish to thank my wife for checking the spelling and punctuation in the manuscript and proof reading the typescript.

The financial support of the Natural Environment Research Council and of Seismograph Service Limited, is gratefully acknowledged.

## LIST OF CONTENTS

Abstract

Acknowledgements

Contents

List of Symbols

CHAPTER 1	INTRODUCTION	1
CHAPTER 2	ADAPTIVE PROCESSING	5
2.1	Introduction	5
2.2	Least-squares Filtering	6
2.2.1	The Normal Equations	8
2.2.2	Solutions of the Normal Equations	8
2.2.3	Error Energy in Finite Least-squares Filtering	9
2.3	Motivation for Adaptive Solutions	9
2.4	From Iterative Solutions of the Normal Equations to Adaptive Filters	11
2.4.1	Introduction	11
2.4.2	Iterative Solutions to Normal Equations	11
2.4.3	Steepest Descent	12
2.4.4	Iterative Methods as Adaptive Filters	13
2.5	LMS Adaptive Algorithm	15
2.5.1	General	15
2.5.2	LMS Theory	16
2.5.3	Details of the Algorithm	29
2.6	Alternative Forms for Adaptive Filters	33
2.7	Discussion	38
CHAPTER 3	DECONVOLUTION	39
3.1	Introduction	39
3.2	Direct Methods and the Need for Approximate Solutions	40
3.3	Least-squares Deconvolution	41
3.3.1	Zero Delay Least-squares Deconvolution	41
3.3.2	Least-squares Deconvolution with Delay.	45

3.3.3	Error Energy in Least-squares Deconvolution	48
3.3.4	Noise Reduction Approaches	52
3.3.5	Examples	55
3.4	Alternative Methods for Deconvolution	59
3.4.1	Lattice Forms	59
3.4.2	Homomorphic Deconvolution	62
3.5	A Comparative Study of Least-squares and Homomorphic Techniques for the Inversion of Mixed Phase Signals	64
3.6	Conclusions	70
CHAPTER 4	OPTIMAL CONTROL DECONVOLUTION	72
4.1	Introduction	72
4.2	Theory: Continuous Time	72
4.2.1	Computation	75
4.2.2	Selection of Parameters	75
4.3	Theory: Discrete Time	77
4.4	Noise Reduction through Control of the Parameters	78
4.5	Application: Velocity Meter	81
4.5.1	The Problem	81
4.5.2	The Model	82
4.5.3	Optimal Control Approach	83
4.5.4	Results	84
4.6	Conclusions	92
CHAPTER 5	GENERALISED COMB FILTERING	94
5.1	Introduction	94
5.2	Preliminaries: Signal Models and SNR Definitions	96
5.2.1	Signal Models	96
5.2.2	Signal-to-Noise Ratio Definitions	97
5.3	Review of Classical SNR Enhancement Techniques	98
5.3.1	Introduction	98
5.3.2	Signal Averaging	99
5.3.3	Matched and Output Energy Filtering	100
5.3.4	Wiener Filtering	102
5.3.5	Adaptive Noise Cancellation	103

5.4	Generalised Comb Filtering	104
5.4.1	Introduction	104
5.4.2	Adaptive Signal Enhancement	105
5.4.3	Generalised Signal Averaging	108
5.4.4	Filter Operation	110
5.5	Application of Generalised Comb Filtering to Enhancement of Voiced Speech	112
5.5.1	Introduction	112
5.5.2	Model of Speech Production	113
5.5.3	Existing Techniques for Speech Enhancement	114
5.5.4	SNR Enhancement of Voiced Speech Segments using Generalised Comb Filtering	117
5.5.5	Simulations	118
5.6	Conclusions	122
CHAPTER 6	ADAPTIVE NOISE CANCELLATION FOR NARROWBAND INTERFERENCES	124
6.1	Introduction	124
6.2	Theory of Adaptive Noise Cancellation for Narrowband Interferences	125
6.2.1	Introduction	125
6.2.2	Approximate Transfer Function-Signal Interfering Tone	126
6.2.3	Time Domain Characteristics	128
6.2.4	Noise in the Reference	130
6.2.5	Approximate Transfer Function-Multiple Interfering Sinusoids	131
6.2.6	Generalised Description of the Adaptive Noise Cancellation System Response	133
6.3	Application of Adaptive Noise Cancellation to Narrowband Interference Rejection	137
6.3.1	Parametric Study set up	137
6.3.2	Results	139
6.3.3	Conclusions	146
6.4	Sparse Adaptive Filters	147
6.4.1	Introduction	147
6.4.2	Theory of Two Point Filter	150
6.4.3	Two Point Filter: Simulations	152
6.4.4	Multi-tone Cancellation using Sparse Adaptive Filters	155

6.5	The Function Elimination Filter	161
6.5.1	Introduction	161
6.5.2	Problems with the Function Elimination Filter	162
6.5.3	Modified Function Elimination Filter	164
6.5.4	Simulations	165
6.6	Conclusions	165
CHAPTER 7	SEISMIC SIGNAL PROCESSING	169
7.1	Introduction	169
7.2	Mechanics of Reflection Seismology	170
7.2.1	Models of Transmission	170
7.2.2	Sources and Receivers	174
7.2.3	Data Gathering	176
7.3	Data Processing	177
7.3.1	Preprocessing and Static Corrections	177
7.3.2	Gain Control	177
7.3.3	Velocity Analysis and Moveout Corrections	178
7.3.4	SNR Improvement	182
7.3.5	Deconvolution	183
7.3.6	The Processing Sequence	187
CHAPTER 8	ADAPTIVE DECONVOLUTION OF SEISMIC DATA	189
8.1	Introduction	189
8.2	Background and Previous Work	190
8.2.1	Introduction	190
8.2.2	Gating the Data	190
8.2.3	LMS Adaptive Deconvolution	191
8.2.4	Deconvolution using the Kalman Filter	194
8.3	Adaptive Deconvolution using Optimal Control	198
8.3.1	Implementation	198
8.3.2	Discussion	206
8.3.3	Application to Synthetic Data	206
8.3.4	Application to Field Seismic Data	212
8.4	Conclusions	214

CHAPTER 9	ADAPTIVE SIGNAL ENHANCEMENT OF SEISMIC DATA	216
9.1	Introduction	216
9.2	SNR Enhancement by Predictive Stack	217
9.2.1	Theory	217
9.2.2	Simulations	220
9.3	SNR Enhancement of Multi-channel Seismic Data by Generalised Comb Filtering	231
9.3.1	Background and Previous Work	231
9.3.2	Generalised Comb Filtering Approach	236
9.3.3	Simulations	240
9.4	Conclusions	246
CHAPTER 10	CONCLUSIONS AND RECOMMENDATIONS	248
REFERENCES		251
APPENDICES I to XIV		258



## List of Symbols

The aim here is to present a list of symbols which have recurrent meaning throughout the work. Every use of a particular symbol is not listed here but no ambiguity should occur since each alternative usage is defined as it arises. In general, upper case letters denote frequency or z domain variables and lower case letters denote time domain variables. Vectors are denoted by underlined lower case letters. The kth vector of a set is denoted by the subscript k, elements of vectors (and matrices) are indicated by parentheses as are elements of time-series. Throughout, standard mathematical notation is used and all quantities having dimension are expressed in SI units.

d	desired signal
e	error signal
<u>f</u>	vector of filter coefficients
f <sub>s</sub>	sampling frequency
<u>g</u>	cross-correlation vector
h	system variable
i	$\sqrt{1}$ index
I	Identity matrix, error energy
j,k,m,n	time indices
L	filter length
n <sub>o</sub>	delay
Q	orthonormal matrix of eigenvalues, specific dissipation constant
R	autocorrelation matrix
t	time
T	sample
w	white noise
x	input variable, state-variable
y	output variable
z	z domain variable
$\alpha$	adaptation constant
$\delta$	Kronecker delta
$\Delta$	delay
$\lambda$	eigenvalue
$\Lambda$	spectral matrix
$\sigma$	standard deviation
$\Phi$	state transition matrix
$\omega$	radian frequency
*	convolution

## CHAPTER 1

### INTRODUCTION

Deconvolution and signal enhancement are important aspects of digital signal processing. Many techniques have been developed to achieve these twin aims, the vast majority, however, were designed to operate upon signals whose properties are fixed in time (stationary). Unfortunately many commonly occurring signals are significantly non-stationary and these methods are rendered at best partially ineffective. Adaptive techniques, by contrast, are specifically designed to give the flexibility to deal with non-stationarity.

The aims of this thesis are to develop novel adaptive approaches to deconvolution and signal enhancement, including both the theoretical aspects relating to such techniques and the consideration of new applications. Adaptive techniques cover a very broad span but essentially can be divided into two classes: a) those which attempt to model the non-stationary behaviour of the system in some manner and b) pragmatic methods which are data adaptive and rely on updating the filter in an empirical or semi-empirical manner. Both approaches are important and examples of each are developed in the thesis and their relative merits are illustrated. The main area of application of the thesis is to signals derived from reflection seismology; However, a number of other applications, for example, to speech and transducer signals are also included, as they arise naturally from the methods developed.

The thesis is divided into three sections, the first section is a general review of adaptive processing together with some new results on aspects of adaptive filter theory. In the second section the main techniques of signal enhancement and deconvolution are developed, whilst in the final section the application of these techniques to reflection seismology is considered. The thesis begins by reviewing the motivation for adaptive solutions to signal

processing problems and the techniques available (Chapter 2). One particular method, the so-called LMS (least mean-square) adaptive algorithm, which is used extensively throughout the thesis is considered in detail. This algorithm has been widely applied but, surprisingly, the theoretical properties of the method have only been established for a few, highly artificial, cases. This existing theory is reviewed and clarified and several new results, particularly in the important area of non-stationary inputs, are presented.

Chapter 3, which is the first chapter of the second section, sets out the main techniques of deconvolution and is included partly as a review, giving background for the more sophisticated approach to deconvolution in Chapter 4. A novel element to the chapter is provided by a comparative study of two of the main techniques for deconvolution in their application to physical systems. Chapter 4 develops the main adaptive deconvolution technique used in the thesis which is based on the theory of optimal control. Although the idea itself is not new, the properties of the method are further developed here. A novel approach to the important problem of noise control is proposed and justified, the method is redeveloped in discrete-time and, for the first time, applied to physical systems (both stationary and non-stationary).

In Chapter 5 the emphasis changes to signal enhancement. After a review of some existing methods, a new approach to signal enhancement is proposed, based on a form of generalised comb filtering. This method is applicable to signals which can be considered to consist of a series of slowly time-varying wavelets which recur at approximately constant intervals. This pseudo-periodic structure is assumed to be corrupted by additive random noise, but where no further a priori knowledge about the signal is assumed and where no assumptions (beyond stationarity) are made about the noise. Signals of this form occur frequently in signal processing. Examples of signals which may, in some instances, be assumed to have this form are provided by voiced speech, reverberant seismic data and E.E.G. signals. Two such applications are considered. The generalised comb filtering method is similar to conventional comb filtering but where the individual 'teeth' of the comb are themselves replaced by LMS adaptive filters.

It is also shown how the generalised comb filtering method of enhancement can be applied to multi-channel processes, where successive input channels have correlated, (but unknown) signal components embedded in noise.

In Chapter 6 a different approach to signal enhancement is examined - that of noise cancellation. In particular the problem of cancellation of narrowband interferences at unknown (and possibly drifting) frequencies is considered. The chapter sets out to evaluate, and establish the limitations of existing techniques for this problem, to improve the theoretical understanding of these methods and to develop alternative methods to overcome some of the limitations. Two distinct sets of circumstances are considered, depending on whether a second measurement, consisting primarily of a set of interferences with similar frequencies to those of the data, is available or not. For the case where such a measurement is available the method of adaptive noise cancellation is examined in detail both by extending the theory to explain aspects of the behaviour of the technique which are not resolved by existing analysis, and through simulations in the form of a parametric study. Although adaptive noise cancellation is a powerful approach to cancellation of a single interfering tone, problems are found for multiple tone cancellation. A new approach is proposed based on the idea of a 'sparse adaptive filter'. This is similar to an LMS filter except that it has relatively few coefficients in relation to its length. The properties of sparse adaptive filters are developed, and the method is shown to be generally superior to adaptive noise cancellation for multiple tone cancellation.

In the case where no secondary reference measurement is available an alternative approach known as the function elimination filter is examined and found to be weak in a number of respects. A modified version of this algorithm is proposed which overcomes some of these weaknesses.

Section 3, the seismic section, begins with a brief review of seismic processing (Chapter 7). The purpose of this chapter is to give sufficient background to the subject to set the novel applications of Chapters 8 and 9 in context. This chapter also includes a description of two methods for generating synthetic seismic data - one single channel, based on a lattice synthetic and one a non-stationary multi-channel synthetic.

Chapter 8 is devoted to adaptive deconvolution of seismic data. Existing techniques are reviewed and a novel approach is proposed based on the method of optimal control. The method is applied both to stationary data and to non-stationary data derived from a model which includes frequency dependent attenuation. The noise reduction process developed in Chapter 4 is also applied and the results contrasted with conventional deconvolution. Both synthetic and field data are considered.

Chapter 9 is devoted to adaptive approaches to signal enhancement of seismic data. Two approaches are proposed, both based on forms of the generalised comb filter developed in Chapter 5. The first approach, dubbed the predictive stack, is a single channel operation for reverberant seismic data and is designed to improve the signal-to-noise ratio of the data by realigning the reverberant energy. The second approach is a multi-channel operation designed to utilise the correlation between signal components on consecutive channels at the expense of noise which is either uncorrelated from trace to trace or is correlated but is propagated at an acoustic velocity which lies outside a specified window. Both of these techniques are applied to synthetic and field seismic data.

The thesis closes with a general conclusions chapter in which recommendations for future work are also included.

One final note on the structure of the thesis; wherever possible in the interests of clarity the more mathematical aspects such as proofs of results have been relegated to the appendices. The results are not included merely for the sake of completeness. Any proof which is given in the appendices appears either because the result itself is new, the proof is novel or the proof is needed as the basis for a further result.

## CHAPTER 2

### ADAPTIVE PROCESSING

#### 2.1 Introduction

In this chapter the ideas of adaptive processing, which will be used throughout this thesis, are introduced. The aim is to discuss, in general terms, the motivation for adaptive solutions, the types of adaptive processing schemes available and the rationale for selecting a particular scheme. However, the chapter also contains a detailed description of the so-called LMS (least mean square) adaptive filter [113] which is used extensively throughout the thesis. The theory of the algorithm is discussed in detail and some new results are presented.

Essentially, only least-squares approaches are considered. This is not because other possibilities do not exist. Least-squares techniques are adopted because they are generally simple (both analytically and computationally) and robust. It is not inferred that such schemes are necessarily 'best' in any particular sense (except least-squares) for a given application. Indeed, in some applications in later chapters, it will be seen that the time domain optimality of least-squares techniques is not matched in other ways which are important from an interpretation viewpoint.

The chapter begins by presenting, as essential background, the least-squares formulation for stationary or 'fixed' filters before discussing the need for adaptive filters (section 2.3). Adaptive filters are then presented as a natural way of developing time-variable solutions to non-stationary least-squares problems (section 2.4). The LMS algorithm is then discussed in depth (section 2.5). The theory of the algorithm is discussed in detail in the context of broadband random inputs (narrowband inputs are dealt with in Chapter 6). Existing theory is clarified, non-stationary inputs (which have received little attention in the literature due to the inherent complexities of the solutions) are considered, and several new results are presented. The implementation and other details of the LMS algorithm are also discussed. In section 2.6, a review of alternative (least-squares) adaptive algorithms is presented. This is intended to illustrate the types of solution available rather than be an exhaustive study. The chapter concludes with a discussion of the relative merits of different adaptive algorithms and different approaches to adaptive processing.

## 2.2 Least-Squares Filtering

### 2.2.1 The normal equations

Least-squares filters are designed to modify a given input signal,  $x(n)$ , in such a way as to minimise the mean-square error between the filter output,  $y(n)$ , and some desired signal,  $d(n)$ , (see fig. 2.2.1).

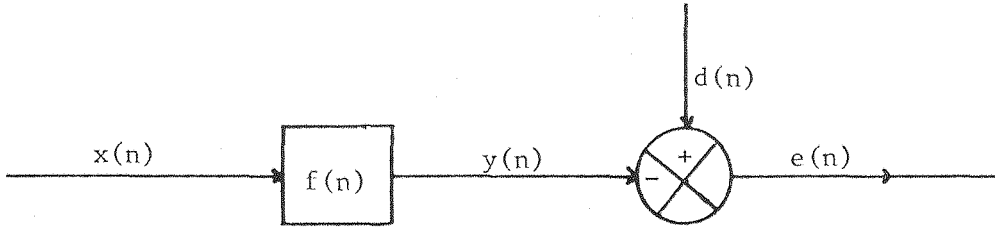


Figure 2.2.1: Least-squares Filtering

That is,  $f(n)$  is designed to minimise:

$$I = \sum e^2(n) \quad (\text{for deterministic signals}) \quad (2.2.1a)$$

where the range of summation remains to be specified,

$$\text{or} \quad I = E\{e^2(n)\} \quad (\text{for random signals}) \quad (2.2.1b)$$

$$\text{where in both cases} \quad e(n) = d(n) - f(n) * x(n) \quad (2.2.2)$$

In either case, the solution is obtained by differentiating  $I$  with respect to  $f(j)$  and equating to zero, which leads to a system of linear equations known as the 'Normal Equations' (see, e.g. [81]) and written in vector form as:

$$R\underline{f} = \underline{g} \quad (2.2.3)$$

where  $\underline{f}$  is the vector whose elements are the filter coefficients,  $f(n)$ ;  $R$  is a matrix whose elements are the autocorrelation coefficients of  $x(n)$ , that is,

$$R(i, j) = \sum x(n + i)x(n + j) \quad (\text{deterministic}) \quad (2.2.4a)$$

$$R(i, j) = E\{x(n + i)x(n + j)\} \quad (\text{random}) \quad (2.2.4b)$$

and  $\underline{g}$  is a vector whose elements are the cross-correlation coefficients between the input  $x(n)$  and the desired signal  $d(n)$

$$g(i) = \sum x(n)d(n + i) \quad (\text{deterministic}) \quad (2.2.5a)$$

$$g(i) = E\{x(n)d(n + i)\} \quad (\text{random}) \quad (2.2.5b)$$

The term Normal Equations arises from the orthogonality of error and input which is implicit in equation (2.2.3). There are two distinct forms for the Normal Equations known as the autocorrelation formulation and the autocovariance formulation [53].

#### (i) Autocorrelation Formulation

The autocorrelation formulation is applicable when the input signals are stationary random processes or when they are deterministic with the minimisation taken over all  $n$ . In this case,

$$R(i, j) = R(i - j) \quad (2.2.6)$$

and the coefficient matrix is highly structured, having a symmetric Toeplitz form (all elements on each diagonal identical). The equations may be written

$$\sum_j R(i - j)f(j) = g(i) \quad (2.2.3a)$$

#### (ii) Autocovariance Formulation

The autocovariance formulation is applicable when the signals are non-stationary random, or when they are deterministic with the minimisation taken over a finite interval. In this case the coefficient matrix is symmetric, but not Toeplitz and the equations may be written:

$$\sum_j R(i, j)f(j) = g(i) \quad (2.2.3b)$$

(strictly  $g(o, i)$  in this case)



Note, however, that the autocorrelation form may be obtained with the minimisation taken over a finite interval by windowing the input signal appropriately (see [14, 53] for more detail).

## 2.2.2 Solutions of the normal equations

### (a) Infinite two-sided filter

For inputs which give rise to the autocorrelation form, recognising that the left hand side of equation (2.2.3a) is the convolution of the filter with the input autocorrelation, then:

$$z \text{ transforming} \quad R(z)F(z) = G(z) \quad \text{where} \quad G(z) = \sum_{i=-\infty}^{\infty} g(i)z^{-i}, \text{ etc.}$$

$$\text{so that} \quad F(z) = \frac{G(z)}{R(z)} \quad (2.2.7)$$

Note, that if the filter is restricted to being of a causal form, the solution cannot then be obtained by simple spectral division, but may still be obtained by a spectral factorisation technique. An example of the properties of such solutions is discussed in Chapter 3.

Note also that, for the autocovariance form, no direct analogue of equation (2.2.7) can be given since the inputs do not have fixed spectral representations.

### (b) Finite causal filter

If, in addition to causality, the filter is also constrained to be finite in length, then the normal equations (2.2.3) become

$$\sum_{j=0}^{L-1} R(i-j) f(j) = g(i) \quad 0 \leq i \leq L-1$$

(for the autocorrelation form) (2.2.3c)

and

$$\sum_{j=0}^{L-1} R(i, j) f(j) = g(i) \quad 0 \leq i \leq L-1$$

(for the autocovariance form) (2.2.3d)

where  $L$  is the filter length.

The resulting set of equations may be solved by any of the standard techniques; however, large increases in computational efficiency are possible due to the symmetry properties of the coefficient matrices (see Appendix I).

### 2.2.3 Error energy in finite least-squares filtering [81]

An expression for the error energy in least-squares filtering may be obtained by expanding (2.2.1a) or (b) as appropriate, and substituting (2.2.4) yielding in either case:

$$I = R_{dd}(0) + \underline{f}^t R_f \underline{f} - 2 \underline{f}^t \underline{g} \quad (2.2.8)$$

where  $R_{dd}$  is the autocorrelation of  $d$ , defined analogously to equation (2.2.4).

Substituting equation (2.2.3) gives

$$I_{\min} = R_{dd}(0) - \underline{f}^t \underline{g} \quad (2.2.9)a$$

$$\text{or} \quad = R_{dd}(0) - \underline{f}^t R_f \underline{f} \quad (2.2.9)b$$

where  $\underline{f} = R^{-1} \underline{g}$ .

These expressions do not directly give any further insight into the form of the least-squares filter but will be needed in the development of adaptive filters in later sections.

## 2.3 Motivation for Adaptive Solutions

The least-squares filtering technique described in the previous section is a powerful approach to filtering in situations where a fixed, finite length filter is applicable. However, there are a number of circumstances where this approach may be less satisfactory. For example, if the input signal is non-stationary, the normal equations (2.2.3) could still be solved but the autocorrelation coefficients cannot be determined from a

single realisation. A further problem which arises is that a least-squares operator as derived in the previous section is a single 'global' operator for the whole of the optimisation interval. In any situation where the operator should be time-variant over intervals which are shorter than that over which the optimisation takes place, the result is effectively averaged over the interval. Whilst there are some circumstances in which such a single 'global' operator is required there are many in which a filter of this form would be inappropriate. Deconvolution is an example of a process for which both types of operator may be desirable in different circumstances (see Chapter 3). One obvious way to overcome this problem is simply to reduce the interval over which the optimisation takes place. This would also be a useful approach for those random processes which might be classed as locally stationary where it may be reasonable to estimate the autocorrelation with respect to a point in time as a short-time average. Examples of such processes might be speech and seismic signals. This technique of subdividing a piece of data into smaller intervals (or gates) over which the signals are considered stationary, is widespread in speech and seismic processing amongst other applications [57, 106]. Attempts have been made to optimise the length of the gates [106] as a trade-off between estimation error in the autocorrelation (which decreases with interval length) and the error implicit in replacing a non-stationary autocorrelation with a time average. However, the resulting formula is somewhat unwieldy to use and is restricted to only a limited class of processes. In any case gating in general can only provide a partial answer to filtering continuously time-variant signals. A more complete solution would be provided by a continuously adaptive filter. In opting for the design of such filters there are two fundamentally distinct approaches:

(i) Modelling the system (or non-stationarity) - this would obviously be desirable in many circumstances but is often impossible. Nevertheless, it is still an important aspect of adaptive signal processing and a powerful example of such a technique is considered in Chapter 4.

(ii) A pragmatic approach based on updating the filter at each point in such a manner as to keep the filter as close as possible to the time-variable solution of the normal equations.

It is this second approach which is considered in detail in the remainder of this chapter.

## 2.4 From Iterative Solutions of the Normal Equations to Adaptive Filters

### 2.4.1 Introduction

In attempting to find continuously adaptive solutions to the normal equations the most obvious approach is simply to recompute the correlations at each point and solve the resulting normal equations. Leaving aside the difficulties implicit in the computation of these correlation coefficients (as discussed in the previous section), such a solution effected by the Levinson recursion, or any other standard technique, involves an enormous computational burden. Nevertheless, one such class of solutions to sets of linear equations - iterative solutions - will now be discussed as these provide the basis for what follows.

### 2.4.2 Iterative solutions to normal equations

Iterative solutions have been applied to stationary systems in place of the Levinson recursion [107]. If the initial approximation is sufficiently close to the optimal value then only a relatively small number of iterations may be required. Recall from section 2.2 that the least-squares filter is obtained from the solution of the normal equation (2.2.3). An iterative solution to these equations is obtained [92] using

$$\underline{f}_{j+1} = \underline{f}_j - \alpha_j \underline{p}_j \quad (2.4.1)$$

where the subscript  $i$  denotes the  $i$ 'th update, and where  $\underline{p}_j$  defines the search direction and has the form

$$\underline{p}_j = D_j \frac{\partial I}{\partial \underline{f}} (\underline{f}_j) \quad (2.4.2)$$

$D_j$  is a matrix whose form is dependent on the particular techniques, and  $\alpha_j$  is a step-size parameter.

The performance index  $I$ , defined by equation (2.2.8) is an  $N$ -dimensional paraboloid surface. The iterative process begins at some point on the surface with an initial guess and attempts to iterate towards the minimum - which is unique for this form of performance index.

A large number of such techniques have been developed; these can be classified by

- (i) specification of initial trial point  $\underline{f}_0$  - usually arbitrary.
- (ii) specification of search direction  $\underline{p}_j$ .

There are two classes:

(a) Direct search methods

These seek the minimum directly by evaluation of the performance index at successive trial points.

(b) Gradient Search Methods

Gradient search procedures make use not only of the performance index, but also of its derivative  $\partial I / \partial \underline{f}$ . Gradient search methods usually require fewer trial points to converge to within a given limit. On the other hand, direct search methods generally need substantially fewer computations per iteration. It is gradient techniques which are of primary interest here, though an example of a direct search method will be discussed in a later section.

(iii) Step-size Parameter

In some algorithms the step-size parameter,  $\alpha_i$ , is chosen arbitrarily, in others it may be chosen to minimise  $I$  at  $\underline{f}_{i+1}$  in a given search direction.

A fourth aspect of the specification may be search termination criteria, though this is not relevant for the purposes of this thesis, and will not be considered further.

#### 2.4.3 Steepest descent (eg. [114])

The method of primary interest here is the steepest descent approach. Other methods to produce faster convergence have been developed, for example, Newton's method and the method of conjugate gradients [92] are designed to produce exact convergence in a finite number of steps. However, these methods invariably incur an increase in computation and complexity over the steepest descent approach.

The philosophy of steepest descent can be described as follows. At each iteration, move (in the space of filter weights) in a direction opposite to the gradient of the performance index, and by a distance proportional to the magnitude of the gradient. In terms of the above specification, this gives

$$D_j = -I; \quad p_j = \frac{\partial I(\underline{f}_j)}{\partial \underline{f}}$$

and  $\alpha_j = \alpha/2$  a constant of proportion where the 2 is introduced for convenience, so that (2.4.1) becomes

$$\underline{f}_{j+1} = \underline{f}_j - \frac{\alpha}{2} \frac{\partial I(\underline{f}_j)}{\partial \underline{f}} \quad (2.4.3)$$

which from (2.2.3) is

$$\underline{f}_{j+1} = \underline{f}_j - \alpha(R\underline{f}_j - \underline{g}) \quad (2.4.4)$$

The term 'steepest descent' arises from the fact that in the neighbourhood of  $\underline{f}_j$  the gradient is normal to lines of equal cost, thus the gradient direction is the line of steepest ascent (in cost terms).

In contrast to many iterative techniques convergence can be analytically established for the method of steepest descent (an example proof is given in Appendix II), subject to the restriction that

$$0 < \alpha < 2/\lambda_{\max} \quad (\text{II.2.4})$$

where  $\lambda_{\max}$  is the largest eigenvalue of  $R$ .

The method may converge only slowly, however, particularly in the region of the minimum.

#### 2.4.4 Iterative methods as adaptive filters

In the previous section iterative methods for the solution of normal equations were discussed. In this section, the manner in which such techniques may be employed as adaptive filters for non-stationary data is considered. It has already been observed that the performance index  $I$

may be considered as an N-dimensional paraboloid with a unique minimum. In the case of non-stationary data the position and orientation of the surface (and its minimum) vary with time. Widrow and Hoff [113] proposed that the adaptive filter should be designed to correspond to the updating procedure of the iterative process. That is, the  $(j + 1)$ 'th update  $\underline{f}_{j+1}$  corresponds to the adaptive filter at  $(j + 1)$ . The procedure may be specified by:

$$\underline{f}_{j+1} = \underline{f}_j - \alpha_j D_j \frac{\partial I(\underline{f}_j)}{\partial \underline{f}} \quad (2.4.1)$$

and

$$y_{j+1} = \underline{f}_{j+1}^t \underline{x}_{j+1} \quad (2.4.5)$$

where  $\alpha_j$ ,  $D_j$  are as defined in section 2.3.

The filter attempts to track variation in the least-squares solution at each point. In the case of steepest descent (see previous section) equation (2.4.1) becomes

$$\underline{f}_{j+1} = \underline{f}_j - \alpha (R_j \underline{f}_j - \underline{g}_j) \quad (2.4.4.a)$$

where  $R_j$ ,  $\underline{g}_j$  are the autocorrelation matrix and cross-correlation vector, respectively, computed with reference to the  $j$ 'th point of the process.

There are two main problems with steepest descent. Firstly, the calculation of  $R$  and  $\underline{g}$  at each point is very expensive computationally. Secondly, as already discussed, it may not be possible to compute  $R_j$  and  $\underline{g}_j$  if only a single realisation of the process is available. These difficulties can be overcome, in part at least, by replacing the gradient  $\partial I / \partial \underline{f}$  by an estimate. The adaptive filtering method which is of primary interest here is based on estimating the gradient of the mean-square error by the instantaneous value. This method, which is due originally to Widrow and Hoff [113], is known as the LMS algorithm. This algorithm is discussed in detail in the next section. However, it is well to stress that it is by no means the only form of adaptive filter and a number of alternative schemes are discussed in section 2.6.

## 2.5 LMS Adaptive Algorithm

### 2.5.1 General

As discussed in the previous section, the LMS adaptive algorithm is based on the steepest descent algorithm of section 2.4.3 with the gradient  $\partial I(\underline{f}_j)/\partial \underline{f}$  replaced by an estimate based on the instantaneous value. That is, the steepest descent update equation (2.4.3) is replaced by

$$\underline{f}_{j+1} = \underline{f}_j - \frac{\alpha}{2} \frac{\partial \hat{I}(\underline{f}_j)}{\partial \underline{f}} \quad (2.5.1)$$

where, again, the constant 2 is included merely for convenience.

Now,  $I$  is the mean squared error defined by equation (2.2.1),  $\hat{I}$  by contrast is the instantaneous squared error and is given by

$$\hat{I} = e^2(j) = (d(j) - \underline{f}_j^T \underline{x}_j)^2 \quad (2.5.2)$$

so that

$$\frac{\partial \hat{I}}{\partial \underline{f}} = \frac{\partial e^2(j)}{\partial \underline{f}} = 2e(j) \frac{\partial e(j)}{\partial \underline{f}} \quad (2.5.3)$$

or

$$\frac{\partial \hat{I}}{\partial \underline{f}} = -2e(j)\underline{x}_j. \quad (2.5.4)$$

Substituting in equation (2.5.1) gives the LMS update equation:

$$\underline{f}_{j+1} = \underline{f}_j + \alpha e(j)\underline{x}_j. \quad (2.5.5)$$

A number of the attractions of the LMS algorithm are immediately apparent from this equation. Firstly, the update equation is computationally simple, requiring no matrix inversions or other computationally expensive operations, and the total update requires just  $L$  multiplies and  $L$  additions per step. Secondly, the algorithm requires no averaging, thus avoiding the difficulties, both analytical and computational, involved in computing correlations. The update equation also indicates, as a consequence of the last two points discussed, the possibility of real-time implementation as a tapped-delay line.



The adaptation constant  $\alpha$  plays a vital role in determining the behaviour of the algorithm. Empirically, increasing the magnitude of this constant increases the ability of the algorithm to track variations in the input signals. However, as will be seen in the next section, increasing  $\alpha$  also increases the propensity of the algorithm to respond to spurious events, that is, to exaggerate noise.

The algorithm has found widespread use in a great variety of applications, e.g. [31, 91, 115] and, indeed, a primary aim in this thesis is to use the algorithm in certain novel situations. The performance of the algorithm has been proved by simulation many times but the analytic properties are less well understood and these are considered in the next section.

### 2.5.2 LMS theory

In contrast to the steepest descent algorithm from which it is derived, and in spite of the apparent simplicity of the LMS filter as expressed by the update equation (2.5.5), the properties of the filter have proved difficult to analyse. Some work has been done and results have been obtained for certain limited types of input. In Chapter 6 these results are developed and extended for the case where the input signal has a narrowband form. In this section the response of the LMS filter to random signals is considered.

In the case of random inputs the difficulties in analysis are due to the fact, expressed by the update equation (2.5.5), that the filter is obtained by recursive, nonlinear combinations of random vectors. Contrast this with the steepest descent method where all operations are defined in terms of second moments. The difficulties implied by this can be illustrated by geometric considerations. As has already been stated the mean-squared error performance index can be represented as an  $L$ -dimensional paraboloid in the space of filter weights. An example is shown in figure 2.5.1, where for convenience  $L = 2$ . The contours represent lines of equal cost. The gradient of the mean-square error,  $\partial I / \partial \underline{f}$ , at any point  $\underline{f}_k$ , is normal to the lines of equal cost [92], so that the limitations

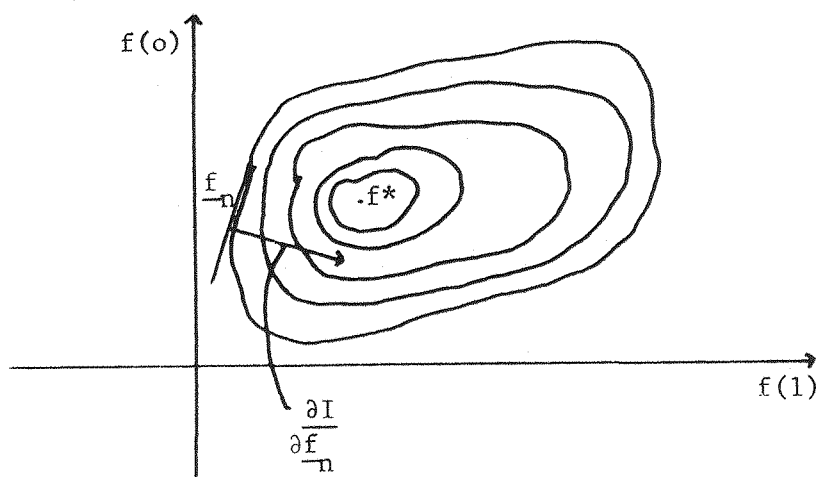


Figure 2.5.1: Diagrammatic Representation of Error-energy Versus Adaptive Filter Coefficients.

on the magnitude of the correction in the direction of the gradient to produce a reduction in the mean-square error can be easily quantified (see section 2.4). In the LMS case, however, the direction,  $\hat{\partial I} / \partial \underline{f}$ , is itself an  $L$ -dimensional random variable. Furthermore, this is itself dependent on  $\underline{f}_k$ . In general the LMS filter will not converge to an exact point due to the random nature of the filter. Consequently, the LMS algorithm is generally far more complex to analyse than the steepest descent algorithm. However, some progress is possible in some circumstances and this will now be discussed.

#### Convergence of the LMS filter (stationary processes)

Consider initially the convergence properties for input processes which are zero mean and (weakly) stationary.

Preliminaries:

##### (1) Bias of gradient estimates

As noted above, the LMS algorithm is based on an estimate of the gradient of the mean-squared error. Many authors have concluded, generally incorrectly, that the LMS gradient is an unbiased estimator of the true gradient of the mean-square error. This can be easily seen by considering the update equation:

$$\underline{f}_{j+1} = \underline{f}_j + \alpha e(j) \underline{x}_j \quad (2.5.5)$$

Now

$$e(j)\underline{x}_j = (d(j) - \underline{f}_j^t \underline{x}_j) \underline{x}_j^t \quad (2.5.6)$$

so that

$$\underline{f}_{j+1} = (I - \alpha \underline{x}_j \underline{x}_j^t) \underline{f}_j + \alpha d(j) \underline{x}_j^t \quad (2.5.7)$$

The gradient estimate is  $-2e(j)\underline{x}_j$ , so that

$$E\{-e(j)\underline{x}_j\} = E\{\underline{f}_j^t \underline{x}_j \underline{x}_j^t\} - \underline{g} \quad (2.5.8)$$

Now

$$E\{\underline{f}_j^t \underline{x}_j \underline{x}_j^t\} = E\{\underline{f}_j^t E(\underline{x}_j \underline{x}_j^t / \underline{f}_j)\} \quad (2.5.9)$$

but  $\underline{f}_j$  is a function of  $\underline{x}_{j-1}, \underline{x}_{j-2}, \dots$ , and  $d(j-1), \dots, d(0)$  so that  $E\{\underline{x}_j \underline{x}_j^t / \underline{f}_j\}$  will only equal  $E\{\underline{x}_j \underline{x}_j^t\}$  if successive input vectors are uncorrelated, that is, if:

$$E\{\underline{x}_{j-k} \underline{x}_k\} = \delta_{jk} I \quad (2.5.10)$$

So that, in general, the gradient estimate is only unbiased if successive input vectors are uncorrelated. Note that equation (2.5.10) is a much stronger condition than white noise and not one which can be utilised in any circumstances with the tapped-delay line form for the adaptive filter.

## (2) Filter coefficient solution

A solution for the filter coefficients does exist, and in fact is easily obtained by repeated application of the update equation as:

$$\underline{f}_j = \underline{f}_0 + \alpha \sum_{i=0}^j e(j-i) \underline{x}_{j-i} \quad (2.5.11)$$

or, alternatively, using (2.5.7):

$$\underline{f}_j = \prod_{i=1}^j (I - \alpha \underline{x}_{j-i} \underline{x}_{j-i}^t) \underline{f}_0 + \alpha \sum_{k=1}^j \prod_{i=1}^{k-1} (I - \alpha \underline{x}_{j-i} \underline{x}_{j-i}^t) d(j-k) \underline{x}_{j-k} \quad (2.5.12)$$

Unfortunately, except in special circumstances (see Chapter 6) these expressions are not very useful. In the case of random inputs the difficulty lies in the evaluation of the higher order moments in equation (2.5.12).

(3) Alternative update form

The LMS update equation may be written

$$\underline{f}_{j+1} = \underline{f}_j - \frac{\alpha}{2} \frac{\partial \hat{I}}{\partial \underline{f}} \quad (2.5.1)$$

This may be used to obtain an alternative update form. Now

$$\frac{\partial \hat{I}}{\partial \underline{f}} = \frac{\partial I}{\partial \underline{f}} - 2N_j \quad (2.5.13)$$

where  $N_j$  is a noise term representing the error in the gradient estimate. The 2 appears for convenience.

Now

$$\frac{\partial I(\underline{f}_j)}{\partial \underline{f}} = 2(R\underline{f} - \underline{g})$$

but  $R\underline{f}^* = \underline{g}$  where  $\underline{f}^*$  is the optimal solution. Hence, defining

$$\underline{v}_j = \underline{f}_j - \underline{f}^* \quad (2.5.14)$$

$$\frac{\partial I(\underline{f}_j)}{\partial \underline{f}} = 2R\underline{v}_j \quad (2.5.15)$$

Substituting (2.5.15) and (2.5.13) into (2.5.1) yields

$$\underline{v}_{j+1} = (I - \alpha R)\underline{v}_j + \alpha N_j \quad (2.5.16)$$

This recursive error equation is very useful for convergence purposes.

The noise term  $N_j$  determines the behaviour of the system

$$N_j = \frac{1}{2} \left\{ \frac{\partial I}{\partial \underline{f}} - \frac{\partial \hat{I}}{\partial \underline{f}} \right\} \quad (2.5.17)$$

$$= (R\underline{f} - \underline{g}) - (d(j)\underline{x}_j - \underline{x}_j \underline{x}_j^t \underline{f}_j) \quad (2.5.18)$$

Hence

$$\begin{aligned} E\{N_j\} &= RE\{\underline{f}_j\} - E\{\underline{x}_j \underline{x}_j^t \underline{f}_j\} \\ &= RE\{\underline{f}_j\} - E\{\underline{x}_j \underline{x}_j^t E(\underline{f}_j / \underline{x}_j \underline{x}_j^t)\} \end{aligned} \quad (2.5.19)$$

Two cases may be distinguished.

(a)  $E\{N_j\} \equiv 0$  (uncorrelated input vectors)

This condition corresponds to independence of  $\underline{f}_j$  and  $\underline{x}_j$  and, as discussed earlier, can only occur for input vectors which are uncorrelated in the sense of equation (2.5.10). In spite of the fact that this is a highly unrealistic situation, it remains one of the few cases where convergence in the mean may be explicitly proved. Widrow [114] has shown that

$$\lim_{j \rightarrow \infty} E\{\underline{v}_j\} \rightarrow 0 \quad \text{if} \quad 0 < \alpha < 2/\lambda_{\max} \quad (\text{III.8})$$

(See Appendix III)

(b)  $E\{N_j\} \neq 0$  (correlated input vectors)

In the more usual case where  $E\{N_j\} \neq 0$  and consecutive input vectors are correlated, no general convergence proof exists. Nevertheless, some work has been done: Griffiths [36] considers the behaviour of the algorithm in the context of linear prediction (single step). For obvious reasons consecutive input vectors cannot be considered uncorrelated. However, Griffiths maintains the assumption that  $\underline{x}_{j-1} \underline{x}_{j-1}^t$  is independent of  $\underline{f}_{j-1}$  by assuming  $\underline{x}(j)$  is zero mean, stationary and Gaussian and that the resulting  $\underline{f}_j$  are also Gaussian. However, this assumption is not generally valid as  $\underline{f}_k$  is formed from a non-linear combination of the  $\underline{x}_i$ 's and it is known [71] that non-linear combinations of Gaussian random variables produce non-Gaussian results.

Kim and Davisson [43] consider input processes which are jointly stationary and M-dependent, in the sense that

$$E\{\underline{x}(j)\underline{x}(k)\} = 0; \quad |j - k| > M \quad (2.5.20)$$

They demonstrate convergence (to a result which is biased from the fixed least-squares solution) for small  $\alpha$  using the modified algorithm

$$\underline{f}_{j+1} = \underline{f}_j + \frac{\alpha}{L} \sum_{n=j-\frac{N}{2}}^{j+\frac{N}{2}} e(n) \underline{x}_n \quad (2.5.21)$$

where  $N \geq 2M + 2L - 1$ , where  $L$  is the filter length. However, these results cannot be applied to the usual LMS algorithm.

Daniell [17] has shown that for processes which, in addition to stationarity and ergodicity, have bounded moments and satisfy a form of asymptotic independence, then the steady-state excess mean-square error (over the fixed least-squares solution) can be made arbitrarily small for sufficiently small  $\alpha$ . The asymptotic independence requirement is defined as follows:

$$\text{If } A_i = \underline{x}_i \underline{x}_i^t - R \text{ and } \underline{c}_i = (d(i)\underline{x}_i - \underline{x}_i \underline{x}_i^t R^{-1} \underline{g})$$

then

$$\text{tr} \left[ E \{ A_L^t A_M | \underline{x}_1, \underline{c}_1, \dots, \underline{x}_i, \underline{c}_i \} - E \{ A_L^t A_M \} \right] < \alpha_k \quad (2.5.22)$$

where  $i < i + k \leq M \leq L$

with  $\lim_{k \rightarrow \infty} \alpha_k = 0$

and where  $\text{tr}$  denotes trace of the matrix.

Note, however, that this is not a complete answer, for which one would require convergence in the mean for fixed  $\alpha$  together with the steady-state excess mean-square error. That is, the concern is with finite adaptation rates, not with the limit as  $\alpha$  tends to zero.

For inputs which are stationary and ergodic or alternatively satisfy a form of asymptotic independence, Bitmead and Anderson [7] demonstrated exponential asymptotic stability for the homogeneous equations which may be obtained if it is assumed that

$$d(k) = \underline{f}^* \underline{x}_k^t \quad (2.5.23)$$

that is, if an exact solution exists.

This is then used to infer 'reasonable' behaviour of the usual (inhomogeneous) equations.

Further insight into the convergence behaviour of the LMS algorithm for correlated inputs may be obtained by considering equation (2.5.19).

Let

$$\underline{\varepsilon}_j = E \{ N_j \} = RE \{ \underline{f}_j \} - E \{ \underline{x}_j \underline{x}_j^t E \{ \underline{f}_j / \underline{x}_j \underline{x}_j^t \} \} \quad (2.5.19)$$

then from (2.5.16)

$$E\{\underline{v}_{j+1}\} = (I - \alpha R)E\{\underline{v}_j\} + \alpha \underline{\epsilon}_j \quad (2.5.24)$$

These equations may be decoupled by factorising  $R$  [114] as

$$R = Q\Lambda Q^t \quad (2.5.25)$$

where  $Q$  is the orthonormal matrix of eigenvectors and  $\Lambda$  is the spectral matrix (diagonal matrix of eigenvalues), assuming distinct eigenvalues.

Defining

$$\underline{v}_j' = Q^t \underline{v}_j \quad (2.5.26)$$

then

$$E\{\underline{v}_{j+1}'\} = (I - \alpha \Lambda)E\{\underline{v}_j'\} + \alpha \underline{\epsilon}_j' \quad (2.5.27)$$

where

$$\underline{\epsilon}_j' = Q^t \underline{\epsilon}_j. \quad (2.5.28)$$

Equations (2.5.27) are now a decoupled set; the  $i$ 'th equation may be written

$$E\{v_{j+1}'(i)\} = (1 - \alpha \lambda_i)E\{v_j'(i)\} + \alpha \epsilon_j'(i) \quad (2.5.29)$$

where  $v_j'(i)$  is the  $i$ 'th component of the vector  $\underline{v}_j'$ , and  $\lambda_i$  is the  $i$ 'th eigenvalue of the autocorrelation matrix  $R$ .

Repeated substitution gives the solution for this equation as

$$E\{v_j'(i)\} = (1 - \alpha \lambda_i)^j E\{v_0'(i)\} + \alpha \sum_{k=0}^{j-1} (1 - \alpha \lambda_i)^k \epsilon_{j-k}'(i) \quad (2.5.30)$$

or

$$E\{v_j'(i)\} = (1 - \alpha \lambda_i)^j v_0'(i) + \alpha h(k) * \epsilon_k'(i) \quad (2.5.31)$$

where

$$h(k) = (1 - \alpha \lambda_i)^k.$$

Several conclusions are immediately possible:

1) The response due to the initial error  $v_0'$  decays to zero provided  $0 < \alpha < \frac{2}{\lambda_i}$  and the rate of decay is determined by  $(1 - \alpha\lambda_i)$ .

2) Subject to the same restriction on  $\alpha$ ,  $h(k)$  is a stable linear system from which it may be inferred that, provided  $\underline{\epsilon}_j$  is bounded for all  $j$ , then so is  $E\{v_j\}$ . Also the contribution due to any given  $\underline{\epsilon}_k$  decays exponentially.

3) If  $\lim_{j \rightarrow \infty} \epsilon_j(i) \rightarrow 0$  then  $\lim_{j \rightarrow \infty} E\{v_j'(i)\} \rightarrow 0$

that is if  $\epsilon_j$  tends to zero the LMS algorithm tends, in the mean, to the fixed least-square solution. In other circumstances the 'steady-state' result will generally be biased. Such a bias has been demonstrated (by simulation) by Senne [86].

Note that conclusions (1) and (2) are similar to those obtained by Bitmead and Anderson [7] but in that case the processes were restricted in addition to stationarity, to being ergodic.

### Steady-state error

The mean-square error  $I$  can be expressed in terms of the excess error over the minimum value for the fixed least-squares solution  $I_{\min}$  using equations (2.2.8) and (2.2.9) as [114]

$$I = I_{\min} + (\underline{f} - \underline{f}^*)^t R (\underline{f} - \underline{f}^*)$$

or

$$I = I_{\min} + \underline{v}^t R \underline{v} \quad (\text{using (2.5.14)})$$

or

$$I = I_{\min} + \underline{v}'^t \Lambda \underline{v}' \quad (2.5.32)$$

(using (2.5.25) and (2.5.26))

Widrow [116] has obtained an expression for the steady-state excess mean-square error using the uncorrelated input vector assumption:



If

$$\frac{\partial \hat{I}}{\partial \underline{f}} = \frac{\partial I}{\partial \underline{f}} - 2\underline{N}_j = -2e(j)\underline{x}_j$$

then in the region of the fixed least-squares solution

$$\frac{\partial I}{\partial \underline{f}} \approx 0 \quad \text{and} \quad E\{\underline{N}_j \underline{N}_j^t\} = E\{e(j)^2 \underline{x}_j \underline{x}_j^t\}$$

By further assuming that  $e(j)$  and  $\underline{x}_j$  are zero-mean, Gaussian and independent:

$$E\{\underline{N}_j \underline{N}_j^t\} = I_{\min} R$$

Using  $\underline{N}_j' = Q^t \underline{N}_j$

$$E\{\underline{N}_j' \underline{N}_j'^t\} = I_{\min} J$$

where  $J$  is the identity matrix (renamed to avoid confusion), then using

$$\underline{v}_{j+1}' = (I - \alpha \Lambda) \underline{v}_j' + \alpha \underline{N}_j$$

it can be shown [114] that  $E\{\underline{v}_j' \underline{v}_j'^t\} = \alpha I_{\min} J$ , in the region of the least-squares solution and, hence, using equation (2.5.30)

$$I = I_{\min} + \alpha I_{\min} \text{tr}\{R\} \quad (2.5.33)$$

Davisson [18] produces a more general result. Assuming stationary inputs and assuming convergence, then the steady-state error variance is bounded by:

$$I \leq I_{\min} + \alpha E\{I_{\min} \underline{x}_{-n}^t \underline{x}_{-n}\} + O(\gamma^{1+\delta}) \quad \delta > 0 \quad (2.5.34)$$

where  $\gamma = \alpha E\{x^2(n)\}$ .

It is also pointed out in the above paper that, for Gaussian processes, this reduces to:

$$I \leq I_{\min} + I_{\min} L \alpha E\{x^2(n)\} + O(\gamma^{1+\delta})$$

$$\text{or} \quad I \leq I_{\min} + \alpha I_{\min} \text{tr}\{R\} + O(\gamma^{1+\delta}) \quad (2.5.35)$$

(cf. equation (2.5.33)).

Note, finally, that Widrow [114] has defined a normalised measure of excess mean-square error termed misadjustment and defined

$$M = \frac{\text{Excess mean-square error}}{\text{Minimum mean-square error}}.$$

### Nonstationary inputs

Processing non-stationary signals is an important application of the LMS filter. Although the ability of the algorithm to deal with at least some types of non-stationarity has been adequately demonstrated in practice, little has been done to establish the analytic properties of the algorithm for such inputs. Widrow et al [19] have investigated a simplified problem where the filter is used to track a non-stationary desired output signal (of a restricted form) but where the input remains stationary. The analysis and simulations demonstrate that the filter performance is a trade-off between tracking errors caused by the non-stationary nature of the solution which are inversely proportional to the rate of adaptation, and misadjustment errors which are directly proportional to the adaptation rate.

In this section a novel description of the behaviour of the algorithm for non-stationary inputs is obtained. It is demonstrated that the equations describing the non-stationary response are similar to those for the stationary response but with an extra driving term proportional to the change in the optimal solution at each step.

From equation (2.2.8)

$$\frac{\partial I(\underline{f}_j)}{\partial \underline{f}} = 2(R_j \underline{f}_j - \underline{g}_j) \quad (2.5.36)$$

where  $R_j$ ,  $\underline{g}_j$  are the correlation matrices and where subscript  $j$  denotes time dependence.

Now

$$R_j \underline{f}_j^* = \underline{g}_j$$

and hence

$$\frac{\partial I}{\partial \underline{f}} = 2R_j (\underline{f}_j - \underline{f}_j^*) \quad (2.5.37)$$

Now

$$\frac{\partial \hat{I}}{\partial \underline{f}} = \frac{\partial I}{\partial \underline{f}} - 2N_j \quad (2.5.13)$$

where

$$\frac{\partial \hat{I}}{\partial \underline{f}} = -2e(j)\underline{x}_j = -d(j)\underline{x}_j + (\underline{f}_j^t \underline{x}_j)\underline{x}_j \quad (2.5.38)$$

and hence, using (2.5.13), (2.5.37) and (2.5.38)

$$N_j = R_j (\underline{f}_j - \underline{f}_j^*) - d(j)\underline{x}_j + (\underline{f}_j^t \underline{x}_j)\underline{x}_j \quad (2.5.39)$$

(this is just the non-stationary version of equation (2.5.18)), but

$$\underline{f}_{j+1} = \underline{f}_j - \frac{\alpha}{2} \frac{\partial \hat{I}}{\partial \underline{f}} \quad (2.5.1)$$

using (2.5.38) and (2.5.39) this is

$$\underline{f}_{j+1} = \underline{f}_j - \alpha R_j (\underline{f}_j - \underline{f}_j^*) + \alpha N_j \quad (2.5.40)$$

Hence

$$(\underline{f}_{j+1} - \underline{f}_{j+1}^*) = (\underline{f}_j - \underline{f}_j^*) - \alpha R_j (\underline{f}_j - \underline{f}_j^*) + (\underline{f}_j^* - \underline{f}_{j+1}^*) + \alpha N_j \quad (2.5.41)$$

or

$$\underline{v}_{j+1} = (I - \alpha R_j)\underline{v}_j + \alpha N_j + (\underline{f}_j^* - \underline{f}_{j+1}^*) \quad (2.5.42)$$

This is the non-stationary version of (2.5.16) and, contrasting the two, it is seen that the difference is that the non-stationary equation has an extra driving term, due to the non-stationarity and proportional to the change in the optimal solution from  $j$  to  $j + 1$ .

The term  $N_j$  is essentially unchanged except that the correlation functions are, of course, non-stationary. The solution to this difference equation is obtained by repeated substitution as

$$\begin{aligned} \underline{v}_j = & \prod_{i=1}^j (I - \alpha R_{j-i}) \underline{v}_0 + \alpha \sum_{k=1}^j \prod_{i=1}^k (I - \alpha R_{j-i}) \underline{N}_{j-k} \\ & + \alpha \sum_{k=1}^j \prod_{i=1}^k (I - \alpha R_{j-i}) (\underline{f}_{j-k}^* - \underline{f}_{j-k+1}^*) \end{aligned} \quad (2.5.43)$$

If the form of the non-stationarity is restricted to changes in power, then  $R_j$  may be factored as

$$R_j = Q \Lambda_j Q^t$$

and one can proceed to obtain decoupled equations as in the previous section. However, this restriction is not necessary since similar results can be demonstrated without decoupling the equations. The basic result required is that:

$$\lim_{k \rightarrow \infty} \left\| \prod_{i=1}^k (I - \alpha R_i) \right\| = 0$$

where  $\| \cdot \|$  is defined by  $\|A\| = \lambda_{\max}$  for a symmetric positive definite matrix  $A$  (example, [112]).

Now

$$\|I - \alpha R_i\| = |1 - \alpha \lambda_j^{(i)}|_{\max j}$$

where  $\lambda_j^{(i)}$  is the  $j$ 'th eigenvalue of  $R_i$ ,

$$= (\alpha \lambda_{\max j}^{(i)} - 1); \quad \alpha > \frac{2}{\lambda_{\max j}^{(i)} + \lambda_{\min j}^{(i)}}$$

$$= (1 - \alpha \lambda_{\min j}^{(i)}); \quad \text{otherwise.}$$

$$\text{Also, } \left\| \prod_{i=1}^k (I - \alpha R_i) \right\| \leq \prod_{i=1}^k \|I - \alpha R_i\| = \prod_{i=1}^k (1 - \alpha \lambda_j^{(i)})_{\max j}$$

So

$$\lim_{k \rightarrow \infty} \left\| \prod_{i=1}^k (I - \alpha R_i) \right\| \leq \lim_{k \rightarrow \infty} \prod_{i=1}^k (1 - \alpha \lambda_j^{(i)})_{\max j}$$

Now, in order to demonstrate that

$$\lim_{k \rightarrow \infty} \prod_{i=1}^k (1 - \alpha \lambda_j^{(i)})_{\max(j)} \rightarrow 0 \quad (2.5.44)$$

the following result, which is a slight generalisation of a result due to Wang[108], will be required.

#### Lemma

If  $(1 - a_r) \leq 1$ ,  $a_r \geq 0 \forall r$  except at most at a finite number of places, and  $|(1 - a_r)| < L < \infty$   $r$ , then

$$\prod_{r=0}^{\infty} (1 - a_r) \rightarrow 0 \quad \text{if} \quad \sum a_r \rightarrow \infty.$$

Proof: Appendix IV.

Now, assuming

$$\alpha \leq \frac{2}{\lambda_{j\max} + \lambda_{j\min}} \quad \forall j$$

at most at a finite number of places and since:

$$0 < \lambda^{(i)} < \infty \quad \forall i,$$

then the conditions of the lemma apply to equation (2.5.44) and

$$\lim_{k \rightarrow \infty} \prod_{i=1}^k (1 - \alpha \lambda_j^{(i)})_{\max(j)} = 0$$

and hence

$$\lim_{k \rightarrow \infty} \left\| \prod_{i=1}^k (I - \alpha R_i) \right\| = 0$$

Finally, applying this result to equation (2.5.43), assuming  $\alpha \leq 2/(\lambda_{j\max} + \lambda_{j\min})$  except at a finite number of places, then:

- 1) The response due to the initial error  $\underline{v}_0$  decays to zero (though not necessarily uniformly).
- 2) Subject to the same restrictions on  $\alpha$  it may be inferred that if  $E\{\underline{N}_j\}$  is bounded, then so is  $E\{\underline{v}_j\}$ .
- 3) Subject again to the same restrictions, the contributions due to any given  $\underline{N}_j$  and  $(\underline{f}_j^* - \underline{f}_{j+1}^*)$  decay to zero (at similar rates).

In effect this is using the convergence of the product form to infer reasonable behaviour of the equations and this is similar in some ways to the results of Bitmead and Anderson [7] previously discussed. Note, however, that these results are somewhat more general since (i) no 'mixing' assumption is required, and (ii) the contributions due to the correlation of the inputs and the non-stationarities are explicitly obtained.

### 2.5.3 Details of the algorithm

#### (1) Selection of adaptation constant

As is clear from the previous section, the adaptation constant  $\alpha$  plays a vital role in determining the behaviour of the algorithm. Equation (III.8) gives the limits on  $\alpha$  for stability for one rather restrictive case, and this result has been found to provide a good rule of thumb for more complex cases.

Now, from (III.8)

$$0 < \alpha < \frac{2}{\lambda_{\max}}$$

but

$$\lambda_{\max} \leq \text{tr}\{R\} = \sum_{i=1}^L E\{x^2(i)\} = \text{input power}$$

so that

$$0 < \alpha < \frac{2}{\sum_{i=1}^L E\{x^2(i)\}} \quad (\text{see [19]}). \quad (2.5.45)$$

This input power may then be approximated by a finite average. However, stability is not the only consideration affecting the choice of adaptation constant. As has already been discussed,  $\alpha$  is usually chosen as a compromise between adequate tracking ability and misadjustment noise. Hence, one would not normally choose a value of  $\alpha$  on the edge of stability. An appropriately modified system might be

$$\underline{f}_{j+1} = \underline{f}_j + \frac{\alpha e(j) \underline{x}_j}{\frac{1}{(2L+1)} \sum_{i=j-L}^{j+L} x^2(i)} \quad (2.5.46)$$

where  $\alpha$  is generally chosen in the range

$$0.1 < \alpha < 0.5. \quad (2.5.47)$$

Note that in some applications [39] it is advisable to apply some smoothing to the denominator function. In this form the LMS bears a remarkable resemblance to another iteration technique known as the 'quick and dirty' technique for non-linear regression [92] which is defined by

$$\underline{f}_{j+1} = \underline{f}_j + \frac{\alpha e(j) \underline{x}_j}{\frac{\underline{x}_j^t \underline{x}_j}{\underline{x}_j^t \underline{x}_j}} \quad (2.5.48)$$

## (2) Computation

As already stated, one of the main attractions of the LMS algorithm is the low computational requirement. For the basic scheme of equation (2.5.5), the filter requires just  $L$  multiplies (and  $L$  additions) to update the coefficients. It will be seen in the next section that this compares favourably with other iterative schemes.

The normalised form of the algorithm (equation (2.5.46)) has an increased computational requirement. However, the actual increase will vary according to circumstances. For applications where the input power is roughly constant, the value need only be computed once. In other

applications it may be necessary to compute input power on a running basis. However, even this does not engender a large increase in computation provided adequate storage is available.

### (3) Initialisation

As discussed in section 2.5.2, the choice of a set of initial values for the filter coefficients does not affect the final convergence of the algorithm. In many instances, no *a priori* information about the filter coefficients will be available and so these must be set arbitrarily.

A common choice is

$$\underline{f}_0 \equiv 0. \quad (2.5.49)$$

In a relatively few instances, some *a priori* knowledge of the coefficients will be available [39] and this can be used appropriately.

### (4) Alternative implementations

Although the implementation of the LMS filter discussed is the most common, it is not the only possibility. The most obvious generalisation is for a set of such filters operating together - as a multichannel filter, e.g., [27,115]. Such schemes will be considered in greater detail in Chapter 5.

Some authors have produced frequency domain versions of the LMS filter. The aim is usually to reduce the computation by allowing the use of the FFT. Dentino et al [19] have produced a scheme which reduces computation for 16 weights or more. In their scheme the input and desired signals are transformed in blocks of  $L$ . Adaptation is then performed independently for each frequency component, that is:

$$f_{k+1}(l) = f_k(l) + \alpha e_l(k) X_l \quad (2.5.50)$$

where  $f_k(l)$  denotes the  $l$ 'th frequency component of the  $k$ 'th update of the filter, where  $X_l$  is the  $l$ 'th frequency component and

$$e_l = D_l - Y_l \quad (2.5.51)$$

where  $D_l$  is the  $l$ 'th frequency component of the desired signal and where



$Y_L = f(L)X_L$  and the outputs are block inverse transformed. However, this multiplication in the frequency domain does not include appending zeroes so that the effect is to produce a circular convolution of  $f$  and  $x$ . Ferrara [26] has produced a modified version of this scheme which replaces circular convolution by linear convolution using the 'overlap-save' method [66]. As in Dentino's scheme, adaptation takes place just once per block but, in contrast, the weights are updated for all gradients in the previous block, that is

$$\underline{f}_{k+1} = \underline{f}_k + \alpha \sum_{i=0}^{L-1} e(kL+i) \underline{x}_{kL+i} \quad (2.5.52)$$

(time domain)

$$\text{where } e(kL+i) = d(kL+i) - \underline{f}_k^t \underline{x}_{kL+i} \quad (2.5.53)$$

(the actual updating is performed in the frequency domain).

In this way, Ferrara claims that the resulting impulse response is identical to that of the time domain implementation. However, in the author's opinion, this is incorrect, since the LMS would be

$$\underline{f}_{k(L+1)} = \underline{f}_k + \alpha \sum_{i=0}^{L-1} e(kL+i) \underline{x}_{(kL+i)}$$

so that the update equations are the same but where

$$e(kL+i) = d(kL+i) - \underline{f}_{(kL+i)}^t \underline{x}_{(kL+i)}$$

that is, the errors do not compare because in Ferrara's scheme the filter is only updated once per block. Computationally this scheme is superior to the usual LMS if  $L > 64$ .

## 2.6 Alternative Forms for Adaptive Filters

Although the LMS algorithm discussed in the previous section is probably the most widely used in signal processing, it is by no means the only possibility. Other schemes based on alternative gradient estimates, direct search methods, etc., have been developed. In fact a very large number of such schemes have been proposed. The intention here is to indicate the types of solution available rather than to give an exhaustive review. It is mentioned in passing that other algorithms exist which do not seek to minimise the mean-squared error, but operate on an alternative criterion either by incorporating constraints or possibly minimising a different norm. Such schemes will not, however, be considered here.

The available techniques may be divided into a number of sections.

### 1. LMS variants

A number of algorithms have been developed which can be classified as LMS variants. These cover a fairly wide range but have the common feature that they start from the LMS solution and attempt to improve on this by incorporating some modification (usually in a fairly empirical way).

The simplest form of modification consists of simply replacing the adaptation constant  $\alpha$  by a time-varying parameter  $\alpha(k)$ . This parameter is then generally chosen to reduce in magnitude as the steady-state solution is approached, for example, Ristow and Kosbahn [79] propose

$$\alpha(k) = \frac{1}{k} . \quad (2.6.1)$$

(see also Chapter 8)

Such an approach has advantages in the case of stationary data, but must be used with caution in other cases. In another approach, Proakis [76] proposes filtering the gradient estimate to improve convergence. In developing these results further, Glover [34] takes the noisy gradient estimate of the LMS filter and attempts to smooth this by low-pass filtering. For example,

$$\underline{f}_{j+1} = \underline{f}_j + \alpha \underline{B}_j \quad (2.6.2)$$

$$\underline{B}_j = \underline{B}_{j-1} + \gamma(e(j)\underline{x}_j - \underline{B}_{j-1})$$

so that in effect  $e(j)\underline{x}_j$  is filtered by:

$$G(z) = \frac{\gamma}{1 - (1 - \gamma)z^{-1}} \quad (2.6.3)$$

and the resulting overall update equation is

$$\underline{f}_{j+1} = \underline{f}_j + (1 - \gamma)(\underline{f}_j - \underline{f}_{j-1}) + \alpha \gamma e(j)\underline{x}_j \quad (2.6.4)$$

Glover compares the behaviour of this second order algorithm with the usual LMS and with a similar third order scheme. However, he finds that the higher order algorithms do not significantly increase convergence or reduce mean-square error. Another LMS variant is provided by the 'double updating' procedure of Ristow and Kosbahn [79]. In this method the LMS algorithm is updated as usual (in normalised form)

$$\underline{f}_{j+1} = \underline{f}_j + \frac{\underline{x}_j^t \underline{x}_j}{\underline{x}_j^t \underline{x}_j} e(j) \quad (2.5.48)$$

where  $y_j = \underline{f}_j^t \underline{x}_j$ , but then the updated filter coefficients are applied to the same data to produce

$$y_j' = \underline{f}_{j+1}^t \underline{x}_j \quad (2.6.5)$$

which is used as the final output at time  $j$ .

## 2. Perturbation Methods [118]

Recall that the LMS algorithm is based on replacing the gradient of the mean-square error in the steepest descent method by an estimate based on the instantaneous value. An alternative method of estimating the

gradient is by direct measurement through finite differences.

For a quadratic function of a scalar variable,  $x$ ,

$$f(x) \approx ax^2 + bx + c \quad (2.6.6)$$

The derivative may be obtained by taking

$$\frac{df(x)}{dx} = \frac{f(x + \delta) - f(x - \delta)}{2\delta} \quad (2.6.7)$$

and this is exact. Since the mean-square error,  $I$ , is a quadratic function, one way to estimate the derivative  $\partial I / \partial \underline{f}$  at  $\underline{f} = \underline{f}_k$  is to perturb each coefficient of the filter in turn and measure the resulting change in error power. These values may then be used to obtain the derivative as

$$\frac{\partial I}{\partial f_k(i)} = \frac{I(f_k(i) + \delta) - I(f_k(i) - \delta)}{2\delta} \quad (2.6.8)$$

$i = 1, \dots, N$

However, in perturbing the filter coefficients, the average error energy is increased by an amount [118]

$$P = \delta^2 \lambda_{av} \quad (2.6.9)$$

(assuming equal 'time' is spent at both  $I(f_k + \delta)$  and  $I(f_k - \delta)$ ) where  $\lambda_{av}$  is the average of the eigenvalues of  $R$ .

Gradients measured in this manner are inexact or noisy, because they are based on imperfect values for  $I$ . In Widrow's scheme [118] each  $I$  is based on an estimate formed from

$$I = \frac{1}{N} \sum_{j=1}^N e(j)^2. \quad (2.6.10)$$

### 3. Alternative gradient methods

The steepest descent method is perhaps the simplest approach to the iterative solution of the normal equations. However, as mentioned in section 2.4, other solutions designed to have better convergence properties have been developed and many of these have been used as adaptive filters. For example, techniques based on Newton's method premultiply the gradient estimate by an estimate of the inverse of  $R$  [119], so that

$$\underline{f}_{j+1} = \underline{f}_j + \alpha \hat{R}^{-1} \frac{\partial \hat{f}}{\partial \underline{f}} \quad (2.6.11)$$

It is clear, however, that although such approaches have improved convergence, they are considerably more complex to implement, involving substantial increases in computation. It has also been reported [32] that algorithms based on Newton's or conjugate gradient methods are very sensitive to noise.

### 4. Direct search methods

The methods discussed thus far have all been examples of iterative solutions to the normal equations based on gradient methods. As discussed in section 2.4, a second class of methods exist, these are known as direct search methods. Far fewer examples of direct search procedures have been implemented as adaptive algorithms, compared to gradient techniques. However, Widrow et al [118] have used a method dubbed linear random search which falls into this class. In a simple random search procedure a random change is made to the filter coefficients and the resulting effect on mean-square error is measured. If the change results in a lowering of the mean-square error then it is accepted, otherwise it is rejected and so on. However, as the authors point out, this method has the drawback that nothing is learned when a trial change is rejected. Instead they propose a more sophisticated approach whereby a small random change is tentatively made in the filter and the mean-square error measured. A permanent change in the filter, proportional to the product of the change in performance and the initial tentative change is then made:

$$\underline{f}_{j+1} = \underline{f}_j + \alpha [I(\underline{f}_j) - I(\underline{f}_j + \underline{v}_j)] \underline{v}_j \quad (2.6.12)$$

where  $\underline{v}_j$  is the random change with covariance  $\sigma^2$ . The authors compare the performance of this algorithm with the LMS but conclude that it is greatly inferior.

## 5. Recursive forms

The adaptive filters so far discussed have in common the fact that they were FIR filters. A number of schemes which do not fit into this category have been developed, e.g., [25, 44, 111]. For example, Feintuch [25] develops a straightforward approach using

$$y(j) = \underline{f}_j^t \underline{x}_j + \underline{g}_j^t \underline{y}_j \quad (2.6.13)$$

with  $e(j) = d(j) - y(j)$ .

The coefficients  $\underline{f}$  and  $\underline{g}$  are updated by the gradient of the mean-square error with respect to  $\underline{f}$  and  $\underline{g}$  respectively, that is,

$$\begin{aligned} \underline{f}_{j+1} &= \underline{f}_j - \alpha_1 \frac{\partial I}{\partial \underline{f}} \\ \underline{g}_{j+1} &= \underline{g}_j - \alpha_2 \frac{\partial I}{\partial \underline{g}} \end{aligned} \quad (2.6.14)$$

As in the usual LMS, correlations are replaced by instantaneous estimates, which leads to:

$$\begin{aligned} \underline{f}_{j+1} &= \underline{f}_j + \alpha_1 e(j) \underline{x}_j \\ \underline{g}_{j+1} &= \underline{g}_j + \alpha_2 e(j) \underline{x}_j \end{aligned} \quad (2.6.15)$$

The filter has the advantage that it can be easily implemented with two transversal adaptive filters using equation (2.6.13).

## 2.7 Discussion

In this chapter an approach to processing signals with properties which are unknown or time-varying, based on adaptive filtering has been considered. The techniques discussed - those based on least-squares optimisation - form only a small subset of the available approaches to adaptive filtering. A number of such methods has been considered but one particular technique (the LMS algorithm) has been seen to have the advantage of simplicity in terms of both computation and implementation. This algorithm is used extensively throughout this thesis and will be seen to have the further advantage of being very robust. It is not claimed that the LMS algorithm is superior to any of the others considered, in any particular situation, but it does have very widespread applicability.

The theory of the LMS algorithm has been considered here in detail. Of particular interest in practical situations are non-stationary inputs. Little analysis of the behaviour of the LMS algorithm for such classes of inputs has been published. In this chapter a novel description of the response to non-stationary inputs has been developed which directly illustrates the effect of the non-stationarity. It is possible to conclude from this that, generally, the robustness of the algorithm is retained for a wide range of non-stationary inputs. Limits on the rate of adaptation for 'reasonable' behaviour of the algorithm were also obtained.

More generally, it cannot be claimed that adaptive algorithms such as these, which operate locally in an empirical way, are necessarily the 'best' approach to non-stationary processing but they do have the advantage that they can be used when input properties are unknown, that is, no models are required. In many circumstances such an approach will be the only possibility.

## CHAPTER 3

### DECONVOLUTION

#### 3.1 Introduction

The aim of inverse filtering or deconvolution is to unravel the effects of a convolution of two signals (or a system and a signal) so as to restore one of the signals. For example, if a signal  $x$  is operated upon by a system with impulse response  $h$ , to produce an output  $y$ , the aim is to design and apply some operator  $f$  which will restore  $x$  (see fig. 3.1.1),

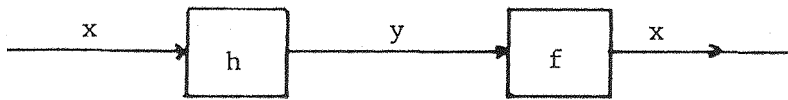


Figure 3.1.1: Deconvolution

where it is assumed throughout that the operation on  $x$  is linear and that  $h$  and  $y$  are known. The operator  $f$  is the 'inverse filter' corresponding to  $h$  and may be denoted by  $h^{-1}$ .

This discussion relates to the deconvolution problem in its barest form. More usually the measurement  $y$  is contaminated by noise and/or the system dynamics are not known exactly. In this chapter the principle techniques of deconvolution are considered in some detail. As such the chapter represents an essential base for the more sophisticated approaches to deconvolution to be discussed in the following chapter and again in Chapter 8.

A main theme of the discussion is the use of least-squares techniques as discussed in Chapter 2 for deconvolution, and the properties of such methods are carefully discussed. Other approaches to deconvolution are also considered beginning with some 'direct' or obvious methods, but more sophisticated approaches based on the cepstrum and lattice methods are also included.

An important and novel aspect of the chapter is a comparative study of the least-squares method and an alternative approach to the inversion of mixed phase signals known as homomorphic prediction.



### 3.2 Direct Methods and the Need for Approximate Solutions

The simplest approach to deconvolution is to invert the system transform. That is, for a signal  $h(n)$  with a rational  $z$  transform:

$$H(z) = \frac{\prod_{i=1}^N (1 - a_i z^{-1})}{\prod_{j=1}^M (1 - b_j z^{-1})} \quad (3.2.1)$$

the inverse is given by

$$F(z) = \frac{1}{H(z)} = \frac{\prod_{j=1}^M (1 - b_j z^{-1})}{\prod_{i=1}^N (1 - a_i z^{-1})} \quad (3.2.2)$$

Whilst this approach is simple, problems can arise if an impulse response  $f(n)$  is required. To clarify this, consider  $H(z)$  written in the form:

$$H(z) = \frac{\prod_{i=1}^k (1 - a_i z^{-1}) \prod_{i=k+1}^N (1 - a_i z^{-1})}{\prod_{j=1}^M (1 - b_j z^{-1})} \quad (3.2.3)$$

where the poles  $b_j$  are such that  $|b_j| < 1$ ;  $j = 1, \dots, M$   
 and the zeros  $a_i$  are ordered such that  $|a_i| < 1$ ;  $i = 1, \dots, k$   
 $|a_i| > 1$ ;  $i = k + 1, \dots, N$

then the inverse transfer function has zeros  $z = b_j$ ;  $j = 1, \dots, M$   
 and poles at  $z = a_i$ ;  $i = 1, \dots, N$  and will only have a stable, causal representation if all the poles are inside the unit circle, that is, if  $H(z)$  is minimum phase. Conversely,  $F(z)$  will have a stable, purely acausal representation in the time domain if all the zeros of  $H(z)$  are outside the unit circle ( $k = 0$ ), that is, if  $H(z)$  is maximum phase. In general,  $H(z)$  will have zeros both inside and outside the unit circle (mixed phase) and  $F(z)$  will only have a stable, two-sided representation.

Further problems arise when the inverse is constructed using finite length discrete Fourier transforms. In general, the sequence  $h^*(n)$  whose

Fourier transform is  $1/H(k)$  is not equal to  $h^{-1}(n)$ . This fact is illustrated by, for example, Oppenheim and Schaffer [65] but is basically a form of aliasing due to the higher terms in the infinite series which usually occurs when a transform is inverted.

It follows from the foregoing that if the inverse filter is constrained for practical reasons to be finite and/or causal, then it will in general only be possible to construct an approximate inverse. Most deconvolution techniques are aimed at constructing such approximate inverses and several methods are considered in the following sections.

### 3.3 Least-squares Deconvolution

#### 3.3.1 Zero delay least-squares deconvolution

In this section a method for approximate deconvolution using least-squares techniques is discussed. Least-squares inverse filters are designed using the approach described in Chapter 2. Given some signal  $h(n)$  - where for simplicity  $h(n)$  is constrained to be causal - the aim is to design a filter  $f(n)$  such that the output  $\hat{\delta}(n)$  is the best least-squares approximation to a delta function (see fig. 3.3.1).

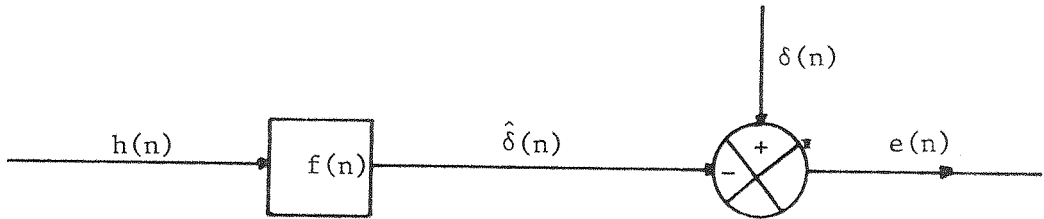


Figure 3.3.1: Approximate Deconvolution

Mathematically this may be expressed as

$$\text{minimise } I = \sum_{n=-\infty}^{\infty} e^2(n) = \sum_{n=-\infty}^{\infty} (\delta(n) - \hat{\delta}(n))^2 \quad (3.3.1)$$

That is, the problem is identical to that described in Section 2, of Chapter 2, but with the desired output equal to a delta function. Accordingly, from that section, the solution is given by the normal equations

$$R\underline{f} = \underline{g} \quad (2.2.3)$$

or

$$\sum_k R(m-k)f(k) = g(m) \quad (2.2.3a)$$

where in this instance

$$g(m) = \sum_{n=-\infty}^{\infty} h(n)\delta(n+m) \quad (3.3.2)$$

is the cross-correlation between the input sequence and the desired output, which for causal  $h(n)$  is

$$\begin{aligned} g(m) &= 0 & m > 0 \\ &= h(-m) & m \leq 0 \end{aligned} \quad (3.3.3)$$

and

$$R(m) = \sum_{n=-\infty}^{\infty} h(n)h(n+m) \quad (3.3.4)$$

Referring to section 2.2, it should be noted that the autocorrelation rather than the autocovariance form has been used here.

For the deconvolution, three separate cases are considered:

(a) Infinite unconstrained filter

If the inverse filter  $f(n)$  is not constrained to be causal the solution may be obtained simply by z-transforming the normal equations (2.2.3a).

Recognizing that the left hand side of these equations represents the convolution of the filter with the input autocorrelation, then

$$R_{hh}(z)F(z) = H\left(\frac{1}{z}\right) \quad (2.2.3b)$$

and hence

$$F(z) = \frac{H(1/z)}{R_{hh}(z)} \quad (3.3.5)$$

However, z-transforming (3.3.4) gives

$$R_{hh}(z) = H(z)H\left(\frac{1}{z}\right) \quad (3.3.6)$$

so that

$$F(z) = \frac{1}{H(z)} \quad (3.3.7)$$

Hence the infinite unconstrained least-squares filter is equal to the ideal inverse.

(b) Infinite causal filter

If the inverse filter  $f(n)$  is constrained to be causal, the normal equations (2.2.3a) become

$$\sum_{k=0}^{\infty} R_{hh}(m-k)f(k) = h(0) \quad m = 0$$

$$= 0 \quad m > 0$$

The solution can be obtained e.g., [69] as:

$$F(z) = \frac{C}{H_{eq_{min}}(z)} \quad (\text{see Appendix V}) \quad (V.14)$$

where  $C$  is a constant and where  $H_{eq_{min}}(z)$  is the equivalent minimum phase version of  $H(z)$  which for  $H(z)$  in the form of equation (3.2.3) is given by

$$H_{eq_{min}}(z) = \frac{\prod_{i=1}^k (1 - a_i z^{-1}) \prod_{i=k+1}^N (1 - a_i z)}{\prod_{j=1}^M (1 - b_j z^{-1})} \quad (V.8)$$

so that  $H_{eq_{min}}(z)$  has all its poles and zeroes within the unit circle.

From equations (V.14) and (V.8)

$$F(z) = \frac{C \prod_{j=1}^M (1 - b_j z^{-1})}{\prod_{i=1}^k (1 - a_i z^{-1}) \prod_{i=k+1}^N (1 - a_i z)} \quad (3.3.8)$$

It follows that the inverse filter  $F(z)$  is minimum phase irrespective of the input and this is an important property of least-squares inverse filters.

The filter output  $Y(z)$  is given by:

$$Y(z) = F(z)H(z) \quad (3.3.9)$$

$$\begin{aligned}
&= \frac{C \prod_{j=1}^M (1 - b_j z^{-1}) \prod_{i=1}^k (1 - a_i z^{-1}) \prod_{i=k+1}^N (1 - a_i z^{-1})}{\prod_{j=1}^M (1 - b_j z^{-1}) \prod_{i=1}^k (1 - a_i z^{-1}) \prod_{i=k+1}^N (1 - a_i z)} \\
&= \frac{C \prod_{i=k+1}^N (1 - a_i z^{-1})}{\prod_{i=k+1}^N (1 - a_i z)}
\end{aligned}$$

which is all-pass. Hence the infinite causal least-squares inverse is only equivalent to the ideal inverse if  $k = N$ , that is, if  $h(n)$  is minimum phase.

### (c) Finite causal filter

If, in addition to causality, the inverse filter is also constrained to be finite in length, then the normal equations (2.2.3) become a set of  $L$  linear equations with

$$R = \begin{bmatrix} r_0 & r_1 & \dots & r_{L-1} \\ r_1 & r_0 & r_1 & \cdot \\ \cdot & r_1 & \cdot & \cdot \\ \cdot & \cdot & \cdot & r_1 \\ r_{L-1} & \cdot & r_1 & r_0 \end{bmatrix}$$

where  $R(i)$  is denoted  $r_i$  for brevity.

$R$  is a positive semi-definite Toeplitz matrix,  $\underline{g}$  is given by

$$\underline{g} = [h(0), 0, \dots, 0]^t$$

and

$$\underline{f} = [f(0), f(1), \dots, f(L-1)]^t$$

As discussed in Chapter 2, this set may be solved by the highly efficient Wiener-Levinson algorithm which exploits the Toeplitz structure of the coefficient matrix  $R$  (see Appendix I). Further, the simplified form of the cross-correlation vector,  $\underline{g}$ , can also be utilised to give

still greater computational efficiency using a modification of the Wiener-Levinson algorithm due to Durbin [24].

It can be shown [89], that the finite filter  $\underline{f}$  will also have a minimum phase structure - irrespective of the phase properties of the input. Consequently, as for the infinite case, the filter performs best when the input sequence  $x(n)$  has the minimum phase lag of all sequences possessing the same amplitude spectrum. When the input is a non-minimum phase sequence, the resulting output is approximately 'all pass'.

### 3.3.2 Least-squares deconvolution with delay

As already seen, constraining the inverse filter to be causal will usually produce considerable errors. However, the quality of the inversion may be radically improved if the inverse operator is delayed. To illustrate this, consider the simple example of a sequence

$$h(n) = (1, a); \quad |a| > 1.$$

Now 
$$H(z) = 1 + az^{-1}.$$

The inverse  $F(z)$  is stable only in reverse time, as

$$F(z) = \frac{1}{H(z)} = \frac{1}{a} z - \frac{1}{a^2} z^2 + \frac{1}{a^3} z^3 - \dots \quad (3.3.11)$$

However, if  $f(n)$  is delayed by  $k$ , say, then

$$z^{-k} F(z) = \frac{1}{a} z^{-k+1} - \frac{1}{a^2} z^{-k+2} + \dots + (-1)^{k+1} \frac{1}{a^k} + (-1)^k \frac{1}{a^{k+1}} z + \dots \quad (3.3.12)$$

truncating the acausal component to form  $\hat{F}(z)$ , say, gives:

$$\hat{F}(z) = \frac{1}{a} z^{-k+1} - \frac{1}{a^2} z^{-k+2} + \dots + (-1)^{k+1} \frac{1}{a^k} \quad (3.3.13)$$

The application of this operator for  $H(z)$  produces an output which is an approximation to a delta function at  $n = k$ . By making  $k$  sufficiently large, that is by delaying the inverse operator sufficiently, the ideal inverse can be approximated arbitrarily closely.

Whilst the incorporation of a delay may improve the quality of an inversion, it is clear that if, in addition to causality, the inverse operator is limited in length and/or the delay  $k$  is finite then the inversion will still be approximate. Furthermore, the design method employed in the example of the previous section (simply truncating the shifted ideal inverse operator) was somewhat arbitrary. It is, however, possible to design an inverse operator which incorporates a delay using the least-squares method. This modified least-squares design problem may be specified as follows: Given an impulse response  $h(n)$  the aim is to design a filter  $f(n)$  such that the output  $\hat{\delta}(n)$  is the best least-squares approximation to a spike delayed by  $k$  units (see fig. 3.3.2).

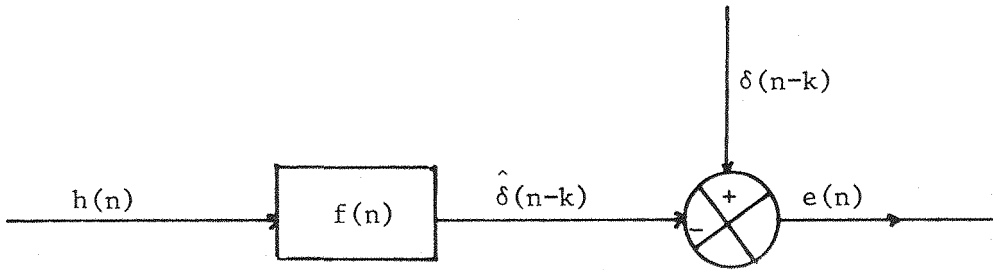


Figure 3.3.2: Approximate Deconvolution with Delay

Mathematically this may be expressed as:

$$\text{minimise } I_k = \sum_n (\delta(n-k) - f_k(n) * h(n))^2 \quad (3.3.14)$$

where  $f_k$  refers to the filter associated with delay  $k$ .

Minimising  $I_k$  gives the normal equations (2.2.3) as usual, but where  $\underline{g}$  is now defined by:

$$g(m) = \sum_{n=-\infty}^{\infty} h(n) \delta(n-k+m) \quad m \geq 0 \quad (3.3.15)$$

For the infinite causal filter it can be shown (see Appendix VI) that

$$F_k(z) = \frac{h_{ap}(0)z^{-k} + h_{ap}(1)z^{-k+1} + \dots + h_{ap}(k)}{H_{eq_{min}}(z)} \quad (VI.21)$$

where

$$H_{ap}(z) = \frac{\prod_{i=k+1}^N (1 - a_i z^{-1})}{\prod_{i=k+1}^N (1 - a_i z)} \quad (3.3.16)$$

is all-pass.

From this it is straightforward to obtain two results which have previously been obtained somewhat differently by Ford [28], namely:

(i) the infinite causal least-squares filter perfectly spikes  $H(z)$  if the output is sufficiently delayed; and

(ii) the performance (defined mathematically in section 3.3.3) is a monotonically non-decreasing function of  $k$  (see Appendix VI).

### Finite Causal Filter

If the causal least-squares filter with delay  $k$  is constrained to be finite, the normal equations (2.2.3) become:

$$Rf_{-k} = [h(k), h(k-1), \dots, h(0), 0, \dots, 0]^t$$

The results of the previous section for the causal infinite filter are not generally applicable for the finite least-squares filter. In particular, the filter performance is not usually a monotonic function of delay. It follows, therefore, that without some *a priori* knowledge of the delay required to produce a desired accuracy the above formulation is not of much value in itself. Fortunately, this is not a serious practical problem, since Simpson [90] has produced a highly efficient algorithm known as the 'Simpson sideways recursion'. Starting from the zero delay solution obtained from the Levinson recursion, the algorithm computes the filters for delays  $k = 1, \dots$ , sequentially (see Appendix VII). Further, it is possible to monitor the performance (defined in section 3.3.3) at each step in the recursion and halt the process when this falls below some pre-determined level. Alternatively, the recursion may be performed over



some pre-set interval and the minimum error selected *a posteriori*.

### 3.3.3 Error energy in least-squares deconvolution

The error energy for the infinite unconstrained least-squares filter is trivially zero since the filter is equal to the ideal inverse. For other cases, the expressions for the error energy for the general least-squares filter derived in Chapter 2 can be modified for the special case of inversion [20]. The expression for the minimum error energy:

$$I_{\min} = R_{dd}(0) - \underline{f}^t \underline{g} \quad (2.2.9a)$$

becomes 
$$I_{\min} = 1 - \underline{f}^t \underline{g}. \quad (3.3.17)$$

For the causal filter with delay  $k$ ,  $\underline{g}$  is given by

$$\underline{g} = [h(k), h(k-1), \dots, h(0), 0, 0, \dots]$$

so that

$$\underline{f}^t \underline{g} = \sum_{i=0}^k f(i)h(k-i) = x_k(k) \quad (3.3.18)$$

where  $x_i(j)$  is the  $j$ 'th output of the filter for delay  $i$ . Hence

$$I_{\min}^{(k)} = 1 - x_k(k). \quad (3.3.19)$$

This expression is valid for both finite and infinite filters. However, for the infinite filter it can also be shown (see Appendix VI) that the output is given by

$$X_k(z) = \left( \sum_{i=0}^k h_{ap}(i) z^{-k+i} \right) H_{AP}(z) \quad (VI.24)$$

from which

$$x_k(k) = \text{coefficient of } z^{-k} \text{ in } \left( \sum_{i=0}^k h_{ap}(i) z^{-k+i} \right) \left( \sum_{j=0}^{\infty} h_{ap}(j) z^{-j} \right) \quad (3.3.20)$$

which gives:

$$x_k(k) = \sum_{i=0}^k h_{ap}^2(i) \quad (3.3.21)$$

and hence from (3.3.19)

$$I_{\min}^{(k)} = 1 - \sum_{i=0}^k h_{ap}^2(i) \quad (3.3.22)$$

In the zero delay case the error energy is given by

$$I_{\min} = 1 - h_{ap}^2(0) \quad (3.3.23)$$

#### Bounds on the error energy

The error energy  $I_{\min}$  for both zero delay and generalised inverse filtering is bounded by

$$0 \leq I_{\min} \leq 1. \quad (3.3.24)$$

This is trivially true since

- (i)  $I_{\min}$  is a squared quantity ( $I_{\min} \geq 0$ ).
- (ii)  $I_{\min} = 1$  if  $\underline{f} \equiv 0$ . Hence, any non-zero  $\underline{f}$  must produce  $I_{\min} \leq 1$  or the error energy would not be minimum.

#### Performance

A natural definition of performance (after Treitel and Robinson [100]) is:

$$P = 1 - I_{\min} \quad \text{for inversion} \quad (3.3.25)$$

so that  $0 \leq P \leq 1$ .

#### Frequency domain interpretation

A discription of the error energy for least-squares inversion may be obtained which provides a qualitative interpretation of the algorithm's performance in the frequency domain. From the previous, the error energy for zero delay inversion is

$$I = \sum_{n=-\infty}^{\infty} e^2(n) = \sum_{n=-\infty}^{\infty} \left( \delta(n) - \sum_{k=0}^{L-1} f(k)h(n-k) \right)^2 \quad (3.3.26)$$

Using Parseval's formula:

$$I = \frac{1}{2\pi} \int_{-\pi}^{\pi} (1 - F(e^{i\omega})H(e^{i\omega}))^2 d\omega \quad (3.3.27)$$

Let 
$$F(e^{i\omega}) = \frac{1}{\hat{H}(e^{i\omega})} \quad (3.3.28)$$

and let 
$$P(\omega) = |H(e^{i\omega})|^2 \quad (3.3.29)$$

and 
$$\hat{P}(\omega) = |\hat{H}(e^{i\omega})|^2. \quad (3.3.30)$$

Now

$$I = \frac{1}{2\pi} \int_{-\pi}^{\pi} \left( 1 - \frac{H(e^{i\omega})}{\hat{H}(e^{i\omega})} \right)^2 d\omega \quad (3.3.31)$$

$$= \frac{1}{2\pi} \int_{-\pi}^{\pi} \frac{|E_R(e^{i\omega})|^2}{|\hat{H}(e^{i\omega})|^2} d\omega \quad (3.3.32)$$

where  $E_R(e^{i\omega}) = \hat{H}(e^{i\omega}) - H(e^{i\omega}), \quad (3.3.33)$

so that

$$I = \frac{1}{2\pi} \int_{-\pi}^{\pi} \frac{|E_R(e^{i\omega})|^2}{\hat{P}(e^{i\omega})} d\omega. \quad (3.3.34)$$

From this expression a qualitative interpretation of the minimisation of  $I$  may be given after Makhoul [53] who distinguishes two properties:

(a) Global

Since  $I$  is a ratio of spectra, there is no inherent bias against areas in the spectrum which have low energy. In other words, the error  $E_R(e^{i\omega})$  will tend to diminish with the energy in the signal  $H(e^{i\omega})$ .

(b) Local

A given value for  $E_R(e^{i\omega})$  will produce a greater contribution to the error energy when  $\hat{H}(e^{i\omega}) < H(e^{i\omega})$  than vice versa. That is,  $\hat{H}(e^{i\omega})$  should be a good estimate of the 'spectral envelope' of  $H(e^{i\omega})$ . For the inverse filter this implies that peaks in the spectrum will be flattened more effectively than dips.

Also for the optimum filter from equation (3.3.17)

$$I_{\min} = 1 - \underline{f}^t \underline{g} = 1 - \underline{f}^t R \underline{f} \quad (3.3.35)$$

$$I_{\min} = \frac{1}{2\pi} \int_{-\pi}^{\pi} \left( 1 - |F(e^{i\omega})|^2 |H(e^{i\omega})|^2 \right) d\omega \quad (3.3.36)$$

Hence

$$I_{\min} = 1 - \frac{1}{2\pi} \int_{-\pi}^{\pi} \frac{P(\omega)}{\hat{P}(\omega)} d\omega \quad (3.3.37)$$

Now, for a given  $h(n)$ ,

$$\frac{1}{2\pi} \int_{-\pi}^{\pi} \frac{P(\omega)}{\hat{P}(\omega)} d\omega = K, \text{ say} \quad (3.3.38)$$

As pointed out by Makhoul, one major disadvantage of the least-squares approach which is made clear by the above expression is error cancellation. That is, a contribution to the integral at a particular frequency such that

$$\frac{P(\omega_1)}{\hat{P}(\omega_1)} > K$$

may be effectively cancelled by another contribution

$$\frac{P(\omega_2)}{\hat{P}(\omega_2)} < K.$$

This fact will be illustrated in a later section by comparison with an alternative method.

### 3.3.4 Noise reduction approaches

#### Inversion in the presence of noise

Thus far only the inversion of signals which can be measured exactly has been considered. In practice a signal will often not be available exactly, that is, the measurement will usually be corrupted by noise. For example, consider the system depicted in fig. 3.3.3, where  $f$  is the desired inverse filter;  $h$  is a known system and  $u$  is a random noise.

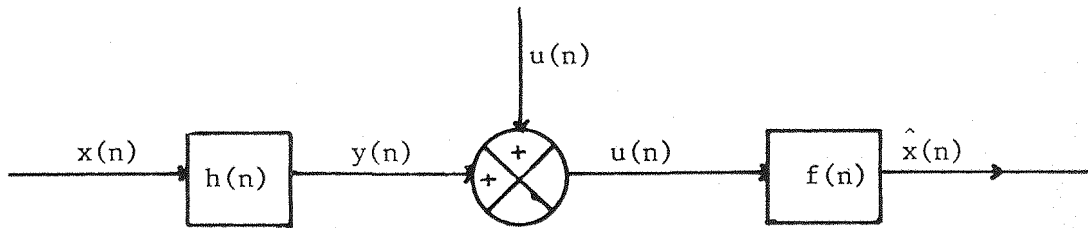


Figure 3.3.3: Deconvolution of Noisy Data

Even if  $f$  is an ideal inverse ( $f = h^{-1}$ ) the input  $x$  is not recovered exactly. Furthermore, in areas of the spectrum where the system,  $h$ , has a low response (for example at high frequencies) the noise,  $u$ , is likely to be significantly enhanced by the amplifying effect of the inverse filter.

A number of authors have considered the problem of noise reduction in deconvolution and in the remainder of this section an outline of the two main techniques is given.

#### Prewhitening

Prewhitening, or ridge regression as it is sometimes known, is the term used to describe the practice of adding a small positive quantity to each element of the leading diagonal of the autocorrelation matrix (that is the zero'th lag of the autocorrelation) in the normal equations. That is the normal equations

$$\underline{R}\underline{f} = \underline{g} \quad (2.2.3)$$

are replaced by

$$(R + \sigma^2 I) \underline{f} = \underline{g} \quad (3.3.39)$$

where  $\sigma^2 = \text{constant}$ .

The term prewhitening arises from the fact that adding some number to the zero'th lag of the autocorrelation is equivalent to raising the level of the spectrum by a constant amount, which is equivalent to adding white noise to the input. However, this whitening of the spectrum is purely hypothetical as far as the input time series  $h(n)$  is concerned, since  $\sigma^2$  is added only to the correlation, and then only for the purposes of computing the inverse operator. In the inversion the raising of the input spectral level causes a corresponding decrease in the level of amplification in the inverse operator.

From a numerical point of view, prewhitening can be seen as a means of improving the stability of the solution. The determination of the filter becomes unstable when the system of normal equations becomes ill-conditioned (when the autocorrelation matrix is almost singular). A number of measures of the condition of a system have been defined amongst which is the idea of condition numbers,  $Q$ ,

$$Q = \frac{|\lambda_{\max}|}{|\lambda_{\min}|} \quad (3.3.40)$$

where  $\lambda_{\max}$  and  $\lambda_{\min}$  denote the maximum and minimum eigenvalues respectively of the coefficient matrix of the system. The larger the value of  $Q$  the worse the condition of the system and, in the limit, if  $\lambda_{\min} = 0$  the matrix is singular. This definition of condition has been used by Treitel and Wang [102] to investigate the effect of prewhitening on the normal equations. Since the autocorrelation matrix is symmetric and positive semidefinite, its eigenvalues are all real and positive (or zero), so that

$$Q = \frac{\lambda_{\max}}{\lambda_{\min}} \quad (3.3.41)$$

These authors used several numerical examples to show that prewhitening generally improves the condition of the system. In fact, it is easy to show that if the matrix  $R$  has eigenvalues  $\lambda_i$  and eigenvectors  $\underline{x}_i$  then the matrix  $R' = (R + \sigma^2 I)$  has eigenvalues  $(\lambda_i + \sigma^2)$  and eigenvectors  $\underline{x}_i$ . Hence the condition number for  $R'$  is

$$Q' = \frac{\lambda_{\max} + \sigma^2}{\lambda_{\min} + \sigma^2} \quad (3.3.42)$$

and  $Q' \leq Q \forall \sigma^2$ ,  $\lambda_{\min}$ ,  $\lambda_{\max}$  with equality holding if, and only if,  $\lambda_{\max} = \lambda_{\min}$ , that is, if the input is white.

The level of prewhitening applied to a system, that is, the value of  $\sigma^2$  is usually given as a percentage of the zero lag autocorrelation coefficient. If  $\sigma^2$  is the prewhitening applied to the system, then

$$PPW = \frac{100 \sigma^2}{r_0} \quad (3.3.43)$$

is the percentage pre-whitening (PPW). Different authors suggest differing levels of prewhitening, for instance, Douze [21] uses 10%, whereas Treitel and Wang [102] adopt 0.1% to 1%.

The main advantages of prewhitening are its simplicity and the fact that well-conditioned systems are insensitive to its application. This latter fact has led to suggestions [102] that its use be adopted as standard for all systems.

#### Noise reduction by shaping

Another approach to the reduction of noise in inverse filtering is to relax the output spike requirement to a more general desired function. This idea has been used by Senmoto and Childers [85], who obtained a 'generalised' inverse (by Fourier methods) of the form

$$F(\omega) = \left[ \frac{D(\omega)}{H(\omega)} \right] \quad (3.3.44)$$

where  $D(\omega)$  is the desired output pulse.

Senmoto and Childers used a Gaussian pulse for  $d(k)$ , but suggested that any function which limits to a spike may be suitable. The width of the pulse generally controls the filter resolution and the output SNR. Narrowing the pulse improves the resolution of the filter but decreases the output SNR since the bandwidth of the inverse filter is increased. Such shaping filters can of course be produced using least-squares methods (see Chapter 2). Note also that the generalised (delayed) formulation may be applied to the shaping filter [20], the optimum delay occurring when the energy distribution of the delayed output is matched with that of the input [81].

### 3.3.5 Examples

In this section the application of the techniques of the previous sections is demonstrated using a few examples. The signals chosen were:

- (i) A minimum phase system with a single pole and a zero;
- (ii) a non-minimum phase system with a single pole and a zero;
- (iii) a half sine wave pulse.

The first two examples were chosen to illustrate the basic properties of least-squares inversion, and the effect of delay. The third is an example of a system which is difficult to invert and illustrates the stabilising effect of prewhitening. In each case the operators were restricted to 256 points in length, though this is purely arbitrary since there is no reason why operators should not be of any desired length (subject only to computational restrictions).

#### (i) Minimum phase system

The impulse response corresponding to a system with a single pole at  $|z_p| = 0.95$ ,  $\arg(z_p) = 0.3$  rads and a single zero at  $|z_p| = 0.95$ ,  $\arg(z_p) = 0.9$  rads is shown in fig. 3.3.4a; the corresponding modulus frequency response is shown in fig. 3.3.4b. The system was inverted using least-squares methods, the modulus of the inverse operator is shown in fig. 3.3.4d. The corresponding approximation to delta is shown in fig. 3.3.4c. As is clear from the diagram, the result is close to the ideal inverse. Also, due to the minimum phase nature of the system there is no need to introduce delay into the inversion.



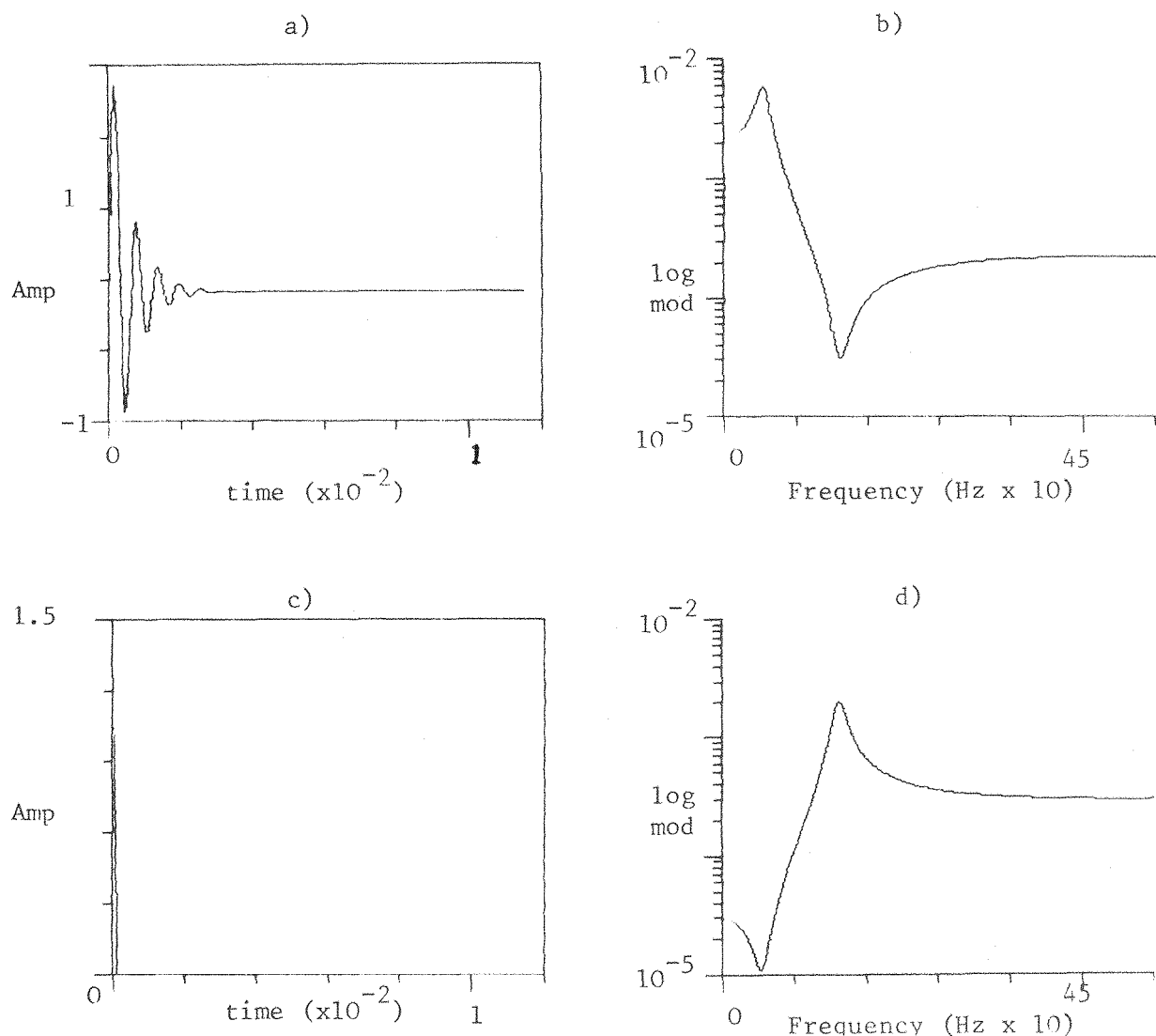


Figure 3.3.4: Inversion of a Minimum Phase System

#### (ii) Maximum phase system

A similar impulse response was generated from a system with a single pole again at  $|z_p| = 0.95$ ,  $\arg(z_p) = 0.3$  rads, but with the zero reflected outside the unit circle at  $|z_o| = 1.05$ ,  $\arg(z_o) = 0.9$  rads. The system has an identical modulus frequency response to that of the previous system (fig. 3.3.4b). The zero delay least-squares inverse also has an identical modulus response to the previous version (fig. 3.3.4d) but the convolution of the inverse and the impulse response leads to a rather different result (compare fig. 3.3.4c and fig. 3.3.5a). In this instance the inversion has failed to produce a single spike due to the maximum phase nature of the input, but has instead left a residual all-pass component. Fig. 3.3.5b shows the effect of the inversion when performed with the optimum delay and clearly very considerable improvements have been achieved. The curve of performance versus delay is shown in fig. 3.3.6.

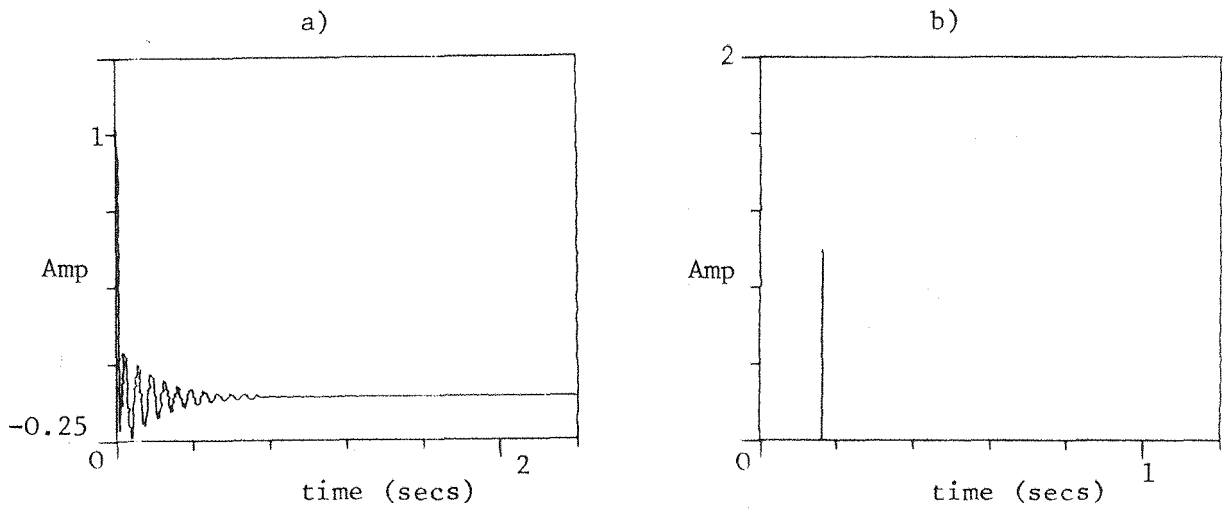


Figure 3.3.5: Inversion of Maximum Phase System

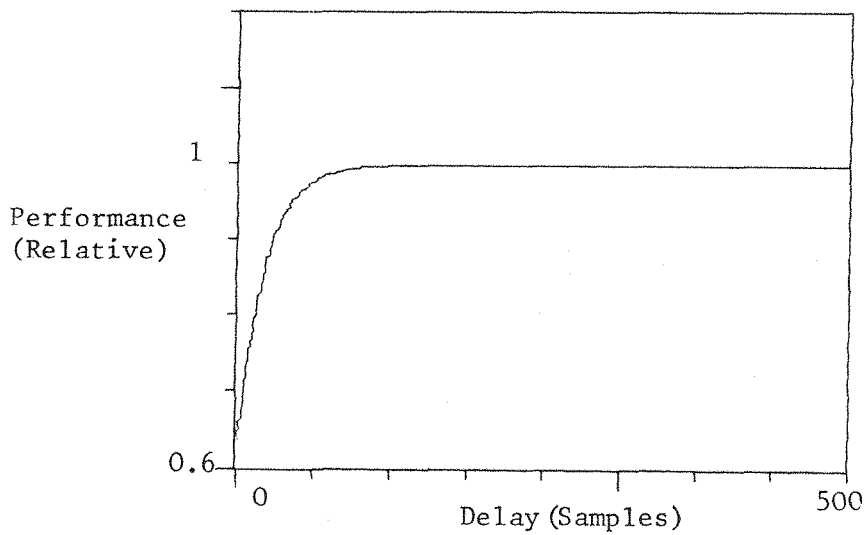


Figure 3.3.6: Performance curve for Maximum Phase Inversion

(iii) Half sine wave

In contrast to the previous signal the half sine wave of fig. 3.3.7a is an example of an impulse response which is difficult to invert due to the presence of sharp zeros in the response. Indeed, without prewhitening

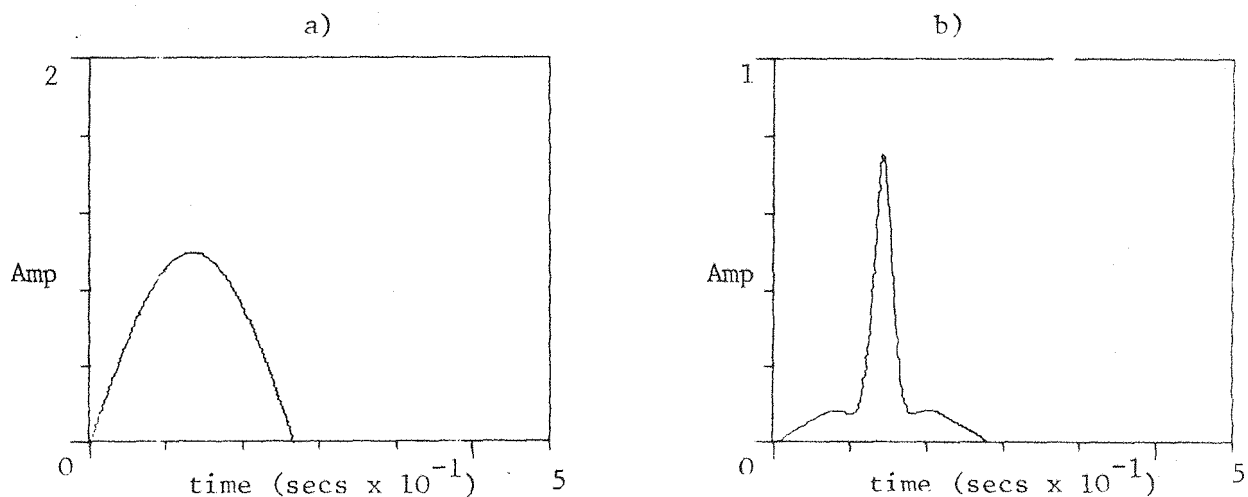


Figure 3.3.7: Inversion of Half Sine Pulse

no results were obtained due to instability in the algorithm (with or without delay). The addition of 1% prewhitening stabilises the algorithm sufficiently to allow the inversion to proceed. The resulting approximation to delta is shown in fig. 3.3.7b. Although the result is clearly imperfect some compression of the half sine wave has occurred so that the inversion is not completely unsuccessful. The curve of performance versus delay is shown in fig. 3.3.8.

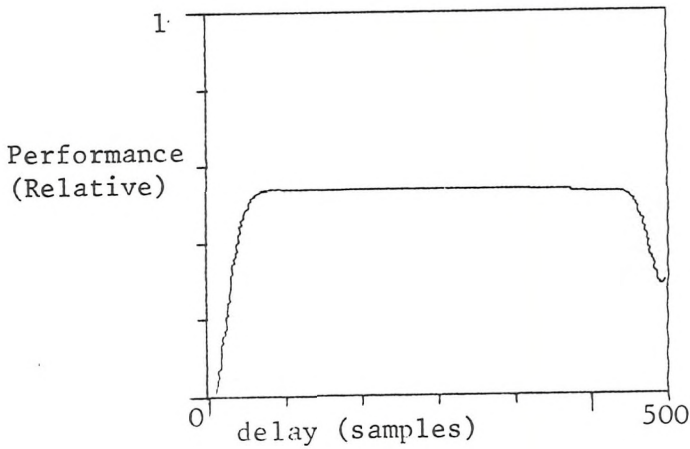


Figure 3.3.8: Performance Curve for Half-sine Inversion

### 3.4 Alternative Methods for Deconvolution

#### 3.4.1 Lattice forms

Lattice forms have been developed for the problem of linear prediction with all-pole (autoregressive) models. Such a predictor has the form:

$$\hat{h}(n) = -a_1 h(n-1) - a_2 h(n-2) - \dots - a_N h(n-N) \quad (3.4.1)$$

The prediction error  $e$  is given by

$$e(n) = h(n) - \hat{h}(n) = h(n) + a_1 h(n-1) + \dots + a_N h(n-N) \quad (3.4.2)$$

Now, it can be shown [70] that the least-squares deconvolution filter for the signal  $h$  of length  $L$  is given by  $(1, a_1, a_2, \dots, a_{L-1})$  and is thus identical to the prediction error filter of equation (3.4.2). It is this fact which makes the lattice of use in deconvolution.

The basic lattice is a network as depicted in fig. 3.4.1 [40].

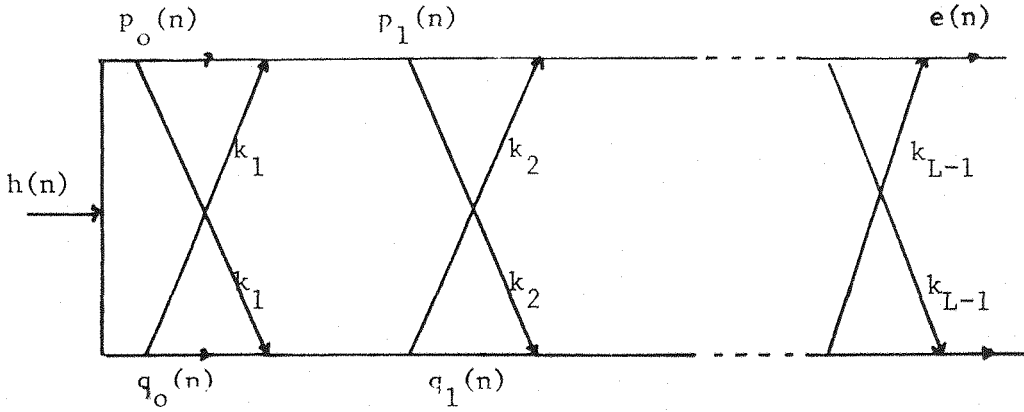


Figure 3.4.1: Lattice Structure for Linear Prediction

From this it can be seen that

$$\begin{aligned}
 p_0(n) &= q_0(n) = h(n) \\
 p_m(n) &= p_{m-1}(n) + k_m q_{m-1}(n-1) \\
 q_m(n) &= k_m p_{m-1}(n) + q_{m-1}(n-1)
 \end{aligned} \tag{3.4.3}$$

z-transforming equations (3.4.3) gives

$$\begin{aligned}
 P_0(z) &= Q_0(z) = H(z) \\
 P_m(z) &= P_{m-1}(z) + k_m z^{-1} Q_{m-1}(z) \\
 Q_m(z) &= k_m P_{m-1}(z) + z^{-1} Q_{m-1}(z)
 \end{aligned} \tag{3.4.4}$$

Now, if  $A_m(z)$  is defined as

$$A_m(z) = \frac{P_m(z)}{H(z)} \tag{3.4.5}$$

and  $B_m$  is defined as

$$B_m(z) = \frac{Q_m(z)}{H(z)} \tag{3.4.6}$$

then from (3.4.4)

$$\begin{aligned}
 A_0(z) &= B_0(z) = 1 \\
 A_m(z) &= A_{m-1}(z) + k_m z^{-1} B_{m-1}(z) \\
 B_m(z) &= k_m A_{m-1}(z) + z^{-1} B_{m-1}(z)
 \end{aligned} \tag{3.4.7}$$

Now

$$P_m(z) = H(z)A_m(z) \quad (3.4.8)$$

From (3.4.6)  $a_m(0) \equiv 1$

so that

$$p_m(n) = h(n) + a_m(1)h(n-1) + \dots + \dots a_m(m)h(n-m) \quad (3.4.9)$$

Now the  $q_i(j)$ 's can be regarded as predictor coefficients so that

$$p_m(n) = h(n) - \left( - \sum_{i=1}^m a_m(i)h(n-i) \right)$$

is the prediction error.

The properties of the prediction coefficients are determined by the  $k_i$ 's (also known as reflection coefficients for reasons which are made clear in Appendix XIV). These reflection coefficients are computed to minimise the mean-squared value of the prediction error  $p_m(n)$  at each stage. It can be shown [54] that the optimal value of  $k_i$  is given by

$$k_i^* = \frac{E\{p_{m-1}(n)q_{m-1}(n-1)\}}{\sqrt{E\{p_{m-1}^2(n)\} E\{q_{m-1}^2(n)\}}} \quad (3.4.10)$$

The essential properties of the lattice in comparison with conventional deconvolution are that the lattice gives guaranteed stability (for  $|k_i| < 1$ ), is less prone to round-off errors [56] and avoids any necessity to window the signal. Against that, the lattice does not minimise any global error criterion, that is, it is a stage-by-stage minimisation. If the input is truly stationary then the results will be identical for both forms, but if as usual this is not the case, the lattice gives suboptimal solutions [54]. It is also worth noting that lattice forms generally engender an increased computational liability over conventional deconvolution.

### 3.4.2 Homomorphic deconvolution

Methods of deconvolution have been developed which are based on the use of the complex cepstrum [65]. In particular a method of deconvolution of mixed phase signals using the cepstrum, dubbed homomorphic prediction has been proposed by Oppenheim et al [66]. The method will be discussed in some detail as the intention is to compare and contrast the properties of this method with those of least-squares. As a preliminary, some discussion of the properties of the cepstrum will be necessary.

#### Homomorphic signal analysis [65]

Let  $h(n)$  be a causal mixed phase signal of finite duration with  $z$  transform  $H(z)$ . Now, the transform can be factorised as

$$(a) \quad H(z) = H_{\min}(z)H_{\max}(z) \quad (3.4.11)$$

where  $H_{\min}(z)$  denotes the minimum phase part of  $H(z)$  whose zeros (and poles) lie within  $|z| = 1$ , and  $H_{\max}(z)$  denotes the maximum phase part of  $H(z)$ , whose zeros lie outside  $|z| = 1$  or

$$(b) \quad \text{as } H(z) = H_{\text{eq}}(z)H_{\text{ap}}(z) \quad (3.4.12)$$

where  $H_{\text{eq}}(z)$  is a minimum phase transform such that  $|H_{\text{eq}}(z)| = |H(z)|$  and contains the zeros of the minimum phase component of  $H(z)$  and the reflection of the zeros of the maximum phase component about the unit circle.  $H_{\text{ap}}(z)$  is an all-pass function. Now the complex cepstrum is defined as the (inverse)  $z$ -transform of the complex logarithm of the  $z$  transform of the original signal.

Now from (a)

$$h(n) = h_{\min}(n) * h_{\max}(n) \quad (3.4.13)$$

and so the complex cepstrum is

$$\hat{h}(n) = \hat{h}_{\min}(n) + \hat{h}_{\max}(n) \quad (3.4.14)$$

Retaining the cepstral components for positive/negative values of  $n$ , the minimum/maximum phase components are obtained. From (b) the sequence  $h(n)$  may be written

$$h(n) = h_{eq}(n) * h_{ap}(n) \quad (3.4.15)$$

and taking the complex cepstrum yields

$$\hat{h}(n) = \hat{h}_{eq}(n) + \hat{h}_{ap}(n) \quad (3.4.16)$$

$\hat{h}_{ap}(n)$ , being the cepstrum of an all-pass sequence, has antisymmetric positive and negative components. Hence, adding the cepstral component for negative  $n$  to that for positive  $n$  yields  $h_{eq}(n)$ .

#### Homomorphic prediction

The cepstral technique described above can be used to invert a mixed phase sequence. This procedure, known as Homomorphic Prediction [66], may be summarised as follows: firstly the sequence  $h(n)$  is separated into  $h_{min}(n)$  and  $h_{max}(n)$  using the method described above. Each of the two components is then inverted separately using standard Fourier or least-squares techniques. As discussed previously,  $h_{min}(n)$  has a stable causal inverse whilst  $h_{max}(n)$  has a stable purely acausal inverse. A single composite mixed phase inverse may then be constructed as

$$h^{-1}(n) = h_{max}^{-1}(n) * h_{min}^{-1}(n) \quad (3.4.17)$$

and this may be rendered causal by the introduction of an appropriate delay.

#### Exponential weighting [65]

The presence of zeros on or close to the unit circle in the transfer function leads to inaccuracy in the cepstral separation of  $h_{min}(n)$  and  $h_{max}(n)$ , (indeed the operation may even fail completely). In such cases, exponential weighting of  $h(n)$  is essential. This can be illustrated as follows. Let



$$H(z) = H_{\min}(z) \cdot H_2(z) \cdot H_3(z) \quad (3.4.18)$$

where  $H_2(z) \cdot H_3(z) = H_{\max}(z)$ .

$H_3(z)$  has zeroes outside a radius  $|z| = 1 + \delta$  ( $\delta > 0$ ) and  $H_2(z)$  has zeroes within the annulus  $1 < |z| < 1 + \delta$ . Now if  $h(n)$  is exponentially weighted to form:

$$h_w(n) = h(n)e^{-\lambda n} \quad (3.4.19)$$

and if  $\lambda = \ln(1 + \delta)$  then all zeros of  $H_2(z)$  are drawn inside  $|z| = 1$ .

Applying cepstral separation results in isolating

$$h'_{\min}(n) = [h_{\min}(n)e^{-\lambda n}] * [h_2(n)e^{-\lambda n}] \quad (3.4.20)$$

and 
$$h'_{\max}(n) = h_3(n)e^{-\lambda n} \quad (3.4.21)$$

Inversion of  $h'_{\min}(n)$  and  $h'_{\max}(n)$  instead of the correct components results in mismatch between the inverse and  $h(n)$ .

### 3.5 A Comparative Study of Least-Squares and Homomorphic Techniques for the Inversion of Mixed Phase Signals

In this section the results of a comparative study between least-squares and homomorphic methods for the inversion of mixed phase signals are presented. The results of the study have also been published in [63].

#### Comparative tests and criteria

The aims of this study are partly to demonstrate the effect of delay in least-squares for physical systems, but also, more importantly, to compare the efficiency of the least-squares and homomorphic techniques for the inversion of mixed phase signals. To this end, the techniques were applied to a number of specific systems, namely: (i) a miniature loud-speaker; (ii) a computer model of a small room [1]; (iii) an absorbent small room. Aspects of the inversion were considered in both time and frequency domains. All impulse response functions were limited to 1024 points in length for computational reasons.

The criteria used were:

(a) Time domain error energy

computed as

$$I_1 = \frac{1}{N} \sum_{n=0}^{N-1} e^2(n) \quad (3.5.1)$$

Note, however, the least-squares technique will always be at least as good as the homomorphic method when judged on this basis.

(b) Frequency domain spectral distortion

A frequency domain measure may be more appropriate perceptually and is chosen as

$$I_2 = \text{standard deviation of the logarithm of the modulus of the Fourier transform of the inverted signal} \quad (3.5.2)$$

This is a measure of spectral distortion.

Results

(a) The effect of delay in least-squares inversion

Least-squares inversion for physical systems is illustrated by the application to the loudspeaker whose response is illustrated in fig. 3.5.1.

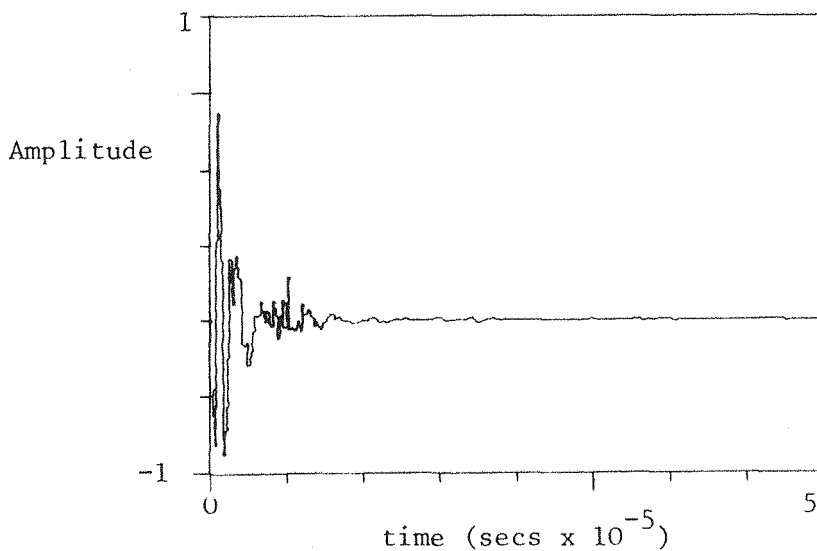


Figure 3.5.1: Loudspeaker Response.

Figures 3.5.2(a) and (c) show the 512 point inverse operators obtained using the zero delay and an optimal delay. The corresponding approximate inversions are shown in figures 3.5.2(b) and (d). Clearly, the introduction of delay considerably enhances the efficiency of the inversion. Figure 3.5.3 illustrates the variation of performance ( $P_k$ , as defined in appendix VI with  $k$ . As can be seen, for all cases examined:

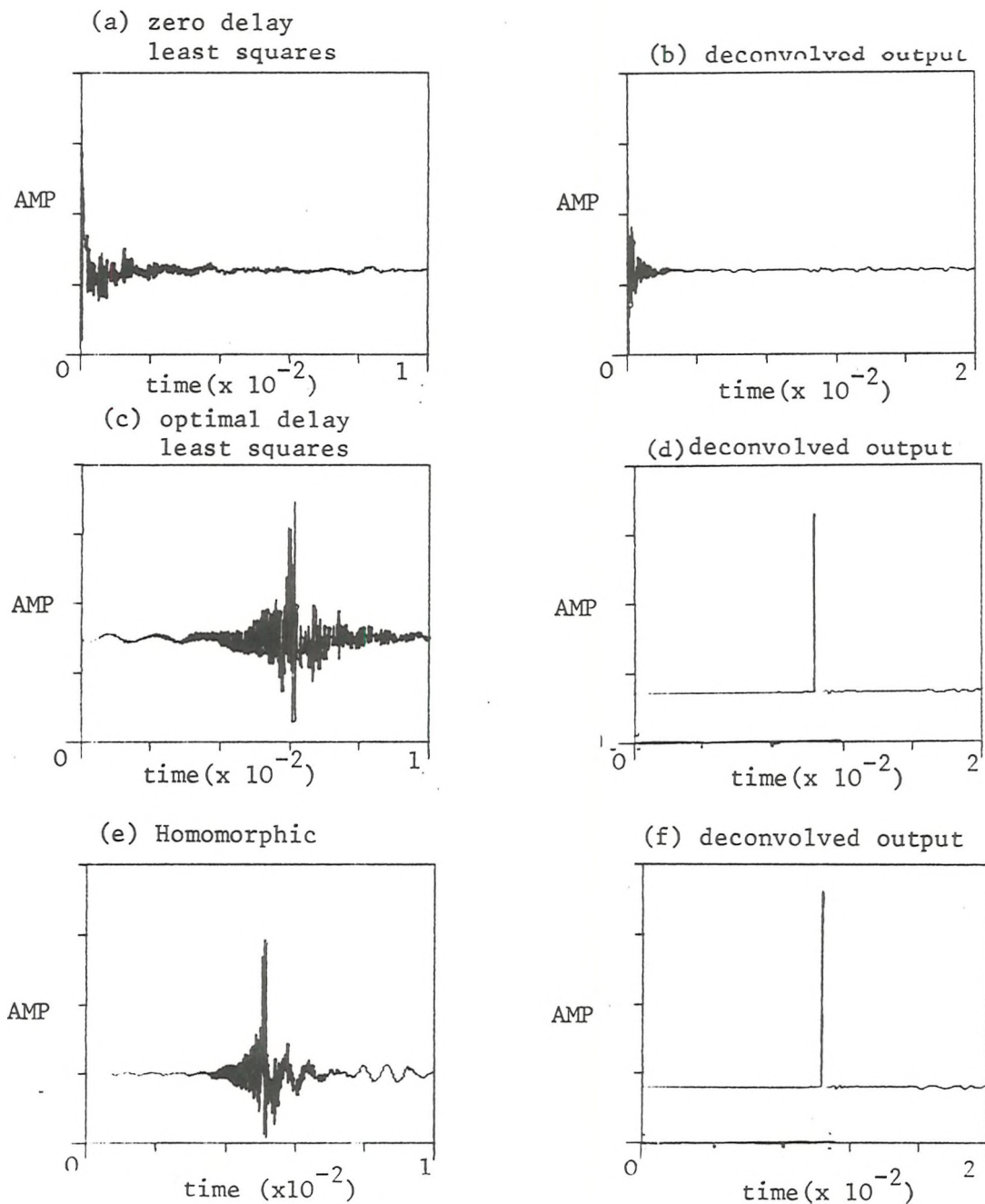


Figure 3.5.2: Least Squares Inversion of Loudspeaker Response.

(i) zero delay inversion is inferior; (ii) the curves exhibit a broad maximum (plateau). As discussed in section 3.3.1, for  $k = 0$ , the output is approximately all-pass and so frequency domain (modulus) criteria will not substantially distinguish between differing  $k$ .

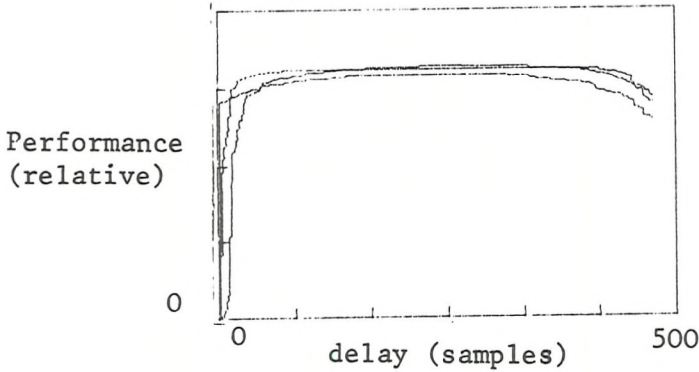


Figure 3.3.5: Performance Curve for Inversion of Responses, for Loudspeaker, Synthetic Room and Real Room.

The effect of exponential weighting on homomorphic inversion

Table 3.5.1 illustrates the effect of exponential weighting on time and frequency domain performance for the loudspeaker using least-squares inversion of the minimum and maximum phase components. (Note that Fourier inversion produces similar results.)

Table 3.5.1 Effect of exponential weighting on homomorphic inversion of the loudspeaker response.

$\lambda$	Error Energy ( $I_1$ )	Spectral Distortion ( $I_2$ )
0.0000	0.024	1.181
0.0025	0.00004	0.066
0.0050	0.00005	0.071
0.0075	0.00006	0.080
0.0100	0.00008	0.089
0.0125	0.00025	0.099
0.0150	0.00028	0.109
0.0175	0.00028	0.119

The performance in both time and frequency domains exhibits an optimum for some value of  $\lambda$ . This value is dependent on the number of zeros near the unit disc.

#### Comparison of Least-Squares and Homomorphic Methods

The results in this section were all obtained using the optimum delay in the least-squares case and the optimum weighting in the homomorphic case. The inverse operators obtained by the two techniques are shown in figs. 3.5.2(c) and (e), respectively. They are similar except for low frequency trends. The resulting inversions are shown in figs. 3.5.2(d) and (f). These results are so close to ideal spikes that it is difficult to distinguish between them visually. Table 3.5.2 shows that the least-squares method is superior for all cases.

Table 3.5.2 Comparison of the error energy  $I_1$ , for least squares and homomorphic inversion.

	Least Squares Inversion	Homomorphic Inversion
Real room	0.000007	0.00018
Model room	0.00002	0.00005
Loudspeaker	0.00001	0.00004

On the other hand, Table 3.5.3 shows that this superiority is not necessarily reflected in the frequency domain. This remains true even if the signal is also exponentially weighted using the optimum weight

Table 3.5.3 Comparison of the spectral distortion  $I_2$ , for least squares and homomorphic inversion

	Least Squares Inversion	Homomorphic Inversion
Real room	0.06848	0.11598
Model room	0.17305	0.09820
Loudspeaker	0.10074	0.06644

prior to least-squares inversion. The frequency domain effect is illustrated in detail for the loudspeaker in Figure 3.5.4 (showing the logarithm of the modulus of the approximate inversions of fig. 3.5.2(d) and (f)). Both



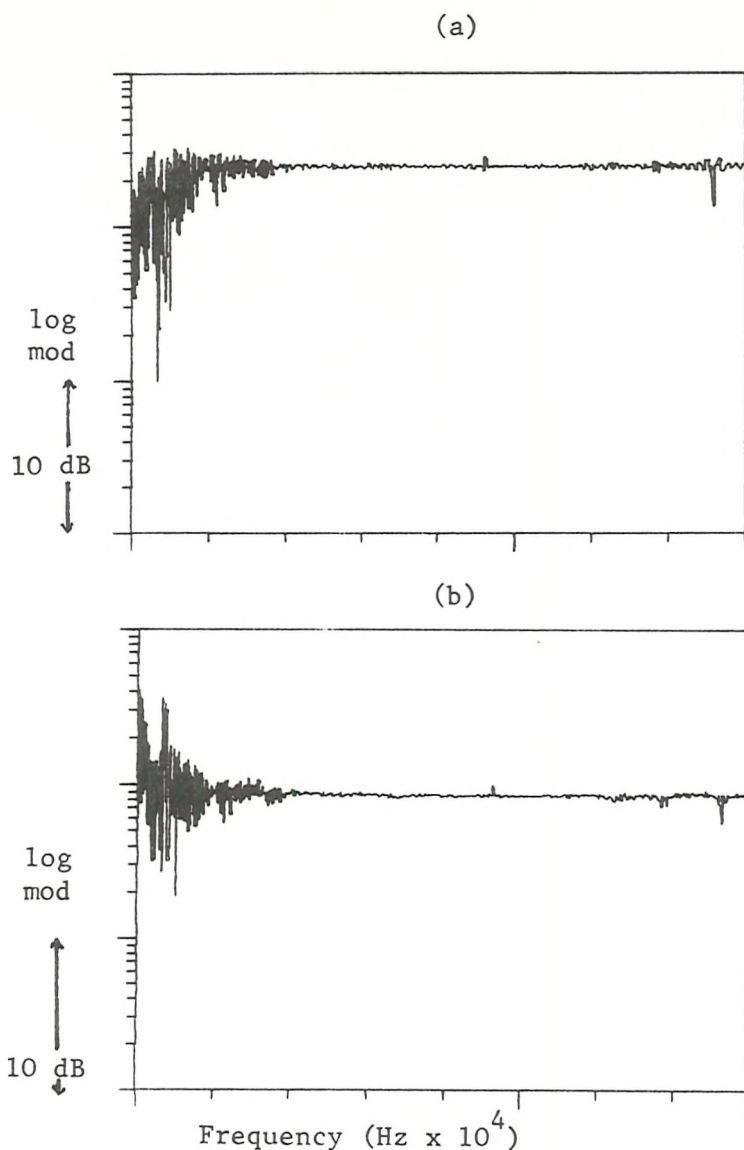


Figure 3.5.4: Log Spectra of Deconvoluted Outputs

have predominantly flat spectra broken by a number of sharp peaks and troughs. In the least-squares case the inversion has clearly been far more effective in flattening peaks than troughs; this behaviour is in accord with the frequency domain interpretation of least-squares inversion given in section 3.3. The homomorphic method, on the other hand, exhibits no such bias.

### 3.6 Conclusions

It has been seen that a system  $H(z)$  can only have a stable causal inverse if it is minimum phase. If the system is non-minimum phase and a causal inverse operator is required then such an inverse must be approximate. If the inverse operator is restricted to finite length then it will usually be approximate even if the system is minimum phase. Many methods for constructing approximate inverse operators exist; in this chapter several have been discussed, but in particular the method of least-squares was considered in detail.

Least-squares inverse operators have the following properties:

- (i) The infinite unconstrained filter is an ideal inverse.
- (ii) The infinite causal filter is equal to the inverse of the equivalent minimum phase system  $H_{eq}(z)$ . That is, it only corresponds to the ideal inverse if  $H(z)$  is minimum phase, when  $H(z)$  is non-minimum phase the output produced by the filter is all-pass.
- (iii) The finite causal filter is obtained from the solution of a set of linear algebraic equations - the normal equations. The solution may be obtained very efficiently via Durbin's algorithm. The resulting inverse operator is minimum phase irrespective of the phase properties of the input. It therefore performs best when the input is minimum phase, in other cases the resulting output is approximately all-pass.

An alternative frequency domain interpretation of the inverse filter may be given which suggests that:

- (a) The inverse in relative terms will be as good, on average, in areas of the spectrum of  $H(z)$  which have little energy, as in those with high energy.
- (b) Peaks in the system  $H(z)$  will be flattened more effectively than dips.

Many of the problems imposed by the restriction of causal inverse operators may be overcome by incorporating a delay in the output. Such a delay may also be built into the least-squares formulation. In the infinite case:

- (i) The error energy is a monotonically non-increasing function of delay.

(ii) The infinite causal filter is equivalent to the ideal filter if sufficiently delayed.

In the finite case these results do not usually hold. In particular the filter performance is not usually monotonic. However, there exists an efficient method of obtaining the filters for all desired delays. Furthermore it is possible to monitor the filter performance at each stage of the computation and select the optimum accordingly.

It was also noted that inversion is a noise enhancing process. Two of the main techniques for reducing this effect are prewhitening and shaping. Prewhitening increases the input spectral level equally at all points, thus decreasing the amplification in the inverse operator. It is simple to apply and generally improves the stability of the solution. In shaping, the output delta function is replaced by a more general desired function. The shape of the desired output is chosen to give the 'best' inversion (in a particular context) whilst causing the minimum decrease in output SNR.

In the application of the least-squares inversion technique, both with and without delay, it was seen that the performance of the least-squares technique is enhanced in general by the incorporation of delay but is often relatively insensitive to changes in the delay over a broad range of values. It was also seen that there are some signals, e.g., half sine pulse, which are not satisfactorily inverted by least-squares methods.

In the application to physical systems the method was compared with an alternative approach known as Homomorphic Prediction. As expected, the least-squares technique was always superior to the homomorphic in the time domain, but this was not always reflected in the frequency domain. The least-squares technique is also computationally more efficient than the homomorphic.



## CHAPTER 4

### OPTIMAL CONTROL DECONVOLUTION

#### 4.1 Introduction

The previous chapter was devoted to the study of conventional deconvolution methods. In this chapter a recent, novel method due to Thomas [96] is explored, which utilises the techniques of optimal control [3]. The aims of this development are three fold. Firstly, the method is applied to certain novel applications involving physical systems. Secondly, a new approach to the treatment of noise is evolved, and thirdly some insight into the relationship of the method to other, more conventional techniques, is obtained.

Thomas's original work was performed in continuous time. Initially, in this chapter, this formulation is retained since it is intended to apply the method to the deconvolution of a transducer signal (velocity meter) which is neatly characterised by an  $s$  domain transfer function. The discrete form of the solution is also developed here and is used throughout the rest of this thesis. This development is made partly for consistency, partly because a discrete form is required for another application in a later chapter, and partly to allow greater insight into the operation of the method. In particular it will be seen that for some signals the parameters of the method can be used to effect noise reduction in the deconvolution. This development is initially made in an empirical manner but it is later demonstrated to be directly analogous to the prewhitening approach to noise reduction in the previous chapter.

In the application to the velocity meter signals described above, the method is found to work well both in the noise free case and in the presence of noise when use is made of the noise reduction method described above.

#### 4.2 Theory: Continuous Time

In the optimal control approach to deconvolution the usual problem - the synthesis of an inverse operator, depicted for an input  $u$  in Figure 4.2.1 - is replaced by a linear tracking system.

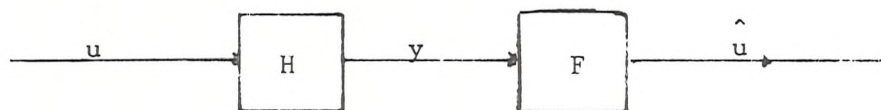


Fig 4.2.1: Deconvolution

The tracking system operates by generating a system  $\hat{u}$  which, when applied to the system  $H$  produces an output  $\hat{y}$ , which is designed to track the true output  $y$  (see Fig 4.2.2).

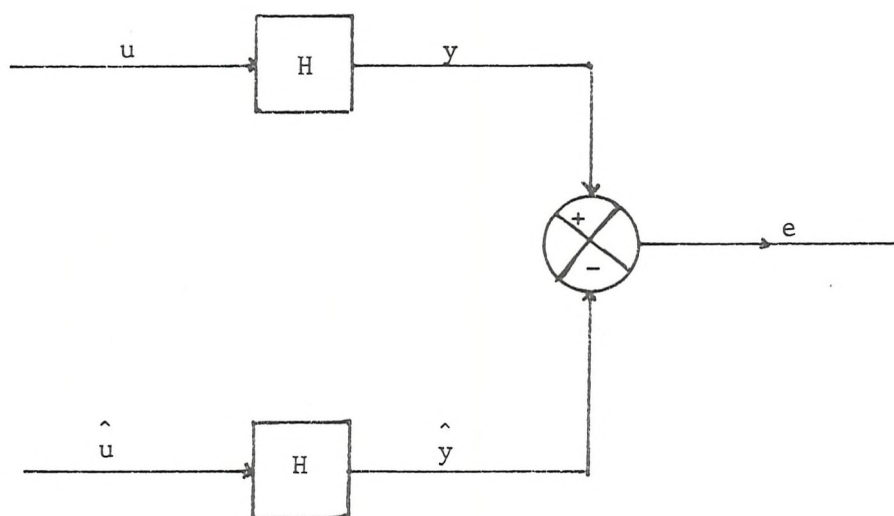


Fig 4.2.2: Deconvolution by Tracking

The quality of the approximation may be ensured by appropriate control of the instantaneous tracking error.

$$e(t) = y(t) - \hat{y}(t) \quad (4.2.1)$$

One approach is to minimise the functional

$$J = \int_0^T (q e^2(t) + r \hat{u}^2(t)) dt \quad (4.2.2)$$

where  $q$  and  $r$  are positive (possibly time-varying) parameters. The interpretation of these parameters will be considered later. To effect the solution the system  $H(s)$  must be expressed in state space form [112]:

$$\dot{\underline{x}}(t) = \underline{A}\underline{x}(t) + \underline{b} \hat{u}(t) \quad (4.2.3)$$

$$\text{with } \hat{y}(t) = \underline{c}^t \underline{x}(t) \quad (4.2.4)$$

where  $\underline{x}(t)$  is the  $n \times 1$  state vector.

$\underline{A}$  is a matrix ( $n \times n$ ) and  $\underline{b}$  and  $\underline{c}$  are vectors ( $n \times 1$ ). Note that in general, in addition to  $q$  and  $r$ ,  $\underline{A}$ ,  $\underline{b}$  and  $\underline{c}$  may be time-varying. Where possible, for simplicity this dependence is not explicitly stated.

The solution for  $\hat{u}$  (stated without proof) may be obtained by standard optimal control techniques [3] as:

$$\hat{u}(t) = r^{-1} \underline{b}^t (\gamma(t) - \underline{K}\underline{x}(t)) \quad (4.2.5)$$

where  $\underline{K}$  is the solution of the matrix Riccati equation.

$$\dot{\underline{K}} = -\underline{K}\underline{A} - \underline{A}^t \underline{K} + \underline{K} \underline{b} r^{-1} \underline{b}^t \underline{K} - \underline{c} \underline{q} \underline{c}^t ; \underline{K}(T) = 0 \quad (4.2.6)$$

and  $\underline{\gamma}(t)$  is the solution of the vector differential equation:

$$\dot{\underline{\gamma}}(t) = -(\underline{A} - \underline{b} r^{-1} \underline{b}^t \underline{K})^t \underline{\gamma}(t) - \underline{c} \underline{q} \underline{\gamma}(t) ; \underline{\gamma}(T) = 0 \quad (4.2.7)$$

A formal analytic solution to equations (4.2.6) and (4.2.7) using partitioning of an augmented state transition matrix does exist, but is inappropriate here and so a numerical solution is adopted. The boundary conditions on  $\underline{K}$  and  $\underline{\gamma}$  preclude a causal solution, however, there are many applications where such an acausal solution is not a significant disadvantage. Indeed, it is the 'global' nature of the solution which is one of the greatest advantages of the method.

Note that one obvious restriction of the method is that the system  $H(s)$  must be known and expressible in state space form.

The solution is depicted in Figure 4.2.3.

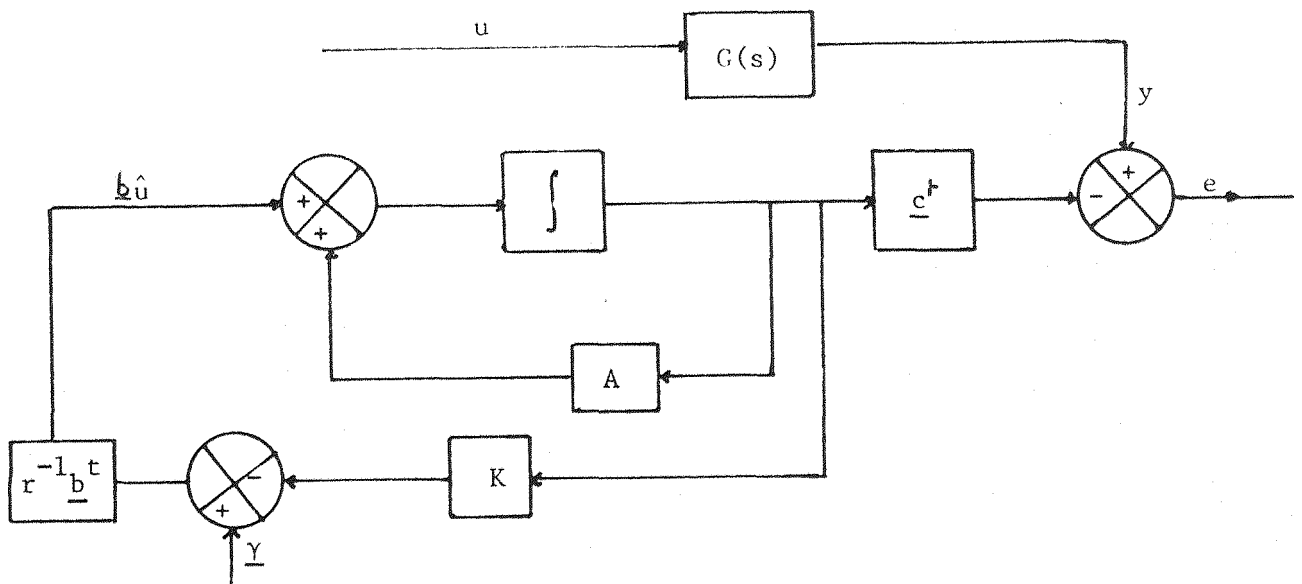


Fig 4.2.3: Block Diagram for Optimal Control Deconvolution.

#### 4.2.1 Computation

As noted in the previous section, the boundary conditions on equations (4.2.6) and (4.2.7) preclude a causal solution to the optimal control deconvolution problem. The numerical solution of these equations must be effected in reverse time beginning at  $t = T$  and proceeding to  $t = 0$ . In the simulations presented later the solution was obtained using a fourth order Runge-Kutta scheme. The values of  $K$  and  $\underline{y}$  at successive sample points are stored. Then, beginning at  $t = 0$ , with the values for  $K(0)$  and  $\underline{y}(0)$  as well as the initial state  $\underline{x}(0)$ , the solution of the coupled system defined by equations (4.2.3) and (4.2.5) is effected in forward time for  $\hat{u}(t)$ .

The above description represents the simplest computational scheme and the one adopted here. However, the memory requirement caused by the necessity to store all the values for  $K$  and  $\underline{y}$  can be considerable. Thomas [97] gives an alternative scheme which avoids this storage load, but at the cost of extra computation.

#### 4.2.2 Selection of Parameters

The parameters  $q$  and  $r$  of equation (4.2.2) have a crucial effect on the optimal control deconvolution. Purely from inspection of (4.2.2) it is clear that the smaller the value of  $r$  (or more correctly the larger

the ratio  $q/r$ ), the more the error is penalised and the less the magnitude of the input. Later the influence of  $q$  and  $r$  will be defined more precisely. In the noise-free case the larger the value of  $q/r$  the closer  $\hat{u}$  approximates  $u$ . Note, however, that  $r = 0$  is not admissible due to the singularity (see equation (4.2.5)).

In many instances, the deconvolution problem is complicated by the presence of measurement noise. Some of the main techniques for dealing with this problem were outlined in Chapter 3. In the case of optimal control deconvolution Thomas [97] suggests prefiltering the input, followed by the application of the deconvolution method as for the noise-free case. The prefiltering can take the form of any standard estimation technique depending on the signal and available knowledge about the statistics of the noise. Here, however, an alternative approach based on the control of the parameters  $q$  and  $r$  is proposed for the case when the signal and noise characteristics are not exactly known.

In this section the method will be developed and justified in an empirical manner. A more solid justification will be given in the next section and further support for the method comes from the simulations later.

$$\text{Suppose; } y_m(t) = y(t) + v(t) \quad (4.2.8)$$

where the noise  $v(t)$  is assumed stationary and zero mean. Now if  $y(t)$  is a transient signal of some sort (for example a shock) then the SNR at a point, which might be defined as:

$$\text{SNR}_{t_1} = \frac{|y(t_1)|}{\sigma_v} \quad (4.2.9)$$

(see also Chapter 5)

will vary with time. Furthermore, it seems intuitively reasonable that for many such transients the variation of the SNR with time may be approximated by the 'envelope' of  $y_m(t)$ . (In this context the term 'envelope' refers to the intuitive concept rather than the mathematical definition because of difficulties with wide band noises).

As is clear from the discussion on selection of parameters, when the SNR is high it is desirable to penalise tracking error heavily and thus to use a large value for  $q/r$ . Whereas in areas where the SNR is low it is less desirable to penalise tracking error heavily since this will cause noise enhancement, and hence a lower value for  $q/r$  should be chosen.

In view of the foregoing a reasonable policy for the selection of  $q/r$  for this type of signal might be:

$$\left(\frac{q}{r}\right) = K \cdot (\text{env } (y_m(t))) \quad (4.2.10)$$

where  $K$  is a constant, and  $\text{env } ( )$  denotes 'envelope' as discussed above and may, in many cases be computed by low pass filtering  $y_m^2(t)$ . It is not possible to claim that this process is optimal in any sense. Indeed, although the time variation of  $(q/r)$  is consistent with the theory, strictly the approach here represents 'state' dependence of  $(q/r)$  - which is not allowable. Nevertheless, some justification will be given in the next section, also the policy is intuitively reasonable and works well in practice (see Section 4.5).

#### 4.3 Theory: discrete time

In this section Thomas's method for deconvolution is redeveloped in discrete form. The aim of this development is partly to bring the theory into line with the remainder of the thesis, partly to facilitate another application of the method (in Chapter 8) and partly to give further insight into the noise reduction method described in the previous section. The discrete equivalent of the optimal control deconvolution method of the previous section can be stated as follows:

Given a measurement sequence  $y(k)$ ,  $k = 1, 2, \dots, N$ .  
 where  $y(k) = h(k) * u(k)$  (4.3.1)  
 the aim is to synthesise a control sequence  $\hat{u}(k)$  such that

$$J = \sum_{k=1}^N (q e^2(k) + r \hat{u}^2(k-1)) \quad (4.3.2)$$

is minimised

$$\text{where } e(k) = y(k) - \hat{y}(k) \quad (4.3.3)$$

The system  $h$  is written in state form as:

$$\underline{x}_{k+1} = \phi \underline{x}_k + \underline{\theta} \hat{u}(k) \quad (4.3.4)$$

with

$$\hat{y}(k) = \underline{c}^t \underline{x}_k \quad (4.3.5)$$

where  $\underline{x}$  is the  $(n \times 1)$  state vector,  $\phi$  is the  $(n \times n)$  state transition matrix, and  $\underline{c}$ ,  $\underline{\theta}$  are  $n \times 1$  vectors, where  $\phi$ ,  $\underline{c}$  and  $\underline{\theta}$  may in general be time-variable.

The solution may be obtained as follows:

$$\text{Let } f_{N-j}(\underline{x}_j) = \min_{\hat{u}} \sum_{k=j+1}^N (q e^2(k) + r \hat{u}^2(k-1)) \quad (4.3.6)$$

$$= \min_{\hat{u}} \{ q e^2(j+1) + r \hat{u}^2(j) + f_{N-(j+1)}(\underline{x}_{j+1}) \} \quad (4.3.7)$$

Now assume,

$$f_{N-j} = \underline{x}_j^t P_{N-j} \underline{x}_j + \underline{x}_j^t \underline{V}_{N-j} + S_{N-j} \quad (4.3.8)$$

where  $P$  is an  $(n \times n)$  matrix,

$\underline{V}$  is an  $(n \times 1)$  vector and  $S$  is a scalar.

Substituting and differentiating gives:

$$\hat{u}_j = G_{N-j} - H_{N-j}^t \underline{x}_j \quad (4.3.9)$$

where

$$G_{N-j} = \frac{-\underline{\theta}^t (-2q \underline{c}^t y(j+1) + \underline{V}_{N-j-1})}{2d_{N-j-1}} \quad (4.3.10)$$

$$H_{N-j}^t = \frac{\underline{\theta}^t (q \underline{c} \underline{c}^t + P_{N-j-1}) \phi}{d_{N-j-1}} \quad (4.3.11)$$

$$\text{where } d_{N-j-1} = \underline{\theta}^t (\underline{qcc}^t + P_{N-j-1}) \underline{\theta} + r \quad (4.3.12)$$

$$P_{N-j} = \phi^t (\underline{qcc}^t + P_{N-j-1}) \phi - d_{N-j-1} \underline{H}_{N-j} \underline{H}_{N-j}^t \quad (4.3.13)$$

$$\text{and } \underline{V}_{N-j} = (\phi^t - \underline{H}_{N-j} \underline{\theta}^t) (-2q \underline{c} y(j+1) + \underline{V}_{N-j-1}) \quad (4.3.14)$$

with  $P_0 = 0$ ,  $\underline{V}_0 = 0$ .

Note that in general  $q$  and  $r$ , as in the continuous case may be functions of time.

As in the continuous form the solution cannot be effected in forward time. The solution proceeds by first finding the values of  $\underline{H}_k$  and  $\underline{G}_k$  sequentially for  $k = N, N-1, \dots, 1$ .

The solution for  $\hat{u}_j$  for  $j = 1, 2, \dots, N$  may then be obtained from the coupled system (4.3.9) and (4.3.4).

Once again the solution has a high storage requirement since all values of  $\underline{G}_k$  and  $\underline{H}_k$  must be retained.

#### 4.4 Noise Reduction through control of the Parameters

In Section 4.2 an empirical interpretation of the role of the parameters  $q$  and  $r$  in the functional (4.2.2) was given. Further insight into these parameters may be obtained by considering the discrete form (4.3.2). First, however, it is necessary to obtain an alternative, less general but more familiar description of these results.

Rewrite (4.3.2) as:

$$I = \sum_{k=0}^{N-1} (q e^2(k+1) + r \hat{u}^2(k)) \quad (4.4.1)$$

with

$$e(k+1) = [y(k+1) - \sum_{j=0}^{N-1} \hat{u}(j) h(k+1-j)] \quad (4.4.2)$$

If  $q$  and  $r$  are restricted to constant values then differentiating (4.4.1) with respect to  $\hat{u}$  and equating to 0, gives:



$$\sum_{j=0}^{N-1} \hat{u}(j) R_{hh}(j,k) + \frac{r}{q} \hat{u}(k) = g(k) \quad (4.4.3)$$

where

$$R_{hh}(j,k) = \sum_{i=1}^N h(i-j) h(i-k) \quad (4.4.4)$$

$$g(k) = \sum_{i=0}^{N-1} y(i) h(i-k) \quad (4.4.5)$$

or

$$\left[ R_{hh} + \left( \frac{r}{q} \right) I \right] \underline{\hat{u}} = \underline{R_{yh}} \quad (4.4.6)$$

where

$R_{hh}$  is the matrix with elements  $R_{hh}(i,j)$ ;  $i,j = 0,1, \dots, N-1$

and

$$\underline{R_{yh}}^t = [g(0), g(1) \dots g(N-1)]$$

These equations (4.4.6) are familiar as the auto-covariance form of the Normal Equations (see Chapter 2). This form has not been developed as an alternative scheme for practical purposes but to clarify the role of the parameters  $(q/r)$ . It is seen, from (4.4.6), that the role of  $(r/q)$  is directly analogous to pre-whitening (see Chapter 3). As such it forms a natural and entirely logical method of noise reduction. To see this more clearly proceed as follows:

$$\text{Note that: } \underline{R_{yh}} = R_{hh} \underline{u} \quad (4.4.7)$$

then (4.4.6) becomes:

$$\left[ R_{hh} + \left( \frac{r}{q} \right) I \right] \underline{\hat{u}} = R_{hh} \underline{u}$$

and hence

$$\left[ I + \left( \frac{r}{q} \right) R_{hh}^{-1} \right] \underline{\hat{u}} = \underline{u} \quad (4.4.8)$$

Now as  $N \rightarrow \infty$  and, using the results of Chapter 3, subject to restrictions on the phase structure of  $h$ ; from (4.4.8):

$$\hat{U}(\omega) \approx \frac{U(\omega)}{\left[ 1 + \left( \frac{r}{q} \right) / |H(\omega)|^2 \right]} \quad (4.4.9)$$

(see Chapter 3).

The influence of  $(q/r)$  is now clear. In general the higher  $(q/r)$  the closer  $\hat{U}(\omega)$  will be to  $U(\omega)$ . But also it is seen that as  $H(\omega)$  increases  $\hat{U}(\omega)$  tends to  $U(\omega)$  and  $q/r$  has greater influence in areas of the spectrum where the system response is low. In such areas  $\hat{U}(\omega)$  becomes small. This is precisely what is required for noise control since it is in areas of low system response that the influence of the measurement noise will be strongest. Although (4.4.9) is subject to the stated restrictions, in practise simulations have verified that it represents a good approximation for both discrete and continuous formulations, for sufficiently long inputs.

Additionally, although this formulation cannot be directly extended to the case of time variable  $(q/r)$ , it is obvious by analogy that this represents a sort of time variable prewhitening, which is clearly a very worthwhile tool for dealing with inputs which have a time varying SNR.

#### 4.5 Application: Velocity Meter

##### 4.5.1 The Problem

Measurements of the motion of a vibrating structure or surface may be obtained using a variety of procedures. For example, velocity meters have traditionally been used to obtain shock and vibration measurements from marine structures. Whilst velocity is the quantity measured it is not uncommon to require, in addition, estimates of structural acceleration. In principle the solution for this problem is simple, but in practice there are complications which must be accounted for such as, (i) the dynamics of the transducer and (ii) instrumentation problems such as amplifier characteristics, pick-up of noise, etc. The aim here is to apply the optimal control deconvolution method described in the previous section to the problem outlined above, that is, to attempt to obtain the input acceleration from a velocity meter signal.

Much of the work to be described in this section has previously been published in [38].

#### 4.5.2 The Model

A velocity meter is mounted on a moving surface (Fig 4.5.1) The input base acceleration is denoted  $\ddot{x}_b$  and the transducer output (velocity),  $\dot{x}_r$ .

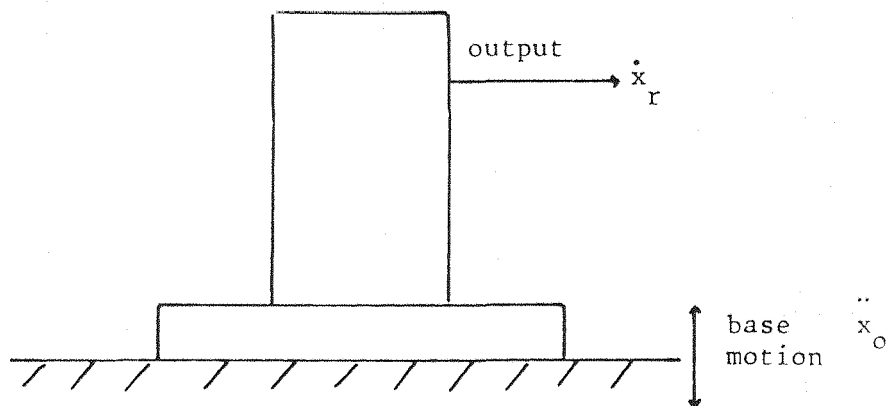


Fig 4.5.1 Velocity Meter

The model used is depicted in Figure 4.5.2.

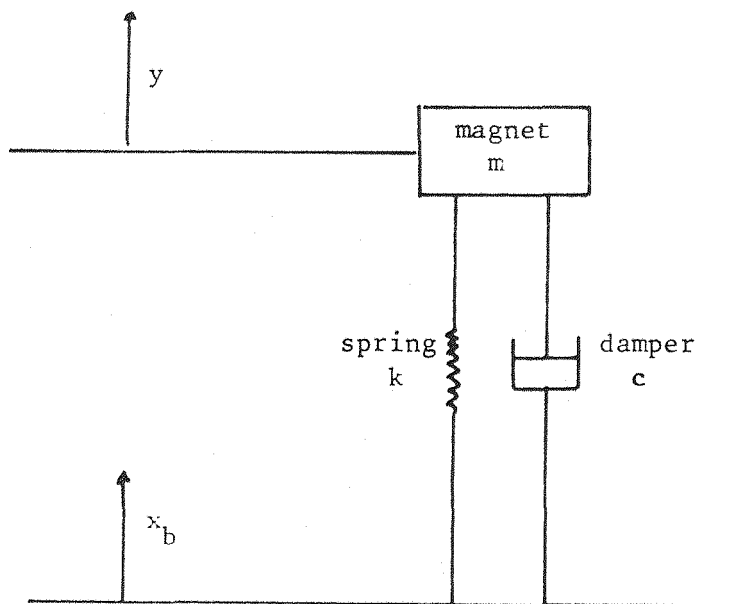


Fig 4.5.2 Model for Velocity Meter

where  $m$  is the mass of the magnet,  $k$  is the spring constant,  $c$  is the damping constant and  $y$  and  $x_b$  are the displacements of the magnet and base respectively.

It is assumed that the transducer output is proportional to the relative velocity between the magnet and the base, that is, proportional to:

$$\dot{x}_r = \dot{y} - \dot{x}_b \quad (4.5.1)$$

If the motion of the system is assumed to be one dimensional then a linear mathematical model is:

$$\ddot{x}_r + 2\xi\omega_o\dot{x}_r + \omega_o^2 x_r = -\ddot{x}_b \quad (4.5.2)$$

where  $\omega_o^2 = \frac{k}{m}$  and  $2\xi\omega_o = \frac{c}{m}$

From this equation a convenient ( $s$  domain) transfer function may be written as:

$$\frac{\dot{x}_r(s)}{\ddot{x}_b(s)} = H(s) = \frac{-s}{s^2 + 2\xi\omega_o s + \omega_o^2} \quad (4.5.3)$$

Written this way the deconvolution problem is as depicted in Figure 4.5.3.

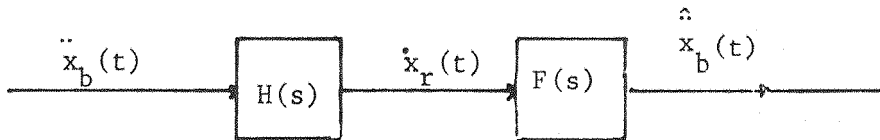


Fig 4.5.3: Deconvolution of the Base Motion

#### 4.5.3. Optimal Control Approach

Using the approach outlined in Section 4.2, let  $\hat{u} = \hat{\ddot{x}}_b(t)$  and  $y = \dot{x}_r$ , so that equation (4.2.2) becomes:

$$J = \int_0^T (q\dot{e}^2(t) + r\hat{\ddot{x}}_b(t))dt \quad (4.5.4)$$

The system  $H(s)$  (equation 4.5.3) may be converted to state-space form using standard methods [3]. The matrices  $A$ ,  $\underline{b}$  and  $\underline{c}$  of equations (4.2.3) and (4.2.7) may be obtained as:

$$A = \begin{bmatrix} 0 & 1 \\ -\omega_o^2 & -2\xi\omega_o \end{bmatrix} \quad \underline{b}^t = (0 \quad 1) \quad \underline{c}^t = (0 \quad -1)$$

The solution for  $\hat{\ddot{x}}_b(\hat{u})$  is then obtained from equations (4.2.3) - (4.2.7), where for the above system these reduce to:

$$\hat{\ddot{x}}_b(t) = r^{-1} (\gamma_2 - K_{12}x_1 - K_{22}x_2) \quad (4.5.5)$$

where

$$\begin{aligned} \dot{K}_{11} &= -2K_{12}\omega_o^2 - \frac{K_{12}^2}{r} ; \quad K_{11}(T) = 0 \\ \dot{K}_{12} &= K_{11} - 2K_{12}\xi\omega_o - \omega_o^2 K_{22} - \frac{K_{12}K_{22}}{r} ; \quad K_{12}(T) = 0 \\ \dot{K}_{22} &= 2K_{12} - 4K_{22}\xi\omega_o - \frac{K_{22}^2}{r} + q ; \quad K_{22}(T) = 0 \end{aligned} \quad (4.5.6)$$

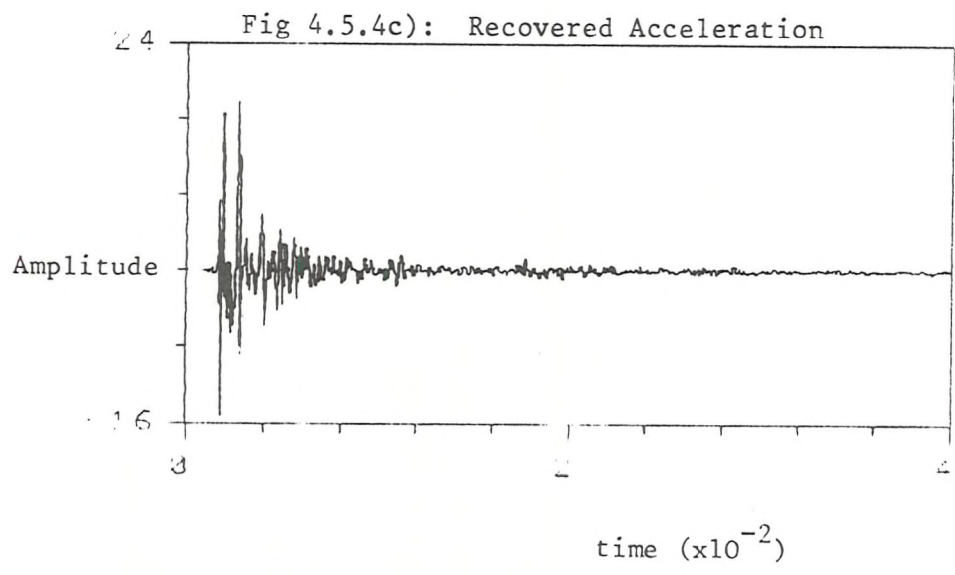
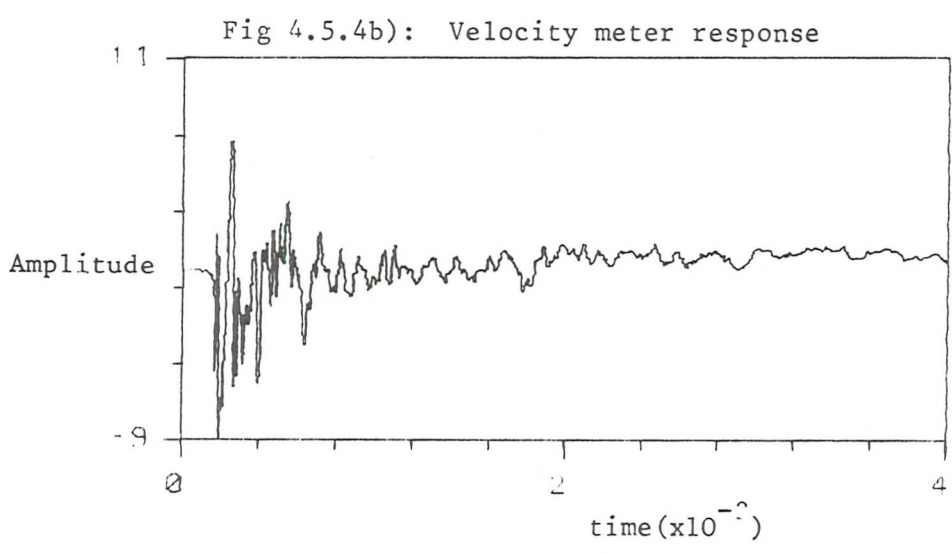
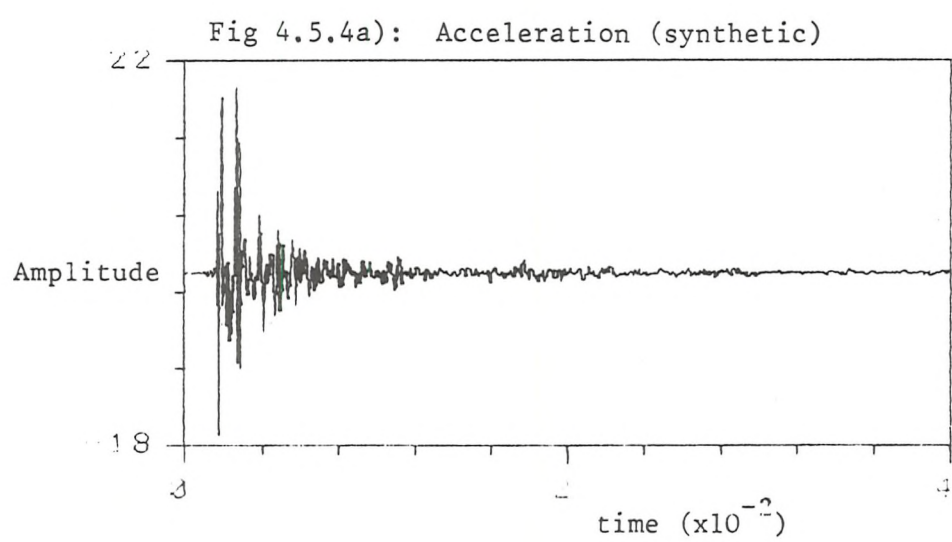
and

$$\begin{aligned} \dot{\gamma}_1 &= (-\omega_o^2 - \frac{K_{12}}{r}) \gamma_2 ; \quad \gamma_1(T) = 0 \\ \dot{\gamma}_2 &= \gamma_1 - (2\xi\omega_o + \frac{K_{22}}{r}) \gamma_2 - \dot{x}_r - q ; \quad \gamma_2(T) = 0 \end{aligned} \quad (4.5.7)$$

#### 4.5.4 Results

a) Noise free synthetic data. A synthetic, 'shock-like' base acceleration of 2000 points in length (Fig 4.5.4a) at a sample rate of 33,000 was created and used as input to the assumed velocity meter system (based on a digital simulation of  $H(s)$ ). The resulting output velocity is shown in Figure 4.5.4(b). Application of optimal control deconvolution with  $q=1$ ,  $r=1 \times 10^{-10}$

produces the results in Figure 4.5.4c). As can be seen, the recovered acceleration is a very good approximation to the true input.



In fact, because of the noise free measurement and the precise accuracy of the system  $H(s)$ , the input can be recovered with almost arbitrary accuracy by choosing the ratio  $q/r$  to be sufficiently large. The effect of varying  $q/r$  can be clearly seen from Figure 4.5.5 which shows the modulus Fourier Transform for the synthetic acceleration together with those for recovered approximations calculated with  $r = 1 \times 10^{-7}$ ,  $r = 1 \times 10^{-8}$ ,  $r = 1 \times 10^{-9}$ , and  $q = 1$ .

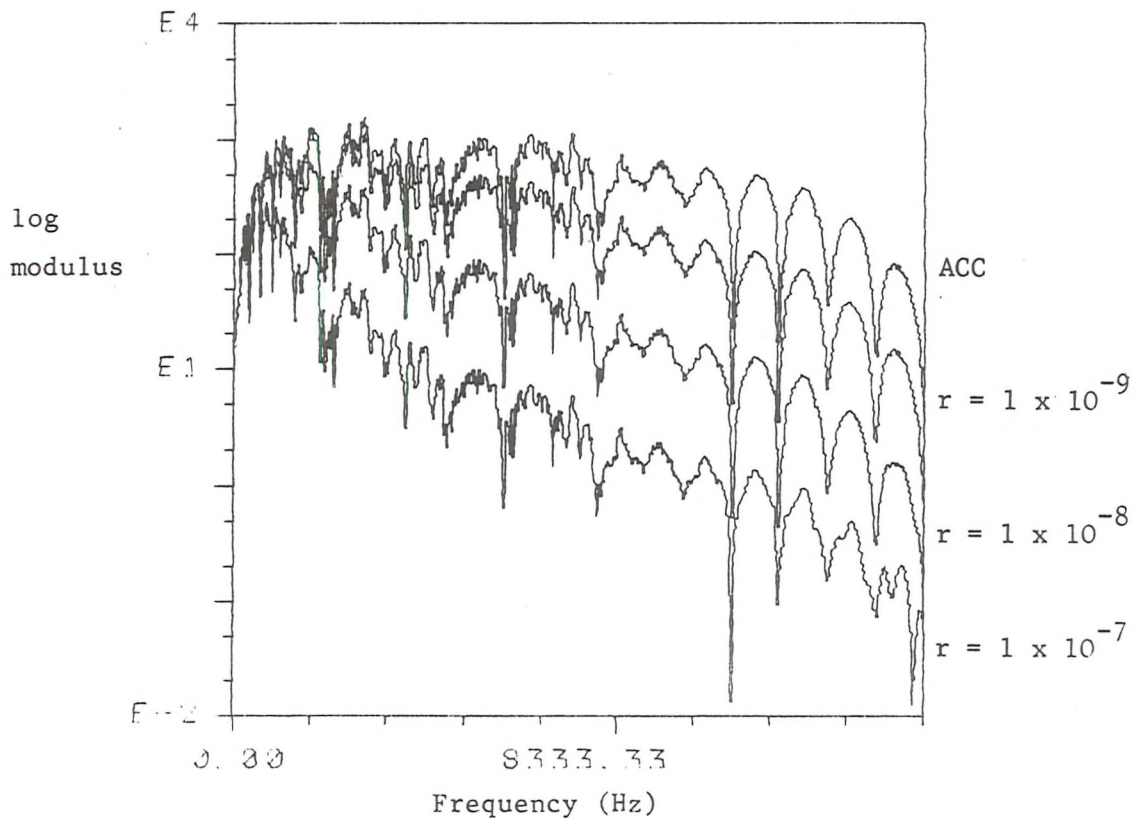


Fig 4.5.5: Mod Frequency Response for Acceleration and Deconvolved Approximations.

From the graph, reducing  $q/r$  appears to give a low frequency weighting to the recovered approximation. It is clear from equation (4.4.9) that this weighting corresponds to the shape of the frequency response of the system  $H(s)$ . In the time domain one way to measure the efficiency (in the synthetic case) of the approximation is to compute

$$I = \frac{[\sum (\ddot{x}_b - \hat{\ddot{x}}_b)^2]^{\frac{1}{2}}}{[\sum \ddot{x}_b^2]^{\frac{1}{2}}} \quad (4.5.8)$$



This is a normalised error energy measure for the deconvolution.

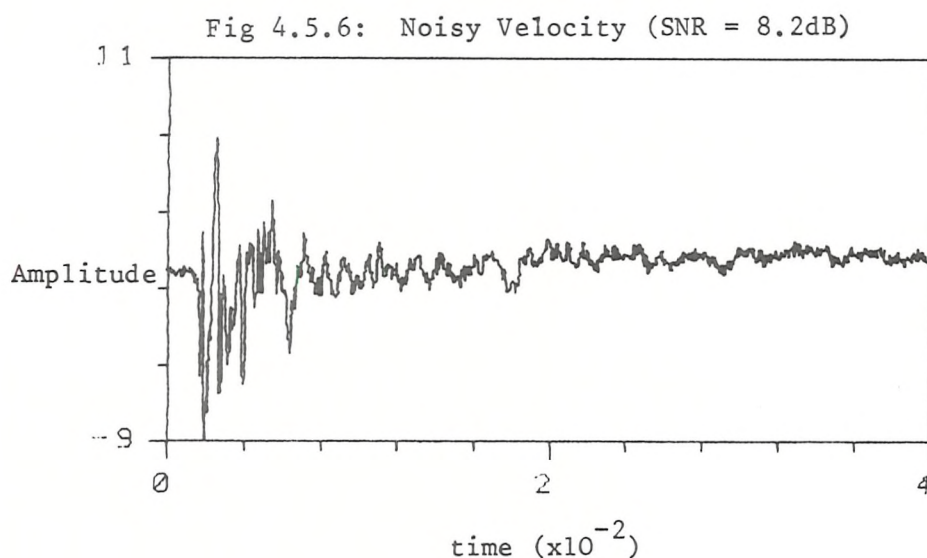
Table 4.5.1 gives values of  $I$  for varying  $(q/r)$ :

$r$	$I$
$1 \times 10^{-7}$	0.96184
$1 \times 10^{-8}$	0.82423
$1 \times 10^{-9}$	0.49625
$1 \times 10^{-10}$	0.08963

Table 4.5.1

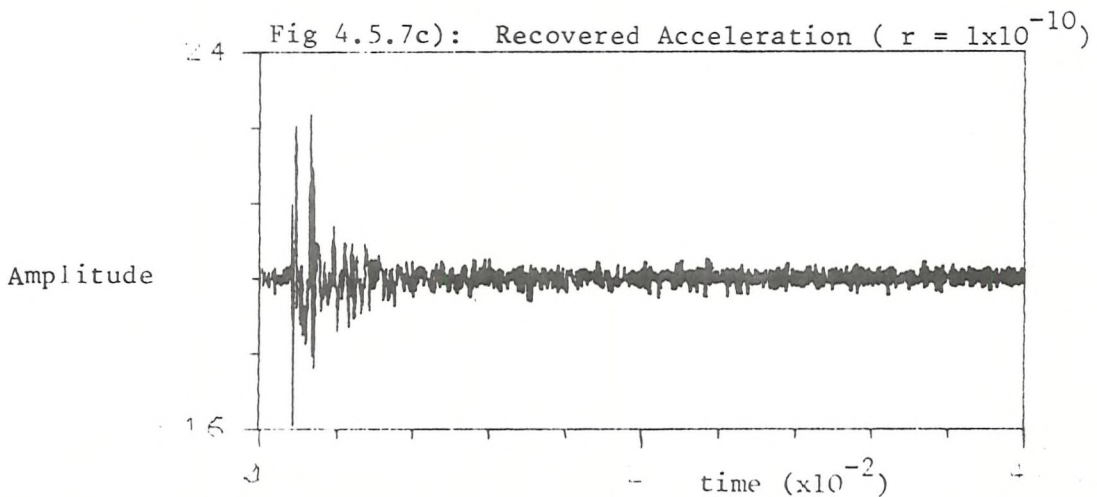
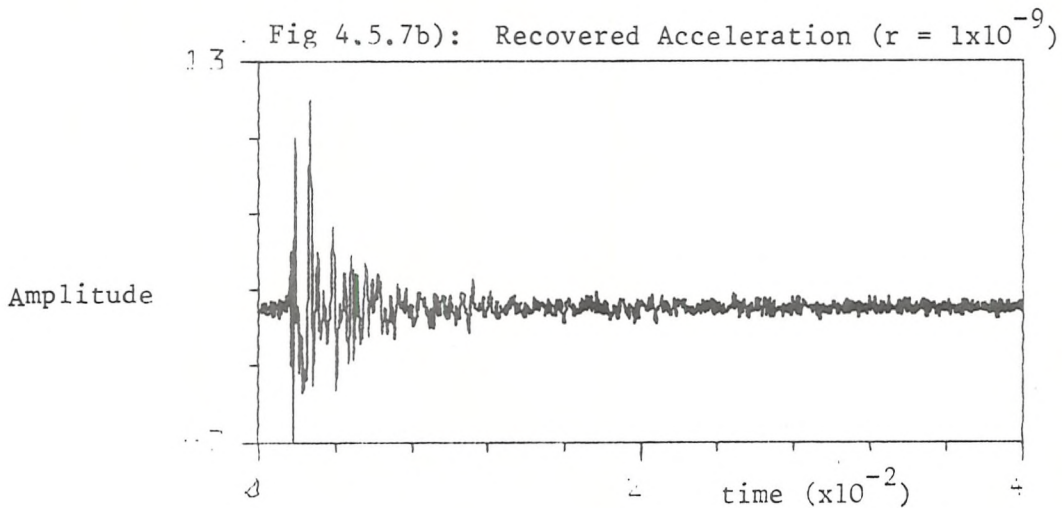
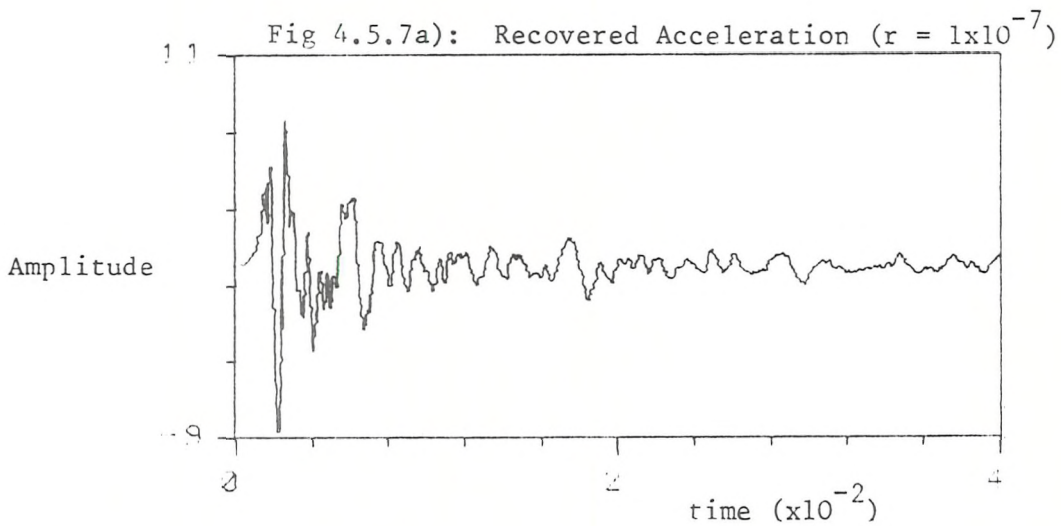
which confirms the tendency for the accuracy to increase as  $r$  decreases.

b) Noise corrupted synthetic. The synthetic velocity meter output (Figure 4.5.4b) was corrupted by additive Gaussian white noise (Figure 4.5.6) to give an average SNR of 8.2dB. (Note, average SNR definitions are used for computation in place of the instantaneous definition of equation 4.2.9, see also Chapter 5). This data was used as input for the optimal control deconvolution.





The resulting approximate deconvolved accelerations obtained using values of  $r = 1 \times 10^{-7}$ ,  $r = 1 \times 10^{-9}$  and  $r = 1 \times 10^{-10}$  are shown in Figure 4.5.7a, b, and c respectively. It is clear from these results that increasing  $q/r$  generally increases the high frequency noise in the resulting recovered acceleration.

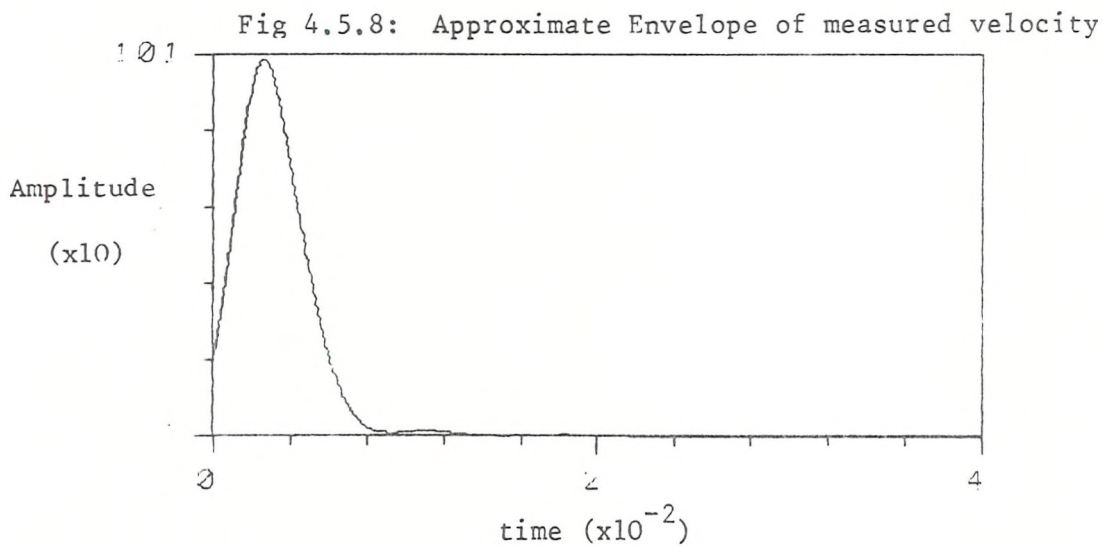


The corresponding values for I (see previous section) are given in Table 4.5.2.

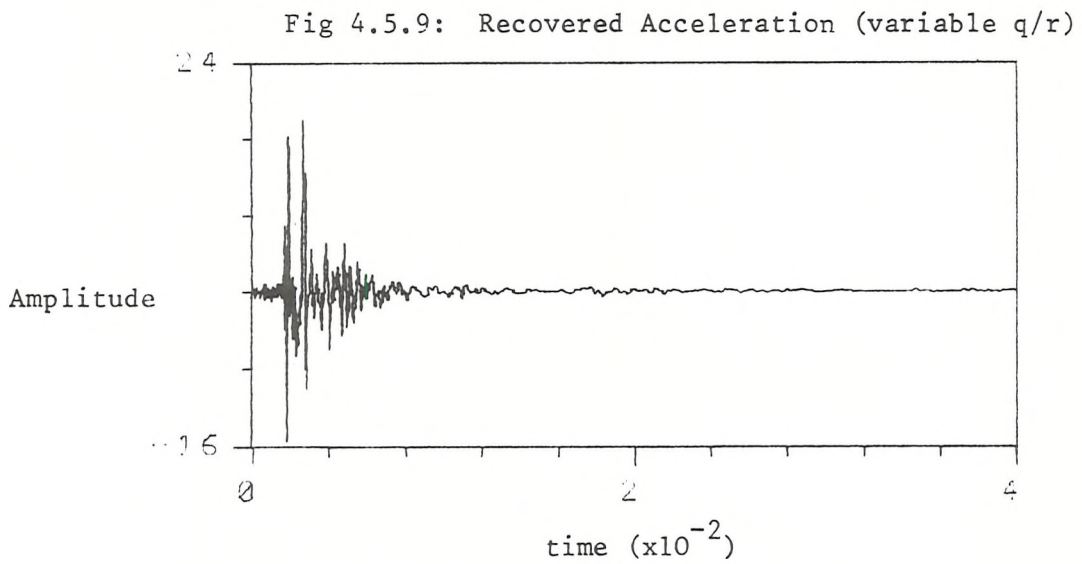
r	I
$1 \times 10^{-7}$	0.962
$1 \times 10^{-8}$	0.825
$1 \times 10^{-9}$	0.522
$1 \times 10^{-10}$	0.535

Table 4.5.2

From this the optimum value appears to be around  $1 \times 10^{-9}$ . The variable q/r method described in Section 4.2 was then applied to the data. From equation (4.2.10) the method requires the envelope of the measured velocity. This was computed (approximately) and is shown in Figure 4.5.8.



q/r was then chosen according to equation (4.2.10) with constant of proportion, K, set at 0.00001. The recovered acceleration obtained in this way is shown in Figure 4.5.9. As is clear from this figure the recovery is considerably better than any of those obtained using constant (q/r) ratios (Fig 4.5.7). The value for I in this case was 0.235, which also demonstrates this superiority, (c.f. Table 4.5.2).



c) Experimental Data. An experiment was conducted in which an accelerometer and velocity meter were mounted on a shaker table which was driven with a swept sine input (from 2Hz to 100Hz in 2 seconds), see Fig (4.5.10).

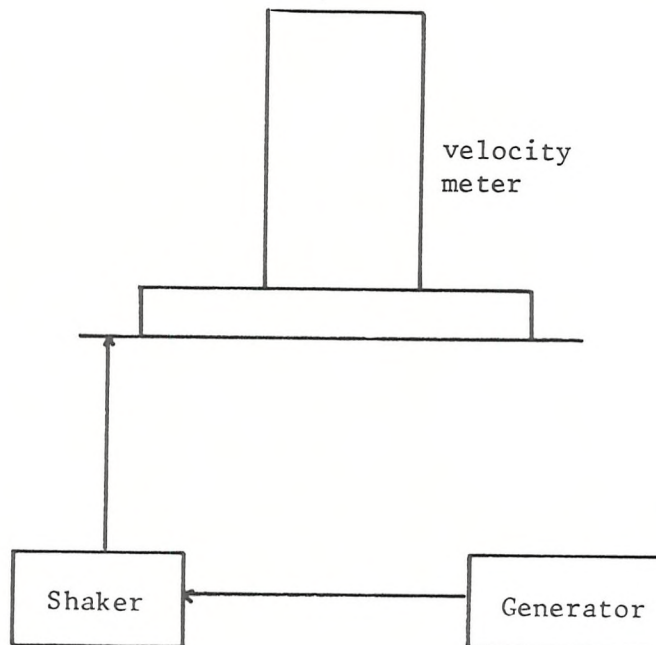


Figure 4.5.10: Experimental set up for Velocity Meter

The response obtained from the accelerometer and from the velocity meter are shown in Figure 4.5.11(a) and (b) respectively.

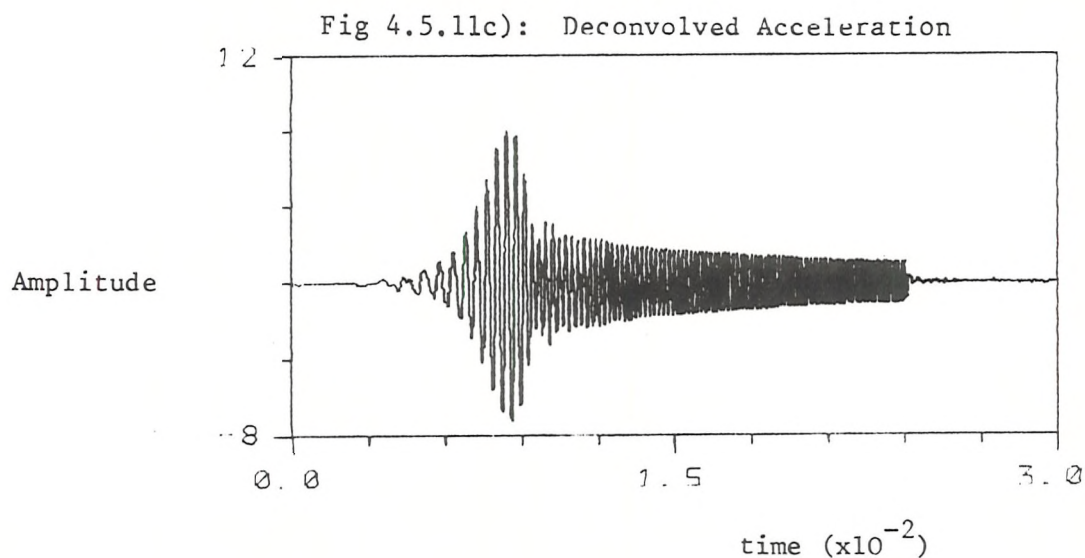
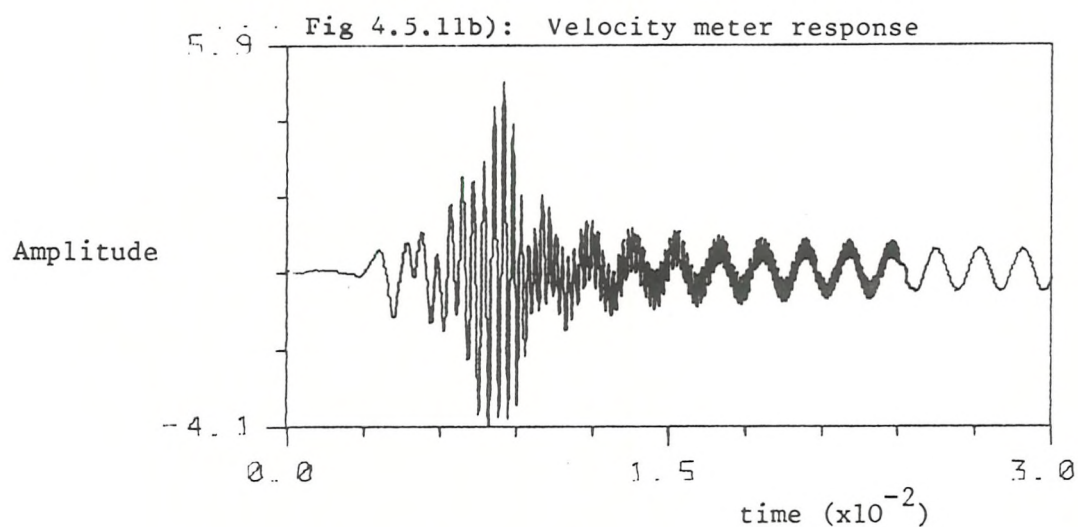
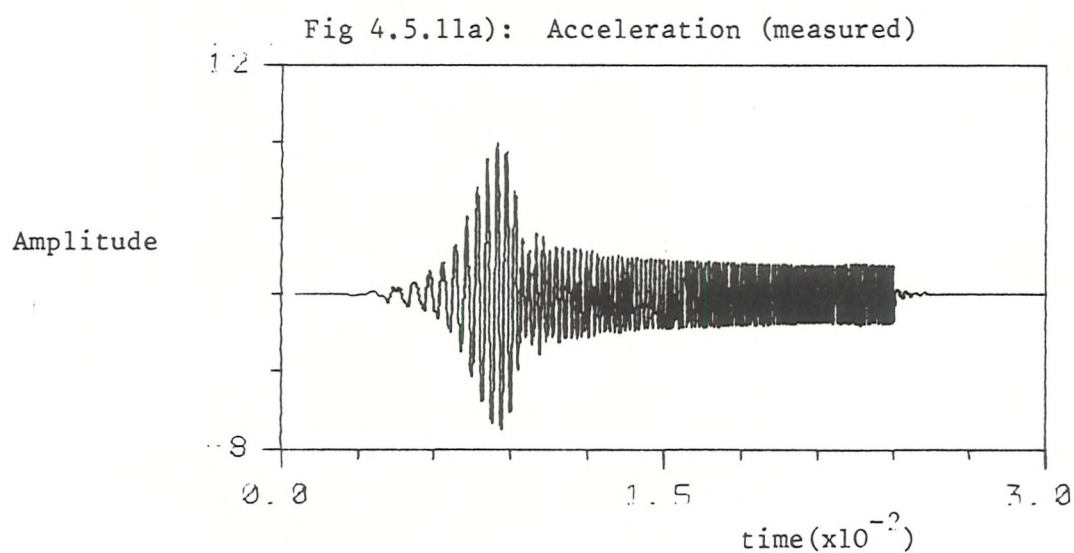




Figure 4.5.11(c) shows the result of applying the optimal control deconvolution method to the velocity meter response using a suitable constant for the ratio  $q/r$  ( $1 \times 10^5$ ). The two signals of Figures 4.5.11(a) and (c) are also shown expanded and overlaid in Figure 4.5.12.

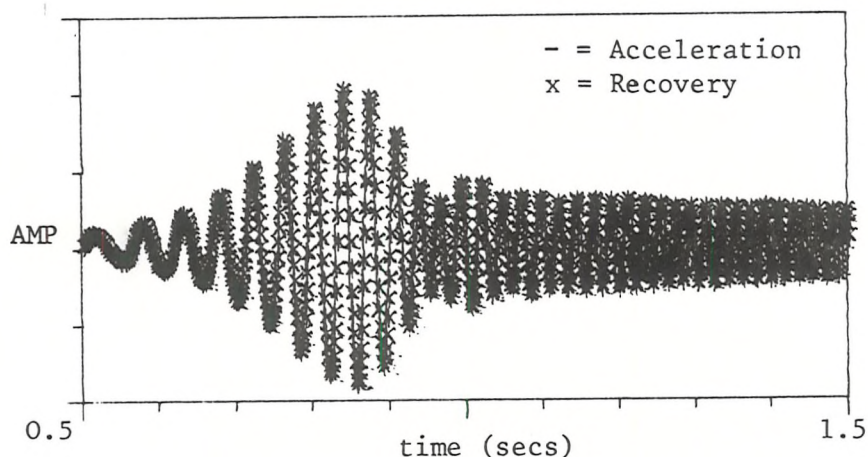


Figure 4.5.12: Acceleration and Deconvolved Recovery

The results show a high degree of agreement between the accelerometer measurement and the deconvolved approximation. This demonstrates both the effectiveness of the deconvolution technique and the close fit of the assumed model.

#### 4.6 CONCLUSIONS

The optimal control method, due to Thomas, described in this chapter provides a novel approach to deconvolution. By reformulating the problem in terms of tracking, the usual deconvolution problem - the synthesis of an inverse system - is avoided entirely. Whether this is advantageous or not depends on the particular application. There are other properties of the method which will also determine its suitability for any particular application. The method has the obvious disadvantage that a state-space description of the system under investigation is required. Also the solution is computationally demanding, both in terms of operations and storage, and can only be performed in an

acausal manner. However, the method also has significant advantages over conventional deconvolution techniques. In the first place, the ease with which non-stationary systems may be incorporated is a big advantage. Another advantage of the method is the flexibility which stems from the form of the functional and in particular the parameters  $q$  and  $r$ . These parameters have a crucial influence on the performance of the method. In the noise-free case it is desirable to have the ratio of  $q$  to  $r$  as large as possible - to penalise error as heavily as possible. However, it was shown that for fixed  $r/q$  the influence of these parameters is directly analogous to the prewhitening method of noise reduction discussed in Chapter 3. As such it is obviously desirable to reduce  $q/r$  (that is, increase the prewhitening) when the signals are noise corrupted.

As a further development of this theme a method, for certain classes of signals, of varying the ratio of  $q/r$  in accordance with changing SNR was evolved. Although not strictly justifiable in terms of the theory, this approach was intuitively reasonable and was found to work well in practice.

Many of the above properties were illustrated using a velocity meter as an example. The method produced good results on both synthetic and real data and the variation of  $q/r$  provided a good technique for handling noisy measurements. A further application of this method (to seismic data) is considered in Chapter 8.

## CHAPTER 5

### GENERALISED COMB FILTERING

#### 5.1 Introduction

In this chapter a novel technique for signal-to-noise enhancement of a certain class of signals will be developed. The type of signals considered are those which consist of a series of slowly time-varying wavelets which recur at approximately constant intervals. This pseudo-periodic structure is assumed to be corrupted by additive random noise. No further apriori information about the signal or noise is assumed. Signals of this form occur frequently in applications. In this chapter the technique proposed is applied to voiced speech sections and in Chapter 9 a further application (to seismic data) is considered. The technique proposed is based on the concept of a generalised comb filter where each 'tooth' of the usual comb structure (Figure 5.1.1a) is itself an adaptive linear filter (Figure 5.1.1b). It is well known that signal averaging (comb filtering) provides a simple and effective method for enhancing the signal-to-noise ratio (SNR) when signal and noise statistics are unknown. However, the comb suffers from two principal limitations, namely: i) successive measurements must contain exact replicas of the signal component and ii) it must be possible to align these signal components precisely.

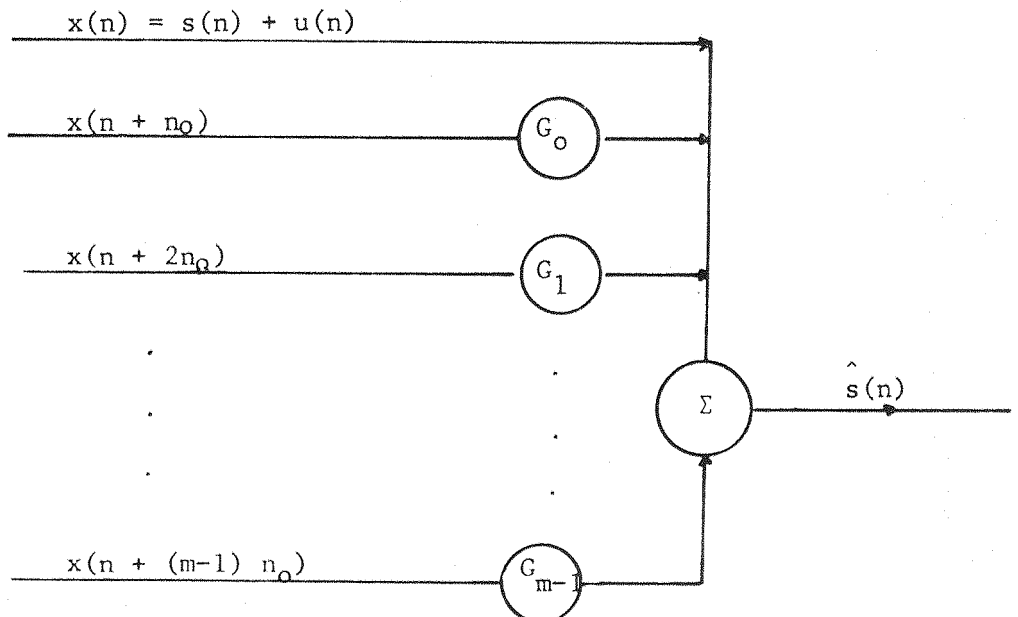


Fig 5.1.1a): Comb Filter Structure

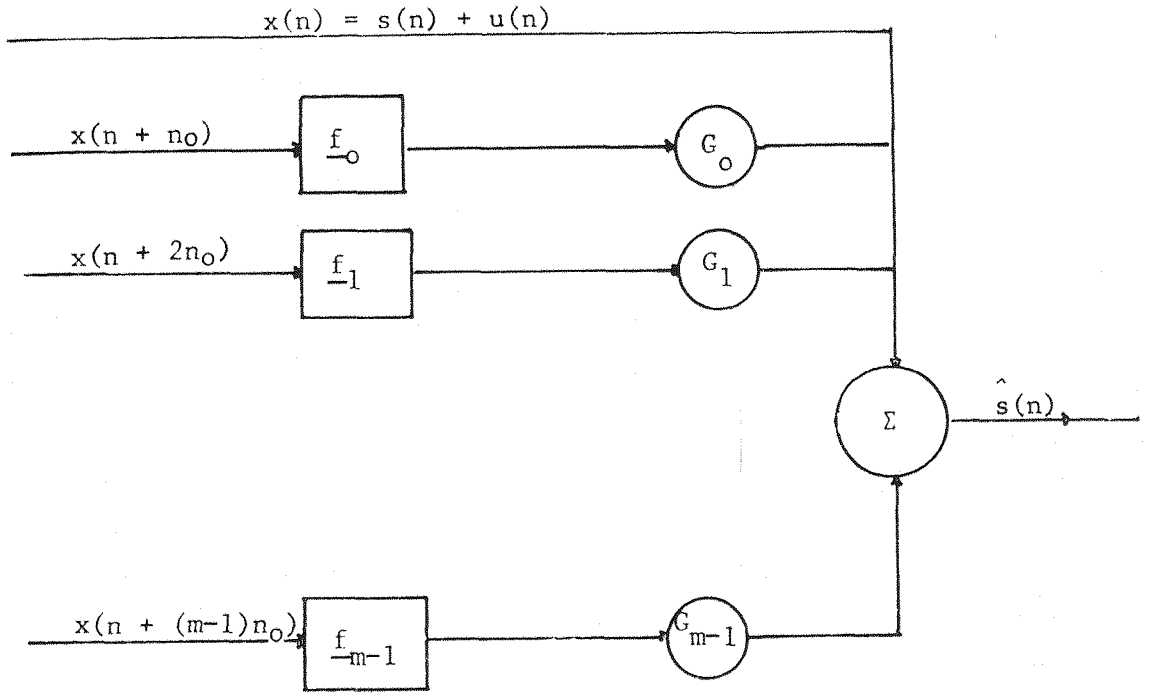


Fig 5.5.1b): Generalised Comb Filter Structure

That is, for signal averaging the inputs must have the form:

$$x(n + kn_0) = \alpha^k s(n) + v(n + kn_0) \quad (5.1.1)$$

where  $s(n)$  is the signal,  $v(n)$  the noise and where  $\alpha$  and  $n_0$  are constants.

The aim in proposing the generalised comb filter is to overcome (at least to some extent) both of the above constraints. The generalised comb filter is designed to give SNR improvement for more general signals of the form:

$$x(n) = s(n) + v(n) \quad (5.1.2)$$

$$x(n + kn_0) = h(n, n + kn_0) * s(n) + v(n + kn_0)$$

where  $h(n, n + kn_0)$  is a linear, possibly time-variant system, and where in addition;  $n_0$  need not be known exactly. A further important property of the generalised comb (in common with the simple comb) is that no apriori knowledge of the statistics of the noise is required. As will be seen, the combination of these properties gives the generalised comb filter considerable advantages over existing techniques, and makes it a useful approach in several applications. Furthermore it will also be demonstrated that the generalised comb filter can be used in a multi-



channel capacity. An application of the filter in this mode (to seismic data) will be considered in Chapter 9.

## 5.2 Preliminaries: Signal Models and SNR Definitions

### 5.2.1 Signal Models

The signal-to-noise ratio enhancing method proposed in this chapter is applicable to signals which consist of a series of slowly time-varying wavelets recurring at roughly equal intervals,  $n_0$  and embedded in random noise. It is assumed that the variation of the wavelets can be described by the action of a linear filter, that is:

$$x(n) = s(n) + v(n) \quad (5.1.2)$$

$$x(n + kn_0) = h(n, n + kn_0) * s(n) + v(n + kn_0)$$

(see Figure 5.2.1)

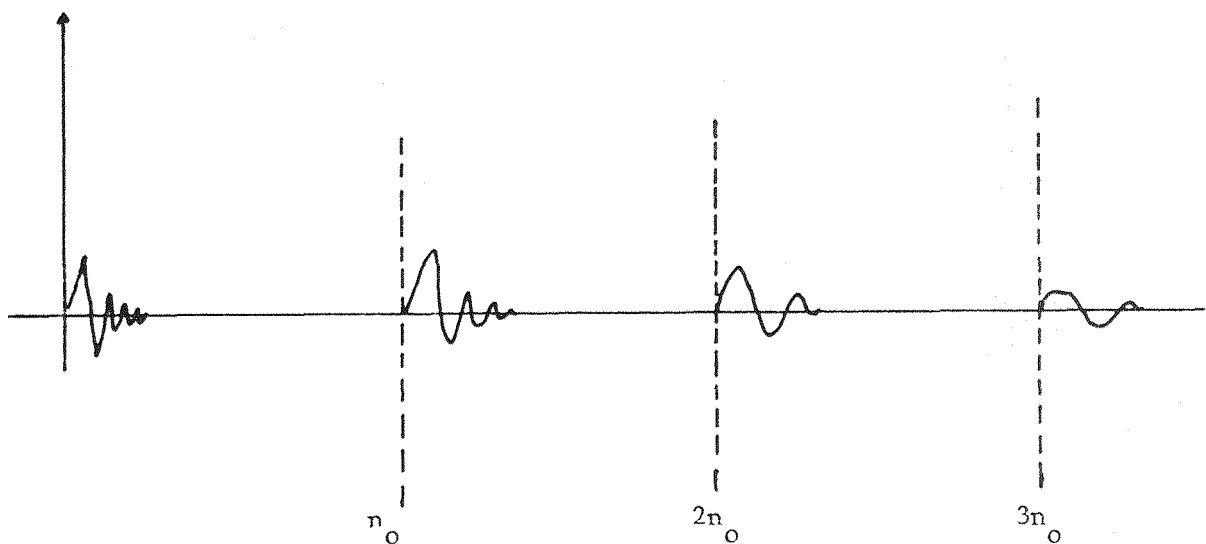


Figure 5.2.1: Signal Model

where  $s(n)$  is the signal component and is considered to be deterministic.

$v(n)$  is a noise term which, unless otherwise stated, will be taken to be stationary and zero mean, and  $h(n, n_1)$  is a linear system, possibly time-varying. That is, the measurement  $x(n + kn_0)$  consists of a linearly filtered version of the signal component  $s(n)$  embedded in random noise  $v(n + kn_0)$ , (possibly correlated with  $v(n)$ ). In general, it is assumed that the system  $h(n)$ , the statistics of  $v(n)$ , and the form of the signal component are all unknown. The interval,  $n_0$ , will generally be assumed to be known only approximately.

It will be seen that these assumptions render the classical signal enhancement techniques ineffective in this case. An example of a signal which may be described by this model is provided by speech signals (see Section 5.5).

### 5.2.2 Signal to Noise Ratio Definitions

The concern in this chapter is not with signal detection/extraction but with the signal-to-noise ratio (SNR) enhancement (contrast this with matched filtering, for example, see Section 5.3). As such it is important to define SNR carefully, in a manner consistent with this objective. The main distinction between detection/extraction and enhancement is that in detection, distortion of the signal waveform is acceptable (desirable even), whereas in enhancement the aim is to reduce the variance of the noise, whilst preserving the signal waveform. Accordingly, given a measurement:

$$x(n) = s(n) + v(n)$$

a definition, consistent with the aims of SNR enhancement is:

$$(\text{SNR}_{x_n}) = \frac{|s(n)|}{\sigma_v} \quad (5.2.1)$$

where  $\sigma_v^2 = E\{v(n)v(n)\}$

and as usual,  $E$  denotes expectation across the ensemble.

More generally, if  $x(n)$  contains a distortion component,  $d(n)$  say, then the definition is modified to take account of the bias implied by this term, to:

$$(\text{SNR}_{x_n}) = \frac{|s(n)|}{(\text{mean square error of } x(n))^{\frac{1}{2}}} \quad (5.2.2)$$

$$\begin{aligned} \text{where mean-square error of } x(n) &= E\{s(n) - x(n)\}^2 \\ &= d^2(n) + \sigma_v^2 \end{aligned} \quad (5.2.3)$$

$$\text{Hence: } (\text{SNR}_{x_n}) = \frac{|s(n)|}{(d^2(n) + \sigma_v^2)^{\frac{1}{2}}} \quad (5.2.4)$$

Note that point SNR definitions are preferred to interval definitions. This is because with an interval definition it is possible to obtain a solution to the problem which satisfies the criterion of improved SNR over the interval, but which is qualitatively unacceptable due to the presence of enhanced distortion at specific points. However, point definitions have the obvious disadvantage that  $(\text{SNR})_{x_n}$  will be zero if the signal component is instantaneously zero, so that some care is necessary in interpreting these values. In any case it is not suggested that the definition be adopted for numerical purposes, only as a design tool for developing and assessing SNR enhancement schemes. For simulation purposes some averaging of values is clearly necessary in order to obtain any meaningful results. Other aspects must then be assessed qualitatively.

### 5.3 Review of classical SNR enhancement techniques

#### 5.3.1 Introduction

In this section the aim is to give a brief review of some of the classical SNR enhancement techniques as applied to digital data. The aim is partly to demonstrate the inapplicability of these techniques (for various reasons) to signals of the type considered here (see Section 5.2), but also to illustrate the relationship between these approaches and the method to be proposed in Section 5.4.

### 5.3.2 Signal Averaging

One of the most straightforward approaches to SNR enhancement is signal averaging [12]. This technique is applicable when the signal has a repetitive (non overlapping) structure, of the form:

$$\begin{aligned} x(n) &= s(n) + v(n) \\ x(n + kn_0) &= \alpha^k s(n) + v(n + kn_0) \\ ; k &= 1, \dots, M-1 \end{aligned} \quad (5.3.1)$$

where  $n_0$  is a known constant,  $\alpha$  is a scale factor and  $E\{v(n)v(n + kn_0)\} \equiv 0$  ;  $k \neq 0$ .

If these representations are now averaged to form:

$$y(n) = \frac{1}{M} \sum_{k=0}^{M-1} x(n + kn_0) \quad (5.3.2)$$

then, in transfer function form, this is

$$\begin{aligned} Y(z) &= \frac{1}{M} \{1 + z^{-n_0} + z^{-2n_0} + \dots + z^{-(M-1)n_0}\} X(z) \\ Y(z) &= \frac{1}{M} \left\{ \frac{1 - z^{-Mn_0}}{1 - z^{-n_0}} \right\} X(z) \end{aligned} \quad (5.3.3)$$

which is a comb filter.

The resulting SNR gains may be evaluated by considering a single addition:

$$y(n) = \frac{1}{2} \{x(n) + x(n + n_0)\}$$

so that

$$E\{y^2(n)\} = \frac{1}{4} [(1+\alpha)^2 s^2(n) + 2\sigma_v^2] \quad (5.3.4)$$

where, as usual,  $E$  denotes expectation taken across the ensemble.

Now, using the SNR definition (5.2.1)

$$(\text{SNR}_y) = \frac{(1+\alpha) s(n)}{\sqrt{2} \sigma_v} \quad (5.3.5)$$

assuming for convenience,  $s(n) \geq 0$ ,  $\alpha \geq 0$ .

From which it follows that provided ( $s(n) \neq 0$ ):

$$\frac{(\text{SNR}_y)}{(\text{SNR}_x)} = \frac{(1+\alpha)}{\sqrt{2}} \quad (5.3.6)$$

Hence, averaging improves the SNR if

$$\frac{(1+\alpha)}{\sqrt{2}} > 1 \quad \text{or} \quad \alpha > \sqrt{2} - 1$$

It follows in general that the improvement obtained by averaging ( $N-1$ ) such representations is given by

$$\left( \frac{1 - \alpha^{N-1}}{1 - \alpha} \right) \cdot \frac{1}{\sqrt{N-1}}$$

From this a condition for averaging of the  $N^{\text{th}}$  representation to produce further improvement is given by:

$$\frac{\sqrt{N}}{\sqrt{N-1}} < \frac{1 - \alpha^N}{1 - \alpha^{N-1}} \quad (5.3.7)$$

The most important factors in determining the success or failure of signal averaging are: (a) that the signals should fit the assumed model and most critically (b) that the interval,  $n_0$ , should be exactly known. In a later section the effects of signal averaging on signals of a more general form will be considered.

### 5.3.3 Matched and Output Energy Filtering

Given a measurement:

$$x(n) = s(n) + v(n)$$

If the signal  $s(n)$  is assumed known and  $v(n)$  is a stationary zero mean process with known properties, then the matched filter eg [69].

is a filter designed to maximise the ratio

$$\rho(n_1) = \frac{|y_s(n_1)|}{\sqrt{E\{y_v(n_1)^2\}}} \quad (5.3.8)$$

where

$$\begin{aligned} y(n) &= y_s(n) + y_v(n) \\ &= f(n) * s(n) + f(n) * v(n) \end{aligned} \quad (5.3.9)$$

The solution for the matched filter is developed using Lagrange multipliers. The solution is then obtained from a set of Normal Equations (see Chapter 2) as:

$$\sum_{i=0}^{L-1} f(i) R_{vv}(k-i) = s(n-k) \quad (5.3.10)$$

$$k=0, 1, \dots, L-1$$

where  $N$  is the filter length, and  $R_{vv}(k)$  is the auto-correlation of  $v$ .

In the special case where  $v(n)$  is white, it is clear by inspection of (5.3.10) that the filter is simply a time reversed version of the signal waveform. It is important to note that the matched filter is a technique for detection/extraction rather than enhancement (obviously, since the signal is already known). This is reflected in the choice of signal-to-noise ratio (compare this with the definition of (5.2.3)).

By contrast, the output energy filter [81] is a filter which is designed to maximise the output power when signal alone is present and minimise the output when noise alone is present. The aim is to maximise:

$$\lambda = \frac{\text{Energy of the filtered signal}}{\text{Power of the filtered noise}} \quad (5.3.11)$$

where from (5.3.9):

$$\text{filtered signal} = f(n) * s(n) = \sum_{k=0}^{L-1} f(k)s(n-k)$$

and hence the energy of the filtered signal is:

$$\sum_{k=0}^{L-1} \sum_{j=0}^{L-1} f(k)f(j)R_{ss}(k-j)$$

and similarly for the power of the filtered noise, so that

$$\lambda = \frac{\sum_{k=0}^{L-1} \sum_{j=0}^{L-1} f(k)f(j)R_{ss}(k-j)}{\sum_{n=0}^{L-1} \sum_{j=0}^{L-1} f(k)f(j)R_{vv}(k-j)} \quad (5.3.11a)$$

The solution to the problem of maximising  $\lambda$ , is again obtained using Lagrange multipliers. The main problem with this technique, however, is that the correlations of both signal and noise must be known.

#### 5.3.4 Wiener Filtering

One of the most widely used methods of SNR enhancement is based on the use of the Wiener filter eg [69]. Given a signal:

$$x(n) = s(n) + v(n)$$

where both  $s(n)$  and  $v(n)$  are stationary, zero mean processes, then the Wiener-Kolmogorov theory gives a linear time invariant operator  $f(n)$ , which minimises:

$$I = E\{ (d(n) - y(n))^2 \} \quad (5.3.12)$$

where  $y(n)$  is the filter output and  $d(n)$  is any desired signal. The solution to this problem is directly analogous to the least-squares shaping filter of infinite length which was described in Chapter 2 (and which stems from this theory), except that the signals involved are random processes.

In particular for enhancement the desired signal  $d(n) = s(n)$  and the solution is obtained from the infinite set of normal equations:

$$[R_{ss}(z) + R_{vv}(z)] F(z) = R_{ss}(z) \quad (5.3.13)$$

where  $R_{ss}(m) = E\{s(n)s(n+m)\}$  and assuming  $s(n)$  and  $v(n)$  are uncorrelated; so that

$$F(z) = \left( \frac{1}{1 + \frac{R_{vv}(z)}{R_{ss}(z)}} \right) \quad (5.3.14)$$

Note that similar operators which are restricted to be finite and/or causal can also be constructed, using the methods discussed in Chapter 2.

However, from (5.3.13) it is clear that the design of all Wiener operators requires apriori information on the spectral properties of both  $s$  and  $v$ .

### 5.3.5 Adaptive Noise Cancellation

The concept of adaptive noise cancellation (ANC) was introduced by Widrow et al [117]. In their paper the authors argued that given some measurement  $d(n)$  which is composed of a signal component  $s(n)$  and a noise component  $v(n)$ , where  $s(n)$  and  $v(n)$  are uncorrelated

$$d(n) = s(n) + v(n) \quad E\{s(k)v(j)\} \equiv 0 \quad ; \quad v_{j,k}$$

together with a second measurement consisting of a noise  $v_1(n)$  correlated with  $v(n)$  but uncorrelated with  $s(n)$ . Then the second measurement may be filtered adaptively to produce a replica of the noise component  $\hat{v}(n)$ , which may then be used to cancel this component from  $d(n)$ . The system is depicted in Figure (5.3.1).



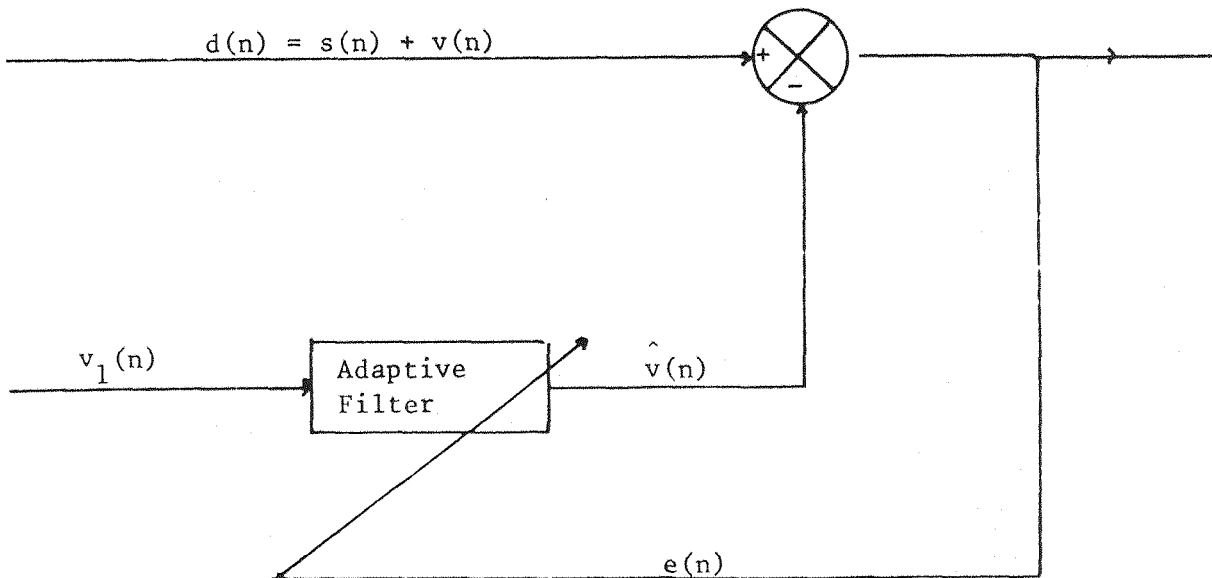


Fig 5.3.1: Adaptive Noise Cancelling System

The adaptive filter used is the LMS algorithm of Widrow and Hoff (see Chapter 2).

In their original paper Widrow et al argued that the adaptive filter would be able to exploit the correlation between  $v_1(n)$  and  $v(n)$  to track the noise, but would be unable to track the signal component. Thus, the filter output would be approximately equal to  $v(n)$  and in turn:

$$e(n) \approx s(n).$$

This argument is an over simplification of the filter operation (see Chapter 2) but serves as a reasonable approximation for illustrative purposes. Adaptive noise cancelling will be considered in much greater detail in the next chapter, for the particular problem of narrowband interferences.

## 5.4 Generalised Comb Filtering

### 5.4.1 Introduction

It is clear from the preceeding section that, for a variety of reasons, the classical approaches to signal enhancement cannot

be directly applied to signals of the type described in Section 5.2. In the case of matched, output energy and Wiener filtering the techniques cannot be used because they require apriori information about the signal and noise which is here assumed unavailable. Adaptive noise cancelling is not directly relevant because no secondary noise source is available. Nevertheless, the approach proposed here contains elements which are similar to ANC but with the roles of signal and noise interchanged. Signal averaging cannot be directly applied because of both the time-varying nature of the waveform and because of approximate knowledge about the spacing between successive repetitions.

Some attempts to achieve SNR enhancement for the class of signals considered here have been made and these will be discussed as they arise. The approach proposed is to use a generalised comb filter structure, where the individual teeth of the comb are themselves replaced by LMS adaptive digital filters (adaptive correlators). As such there are two separate aspects to the overall scheme, namely the combing (averaging) and the adaptive filtering and these will be discussed separately in the following sections, prior to consideration of the complete scheme in Section 5.4.4.

#### 5.4.2 Adaptive Signal Enhancement

In Section 5.3.5 it was seen that the method of adaptive noise cancellation provides a technique for attenuating the noise component of a signal when a second measurement consisting entirely of a correlated noise source is available. The adaptive signal enhancement technique to be described here, as a part of the generalised comb filter, is a form of adaptive noise cancellation with the roles of signal and noise interchanged. Given a signal  $x(n)$  of the form of equation (5.1.3), where for the moment it is assumed that  $E\{v(n)v(n + kn_0)\} = 0$  for  $k \neq 0$ ,  $x(n)$  and  $x(n + kn_0)$  are supplied as reference and primary inputs respectively to an adaptive noise cancelling system (see Figure 5.4.1). The hope is that the filter will exploit the correlation between the signal components, as expressed by the linear system  $h$ , to cancel

these at the output. In order for this to occur the filter output  $y$  must be a replica of the signal component of the primary. Obviously the extent to which this occurs depends on the extent to which the adaptive filter tends to mimic the system  $h$  (or its inverse depending on which measurement is primary and which reference).

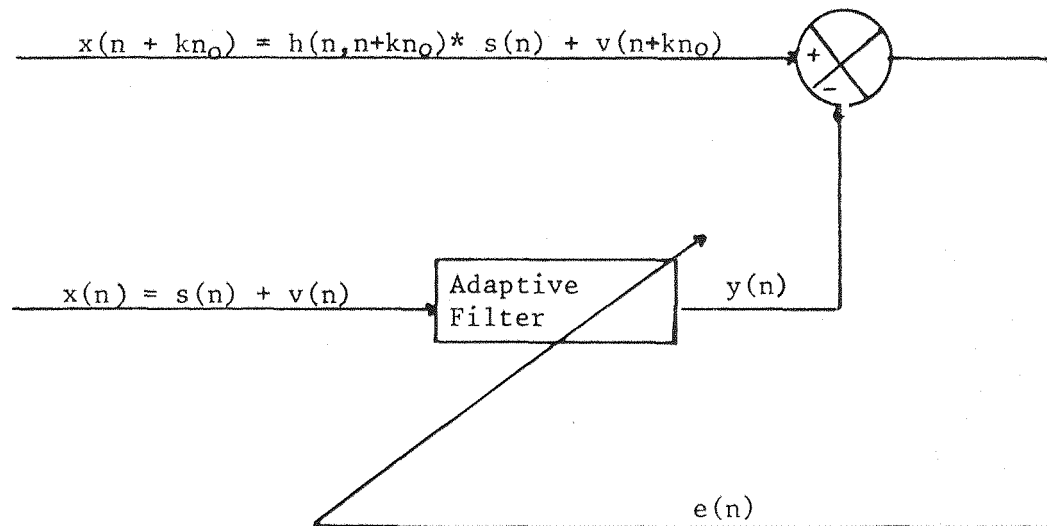


Fig 5.4.1: Adaptive Signal Enhancement Structure

Now, from the figure,

$$e(n) = h(n, n + kn_0) * s(n) + v(n + kn_0) - y(n) \quad (5.4.1)$$

where  $y(n) = f(n) * x(n)$

Squaring (5.4.1) and taking expectation yields:

$$E\{e^2(n)\} = \sigma_v^2 + (h(n + kn_0) * s(n) - y(n))^2 \quad (5.4.2)$$

Recall from Chapter 2 that the LMS filter which drives the adaptive noise cancelling system is designed to minimise  $E\{e^2(n)\}$ . From (5.4.2) it is clear that since  $\sigma_v^2$  is constant,  $E\{e^2(n)\}$  is minimised when  $(h(n, n + kn_0) * s(n) - y(n))^2$  is minimised, that is when the system output is the best least-squares estimate of  $h(n, n + kn_0) * s(n)$ . Obviously the performance of the system in attaining this goal is determined by the behaviour of the adaptive filter. From Chapter 2 it is known that, subject to certain restrictions, the steady-state response of the LMS filter tends, in the mean, towards the fixed Wiener filter. One way of analysing the filter behaviour is to assume that such a steady-state solution

exists and obtain the appropriate Wiener filter. Such an approach has been used in an analogous context by Widrow et al [117]. Using this method the adaptive filter response is approximated by an ideal Wiener filter (infinite and, in general, two sided). Obviously, this cannot take into account the issues of finite filter length and causality which are important in practical applications. Nor, indeed, does this approach account for factors such as misadjustment which are related to the adaptive nature of the system,  $h$ , (all of which are considered in greater detail in Chapter 2). Nevertheless, the resulting expressions can provide useful approximations to the behaviour of the adaptive system. Using this approach an approximation to the adaptive filter response is given by:

$$F(z) = \frac{H(z)}{1 + \frac{R_{vv}(z)}{|S(z)|^2}} \quad (\text{VIII.8})$$

where  $R_{vv}(m) = E\{v(n)v(n+m)\}$  etc.

$$\text{Now, } R_{yy}(z) = |F(z)|^2 R_{xx}(z) \quad * \quad (\text{VIII.5})$$

where the input spectrum is given by

$$R_{xx}(z) = |S(z)|^2 + R_{vv}(z)$$

Hence the output spectrum is given by

$$R_{yy}(z) = \frac{|H(z)|^2 |S(z)|^2}{1 + \frac{R_{vv}(z)}{|S(z)|^2}} \quad (\text{VIII.9})$$

To facilitate the evolution of the response, define the signal-to-noise density ratio,  $\rho$ , (analogously, though not identically to [117]), for a signal

$$x(n) = s(n) + v(n)$$

$$\text{as } \rho_x(z) = \frac{|S(z)|^2}{R_{vv}(z)} \quad (\text{VIII.10})$$

\* It is noted that these equations are valid on the unit circle, ie, where  $F(Z^{-1}) = F^*(Z)$ .

As such  $\rho$  is a way of expressing the signal-to-noise ratio of  $x$  as a function of frequency.

$\rho_y(z)$  may be evaluated (see Appendix VIII) as:

$$\rho_y(z) = \frac{R_{xx}(z)}{R_{vv}(z)} \quad (\text{VIII.13})$$

So that the output signal-to-noise ratio (as a function of frequency) is determined by the ratio of the input spectrum to the noise spectrum. For frequencies where the noise spectrum is low, the signal-to-noise density is high and conversely, when the input noise  $v$  is correlated over  $kn_0$  samples the situation is more complex to analyse. The filter enhances events which are correlated, and this applies as much to noise as to signal. The result is that correlated noises degrade the enhancement and that the extent of the degradation is determined by the ratio of the correlation between the noises to the correlation between the signals.

#### 5.4.3 Generalised Signal Averaging

In Section 5.3.2 the main results of signal averaging for two or more representations of the same signal embedded in white noise were restated. In this section the effects of averaging when the signals have a more complex form are investigated:

Given signals

$$y_0(n) = s(n) + v_0(n) \quad (5.4.3)$$

and  $y_1(n) = \alpha s(n) + d(n) + v_1(n)$

where  $\alpha$  is a constant (scale factor),  $d(n)$  is a deterministic distortional component and

$$\begin{aligned} E\{u_0(n)u_0(n)\} &= E\{u_1(n)u_1(n)\} = \sigma_u^2 \\ E\{u_0(n)u_1(n)\} &= k\sigma_u^2 \quad k < 1 \end{aligned}$$

Now forming

$$y(n) = \frac{1}{(1+\alpha)} \{ y_0(n) + y_1(n) \}$$

(the scale factor simplifies the analysis, but of course cannot affect the resulting SNR).

Then, using the definition (5.2.2), it can be shown (Appendix IX) that,

$$\left( \frac{\text{SNR}_y}{\text{SNR}_{y_0}} \right) > 1 \quad \text{if} \quad \alpha > \left\{ 2(1+k) + \frac{d^2(n)}{\sigma_u^2} \right\}^{\frac{1}{2}} - 1 \quad (\text{IX.8})$$

That is, the averaged representation has an improved SNR only if  $\alpha$  satisfies this equation. However, if a gain,  $G$ , is introduced so that

$$y(n) = \frac{1}{(1+G\alpha)} \{y_0(n) + Gy_1(n)\}$$

then

$$\left( \frac{\text{SNR}_y}{\text{SNR}_{y_0}} \right) = \frac{(1 + G\alpha)}{\left\{ G^2 \frac{d^2(n)}{\sigma_u^2} + 1 + G^2 + 2Gk \right\}^{\frac{1}{2}}} \quad (\text{IX.13})$$

Furthermore, it is possible to obtain an optimal value for  $G$  as

$$G_{\text{opt}} = \frac{(\alpha-k)}{\left\{ \frac{d^2(n)}{\sigma_u^2} + (1-k\alpha) \right\}} \quad (\text{IX.14})$$

and it follows that with this choice for  $G$  the corresponding expression for  $G_{\text{opt}}$  is given by equation (IX.15) from which it can be shown (Appendix IX) that

$$\left( \frac{\text{SNR}_y}{\text{SNR}_{y_0}} \right) > 1 \quad \text{for any finite distortion}$$

provided only that  $\alpha > k$ .

Note that, in the simple case of signals in white noise discussed in Section 5.3.2, the results given there may be recovered here by setting  $k = d(n) = 0$  in equation (IX.8), so that for SNR improvements  $\alpha > \sqrt{2} - 1$  which is the result given in Section 5.3.2. If a gain,  $G$ , is used then the optimal gain is obtained by setting  $k = d(n) = 0$  in (IX.14) as:

$$G_{\text{opt}} = \alpha$$

and with this choice of gain

$$\frac{\text{SNR}_y}{\text{SNR}_{y_0}} = (1+\alpha)^{\frac{1}{2}} > 1 \quad \forall \quad \alpha$$

#### 5.4.4 Filter Operation

The overall operation of the generalised comb filter is a combination of the adaptive filtering and averaging operations discussed in the previous two sections. The structure of the filter is depicted in Figure 5.1.1b), where  $\underline{f}_0, \dots, \underline{f}_{M-1}$  are the set of  $M$  adaptive filters and  $G_0, G_1, \dots, G_{M-1}$  are averaging gains. That is the filter is a set of  $M$  adaptive signal enhancers of the form discussed in Section 5.4.2, whose outputs are subsequently averaged, with suitable gains,  $G_i$ .

The  $M$  inputs are obtained from different points on a single input signal  $x(n)$ . The signal is assumed to have the structure of equations (5.1.2).

$$\begin{aligned} x(n) &= s(n) + v(n) \\ x(n + kn_0) &= h(n, n + kn_0) * s(n) + v(n + kn_0) \end{aligned} \quad (5.1.2)$$

where the interval  $n_0$  is assumed to be approximately known and approximately constant. The interval  $n_0$  need only be known to within  $L$  points where  $L$  is the length of the adaptive filters. Within this range the filters will tend, as a fundamental property of least-squares filters, to align events automatically. This property is discussed more fully in Chapter 7.

The inputs to the enhancing system are provided by

$$x_0(n) = x(n - \frac{M}{2} n_0)$$

$$x_1(n) = x(n - (\frac{M}{2} - 1) n_0)$$

$$x_{M-1}(n) = x(n + \frac{M}{2} n_0)$$

where the aim is to enhance the signal at  $x(n)$ . An example of a signal of this form is considered in Section 4.5 and a second example is presented in Chapter 9. A second form of the GCF is possible, for multi-channel processes, with the input provided by the separate channels. If it is assumed that the signals have the form:

$$x^{(i)}(n) = s(n) + v^{(i)}(n) \quad (5.4.4)$$

$$x^{(i+k)}(n) = h^{(k)}(n) * s(n) + v^{(i+k)}(n)$$

where  $x^{(i)}(n)$  is the  $n$ th sample from the  $i$ th input channel; where  $v^{(i)}(n)$  is the  $n$ th noise sample from the  $i$ th channel, and where  $h^{(k)}(n)$  is a linear, possibly time-variant, system which expresses a correlation between the signal components on the  $i$ th and  $(i+k)$ th channels. Comparison of equations (5.4.4) and (5.1.2) shows that the signal structures are essentially equivalent for both the single and multi-channel signals and hence the GCF may in fact be applied to either. It is interesting to note that this multi-channel version of the GCF is very similar to a multi-channel signal enhancement scheme proposed by Ferrara and Widrow [27], (though not applied to any real signals). However, their scheme is less flexible since there is no provision for varying the gains in the averaging, that is, in effect these are always set to 1.

The final component in the adaptive comb filter structure is the selection of the averaging gains. After adaptive enhancement using the technique of Section 5.4.2, the signals to be averaged will have the form of equations (5.4.3), where the type of distortion is determined by the adaptive filter (an appropriate form for which was derived in equation (VIII.4)).





As seen in the previous section, averaging of signals of this type will only be successful subject to certain restrictions on the distortion etc. Ideally, the gains  $G_i$  should be chosen consistent with equation (IX.13). Unfortunately this is not possible since the determination of  $G_{opt}$  requires knowledge of the adaptive filter structure which in turn requires apriori information concerning the signal and noise structure. Thus, the gains must be selected using an ad-hoc procedure, on a similar basis to that for comb filtering. The gains may be chosen as coefficients from a conventional window (rectangular, Hamming, etc.) The choice of gain is a reflection of confidence felt in the relative merits of the minimisations for different filters. In many cases there may be no apriori reasons for assuming any of the  $M$  outputs will be a better representation of  $s(n)$  than others and so a rectangular window would be appropriate. In other cases it will be logical to assume the correlation will fall with separation and to adjust the gains accordingly (for example, as a Hamming window). It must be pointed out, however, that from the results of Section 5.4.3, without an optimal policy for selection of the gains, SNR improvements cannot be guaranteed from the operation of the GCF. In practise, however, as will shortly be seen, the operation of the GCF produces improvements in SNR for a wide range of gains.

## 5.5 Application of generalised comb filtering to enhancement of voiced speech

### 5.5.1 Introduction

In this section the aim is to apply the generalised comb filtering technique developed in Section 5.4 to the problem of enhancing speech which has been degraded by the addition of random noise. There are a number of situations in which it is desirable to enhance speech and considerable effort has gone into the development of techniques to achieve this end. These methods can be broadly classified according to the assumptions made about both speech and interference [51]. The choice of a particular algorithm will, however, usually depend both on the type of interference and the objectives of the enhancement. The

reason for the importance of the objectives in a particular application is that care must be taken to draw a distinction between SNR improvement, increasing intelligibility, listener fatigue, etc. Whilst it is straightforward (for synthetic examples at least) to measure changes in SNR, it is far more complex to measure the latter two objectives (indeed, the nature of the intelligibility tests themselves will vary according to the particular application). This is an unfortunate feature of speech enhancement since it is quite possible (indeed, very likely) that a particular enhancement technique will improve the SNR but will at best leave the intelligibility unchanged and at worst cause some degradation.

The acceptability, or otherwise, of this situation must depend heavily on the particular application. Whilst it is clear that in many instances the intelligibility of the speech will be of central importance, this need not always be so [51].

As far as the generalised comb filter, is concerned, the technique has been designed as a method for SNR improvement rather than subjective improvement of speech. Accordingly the success of the technique will be quantified in these terms and consideration of intelligibility will be restricted to a few passing comments.

#### 5.5.2 Model of Speech Production

Figure 5.5.1 shows a simple digital model of speech production [77]. The system consists of a time-varying digital filter whose input is derived from one of two sources: For voiced speech (typically vowel sounds) the input is a series of impulses (at intervals of  $n_0$  samples) corresponding to discrete puffs of air caused by the action of the vocal chords (which are tensed for voiced sounds) on the air forced out from the lungs through the trachea. The interval  $n_0$  is referred to as the pitch period.

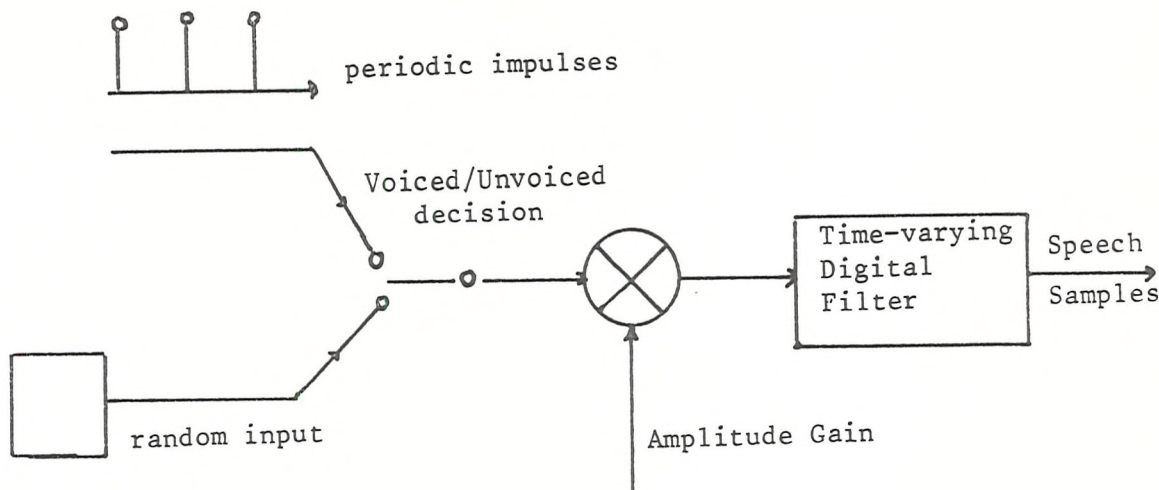


Fig 5.5.1: Model of Speech Production

For unvoiced speech (typically consonants) the input is provided by a random number generator simulating both the random turbulence and pressure build-up which characterise unvoiced sounds.

The filter response itself simulates the vocal tract system. The response is characterised by a set of resonant frequencies, referred to as the formants. The vocal tract changes shape as different sounds are generated and thus the filter must have a time-varying transfer function. It is, however, reasonable to model the system as slowly varying due to mechanical and physiological constraints.

### 5.5.3 Existing Techniques for Speech Enhancement

As was indicated in Section 5.5.1 SNR enhancing methods for speech may be classified according to the assumptions made about both speech and interference. The simplest form of enhancement is simple bandpass filtering to remove interferences outside the perceptually important regions. A different system, which relies on human perception, was proposed by Drucker [22], for systems degraded by wide-band random noise. The method consists of inserting short pauses immediately preceeding the plosive sounds (such as 'P's, assuming these can be identified) and high

pass filtering the fricative 's' sound. The justification for this approach was provided by perceptual tests which indicated that additive wide band noise causes confusion amongst the fricative and plosive sounds. Interestingly, this is an example of a system which increases intelligibility whilst actually decreasing SNR.

Another class of techniques attempts in some way to estimate the short time spectrum of the speech and then enhance this. These techniques include those in which the short time spectral amplitude is estimated directly from the degraded speech and then enhanced using some form of spectral subtraction (eg [50]). Also included are optimum filtering techniques such as Wiener filtering. The problem with all these methods, however, is that the spectral properties of the noise must either be known or be estimable from periods of silence in the speech.

Yet another class of enhancement techniques is based on the idea of estimating the parameters of the speech model rather than the speech itself, and then using these parameters to synthesise the speech, that is to enhance speech using an analysis-synthesis system e.g. [48].

The class of techniques which are of primary interest here are those which exploit the pseudo-periodic nature of voiced speech. A number of such approaches exist:

- 1) Adaptive Comb Filtering. Shields [88] developed an approach to (voiced) speech enhancement based on comb filtering the speech. The spacing of the comb teeth is set approximately equal to the pitch period and the value chosen may be replaced for different sections of the speech. The amplitudes of the teeth are fixed (for example as a standard Hamming window), see Figure 5.5.1a). It was noticed that this scheme introduces distortion due to the fact that local variations in the pitch period exist. Frazier et al [24] suggested a modification which uses a pitch period extractor to estimate the local variations in the pitch periods of the speech (Figure 5.5.1b).

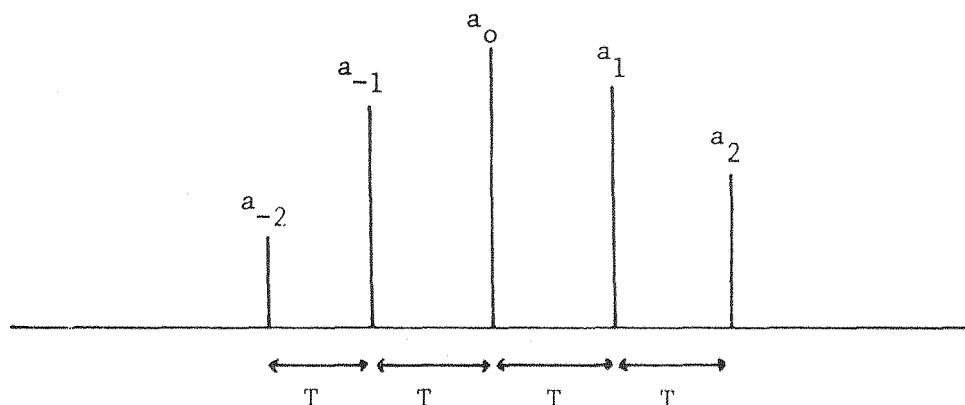


Fig 5.5.1a): Standard Comb Filter

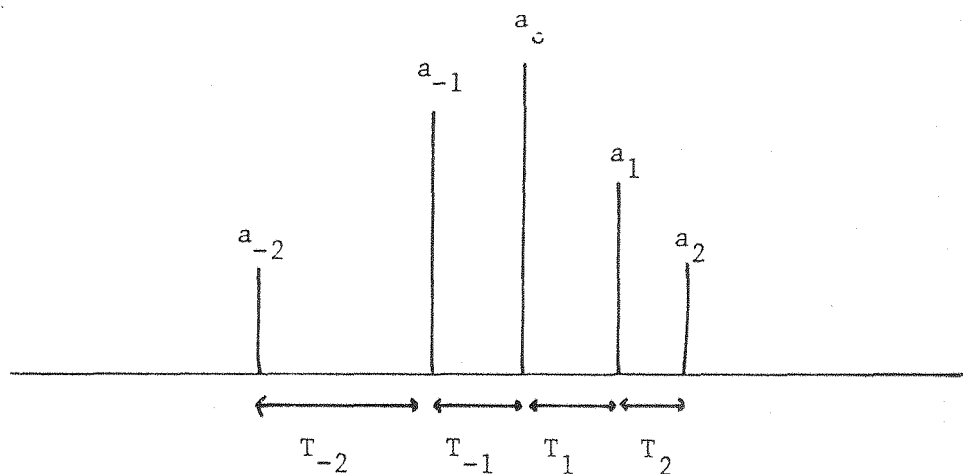


Fig 5.5.1b): Comb Filter with Pitch Period Variation

Tests performed on the Frazier method [49] (generally superior to Shields approach) have indicated that whilst the method can produce improvements in SNR it generally decreases intelligibility and this decrease appears proportional to the number of coefficients in the comb filter.

The main problem with this approach is that the comb filter fails to take account of the time-variable nature of the speech waveform.



2) Adaptive Noise Cancelling. If a second measurement containing a correlated noise source alone can be obtained then the adaptive noise cancelling system described in Section 5.3 can be applied to the speech enhancement problem. (see Chapter 6). However, for cases when a reference measurement is not available Sambur [82] has developed an adaptive noise cancelling system which utilises the periodicity of the voiced speech. This is achieved by using, as a reference measurement, a delayed version of the input, where the delay is set equal to the pitch period (see Figure 5.5.2).

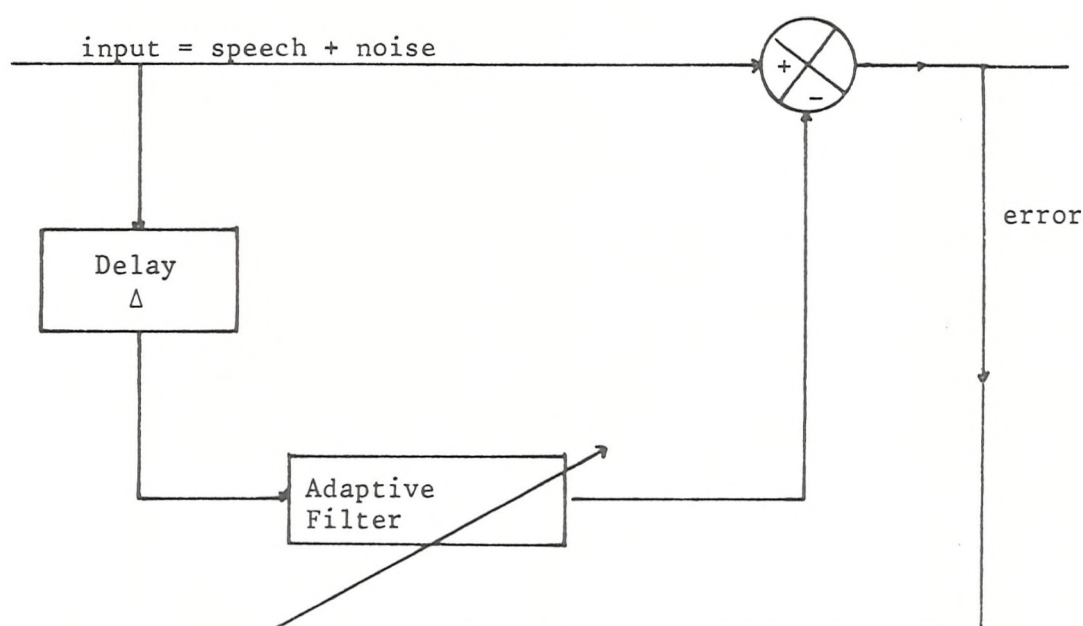


Fig 5.5.2: Adaptive Noise Cancelling with Internal Reference

It is hoped that the delay will serve to decorrelate the noise but it will not, of course, decorrelate the voiced speech due to its pseudo-periodic nature. Hence the filter output will be an estimate of the correlated component, namely the speech.

#### 5.5.4 SNR Enhancement of Voiced Speech Segments using Generalised Comb Filtering

In this section the generalised comb filtering method described in Section 5.4 will be applied to the problem of SNR enhancement for speech signals. Within the context of the existing

methods described in the previous section it is clear that this technique falls into the category of those which enhance voiced speech segments by exploiting their pseudo-periodic nature. In fact, it can be seen that the method is actually a combination of the two approaches described in that category, namely: i) comb filtering and ii) adaptive noise cancellation.

The combination represents a generalisation of the adaptive noise cancellation scheme and overcomes (in part at least) the two main restrictions of Frazier's comb filter. These restrictions are the inability of the comb to deal with changes in the waveform shape, and the necessity for precise information regarding the pitch period. Neither of these constraints is shared by the generalised comb structure proposed here since, as seen in Section 5.3, i) the filter is designed to handle input waveforms with a slowly varying structure and ii) the separation between successive repetitions (pitch period) need only be known approximately.

#### 5.5.5 Simulations

The generalised comb filter was tested using a small section of voiced speech containing the vowel sound 'e'. The signal corresponding to this sound, as expressed by a male speaker, is shown in Figure 5.5.3a. Gaussianly distributed white noise was added synthetically to this signal (Fig 5.5.3b), at several different SNR's. The generalised comb filter was evaluated using this data as a function of the algorithm's parameters. The pitch period was assumed to be 82 samples for the first half of the data, and 83 samples for the remainder. In fact some local variations in pitch period exist within the data.

Note that the SNR improvement figures quoted are log. average figures obtained from

$$\text{SNR}_{\text{imp}} = 20 \log_{10} \left( \frac{\sigma_v}{\sigma_e} \right) \quad (5.5.1)$$

where  $\sigma_v$  is the standard deviation of the input noise and  $\sigma_e$  is the standard deviation of  $e(n) = y(n) - s_p(n)$  where  $y(n)$  is the enhanced output and  $s_p(n)$  is the raw (noise free) speech.

The performance was first tested as a function of the adaptive filter length and adaptation rate. Table 5.5.1(a) and (b) gives SNR improvements obtained as a function of these parameters, with typical (though fixed) values for other parameters.

Filter Length (L)	SNR Improvement (dB)
10	7.31
20	7.49
30	7.60
40	7.42

TABLE 5.5.1(a) - SNR Improvement versus Filter Length  
(Input SNR = 3.30, 4 teeth, rectangular window,  $\alpha = 0.2$ ).

Adaptation Rate ( $\alpha$ )	SNR Improvement (dB)
0.05	7.54
0.1	7.71
0.2	7.49
0.3	6.93
0.4	6.31

TABLE 5.5.1(b) - SNR Improvement versus Adaptation Rate  
(Input SNR = 3.30, 4 teeth, rectangular window, L = 20).

The results show significant SNR improvements over a broad range of values of both adaptation rate and filter length, indicating usefully, that algorithm performance is not critically dependent on either parameter. A typical enhanced waveform is shown in Figure 5.5.3(c). The effect of varying the number of teeth in the comb and the criterion for selecting the comb gains were also evaluated. Table 5.5.2(a) shows the SNR improvements for 2, 4 and 8 'teeth' in the comb with all gains equal to one (rectangular window).



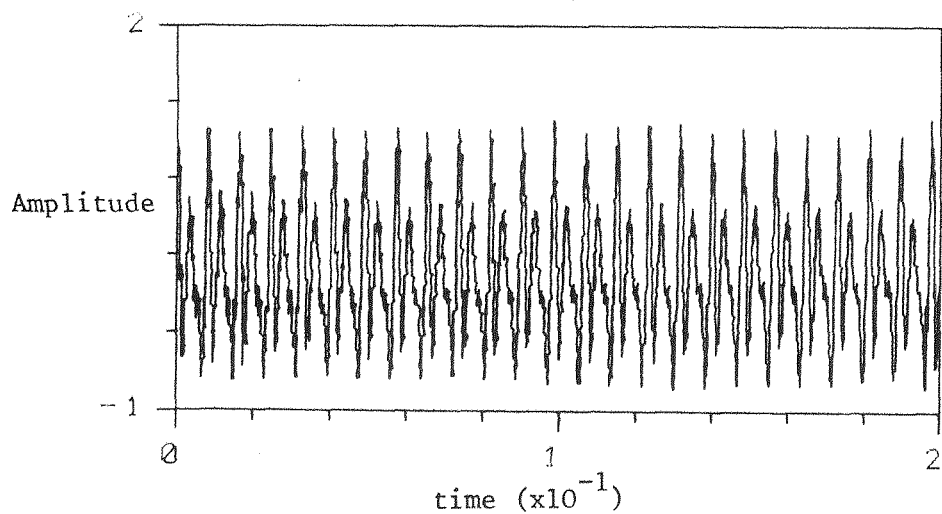


Figure  
5.5.3a

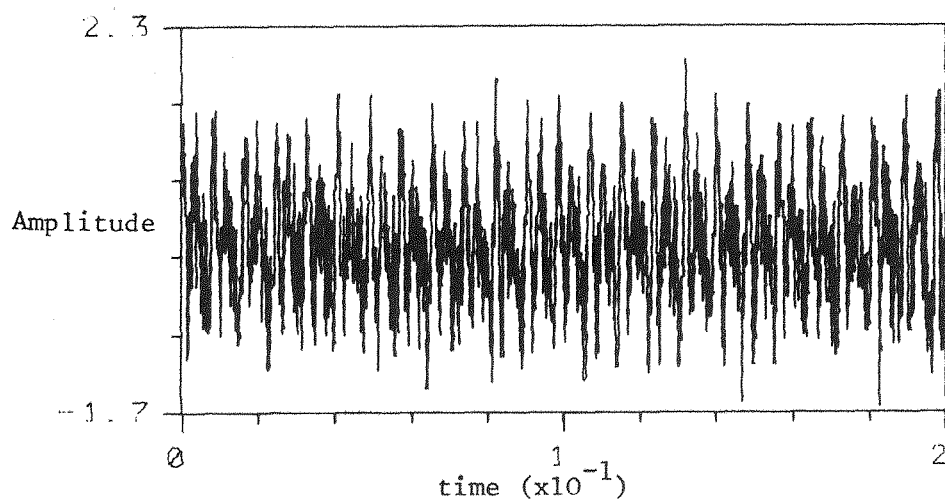


Figure  
5.5.3b

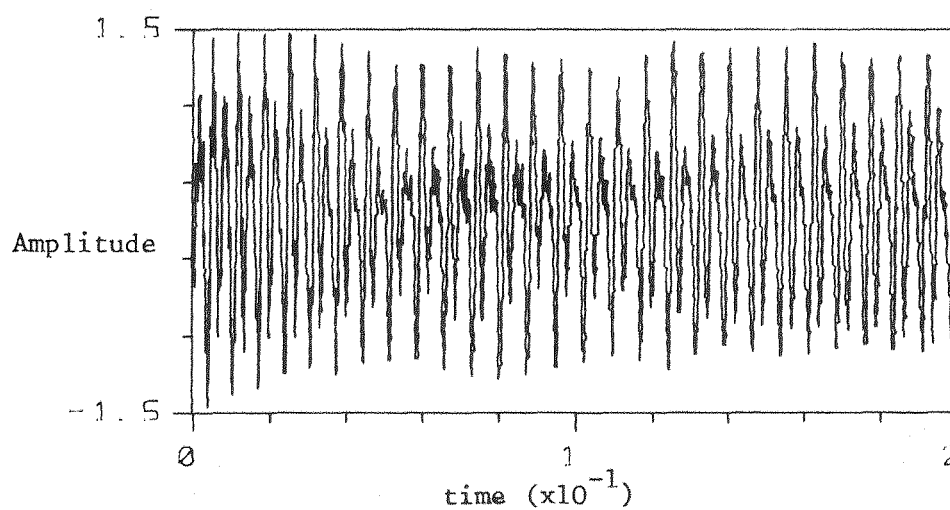


Figure  
5.5.3c

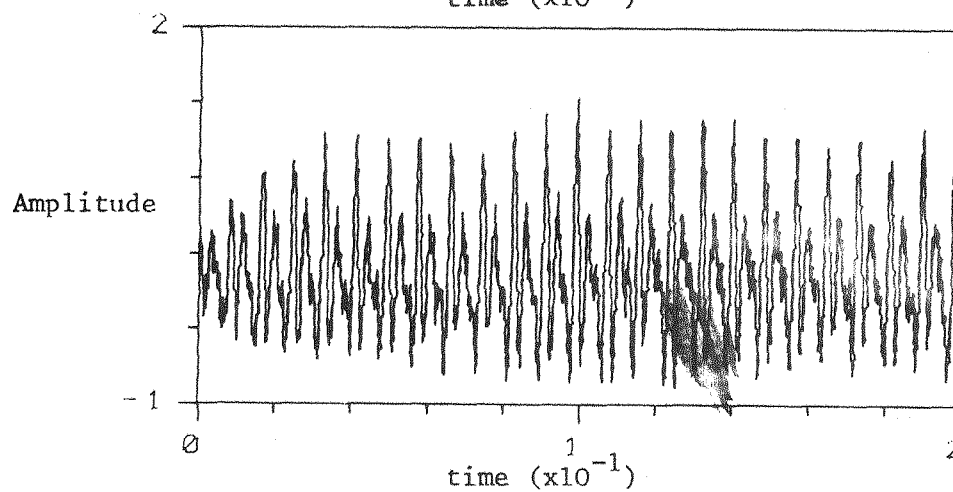


Figure  
5.5.3d

Teeth	SNR Improvements (dB)	
	(a) Rectangular	(b) Hamming
2	5.76	3.22
4	7.49	5.77
8	7.78	7.33

TABLE 5.5.2(a) and (b) - SNR Improvement versus Number of Teeth  
(Input SNR = 3.30,  $L = 20$ ,  $\alpha = 0.2$ ).

From the table, increasing the spread of the comb increases the enhancement. However, this increase is not linear, this is due to the time-variable nature of the speech waveform which causes the correlation between the signal components to decrease with increasing separation. Table 5.5.2(b) gives similar results when the gains are selected as coefficients from a Hamming window (see Section 5.4). The Hamming coefficients give inferior results to the rectangular gains, but the inferiority is less marked for larger numbers of weights, as may be expected.

All of the above results were obtained using data at a single input SNR. If this is varied the performance varies. Table 5.5.3 shows results obtained with similar parameters to those of previous results but with varying SNR. As is clear, the performance of the enhancing system generally increases as the SNR decreases.

Input SNR (dB)	SNR Improvement
+9.32	4.38
+3.30	7.49
-10.68	10.76

TABLE 5.5.3 - SNR Improvement versus Input SNR  
(4 teeth, rectangular window,  $L = 20$ ,  $\alpha = 0.2$ ).

All filters undergo a reasonably short learning period, a typical example is shown in Figure 5.5.3(d).

As discussed in Section 5.5.1, the primary difficulty with the evaluation of speech enhancement techniques is the determination of the relevant criteria with regard to the importance of SNR, intelligibility, etc. In these examples only the question of SNR improvement has been considered, other issues have been ignored. This, of course, says very little about the effect of the method on the intelligibility of the speech. It is quite possible that this method, in increasing the SNR of the speech, may leave unchanged or actually decrease intelligibility, though this has not been determined. This does not, of course, detract from the methods success in enhancing SNR. In fact, as discussed in Section 5.5.3, such a situation occurs in the vast majority of speech enhancement systems[51]. In the author's opinion it is likely that this particular system increases intelligibility at low SNR's and decreases it at higher SNR's.

## 5.6 Conclusions

In this chapter the problem of SNR enhancement for a class of signals which consist of a slowly time-varying waveform recurring at approximately constant intervals, embedded in additive noise has been considered. It has been seen that classical approaches are inappropriate in this instance due to the lack of apriori information about signal and noise, and/or the time varying structure of the signal. A technique to achieve SNR enhancement for signals of this form, was proposed. The scheme involves replacing the simple averaging of comb filtering by adaptive filtering and averaging and as such is dubbed the generalised comb filter. The generalised comb filter has two principal advantages over the conventional comb: (i) It can handle input waveforms of a time-varying nature (due to the adaptive filters) and (ii) It can handle misalignment. The adaptive filter uses the correlation between the signals to reduce the distortion prior to averaging. In all but the most unrealistic cases the generalised comb filter should considerably out-perform the conventional comb. Although, naturally, the generalised comb has increased computation compared to the conventional comb. However, the generalised comb filter is a mechanism which exploits correlation -

it cannot distinguish between correlated signal or correlated noise and as such it cannot be used to attenuate coherent noise. A second mathematical mode of operation of the generalised comb was identified. An example of this multi-channel operation is considered in a later chapter. In this chapter the operation of the generalised comb filter was demonstrated on a single channel problem: the enhancement of voiced speech sections. Some work has been done on voiced speech enhancement using adaptive noise cancellation and a separate attempt used comb filtering. The generalised comb filter proposed here is a combination of these approaches and has the effect of generalising the adaptive noise cancelling method and overcoming the two main restrictions of the conventional comb as described above. The results indicate that significant SNR gains are possible with the generalised comb over a broad range of parametric variation. It is also clear that the resulting gains are inversely proportional to the input SNR.

Two further applications of the GCF (one single and one multi-channel) are developed in Chapter 9.

ADAPTIVE NOISE CANCELLATION FOR NARROWBAND INTERFERENCES

6.1 Introduction

In this chapter a different approach to signal-to-noise enhancement is considered via the process of noise cancellation. In particular this study centres round the problem of signals corrupted by narrowband interferences. The aims of the chapter are to evaluate and establish the limitations of existing techniques for the cancellation of narrow band interferences, to improve the theoretical understanding of these methods and to develop alternative methods which will overcome some of the limitations.

The undesirable interferences in the signals will be assumed to consist of a number of distinct sinusoids of differing amplitudes and frequencies. In general these frequencies will be assumed to be unknown and possibly time-varying, which immediately discounts the possibility of using conventional notch filtering for the purposes of noise cancellation.

Broadly speaking, there are two distinct sets of circumstances depending on whether a separate, secondary (reference) measurement is available or not. Where a reference measurement is present it will be assumed to consist of a set of sinusoidal interferences of different amplitudes and phase, but with the same frequencies as those of the primary interferences. For such circumstances Glover [33] has used the method of adaptive noise cancellation (ANC) described briefly in the previous chapter. This method is examined in detail and its performance evaluated carefully. Although it is found that the adaptive noise cancellation technique is a powerful and flexible approach to noise cancellation for single interferences, in general it performs far less well for multiple sinusoidal interference cancellation. The existing theory (again due to Glover) does not adequately describe the system behaviour in these cases and so a more general description of the response is developed. An alternative approach which is designed to overcome the weakness of conventional adaptive noise cancellation for the cancellation of multiple sinusoidal interferences is proposed. The novel method is based on the idea of a 'sparse' adaptive filter, that is one with relatively few coefficients in relation to its length or time span.

The properties of the new approach are carefully evaluated and contrasted with those of conventional ANC and found to be generally advantageous. A further novel application of a sparse filter with just two coefficients to slow sweep testing is also included.

In the second case of interest - where no reference measurement is available - a modified form of adaptive noise cancellation which uses a delayed version of the primary input for a reference has been used[117] but this approach is generally limited by the quality of the reference which is corrupted by the presence of signal. Also, in some applications there is insufficient data to introduce a large enough delay.

A second approach for such cases has been developed by Plotkin [72] and dubbed the function elimination filter (FEF). The idea of the function elimination filter is to process the signal using a filter whose form is fixed as a notch centred on some frequency  $\omega_0$ . The value of  $\omega_0$  is a least-squares estimate (possibly adaptive) of the interference frequency.

The performance of the FEF in simple situations is examined and found to be weak in two important respects, namely (i) bias of the notch centre frequency and (ii) the width of the notch. A modification to the FEF is proposed which overcomes the latter restriction by introducing a pair of poles into the transfer function. This scheme is shown to be viable in some situations.

## 6.2 Theory of Adaptive Noise Cancellation for Narrowband Interferences

### 6.2.1 Introduction

In this section a method of eliminating sinusoidal interferences from signals using a modified form of the ANC technique described in Chapter 5 and due to Glover[33] is discussed in detail. The scheme is depicted in Figure 6.2.1.



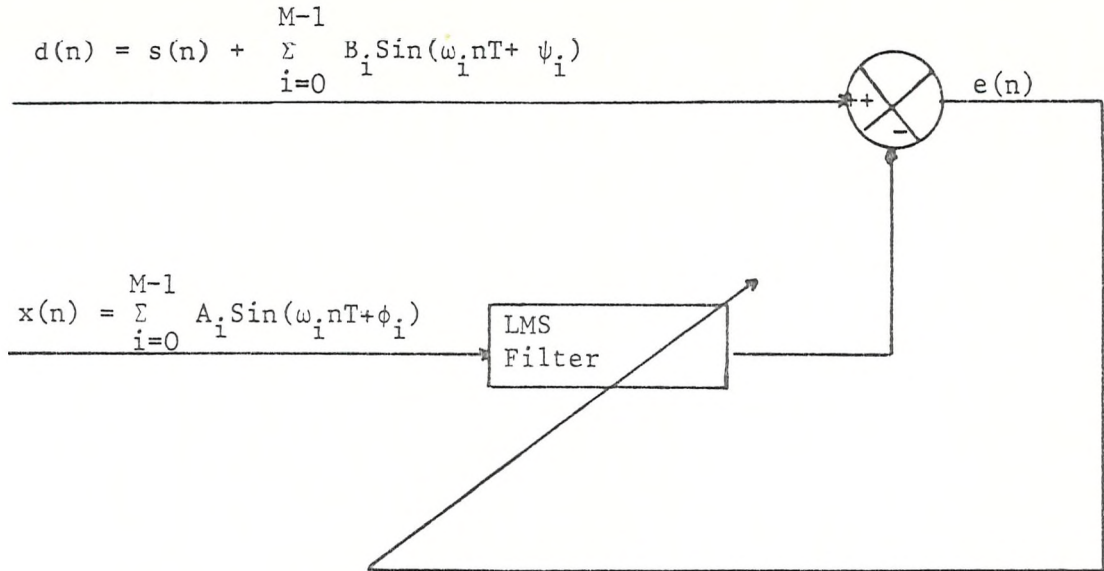


Fig 6.2.1: ANC for Narrowband Interferences

The primary input consists of the signal plus a set of  $M$  interfering sinusoids with amplitudes  $B_i$ , phase angles  $\psi_i$  and frequencies  $\omega_i$ . A reference measurement is assumed available consisting of a set of sinusoids of similar frequencies to those of the primary input but with amplitudes  $A_i$  and phases  $\phi_i$ . The aim is to filter the secondary (reference) input in such a way as to cancel the sinusoidal components from the primary inputs,  $d(k)$ . Moreover, the adaptive nature of the solution should allow the filter to track variations in the pitch of the interferences. Although, generally a reference measurement of the above form is assumed to be available an alternative formulation due to Widrow et al[117] which requires no external reference can also be used. In this approach a reference input is formed simply by delaying the primary (Figure 6.2.2).

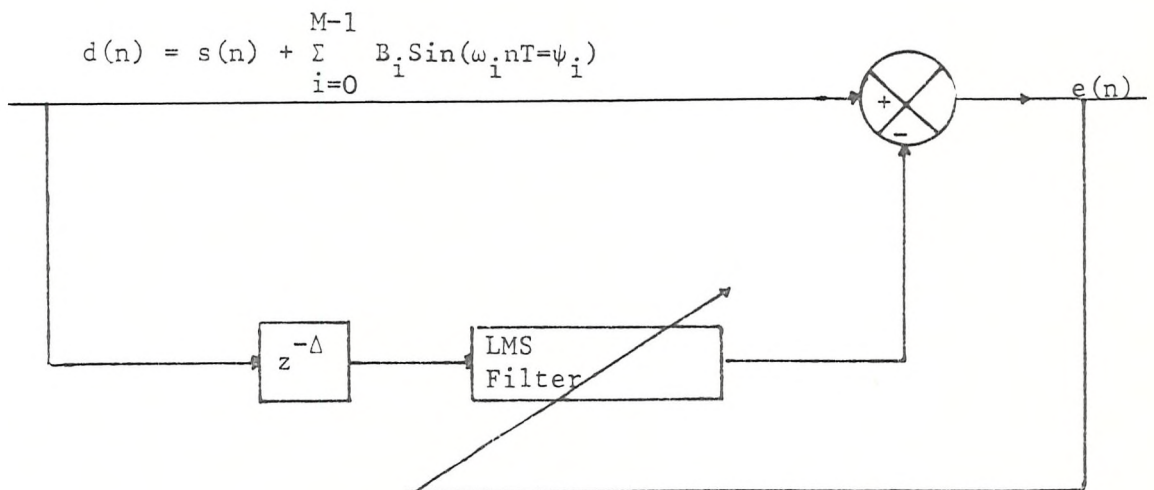


Fig 6.2.2: ANC for Narrowband Interferences with Internal Reference.

It is hoped that the delay will serve to 'decorrelate' the signal components, whilst the sinusoids will remain correlated. Note that in this form the scheme is essentially the same as the so-called Adaptive Line Enhancer (ALE), [117] which has been the subject of considerable attention in the literature recently e.g. [98, 104, 123].

### 6.2.2 Approximate Transfer Function - Single Interfering Tone

Glover [33] has shown that the adaptive noise cancelling system depicted in Figure 6.2.1 with a single interfering tone ( $M=1$  in Figure 6.2.1) of frequency  $\omega_o$ , can be approximated by a linear time invariant system, with system function  $H(z)$  given by:

$$H(z) = \frac{E(z)}{D(z)} = \frac{1 - 2z^{-1} \cos \omega_o T + z^{-2}}{(1 - \alpha \frac{LA^2}{2})z^{-2} + (\alpha \frac{LA^2}{2} - 2)z^{-1} \cos \omega_o T + 1} \quad (X.10)$$

where  $L$  is the number of weights in the adaptive filter,  $\alpha$  is the adaptation constant associated with the adaptive filter and  $T$  is the sample interval for the inputs  $x(k)$  and  $d(k)$ .

Hence the system of figure 6.2.1 has been replaced by an equivalent system depicted by:

$$D(z) \frac{1 - 2z^{-1} \cos \omega_o T + z^{-2}}{(1 - \alpha \frac{LA^2}{2})z^{-2} + (\alpha \frac{LA^2}{2} - 2)z^{-1} \cos \omega_o T + 1} E(z)$$

Fig 6.2.3: Equivalent Transfer Function for ANC System

The transfer function (X.10) is exact if  $L$  satisfies,

$$L = \frac{N\pi}{\omega_o T} \quad ; \quad N = 1, 2, \dots \quad (6.2.1)$$

whilst in other cases the representation is only approximate, the accuracy of the approximation increases with  $L$ .



The system has zeroes at  $z = e^{\pm i\omega_o T}$  and for small adaptation rates the poles lie approximately at

$$z = \left(1 - \alpha \frac{LA^2}{4}\right) e^{\pm i\omega_o T}.$$

That is, on the same radial line as the zeroes but  $\frac{\alpha LA^2}{4}$  inside the unit circle. (see Figure 6.2.4)

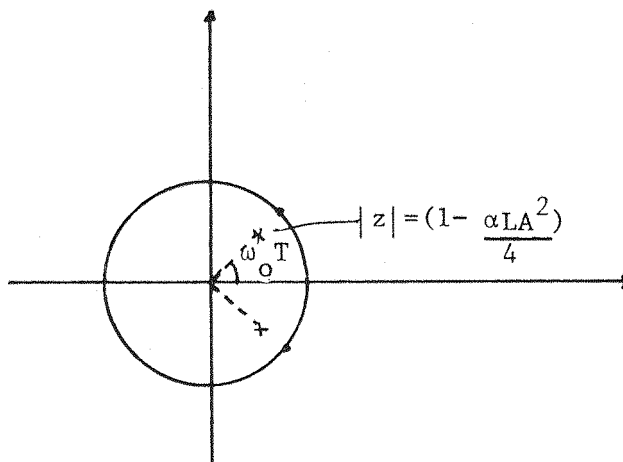


Fig 6.2.4: Pole-zero Plot for ANC System

The composite system is thus a notch centred on frequency  $\omega_o$ . The bandwidth of the notch is controlled by the distance of the poles from the unit circle, and thus by,  $\alpha$ ,  $L$  and  $A$ .

### 6.2.3 Time Domain Characteristics

It is not unreasonable to investigate time domain (convergence) properties of the system by considering the response to a pure sine wave, as the interference is usually the dominant component. If the primary input is  $d(k) = B \cos(\omega_o kT + \psi)$  with this input the response in terms of the approximate transfer function is easily obtained by inverse transforming as:

$$e(k) = c \left(1 - \alpha \frac{LA^2}{4}\right)^k \cos(\omega_o kT - \xi) \quad k \gg 1 \quad (X.16)$$

where;

$c$  and  $\xi$  are constants given by equations (X.17) and (X.18) respectively.

Thus the form of the response is a damped sine wave at frequency  $\omega_0$ . This curve has peaks at intervals of  $k = \frac{2\pi}{\omega_0 T}$ , at the peaks

$$e(k) = c' \left(1 - \alpha \frac{LA^2}{4}\right)^k \quad (X.19)$$

Hence:

$$\text{Log } e(k) = \text{log } c' + k \text{ log } \left(1 - \alpha \frac{LA^2}{4}\right)$$

Hence the logarithm of the peaks of the response versus  $k$  is a straight line with gradient  $\text{log}(1 - \alpha \frac{LA^2}{4})$ .

A time constant  $T_m$  may also be defined as the time for the error to fall to  $1/m$  times the initial peak value. This is given by

$$T_m = \frac{-\log_{10} m}{\log_{10}(1 - \alpha \frac{LA^2}{4}) \times (\text{sample rate})} \quad (X.21)$$

(see Appendix X)

It is also possible using these results to obtain relationships between differing parameters giving equivalent convergence rates (as defined by  $T_m$ ).

For a particular number of weights,  $L_1$  and reference amplitude  $A_1$ , with adaptation constant  $\alpha_1$ , then a second filter with  $L_2$  weights and reference amplitude  $A_2$  will have the same convergence rate if  $\alpha_2$  is chosen according to:

$$\alpha_2 = \left(\frac{L_1 A_1^2}{L_2 A_2^2}\right) \alpha_1 \quad (X.22)$$

(See Appendix X)

#### 6.2.4 Noise in the Reference

If, in the adaptive noise cancelling scheme of Figure 6.2.1 the reference measurement is corrupted by additive random noise, then the theory of previous sections is no longer appropriate for the analysis of the system.

At the simplest level and consistent with the argument given by Widrow et al [117] if the noise is uncorrelated with the primary signal it will have no effect since the filter cannot adapt to cancel uncorrelated components. Whilst this may represent a good approximation, it is known that the noise will have some effect through the phenomenon of misadjustment (see Chapter 2). Some work on the quantification of this effect has been done, mainly in connection with the Adaptive Line Enhancer. Treichler [98] uses an input of the form:

$$x(k) = A \cos(\omega_0 kT + \theta) + w(k) \quad (6.2.2)$$

where  $\theta$  is uniformly distributed on  $(-\pi, \pi)$  and  $w(k)$  is white, to demonstrate that:

$$\lim_{k \rightarrow \infty} E\{\underline{f}_k\} \rightarrow \underline{f}^* = \text{The Wiener solution}$$

and goes on to obtain  $\underline{f}^*$  using approximate values for the eigenvalues of the autocorrelation of  $x(k)$ .

However, the derivation requires the assumption that

$$E\{x_{-k} x_{-k}^t f_{-k}\} = E\{x_{-k} x_{-k}^t\} E\{f_{-k}\} \quad (6.2.3)$$

which although as Treichler claims, may work well in practise, is very dubious due to the highly correlated nature of the inputs (for high SNR references at any rate).

Nevertheless, this result has been used by both Rickard and Zeidler [78] and Shensa [87] who have attempted to quantify the second order statistics. Rickard and Zeidler obtain an

expression for the output spectrum which is valid only for very low SNR and is thus inappropriate for the purposes of this work. Shensa on the other hand obtains an expression for the error spectrum (to order  $\alpha^2$ ), however this requires the stronger restriction that the noise  $v(j)$  has the form:

$$E \{ \underline{v_k} \underline{v_j}^t \} = \sigma^2 \delta_{jk} I \quad (6.2.4)$$

Also the resulting spectrum is difficult to interpret due to the presence of terms in  $F(z)$  - the filter itself.

#### 6.2.5 Approximate Transfer Function (Multiple Interfering Sinusoids)

The transfer function form of Section 6.2.2 can easily be generalised to the case of multiple interferences.

Consider the system depicted in Figure 6.2.1 where for simplicity  $M$ , the number of interfering tones, is restricted to two (the result can easily be generalised). Glover [33] has shown (see Appendix X), that the system can be approximated by a linear time invariant system with system function given by:

$$Y(z) = E(z) [G_1(z) + G_2(z)] \quad (X.28)$$

where

$$G_1(z) = \frac{\alpha_L A_0^2}{2} \left( \frac{z^{-1} \cos \omega_0 T - z^{-2}}{1 - 2z^{-1} \cos \omega_0 T + z^{-2}} \right)$$

and

$$G_2(z) = \frac{\alpha_L A_1^2}{2} \left( \frac{z^{-1} \cos \omega_1 T - z^{-2}}{1 - 2z^{-1} \cos \omega_1 T + z^{-2}} \right)$$

$$\text{also } E(z) = D(z) - Y(z)$$

so that

$$\frac{E(z)}{D(z)} = \frac{1}{1 + G_1(z) + G_2(z)}$$

which is depicted in Figure 6.2.5.

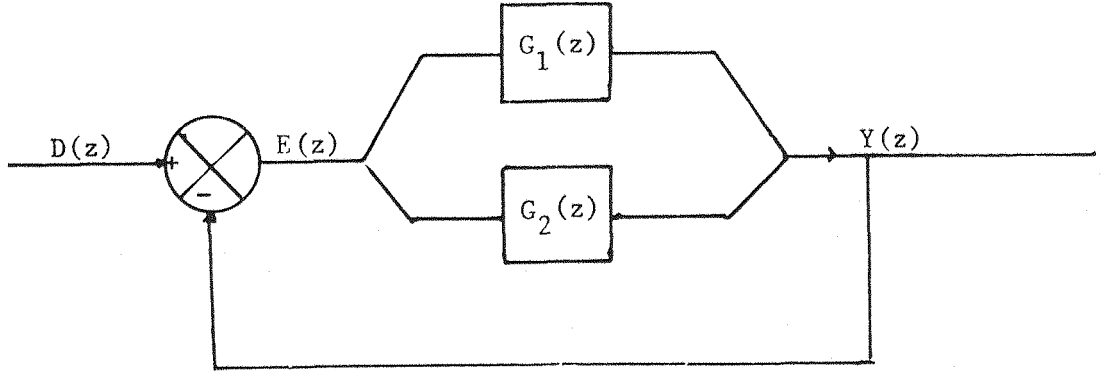


Fig 6.2.5: Equivalent ANC System (two interfering tones)

This system has zeroes at  $z = e^{\pm i\omega_0 T}$  and  $z = e^{\pm i\omega_1 T}$  and, neglecting terms involving  $\alpha^2$ , poles at

$$z = \left(1 - \frac{\alpha L A_0^2}{4}\right) e^{\pm i\omega_0 T} \quad \text{and}$$

$$z = \left(1 - \frac{\alpha L A_1^2}{4}\right) e^{\pm i\omega_1 T}.$$

Thus the system corresponds to a pair of notch filters centred at  $\omega_0$  and  $\omega_1$ .

In contrast to the transfer function for a single interfering tone (equation (X.10)), this system is exact only if it satisfies equation (6.2.1) for both  $\omega_0$  and  $\omega_1$  and for the sum difference frequencies,  $\omega_0 + \omega_1$  and  $\omega_0 - \omega_1$ . Note that these assumptions will be particularly inappropriate for close frequencies, since  $\omega_0 - \omega_1$  will be small and hence the number of weights required to span  $\pi$  samples will be large.

These results extend in a logical manner for an arbitrary number of interfering tones. However, the transfer function becomes increasingly approximate due to contributions from all the combinations of sum and difference frequencies present.

### 6.2.6 Generalised Description of the Adaptive Noise Cancelling System Response

As was seen in the previous section the existing transfer function description of the ANC response, whilst having the advantage of being simple, has the disadvantage that it gives an increasingly inaccurate description of the response as the number of interfering tones increases. In particular, in the case of  $M$  interfering sinusoids the response obtained using the transfer function would simply be  $M$  parallel notches at the relevant frequencies. In fact such a description would not be appropriate since in practise other significant components occur in the response. As multiple tone cancellation is an important consideration it is important to try to quantify these extra effects in some way. In this section a more general (though still approximate) description of the ANC response is developed. This description has the disadvantage that it is considerably more complex than that of Glover but has the advantage of giving a satisfactory description of the response for multiple tone cancellation.

Single Interfering Sinusoid. Beginning with a single sinusoidal interference ( $M = 1$  in Figure 6.2.1), then by neglecting  $O(\alpha^2)$  it can be shown (Appendix XI) that:

$$E(z) = H(z) [D(z) + G_1(z)H(ze^{-2i\omega_o T})D(ze^{-2i\omega_o T}) + G_2(z)H(ze^{2i\omega_o T})D(ze^{i2\omega_o T})] \quad (XI.13)$$

where

$H(z)$  is the transfer function of equation (X.10) and

where

$$G_1(z) = -\frac{\alpha A^2}{4} \left( \sum_{i=0}^{L-1} e^{i2\phi_i} U(ze^{-i\omega_o T}) \right) \quad (6.2.5)$$

$$G_2(z) = -\frac{\alpha A^2}{4} \left( \sum_{i=0}^{L-1} e^{-i2\phi_i} U(ze^{i\omega_o T}) \right) \quad (6.2.6)$$

and where

$$U(z) = \frac{1}{z - 1}$$

this may be represented diagrammatically as in Figure 6.2.6.

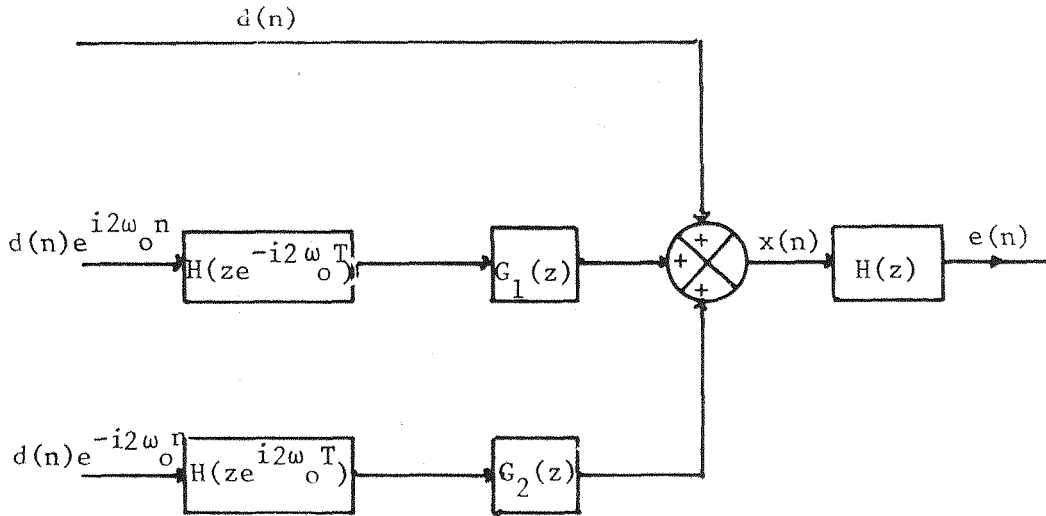


Figure 6.2.6: Block Diagram of Generalised Response

Hence the response is no longer a conventional linear transfer function between  $d$  and  $e$ , although this is not unexpected. It is instead the sum of three components. The first component is the usual linear transfer function relation, the other two are obtained by heterodyning  $d(n)$  at twice the reference frequency, notch filtering using  $H(z)$  rotated in the same manner and then filtered with a first order system. These components are summed and passed through the usual notch. Note that the last two terms are identically zero if

$$\sum_{i=0}^{L-1} e^{\pm i2\phi_i} = 0, \text{ that is if } L = \frac{N\pi}{\omega_0 T}, \quad N = 1, 2, \dots$$

and the response reduces to the usual transfer function. Whilst the general response is not exact, simulations verify that the form provides a description of the response which is entirely adequate for most purposes. The effect of the non-linear components of the response is, primarily, to create an amplitude scaled and rotated (in frequency) version of the linear response. This is illustrated in Appendix XI, using two examples.

The magnitude of these components is determined from  $G_1(z)$ ,  $G_2(z)$  of equations (6.2.5) and (6.2.6) by terms of the form:

$$F = \sum_{j=0}^{L-1} e^{\pm 2i\phi_j} \quad \text{where } \phi_j = \omega_0 jT$$

Now

$$\left| \sum_{j=0}^{L-1} e^{2i\omega_j T} \right| = \left| \frac{\sin L\omega_o jT}{\sin \omega_o jT} \right| \quad (6.2.7)$$

this is displayed in Figure 6.2.7 as a function of  $\omega_o$ . It can be seen from this that the magnitude of the non-linear terms of the response increases as  $\omega_o \rightarrow 0$  or  $\pi$ .

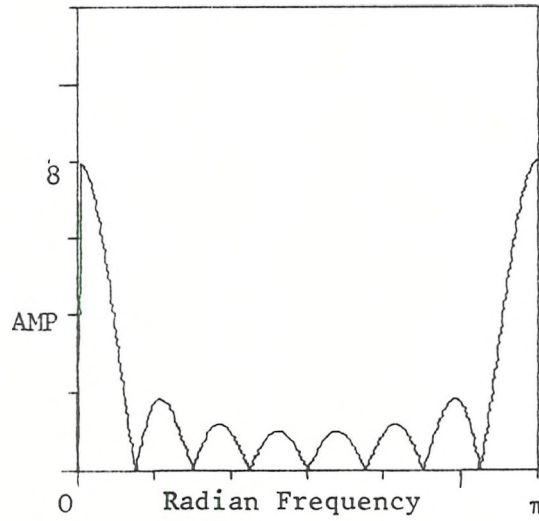


Figure 6.2.7:  $\left| \frac{\sin L\omega_o jT}{\sin \omega_o jT} \right|$  versus  $\omega_o$  ( $L=8$ )

### Time Domain Behaviour

It is possible to obtain some insight into the time domain behaviour in terms of the generalised response described above. If, as before, it is assumed that the interference will be the dominant component of the input it is reasonable to investigate the time domain behaviour by considering the response to a primary which consists solely of the sinusoidal component at frequency  $\omega_o$ . The time domain response as predicted by the theory of the previous section may be obtained by partial fractioning (XI.24). The dominant components in the response again lie near the reference frequency and in this area the response has the form:

$$e(k) = Er^k \cos(\omega_o kT + \theta_1) + kDr^k \cos(\omega_o kT + \theta_2)$$

(6.2.8)



where  $E$ ,  $D$ ,  $\theta_1$  and  $\theta_2$  are constants whose values are determined in the partial fractioning.

The first term of the response is similar to that for the approximate transfer function (equation (X.10)), whilst the second term is caused by the second order pole in equation (X.14). Whilst the change in convergence rate cannot be quantified exactly from equation (6.2.8) due to the complexity of the expressions for  $E$  and  $D$  it may be inferred that the effect of the second term of (6.2.8) is always to decrease the convergence rate ( $kr^k \rightarrow 0$  more slowly than  $r^k$ ). This, in turn, means that consideration of the transfer function form for the response generally leads to over-estimation of the convergence rate. Furthermore, the magnitude of the constant  $D$ , and thus the second term of (6.2.8), is proportional to a term of the form of equation (6.2.7) displayed in Figure 6.2.7. Hence the overall convergence decreases as the magnitude of this function increases and is slowest when  $\omega_0$  is close to 0 or  $\pi$ .

### Multiple Sinusoidal Interferences

If now the response is assumed to consist of a set of  $M$  sinusoids at differing frequencies, where for simplicity  $M$  is restricted to two (again the results generalise in a natural way). Using the same approximation technique employed in the previous section it can be shown (Appendix XI) that:

$$\begin{aligned}
 E(z) = & H(z) \left[ D(z) + G_1(z) H(z e^{-2i\omega_0 T}) D(z e^{-i2\omega_0 T}) + \right. \\
 & G_2(z) H(z e^{i2\omega_0 T}) D(z e^{i2\omega_0 T}) + G_3(z) H(z e^{-2i\omega_1 T}) D(z e^{-i2\omega_1 T}) + \\
 & G_4(z) H(z e^{i2\omega_1 T}) D(z e^{i2\omega_1 T}) + G_5(z) H(z e^{i(\omega_1 - \omega_0) T}) D(z e^{i(\omega_1 - \omega_0) T}) + \\
 & G_6(z) H(z e^{i(\omega_0 - \omega_1) T}) D(z e^{i(\omega_0 - \omega_1) T}) + G_7(z) H(z e^{i(\omega_0 + \omega_1) T}) \\
 & \left. D(z e^{i(\omega_0 + \omega_1) T}) + G_8(z) H(z e^{-i(\omega_0 + \omega_1) T}) D(z e^{-i(\omega_0 + \omega_1) T}) \right]
 \end{aligned}$$

(XI.15)

where  $G_1(z)$ ,  $G_2(z)$ , . . . ,  $G_8(z)$  are given by equations (XI.16) through (XI.23).

As can be seen from equation (XI.15), in addition to containing the linear time invariant response due to the approximate transfer function  $H(z)$ , the response also contains components due to the response rotated at both the reference frequencies and components rotated at the sum and difference frequencies.

Once again the magnitude of each of the extra components is determined by terms of the form:

$$F = \sum_{j=0}^{L-1} e^{\pm i\phi_j} \quad (6.2.9)$$

where, in this case,  $\phi_j = \omega_j T$  where  $\omega$  may be twice either of the interfering frequencies or the sum and difference of the frequencies. This is particularly important in the case of closely spaced interfering frequencies where  $\omega = \omega_1 - \omega_0 \rightarrow 0$ , since from Figure 6.2.7 this gives rise to a large non-linear component.

These results generalise to the case of  $M$  sinusoids in a straightforward manner so that, in addition to the notch at each interfering frequency the response also contains components rotated at sums and difference frequencies and combinations thereof so that as the number of interferences increases the response contains a rapidly increasing number of rotated components.

### 6.3 Application of Adaptive Noise Cancellation to Narrowband Interference Rejection

#### 6.3.1 Parametric Study Set Up

To illustrate the results of the previous section a parametric study of the application of the ANC technique to narrowband interference has been undertaken. The study was based on the problem of cancellation of sinusoidal interferences from speech signals. A short section of speech was synthetically corrupted by various sinusoids and the performance of the ANC

technique was evaluated as a function of the algorithm's parameters. The criteria used for performance evaluation of the ANC were as follows:

i) **Steady-State In-band Attenuation:** The steady state attenuation within the one third octave band containing the interference(s) is defined for the purposes of this study as follows:

$$E(n) = s_p(n) - \hat{s}_p(n) \quad n > \text{some value, say}$$

to exclude convergence effects,

where  $s_p(n)$  is the speech signal and  $\hat{s}_p(n)$  is the speech signal estimate produced by the ANC, and then;

$$\text{Attenuation} = 10 \log_{10} \left( \frac{S_{EE}(\omega)}{S_{\sin}(\omega)} \right) \quad (6.3.1)$$

where  $S_{EE}(\omega)$  denotes the integrated power spectral density in the sinusoidal interference band, and  $S_{\sin}(\omega)$  is the integrated power spectral density of the sinusoidal in the band.

ii) **Steady-State Distortion Out of Band:** As a measure of steady-state distortion outside the one third octave which contains the sinusoid (out of band for short) the following definition is used:

$$\text{Distortion} = 10 \log_{10} \left( \frac{S_{EE}(\omega)}{S_{s_p s_p}(\omega)} \right) \text{ in one third octave bands} \quad (6.3.2)$$

where  $S_{EE}(\omega)$  is as previously defined and  $S_{s_p s_p}(\omega)$  is the integrated power spectral density of the speech signal.

Thus a characteristic plot of out of band distortion is created for each trial.

iii) Convergence Constant: The convergence was measured for the hypothetical case of both reference and primary pure sinusoids (see also Section 6.2.3). The resulting measure is thus a comparative result (between different parameter sets) and not necessarily an absolute measure of the ANC convergence for any given signal. The convergence constant,  $T_m$ , is then defined as the time for the absolute value of the error to fall below some preset level and remain below this threshold. The value chosen, generally, for convergence level was:

$$(\text{convergence level}) = \left( \frac{\text{initial error}}{1000} \right) \quad (6.3.3)$$

iv) Trials: The trials performed were as follows:

- a) Single interfering sine wave and noise free reference.
- b) Single interfering sine wave and noise corrupted reference.
- c) Double interfering sinusoids.

In each case interferences at various frequencies were used, and the amplitudes and phases of the reference inputs were varied.

Tests were performed using varying numbers of filter weights (from 8 - 24) and adaptation constants ( $\alpha = 0.001$  to  $\alpha = 0.051$ ).

### 6.3.2 Results

The results are presented in summary form together with appropriate references to tables/plots.

#### 1) Single Interfering Sine Wave with Noise Free Reference

In tests with a single interfering sine wave and noise free reference it was found that:

- a) The steady-state attenuation always exceeded 50dB.
- b) The convergence time,  $T_m$ , decreases as  $\alpha$  increases. The values from the trials have been plotted against those obtained theoretically (equation (X.21)). (Figure 6.3.1).

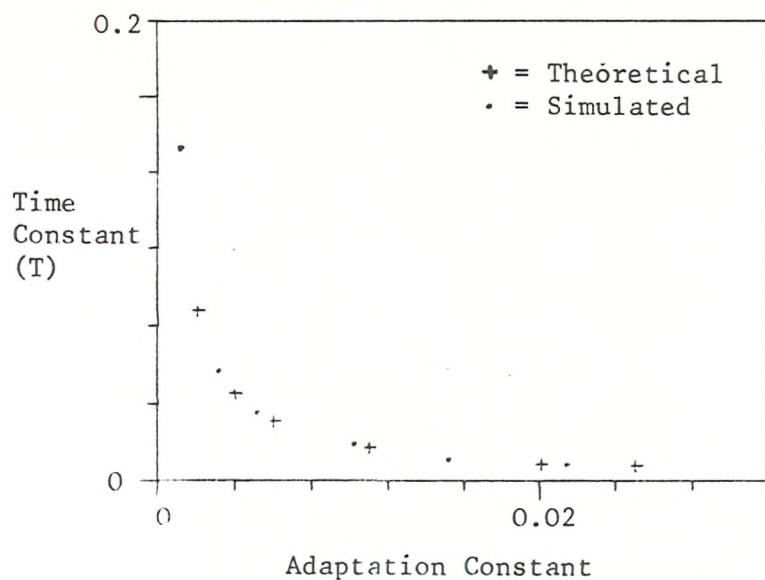


Figure 6.3.1: Time Constants for 16 Coefficients Theoretical and Simulated

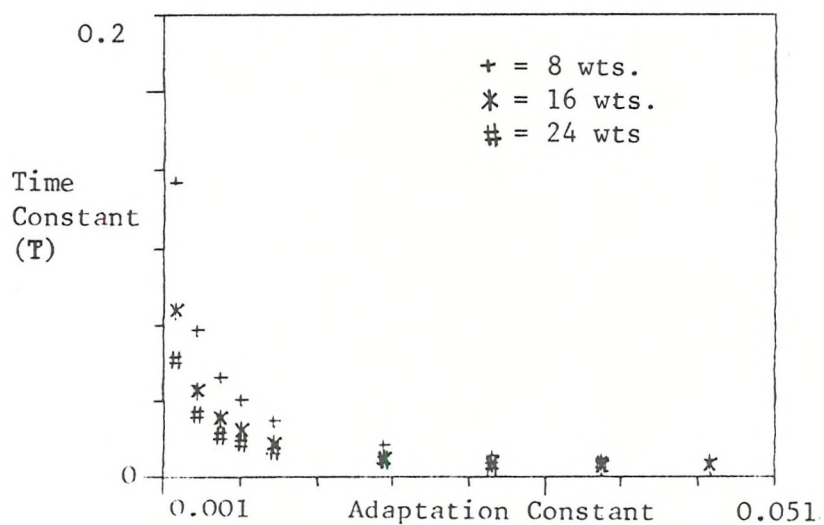


Figure 6.3.2: Time Constants versus Adaptation Rate

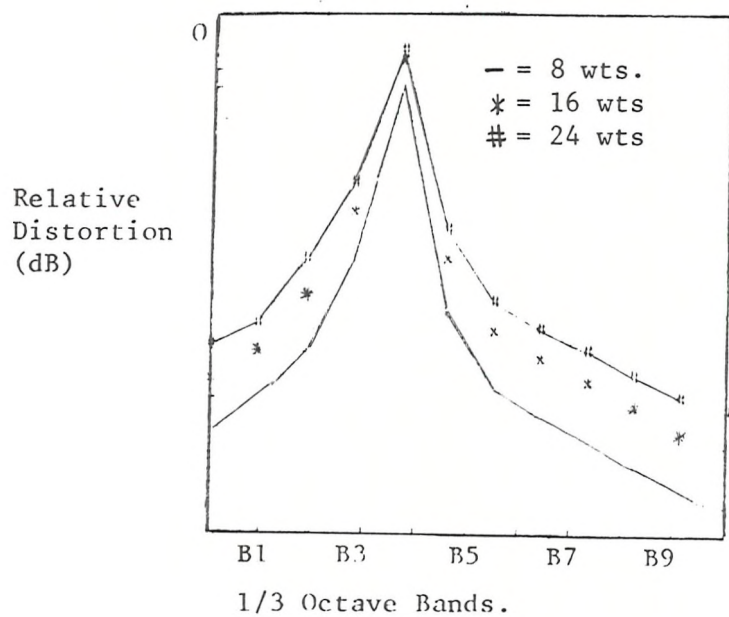


Figure 6.3.3: Distortion in 1/3 Octave Bands

c) At a given value for the adaptation constant , the convergence time decreases as the number of weights increases (Figure 6.3.2).

d) The out of band distortion increases in proportion to the number of weights (Figure 6.3.3).

Note, however, that it is not the adaptation constant but the rate of convergence which is important. The relevant question is:- At a given rate of convergence what is the relationship between the out of band distortion for varying numbers of weights?

In order to address this question, points of equal convergence time,  $T_m$ , were selected graphically and their out of band distortions compared. The results (Figure 6.3.4) show that all are remarkably similar.

e) Changing the phase of the reference input relative to the primary causes little significant change to either the out of band distortion or steady-state attenuation. Some reduction in convergence rates was experienced for small numbers of weights. This is probably a consequence of the fact that at most frequencies a small number of weights does not 'span' a complete cycle of the sinusoid.

f) Changing the amplitude of the interference in the primary has no significant effect on the performance of the ANC.

g) Changing the amplitude of the interference in the reference causes a change in the convergence rate and it was found that to produce an equivalent convergence rate,  $T_m$ , the adaptation constant must be varied according to the inverse square of the amplitude of the sinusoid (Figure 6.3.5). Note this result was also demonstrated in the previous section (equation (X.22)). If the adaptation constant is scaled in this manner then varying the reference amplitude has no significant effect on either the out of band distortion or the steady-state attenuation.

Relative  
Distortion  
(dB)

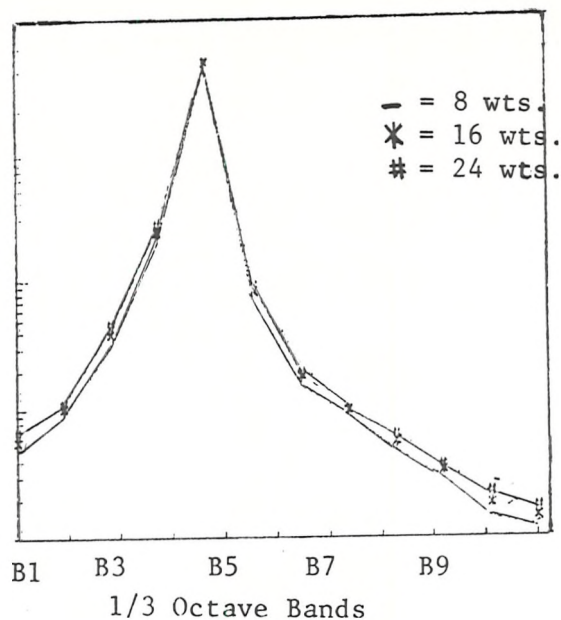


Figure 6.3.4: Distortion in 1/3 Octave Bands: Equal Convergence

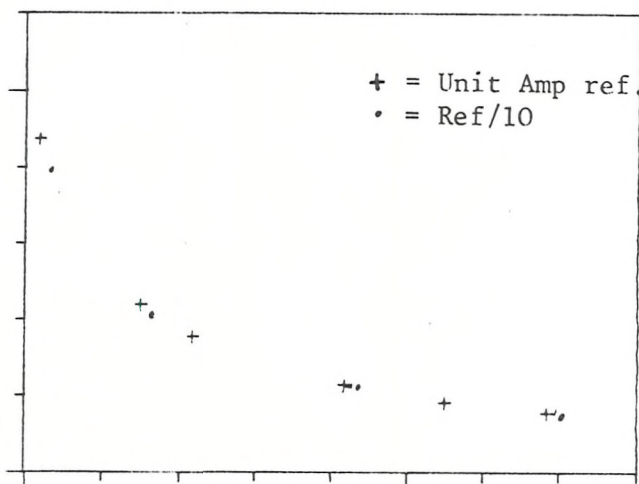


Figure 6.3.5: Time Constants for Amplitude Scaled Reference  
for 16 weights

Relative  
Distortion  
(dB)

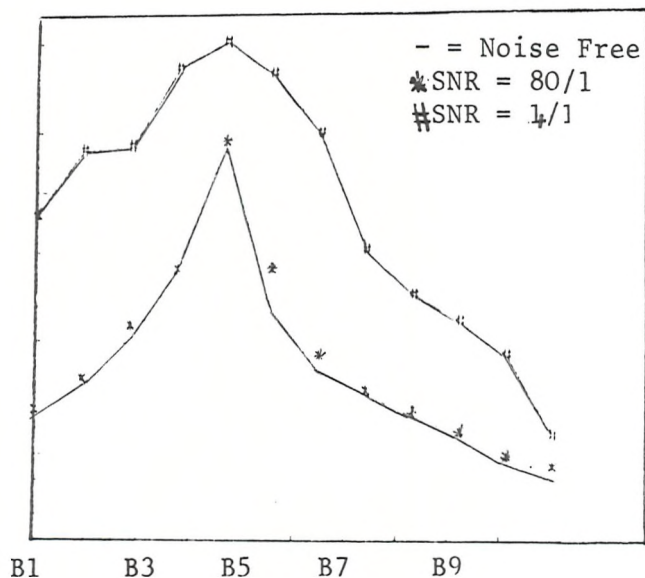


Figure 6.3.6: Distortion in 1/3 octave Bands for Reference  
Corrupted by Uncorrelated Noise (16 wts).



## 2) Single Interfering Sine Wave with Noisy Reference

a) If the reference is corrupted by additive white noise the steady-state attenuation remained above 50dB for all trials performed though clearly there must be some limits to this in relation to the reference SNR.

b) Increasing the noise level causes an increase in the out of band distortion (Figure 6.3.6).

c) With a white noise corrupted reference, convergence rates appear to be unchanged (Figure 6.3.7) but it was not possible to measure this in terms of the time constant  $T_m$ , as the steady-state errors were not sufficiently small.

d) At a given noise level with a given number of weights the steady-state errors are very similar for differing adaptation rates (that is, the steady-state error is primarily a function of noise level rather than parameters).

e) If the reference signal is corrupted by the addition of noise correlated with the primary signal then the performance is severely degraded by the introduction of even low levels of such noise.

## 3) Two Interfering Sinusoids

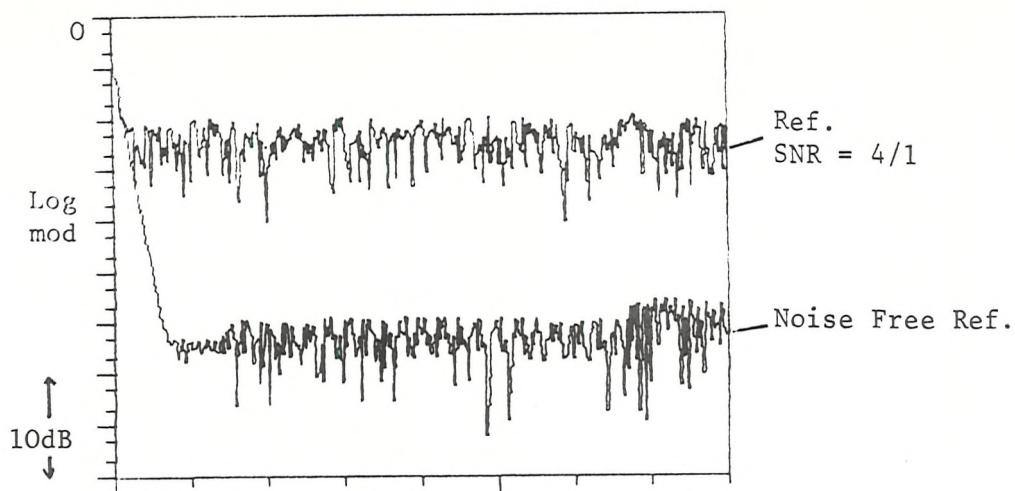
If the speech signal is corrupted by the addition of two sinusoidal interferences and a noise free reference is supplied the following results are generally observed:

a) The 'in-band' steady-state attenuation increases as the number of weights increases (table 6.3.1).

b) The out of band distortion increases as the number of weights increases (see Figure 6.3.8).

c) The time constant  $T_m$  decreases as the number of weights increases at a fixed adaptation constant.





Convergence (Relative)  
Figure 6.3.7: Convergence Curves for ANC

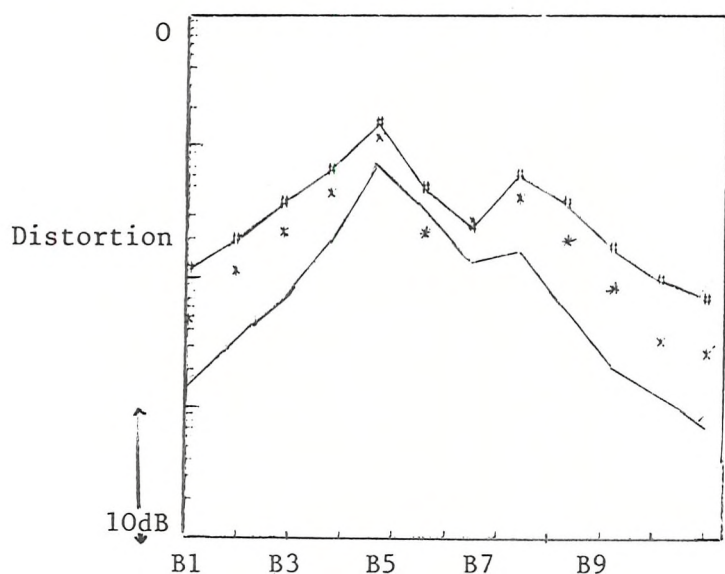


Figure 6.3.8: Distortion in 1/3 Octave Bands for ANC  
2 Interfering Tones

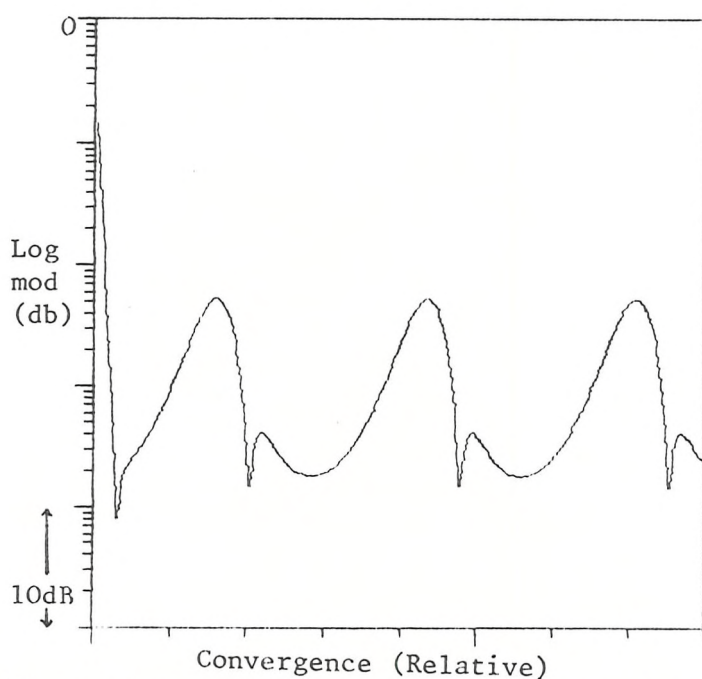


Figure 6.3.9: Convergence Curve for ANC with 2 Interfering  
tone (740 Hz and 750 Hz)

Table 6.3.1

## Steady-State Attenuation for Two Interfering Tones

Trial	Weights	Adaptation Constant	Attenuation (dB)	
			Lower	Upper
Interfering frequencies 400 Hz and 750 Hz	8	.001	-9.92	-36.26
	8	.006	-18.78	-50.40
	8	.011	-20.52	-52.24
	8	.016	-22.34	-34.05
	16	.001	-30.49	-57.80
	16	.006	-40.96	-69.89
	16	.011	-40.64	-67.92
	16	.016	-40.32	-67.25
	24	.001	-41.34	-77.12
	24	.006	-40.63	-70.53
	24	.011	-40.19	-69.19
	24	.016	-40.04	-68.49
Interfering Frequencies 750 Hz and 1000 Hz	8	.001	-19.35	-22.93
	8	.006	-28.51	-32.33
	8	.011	-32.68	-36.40
	8	.016	-36.85	-40.38
	16	.001	-28.53	-31.28
	16	.006	-56.82	-58.93
	16	.011	-55.76	-57.93
	16	.016	-55.08	-56.98
	24	.001	-60.77	-62.95
	24	.006	-55.76	-55.52
	24	.011	-54.77	-57.22
	24	.016	-54.05	-56.62
Interfering Frequencies 750 + 1500 Hz	8	.001	-40.54	-45.58
	8	.006	-73.02	-75.24
	8	.011	-71.79	-77.09
	8	.016	-70.69	-69.85
	16	.001	-77.09	-76.34
	16	.006	-71.11	-72.08
	16	.011	-69.61	-68.24
	16	.016	-68.79	-66.10
	24	.001	-74.40	-77.25
	24	.006	-69.67	-69.50
	24	.011	-68.31	-65.98
	24	.016	-67.50	-64.23

If the two interfering tones are close in frequency the results are similar to the above except that the convergence time  $T_m$  cannot be computed due to the behaviour of the error (Figure 6.3.9). Difficulties with close frequencies were foreseen in the theory section where it was pointed out that the approximate transfer function derived there would be particularly inaccurate in this case.

### 6.3.3 Conclusions

All of the above results serve to confirm the work of the previous section. For the single interference case this shows the validity of the existing theory both in terms of frequency characteristics and convergence rates. For the multi-sinusoid case, as demonstrated here with just two interferences, it is clear that the approximate transfer function theory can only provide an adequate description for large numbers of weights. These difficulties are particularly acute in the case of interfering tones which are closely spaced (in frequency). All of this is as predicted by the theory of Section 6.2, that the deviations from the transfer function theory are due to the effects predicted by the generalised response will be illustrated in the next section.

It is clear from the results that for the case of a single interfering tone the adaptive noise cancellation method provides an effective approach to narrowband attenuation. However, for the case of multiple interferences the performance deteriorates. Furthermore, this deterioration is particularly marked when the interfering tones are closely spaced. Although the problem can be alleviated by increasing the number of weights in the filter this solution rapidly becomes impractical as the number of interferences increases. In the following section an alternative approach aimed at overcoming (in part) these problems is proposed.

## 6.4 Sparse Adaptive Filters

### 6.4.1 Introduction

In this section an alternative approach to narrowband interference rejection based on the concept of sparse adaptive filters is developed. The main aim of this development is to provide an alternative approach to the conventional ANC for the case of multiple interfering sinusoids. However, a novel application of these filters to frequency response tracking is also considered. A sparse filter is a filter which has relatively few non-zero coefficients, separated by non-uniform time intervals. For a transversal implementation of such a filter the output would thus have the form:

$$y(k) = f(0)x(k) + f(1)x(k - n_0) + \dots f(L)x(k - n_{L-1}) \quad (6.4.1)$$

The interest here is in adaptive sparse filters where the coefficients are updated using the LMS algorithm. The simplest example of a sparse filter has just two points (see Figure 6.4.1).

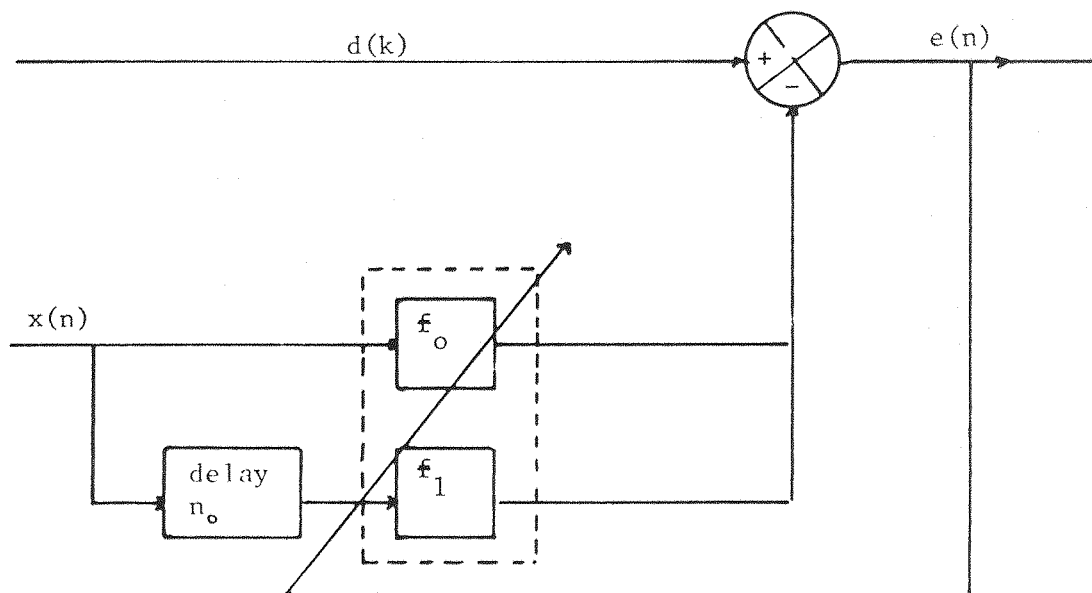


Figure 6.4.1: Two-point Filter Structure

The idea of 2 point adaptive filters is not new, having been used for some years in processing narrowband signals in antenna arrays . Such filters have also been suggested for notching a single tone in an adaptive noise cancelling system [117]. The use of sparse filters with more than 2 coefficients for multi-tone cancellation can be considered as a natural generalisation of this.

For the 2 point filter tone cancellation is achieved using the system shown in Figure 6.4.1. The set up is similar to that for conventional ANC with both a primary and reference measurement. The interval between the coefficients,  $n_o$ , is an integer multiple of the sample interval, chosen to delay the reference sinusoid by  $90^\circ$  (as nearly as possible), that is:

$$\omega_o n_o T = \frac{\pi}{2} \quad ; \quad \omega_o = 2\pi f_o$$

Hence

$$n_o = \frac{1}{4f_o T} \quad (6.4.2)$$

such an interval will henceforth be referred to as  $\pi/2$  samples. The reasoning behind this choice of delay will be examined shortly.

In addition to its function as a single notch, Glover [33], has also suggested that in the case of  $M$  sinusoids, provided that each interfering tone was available as a separate reference input, then each tone might be cancelled separately by the use of a 2 point filter (see Figure 6.4.2).

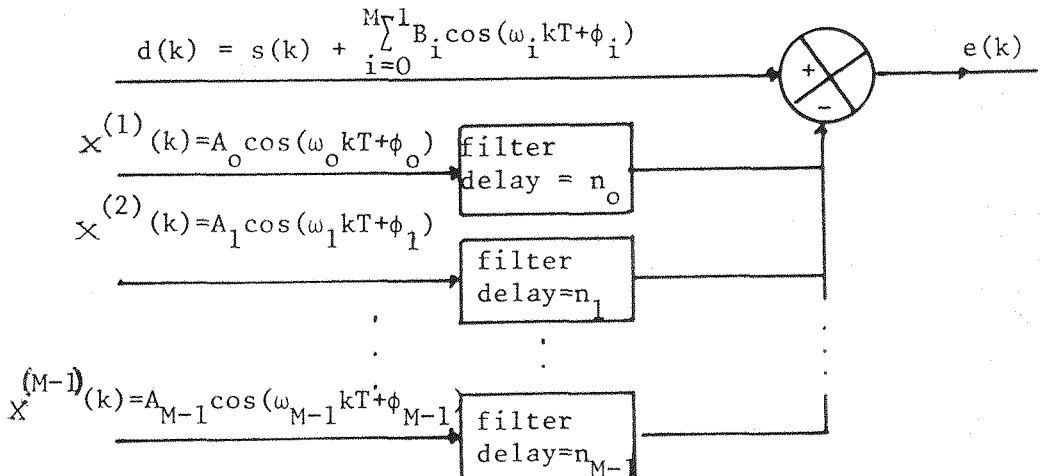


Figure 6.4.2: Multi-tone Cancellation with Separate References

Unfortunately this situation is fairly unrealistic since it is unlikely that one would have  $M$  separate references available (particularly if the frequencies were closely spaced).

The approach suggested here - for the more usual case when separate reference inputs are not available for each tone - is to use a sparse adaptive filter. The set up of the system is shown in Figure 6.4.3. One extra coefficient is used for each extra tone to be cancelled. That is, if there are  $M$  tones to be cancelled there will be a total of  $M+1$  filter coefficients,

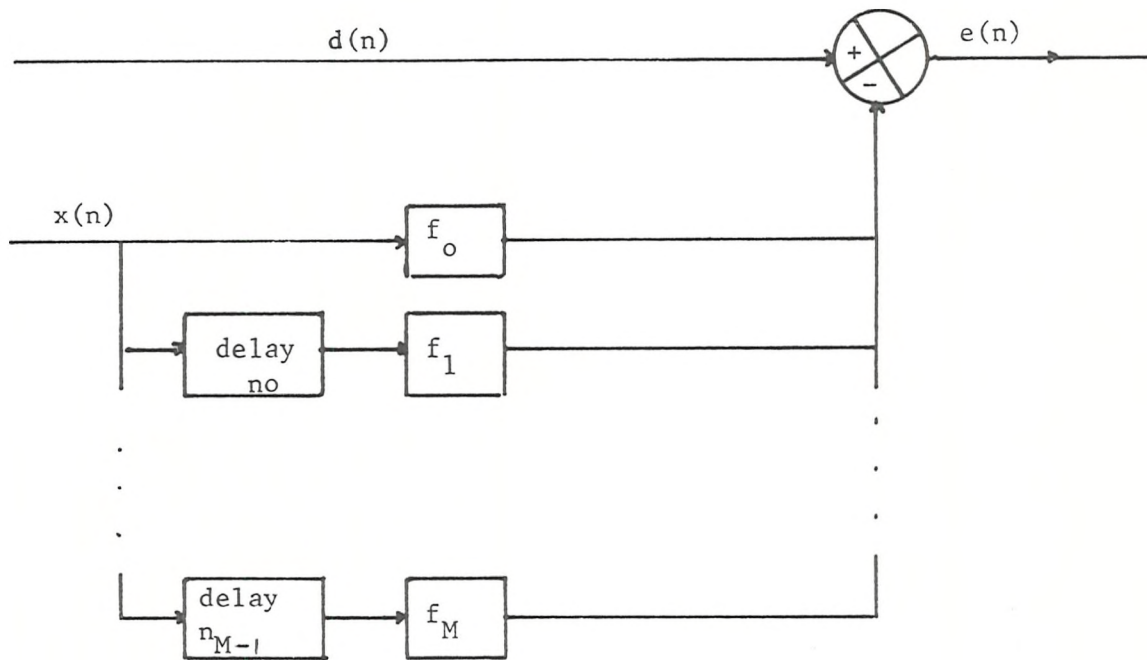


Figure 6.4.3: Multi-tone Cancellation with Single Reference Input

and where in each case the delay  $n_i$  is set approximately equal to  $\pi/2$  samples at the corresponding interference frequency. In this section it will be demonstrated that such filters will usually give superior performance to conventional ANC filters of equivalent (and often greater) lengths.

The principles of sparse filter behaviour in an ANC system are initially demonstrated both in theory and practise using the simplest case - the 2 point filter. The behaviour of the more general sparse filter in cancelling multiple tones will then be examined and contrasted with ANC.

A novel application of the two point adaptive filter is developed in the area of frequency response determination. Because this application is not strictly relevant to the thesis it is restricted to an Appendix (XIII), it is included, however, because it is an interesting and novel application of sparse adaptive filters, and because it is illustrative of the properties of these systems.

#### 6.4.2 Theory of Two Point Filter

##### 1) Approximate Transfer Functions

Consider the system depicted in Figure 6.4.3, where initially it is assumed that there is a single interfering tone ( $M=1$ ). An expression for the approximate transfer function for this system may be obtained simply by setting  $L=2$  in equation (X.10), giving:

$$H(z) = \frac{1 - 2z^{-1} \cos \omega_o T + z^{-2}}{(1 - \alpha A_o^2) z^{-2} + (\alpha A_o^2 - 2) z^{-1} \cos \omega_o T + 1} \quad (\text{X.10a})$$

(this can easily be verified using methods analogous to those of Appendix X).

This transfer function has zeroes at  $z = e^{\pm i\omega_o T}$  and poles approximately at  $z = (1 - \frac{\alpha A_o^2}{2}) e^{\pm i\omega_o T}$  and is exact when  $\omega_o = \pi/2$ , but is approximate in other cases.

Similarly if there are two interfering tones the direct analogy with the results of section 6.2.5, the response can be approximated by a system of the form:

$$H(z) = \frac{1}{1 + G_1(z) + G_2(z)} \quad (6.4.3)$$

where

$$G_1(z) = \alpha A_o^2 \left( \frac{z^{-1} \cos \omega_o T - z^{-2}}{1 - 2z^{-1} \cos \omega_o T + 1} \right)$$



$$\text{and } G_2(z) = \alpha A_1^2 \left( \frac{z^{-1} \cos \omega_1 T - z^{-2}}{1 - 2z^{-1} \cos \omega_0 T + z^{-2}} \right)$$

This system has zeroes at  $z = e^{\pm i\omega_0 T}$  and  $z = e^{\pm i\omega_1 T}$  and poles approximately located at:

$$z = \left(1 - \frac{\alpha A_0^2}{2}\right) e^{\pm i\omega_0 T} \quad \text{and}$$

$$z = \left(1 - \frac{\alpha A_1^2}{2}\right) e^{\pm i\omega_1 T}$$

## 2) Generalised Response

Recall that in the single interference case for the L point filter, the transfer function is exact if the spacing between filter coefficients is an integer multiple of  $\pi/L$  samples at the reference frequency. Hence in this case the requirement is for the space between each filter coefficient to be  $\pi/2$  samples. In the multiple sinusoid case the requirement is that the filter spacing be an integer multiple of  $\pi/2$ , both at all the individual interference frequencies and at the sums and differences thereof. If these conditions do not hold the accuracy of the approximation increases with the length of the filter.

Bearing this in mind it is clear that the transfer function will be particularly inaccurate in the case of the 2 point filter.

The generalised response for the 2 point filter may be obtained directly from the results of Section 6.3.5. For the single interfering sinusoid ( $x(k-i) = A \cos(\omega_0(k-i)T)$ ), the response satisfies (XI.13) with:

$$\begin{aligned} G_1(z) &= \frac{-\alpha A^2}{4} (e^{i2n_0 \omega_0 T} + 1) U(z e^{-i\omega_0 T}) \\ G_2(z) &= -\frac{\alpha A^2}{4} (e^{-2n_0 \omega_0 T} + 1) U(z e^{i\omega_0 T}) \quad (\text{see Appendix XI}) \end{aligned}$$

That is, the response has exactly the same form as for the L point filter, (see Section 6.2.6) only the complex scale factor for the non-linear terms varies.



Similarly for the multi-sine input case the form of the response is identical but

$$\sum_{i=0}^{L-1} e^{2i\phi_{1i}} \text{ becomes } (1 + e^{i2n_o\omega_o T}) \text{ and}$$

$$\sum_{i=0}^{L-1} e^{2i\phi_{2i}} \text{ becomes } (1 + e^{i2n_o\omega_o T}) \text{ in equations (XI.16)}$$

to (XI.23), where it may be recalled from Section 6.2.6 that the magnitude of these terms determines both the convergence time of the system, and the magnitude of the spurious components in the frequency response.

$$\text{Now, } |1 + e^{i2n_o\omega_o T}| = |2 \cos n_o\omega_o T|$$

Accordingly these terms are largest - and thus the response is poorest - when  $n_o\omega_o T \rightarrow 0$  or  $\pi$  and become smallest as  $n_o\omega_o T \rightarrow \pi/2$  (which explains why this choice of  $n_o$  is made where possible). Note that at  $\pi/2$  these terms are zero and thus the transfer function form is exact.

#### 6.4.3 Two Point Filter: Simulations

The above results can be illustrated with a few simple examples. It is also interesting to compare these results with the pole-zero plots for the same systems (Appendix XI).

$$\text{a) } \underline{d(k) = B \cos(\omega_o kT + \psi), \quad \text{Ref} = A \cos(\omega_o kT)}$$

A single sine wave (at frequency 500Hz, sample rate = 10KHz) was supplied as reference and as primary to a 2 point filter. The delay  $n_o$  between the coefficients was varied. Figure 6.4.4(a) and (b) show the modulus frequency response for delays  $n_o = 5$  ( $\pi/2$  samples) and 3 respectively. As can be seen the main distinction between the two responses is the 'glitch' in the latter at a frequency of  $3\omega_o$  caused by the rotation of the response through  $2\omega_o$ . This is of course as predicted by the generalised response.

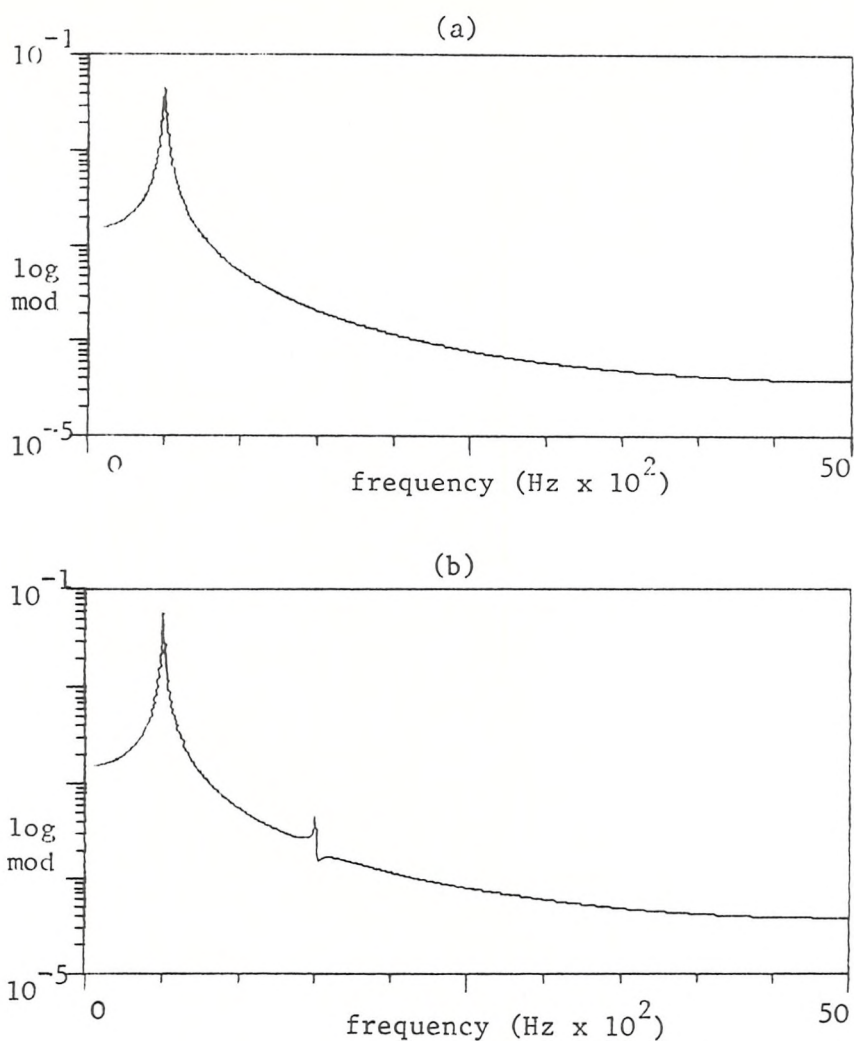


Figure 6.4.4: Modulus Response Curves for 2 point Filter with  $n_o = 5$ (a) and  $n_o = 3$ (b)

Figure 6.4.5 shows the convergence curves obtained from the log peak response curves for  $n_o = 2, 3, 4$  and 5. As is clear from this plot the convergence reduces as  $n_o$  becomes further from  $5, (\pi/2)$  samples, which again is in line with the predictions of Section 6.4.3.

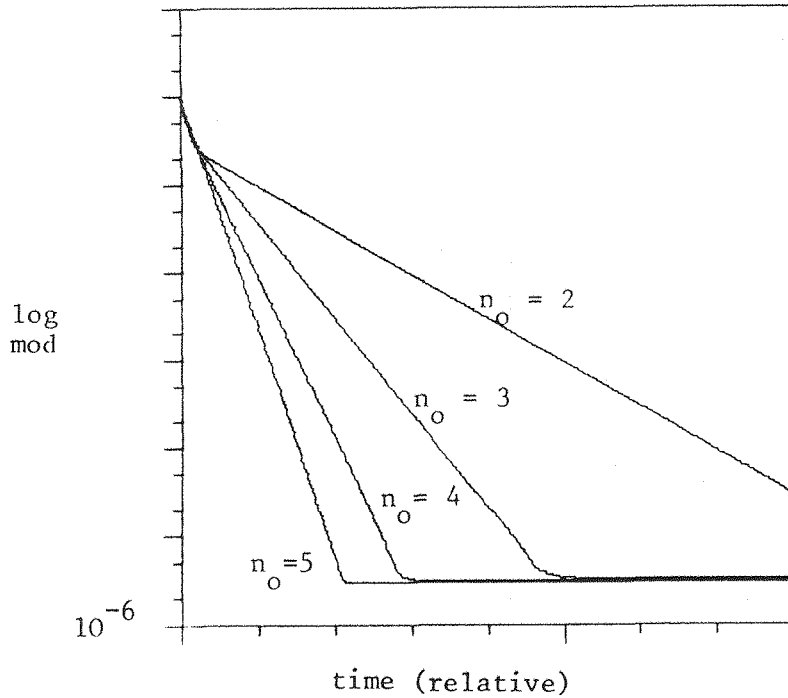


Figure 6.4.5: Convergence Curves for  $n_o=2, 3, 4$ , and  $5$ .

$$b) \quad \frac{d(k) = B \cos(\omega_o kT + \psi) + C \cos(\omega_1 kT + \psi)}{\text{ref} = A \cos \omega_o kT}$$

A single sine wave at frequency  $\omega_o$  (500Hz, sample rate = 10KHz) was supplied as reference to a two point filter. The primary consisted of the reference sinusoid plus a second sine at frequency  $\omega_1$  (800Hz). The modulus frequency responses for  $n_o = 5$  and  $3$  are shown in Figures 6.4.6(a) and (b) respectively. The main distinction is two extra components, one at 1800Hz and one at 200Hz. The first corresponds to a component from  $\omega_1$  heterodyned by  $2\omega_o$ , the second is due to a component from  $-\omega_1$  again heterodyned by  $2\omega_o$ , and both are predictable from equation (XI.13). (See Appendix XI). Closer inspection reveals a smaller, again predictable, element at  $3\omega_o$ .

These extra components in the response may appear relatively minor aspects of the overall response but it is worth remembering that these are very simple examples, as the input signals increase in complexity so to do the resulting responses.

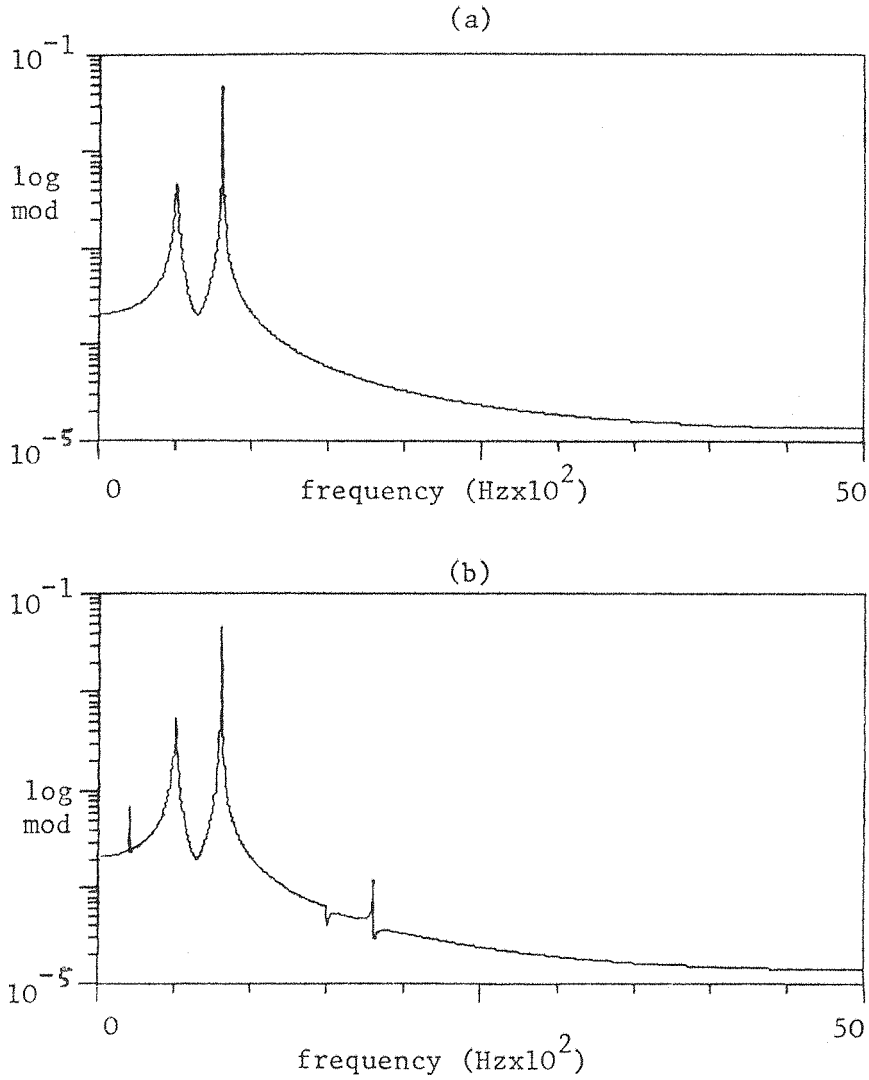


Figure 6.4.6: Modulus Response for 2 pt Filter with  $n_o=5$ (a) and  $n_o=3$ (b)

#### 6.4.4 Multi-tone Cancellation using Sparse Adaptive Filters

The aim in this section to investigate the relationship between the use of the conventional single L point ANC scheme and sparse adaptive filters for multi-tone cancellation. For obvious algebraic reasons this study is restricted to just two sine waves. To be strictly comparable in computational as well as other terms  $L = 3$  should be used, but it will be seen that often the sparse implementation will be superior to the conventional formulation for larger numbers of weights.

If the reference input is assumed to be:

$$x(k) = A_o \cos(\omega_o kT) + A_1 \cos(\omega_1 kT)$$
 then for the sparse as in Figure 6.4.3, with  $M=2$ , the approximate transfer function

can be shown (using methods analogous to Appendix X) to be identical to that for the single L point filter with  $L = 3$ . However, there are significant differences in the behaviour of the two implementations and these are apparent from the non-linear components described in Section 6.3. It can be shown (Appendix XII) that the response for the sparse filter has the same form as that of the single L point filter (Equation XI.15). It is the complex scale factors for the  $G_i(z)$  which vary. For the L point case these are obtained from equations (XI.16) - (XI.23), whilst for the sparse formulation they are given by equations (XII.4) - (XII.12). (see Appendix XII). For the case of  $M=2$  and where, for simplicity, each coefficient has a delay equal to  $\pi/2$  samples at the corresponding frequency, these become equations (XII.14) - (XII.21). Hence, in order to evaluate the performance of the two approaches it is necessary to compare the magnitudes of these coefficients with those of (XI.16) - (XI.23).

As discussed in Section 6.2 in the case of the L point filter all terms have the form:

$$\sum_{j=0}^{L-1} e^{i\theta j T} \quad \text{where, for example; for } G_5 \quad \theta = \omega_1 - \omega_0.$$

Now,

$$\left| \sum_{j=0}^{L-1} e^{i\theta j T} \right| = \left| \frac{\sin \frac{L\theta j T}{2}}{\sin \frac{\theta j T}{2}} \right| \quad (6.4.4)$$

This function is displayed in Figure 6.2.7 (as a function of  $\frac{\theta}{2}$ ). For the sparse form the first four terms have the form:

$$|e^{i\theta}| = 1 \quad (6.4.5)$$

whilst the remaining terms have the form:

$$|1 \pm i e^{i\theta} \pm i e^{i\phi}| < 3 \quad (6.4.6)$$

Contrasting (6.4.5) and (6.4.6) with (6.4.4), it is clear that the sparse form will have smaller coefficients than the two point for frequencies  $2\omega_i < \frac{2\pi}{L}$ . For the sum and difference frequencies similar rules will apply, that is, if the sum and/or difference frequencies are less than  $\frac{2\pi}{L}$ , then the sparse formulation will be superior. The difference frequency is particularly relevant if the sinusoids are closely spaced since the difference will then usually be  $< \frac{2\pi}{L}$  unless  $L$  is very large, and the sparse filter will be considerably superior. Note that in the case of  $L=3$ , the relevant frequency is  $\frac{2\pi}{3}$  or two thirds of the folding frequency. In addition to the likely superiority (for small  $L$ ) of the sparse formulation in terms of these coefficients, the same form will also generally have superior convergence properties. This latter characteristic is a consequence of the fact, asserted in Section 6.2, that the convergence is decreased as the filter spacing moves away from  $\pi/L$  at the relevant frequencies.

Of course, as the number of interfering tones increases so does the number of coefficients in the sparse filter, and thus so will the extraneous terms. However, the important point is that the number of coefficients in the sparse filter will always be small in relation to the number required for comparable performance from the conventional ANC. Hence the number of damaging extra components in the response will be less in the sparse filter than the conventional ANC. A further bonus as a consequence of the lower number of weights required by the sparse filter is a reduced computational burden.

Simulations. The above observations are illustrated by a few simulations. Figure 6.4.7 shows the responses for a single 4 point ANC and a sparse 3 point filter when supplied with 2 sine waves (500Hz and 833.3Hz) as both reference and primary.

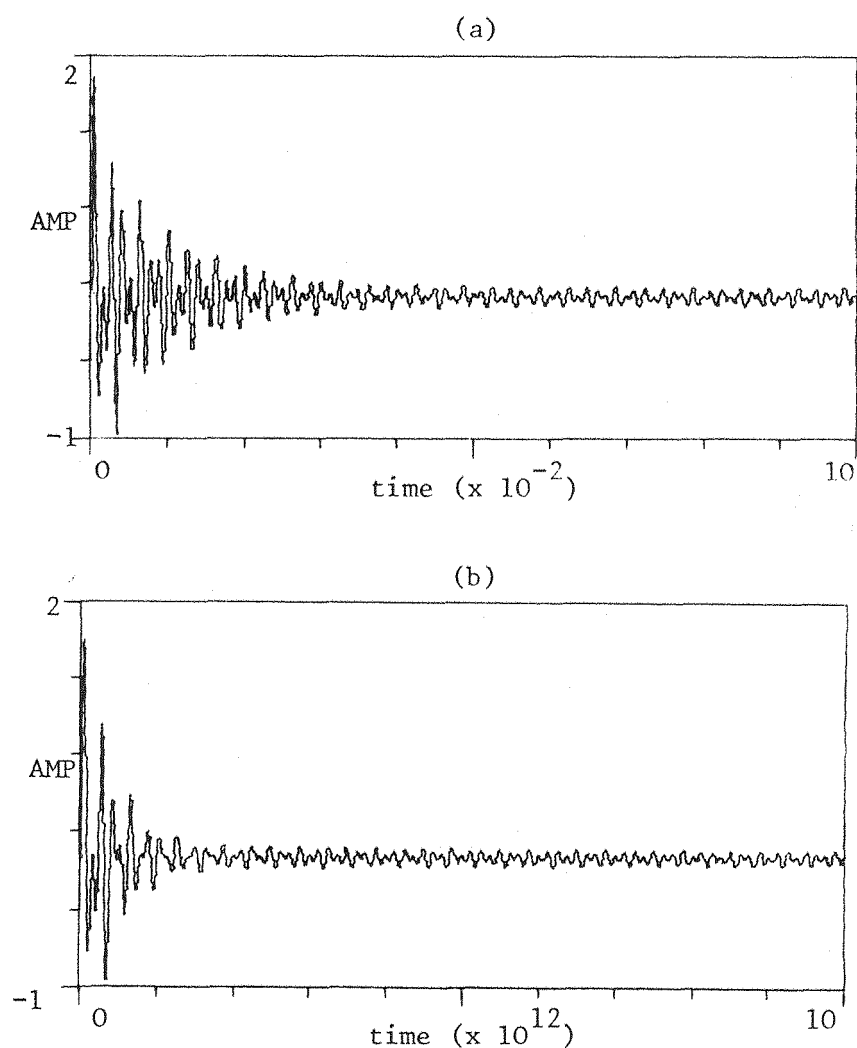


Figure 6.4.7: Convergence of 4 weight ANC (a) and Sparse Filter (b)

Both filters had the same adaptation constant ( $\alpha = 0.01$ ) but it is clear that the sparse filter converges much more quickly. The modulus frequency responses are shown in Figure 6.4.8. It is apparent that the sparse formulation has led to a reduction in the heterodyned components of the response.

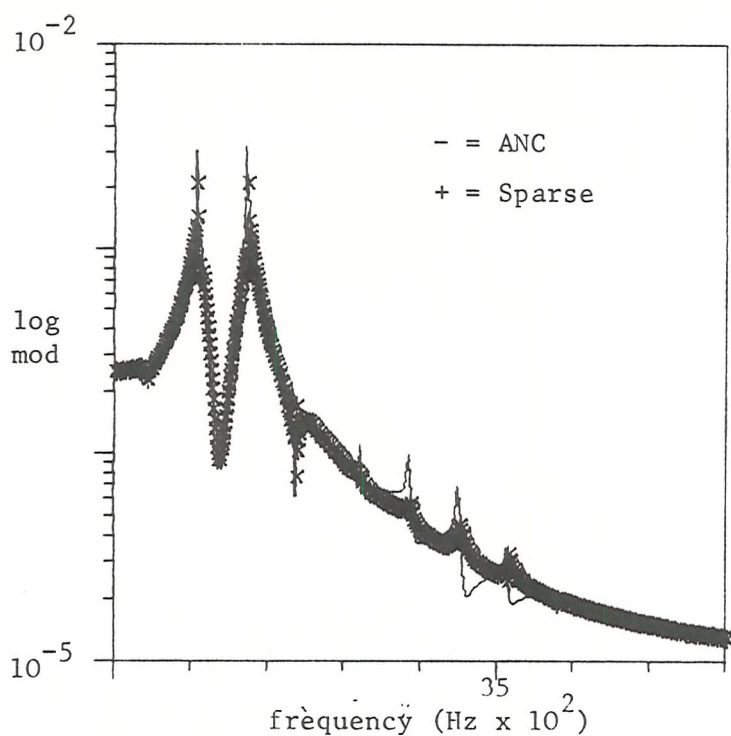


Figure 6.4.8: Modulus Responses for Adaptive Noise Cancellation (4 weights) and Sparse Filter.

Hence it may be concluded that this has improved considerably on the 4 point ANC. When compared with the 16 point ANC response the sparse response is no longer markedly superior but is broadly comparable (Figures 6.4.9 and 6.4.10) but, of course, now has considerable computational advantages.



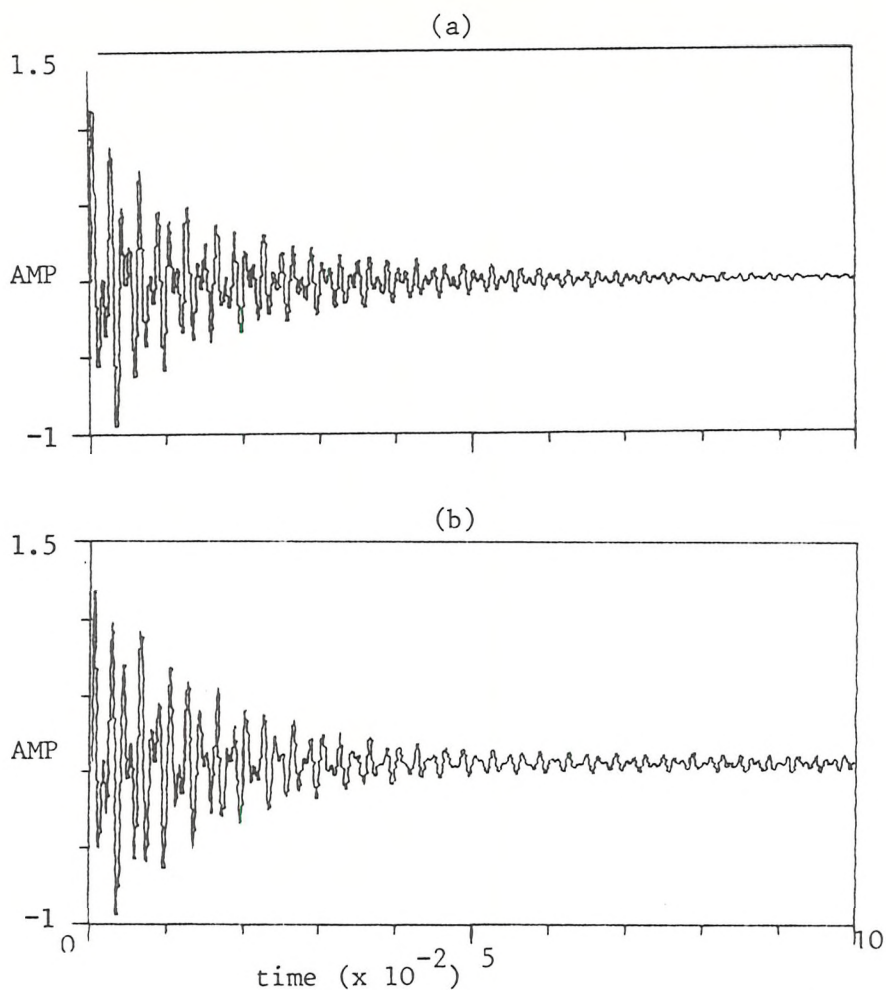


Figure 6.4.9: Response for 16 point ANC (a) and Sparse Filter (b) ( $\alpha = 0.0025$ )

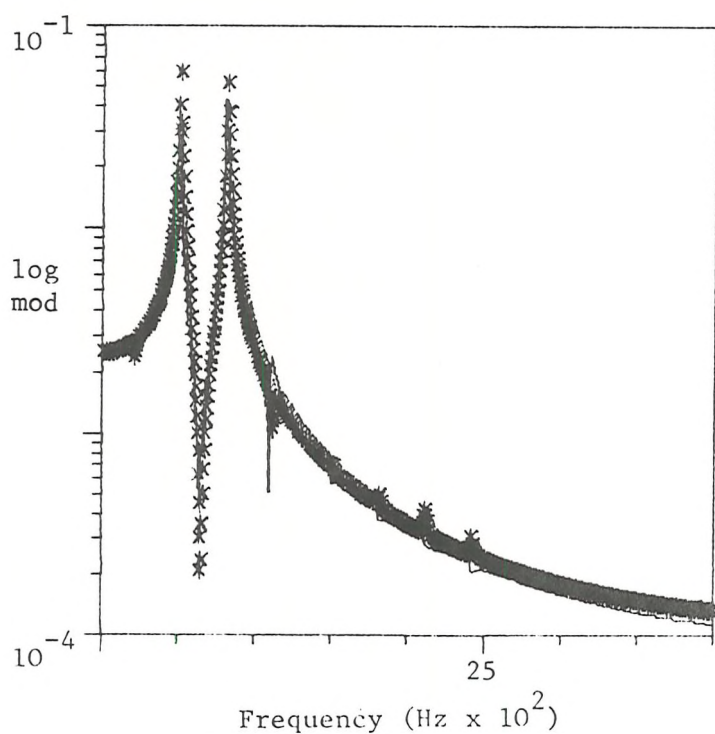


Figure 6.4.10: log modulus Response for 16 point ANC and Sparse Filter ( $\alpha = 0.0025$ )

## 6.5 The Function Elimination Filter

### 6.5.1 Introduction

Plotkin [72-74] has described an alternative approach to tone cancellation which he has dubbed the function elimination filter (FEF). FEF is mainly intended to be used when no external reference is available and when there is not a sufficiently long data section to allow the use of delay as depicted in Figure 6.2.2. The basic idea of FEF is to filter the signal using a filter whose form is fixed as:

$$F(z) = 1 - 2 \cos \omega_0 T z^{-1} + z^{-2} \quad (6.5.1)$$

This filter is a notch and the algorithm estimates a single parameter, the notch frequency  $\omega_0$ , using a least-squares technique. If the input is

$$x(k) = A \cos(\omega_0 kT - \theta) \quad (6.5.2)$$

then convolving with (6.5.1) shows that the output  $y(k) = 0$  for  $k \geq 2$ . That is

$$y(k) = 0 = x(k) - 2 \cos \omega_0 T x(k-1) + x(k-2) \quad (6.5.3)$$

;  $k \geq 2$ , so that

$$x(k) = 2 \cos \omega_0 T x(k-1) - x(k-2)$$

or

$$x(k) = c_1 x(k-1) - x(k-2) \quad (6.5.4)$$

$c_1$  is unknown but could be computed from (6.5.4). However if  $x(k)$  is corrupted by noise (or another signal) then equation (6.5.3) no longer holds. Plotkin suggests that:

$x_k$  can be estimated by:

$$\hat{x}(k) = \hat{c}_1 x(k-1) - x(k-2) \quad (6.5.5)$$

and  $\hat{c}_1$  by a least-squares fit, that is

$$\text{minimise } I = \sum_{N_e} (x(k) - \hat{x}(k))^2 \quad (6.5.6)$$

where  $N_e$  is the estimation interval.

The solution of (6.5.6) is easily obtained as:

$$\hat{c}_1 = \frac{\sum_{N_e} (x(k-2) + x(k)) x(k-1)}{\sum_{N_e} x(k-1)} \quad (6.5.7)$$

### 6.5.2 Problems with The Function Elimination Filter

There are two main problems with FEF:

a) Bias of Estimates: In general the estimate of the parameter  $c_1$  produced by the FEF will be biased. To see this consider the estimation procedure of equation (6.5.7)

if now  $x(k) = s(k) + v(k)$  where

$$s(k) = A \cos(\omega_0 kT + \phi)$$

$v(k)$  is stationary, zero mean and ergodic, then this becomes

$$\begin{aligned} \hat{c}_1 &= \frac{\frac{1}{N_e} \sum_{N_e} (s(k-1) + v(k-1))(s(k) + v(k) + s(k-2) + v(k-2))}{\frac{1}{N_e} \sum_{N_e} s^2(k-1) + \frac{1}{N_e} \sum_{N_e} v^2(k-1) + \frac{2}{N_e} \sum_{N_e} s(k-1)v(k-1)} \end{aligned} \quad (6.5.8)$$

Now the true value  $c_1$  is:

$$c_1 = \frac{s(k) + s(k-2)}{s(k-1)} \quad (6.5.9)$$

Hence combining (6.5.8) and (6.5.9)

$$\hat{c}_1 = \frac{1}{N_e} \frac{\sum}{N_e} \left[ \frac{s^2(k-1) c_1 + s(k-1) (v(k) + v(k-2)) + v(k-1) (s(k) + s(k-2)) + v(k-1) (v(k) + v(k-2))}{(v(k) + v(k-2))} \right]$$

$$\frac{1}{N_e} \sum s^2(k-1) + \frac{1}{N_e} \sum v^2(k-1) + \frac{2}{N_e} \sum s(k-1)v(k-1)$$
(6.5.10)

Now  $\lim_{N_e \rightarrow \infty} \frac{1}{N_e} \sum s(k)^2 \rightarrow \frac{A^2}{2}$  (6.5.11)

and by assumption:

$$\lim_{N_e \rightarrow \infty} \frac{1}{N_e} \sum v(k)v(k-i) \rightarrow R_{vv}(i) \quad (6.5.12)$$

(the correlation coefficient)

If it is further assumed that:

$$\lim_{N_e \rightarrow \infty} \frac{1}{N_e} \sum s(k)v(j) \rightarrow 0 \quad \forall k, j \quad (6.5.13)$$

then in the limit

$$\hat{c}_1 \rightarrow \frac{\left(\frac{A^2}{2}\right) c_1 + 2 R_{vv}(1)}{\left(\frac{A^2}{2}\right) + R_{vv}(0)} \quad (6.5.14)$$

For example if  $v(k)$  were white noise, of variance  $\sigma^2$ , then

$$\hat{c}_1 \rightarrow \frac{c_1}{\left[ \frac{\sigma^2}{\left(\frac{A^2}{2}\right)} + 1 \right]} = \frac{(\text{interference power})}{(\text{total noise})} \cdot c_1 \quad (6.5.15)$$

Hence equations (6.5.14) and (6.5.15) show that in general  $\hat{c}_1$  is biased. Note, however, that given knowledge of the power of the interference and the first two correlation coefficients of the input noise, equation (6.5.14) could be used to remove the bias from the estimate so that with this correction FEF may still be useful in some circumstances. Also, of course, none of the foregoing applies when a noise-free reference measurement is available.

b) Notch Width: The other main problem with FEF is the notch width. The transfer function

$$F(z) = z^{-2} - z \cos \omega_o T z^{-1} + 1$$

has zeros on the unit circle at  $z = e^{\pm i\omega_o T}$  and is thus a notch at these frequencies. However, the notch width is completely uncontrollable and is far too great for most purposes (as will be seen in the simulations).

### 6.5.3 Modified Function Elimination Filter

The problem of the notch width in FEF can be overcome using a novel modification which is obtained by replacing the transfer function (6.5.1) by

$$\frac{z^{-2} - c_1 z^{-1} + 1}{1 - c_1 \rho z^{-1} + \rho^2 z^{-2}} \quad (6.5.16)$$

where  $c_1 = 2 \cos \omega_o T$  as before and  $\rho$  is a fixed parameter.

The effect of this modification is to put a pair of poles into the transfer function on the same radial lines as the zeros at a distance  $(1-\rho)$  from the unit circle, see Figure 6.5.1.

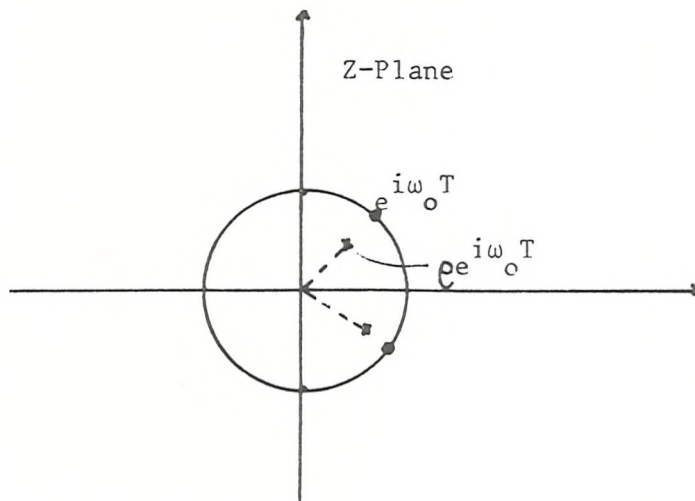


Figure 6.5.1: Pole/zero plot for Modified Function Elimination Filter

The parameter  $\rho$  determines the bandwidth of the notch, it is fixed in advance, and the estimation procedure (for  $c_1$ ) remains unchanged, thus avoiding problems of non-linearity in the estimation procedure.

Hence in the modified FEF the notch width is completely controllable, however, the bias problems discussed in the previous sections remain.

#### 6.5.4 Simulations

The function elimination filter and modified function elimination filter were applied to synthetic data created by adding a single sinusoid at 750Hz to a background of Gaussian white noise normalised to give a variance = 1/100 the level of the sinusoid power (Figure 6.5.2(a)).

Figures 6.5.2(b) shows the result of applying the Function Elimination Filter to the sine wave plus noise, without a reference measurement. The problems are immediately apparent - firstly the notch is far too wide, and secondly the notch position is biased. (The bias in this case should be 30.3 Hz according to equation (6.5.15) that is  $\hat{\omega}_0 = 780.3$  Hz, and this appears to be borne out).

When a noise-free reference measurement is available the bias is avoided and the results of Figure 6.5.2(c) are obtained. However, the notch width remains far too great. This is overcome using the modified FEF of equation (6.5.16), shown in Figure 6.5.2(d) and (e), for  $\rho = 0.9$  and  $0.99$  respectively, assuming again that a reference measurement is available. As expected the notch becomes increasingly narrow as  $\rho \rightarrow 1$ . Hence the modified FEF can be used to produce an arbitrarily sharp notch.

#### 6.6 CONCLUSIONS

In this chapter the problem of signal-to-noise enhancement by narrowband interference rejection has been considered. The Adaptive Noise Cancellation technique has been examined and found to be a powerful approach to the cancellation of a single or small number of tones where a reference measurement consisting almost entirely of the



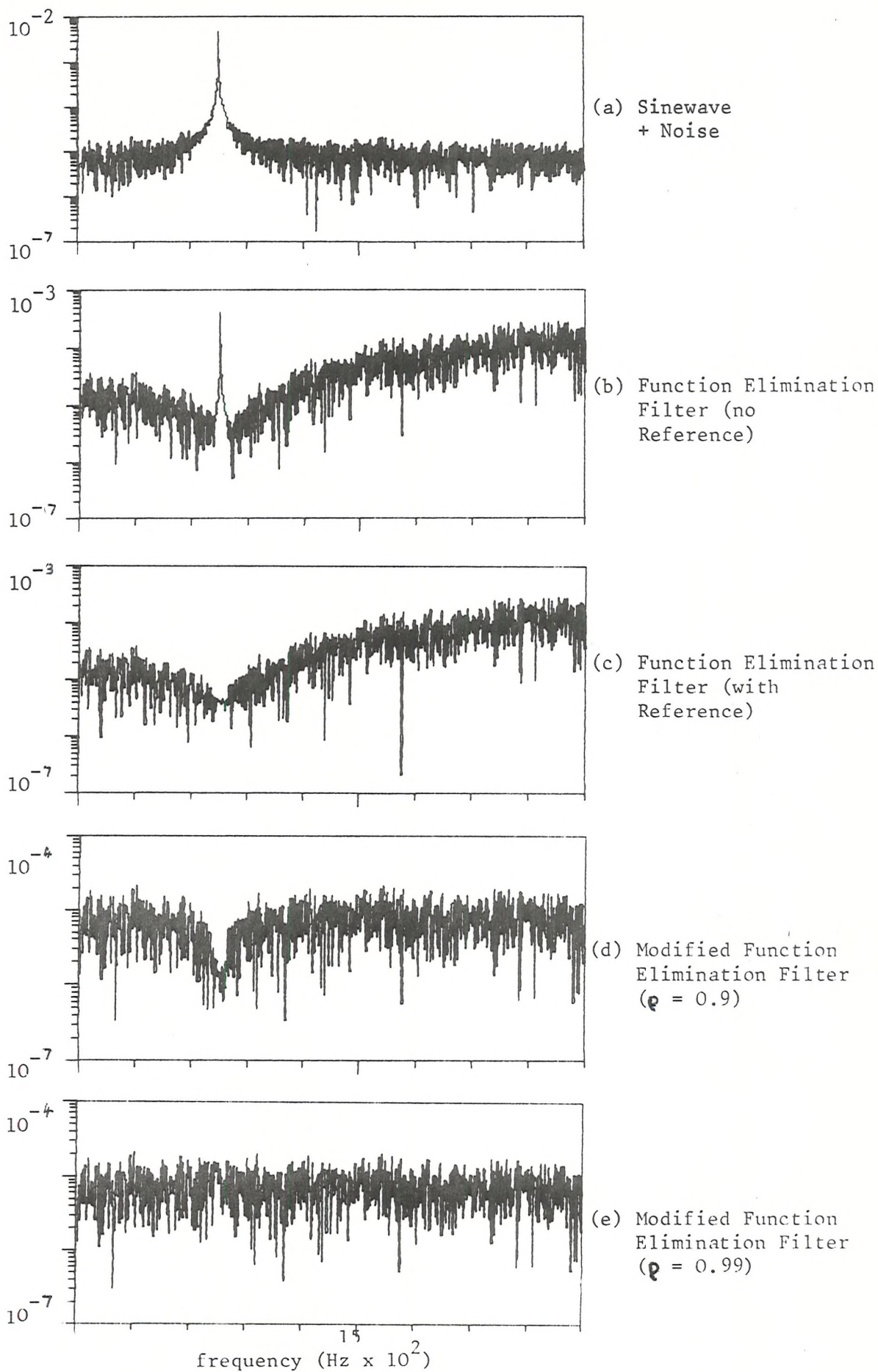


Figure 6.5.2: Function Elimination Filter Simulations

interferences alone is available. It was also found that in such circumstances the existing transfer function theory provides a good description of the system behaviour. However, this study has also indicated two main weaknesses of the ANC approach, which have been addressed:

1) Multiple Tone Cancellation

The adaptive noise cancelling method performs far less well on the cancellation of larger numbers of tones, particularly on tones which are closely spaced (in frequency) and even on small numbers of tones when the filter is not sufficiently long. In all these cases the filter fails to attenuate the interferences to a sufficient degree and also introduces cancellation at spurious frequencies. None of these phenomena are predictable from the existing transfer function theory and so a novel extension of this theory which provides a description of these aspects of the system behaviour has been produced. An alternative approach to narrowband cancellation in these circumstances has also been produced based on the idea of sparse adaptive filters. Using the extra theory the behaviour of the new formulation has been compared to that of the conventional ANC. It was found that the new formulation is likely to be superior in many instances, in terms of steady-state distortion, rate of convergence and computational requirement.

2) Reference Measurement Unavailable

The second major weakness of ANC is the circumstances when it cannot be applied - namely when a reference measurement is unavailable and delay cannot be used (either because there is insufficient data, or the delay needed to decorrelate the signal is unacceptable).

Plotkin has produced a method known as the Function Elimination Filter, which can be used in such circumstances. The function elimination filter has been examined and found to be weak in two respects:

a) Bias: It has been found that the function elimination



filter generally gives biased estimates of the parameters - causing the notch to be incorrectly located. An expression for the bias, for certain types of input signal, has been found and hence, given sufficient information, this could be used to correct the bias.

b) Notch Width: The existing function elimination filter gives a very wide notch - too wide for most purposes. A modified function elimination filter has been proposed here which overcomes this problem and allows the notch width to be selected apriori.

SEISMIC SIGNAL PROCESSING

7.1 Introduction

In this chapter an introduction to and brief review of seismic signal processing is given. The aims of the chapter are to give sufficient background to the subject to set the more detailed consideration of adaptive deconvolution (Chapter 8) and seismic SNR enhancement by adaptive processing (Chapter 9) in context. The novel techniques of those chapters will be tested, in part, on synthetically generated data and a further aim of this chapter is to discuss the mechanisms by which such synthetics are generated.

In reflection seismology elastic waves initiated by seismic energy sources propagate through the earth. Changes in acoustic impedance caused by interfaces between geological strata give rise to partial reflection of incident wavefronts. Surface measurement of reflected waves gives arrival times of reflections from which information about the location and possibly the nature of the subsurface strata can be determined. Whilst the principles may be straightforward, the presence of many boundaries gives rise to complex patterns of reflections. Additionally, as a medium the earth is heterogeneous and subject to sharp discontinuities due to geological phenomena such as faults. These and other complexities render the interpretation of seismic records an exceptionally difficult task in signal processing terms. Because of the complexity of the physical mechanisms, a systems approach to the processing is adopted - the seismic source is considered to be the input, the received signal is the output and the earth is the system. The problem then becomes one of system identification.

Reflection seismology in general can be divided into three sections: (i) data acquisition, (ii) processing and (iii) interpretation. In this chapter (and this thesis) the primary consideration is the processing. Acquisition will only be considered in so far as this is necessary, and relevant to understanding the processing. Interpretation will hardly be considered at all. The dangers in such an approach are obvious since the ultimate aim of processing must be to improve the interpretation of the data. For example, it is relatively easy to devise processing techniques

which improve the SNR of the data but which are actually detrimental to interpretation. To avoid this pitfall, great care must be taken to ensure always that any processing undertaken is at least consistent with the physical mechanisms of reflection seismology. With this in mind the chapter begins with a discussion of the physical processes underlying reflection seismology. The processing sequence, which contains a number of distinct operations, is then discussed in section 7.3.

Finally, mention is made of the fact that much of this chapter is based on three excellent texts: "Reflection Seismology" by K.H. Waters [109], "A Review of Seismic Signal Processing" by D.W. March [55] and "Seismic Signal Processing" by L.C. Wood and S. Treitel [121]. Material in the text which is not directly referenced may be assumed to be derived from one of these three sources.

## 7.2 The Mechanics of Reflection Seismology

### 7.2.1 Models of transmission

Waves emitted by a seismic source travelling through the surface of the earth may be of two types, referred to as compressional (P) (otherwise known as acoustic waves) and distortional (S) waves. In reflection seismology only one type, the compressional waves, are utilised. This is because most seismic experimentation is done with instruments which receive and generate only compressional waves. In any case, for marine seismology, fluids cannot support S waves since they have no shear strength.

Wavefronts travelling outward from a seismic source through an homogeneous isotropic medium are spherical, though in other cases (when the medium is inhomogeneous, etc.) the form of the wavefront is determined by the velocity distribution of the medium. On encountering an interface between two media of differing acoustic impedances the wave is partially reflected and partially transmitted. The situation is complicated by the fact that mode conversion (between P and S waves) occurs at the boundary. In reflection seismology the conventional assumption is that all reflections take place at normal incidence. Under these circumstances

the reflection and transmission relationships are simplified considerably by the fact that no mode conversion takes place. It should be pointed out, however, that the normal incidence assumption is not generally valid due both to horizontal offsets between source and receiver (see section 7.2.3) and non-horizontal reflectors. For waves at normal incidence to a boundary between two media characterised by velocities  $v_1, v_2$  and densities  $\rho_1, \rho_2$ , the reflection coefficient  $r_{12}$  can be easily shown [109] to be:

$$r_{12} = \frac{\rho_1 v_1 - \rho_2 v_2}{\rho_1 v_1 + \rho_2 v_2} \quad (7.2.1)$$

and the transmission coefficient

$$T_{12} = 1 + r_{12} = \frac{2\rho_1 v_1}{\rho_1 v_1 + \rho_2 v_2} \quad (7.2.2)$$

Note that from (7.2.1)

$$r_{21} = -r_{12} \quad (7.2.3)$$

and

$$T_{21} = 1 - r_{12} \quad (7.2.4)$$

so that from (7.2.2) and (7.2.4) the two-way transmission coefficient  $T$  is

$$T = T_{12}T_{21} = 1 - r_{12}^2. \quad (7.2.5)$$

The surface of the earth may contain many such reflectors. However, typical reflection coefficients are small (generally less than 0.1). In some circumstances though, notably sea bottom reflections in marine seismology, the reflection coefficient may be considerably larger.

It is interesting to note that the energy loss caused by two-way transmission through the reflectors is greater for areas which have a large number of reflectors with small changes in acoustic impedance than for those with a few relatively large amplitude reflectors. In some areas this may be the single largest cause of energy loss in seismic wave propagation [64].



A simple earth model is that of a set of  $N$  horizontal, homogeneous layers bounded by a free surface and with coincident source and receiver (thus ensuring normal incidence reflections). As energy travelling downwards from a source located at the surface encounters each reflector it is partially reflected and partially transmitted. Each reflection gives rise to upward travelling waves which, on encountering an interface, are themselves partially reflected and partially transmitted. The upgoing transmitted waves return to the surface, but the downgoing reflections represent energy which has become trapped or reverberated around a layer or layers (see fig. 7.2.1). Such reverberant energy may eventually return to the surface where it interferes with the first bounce (or primary)

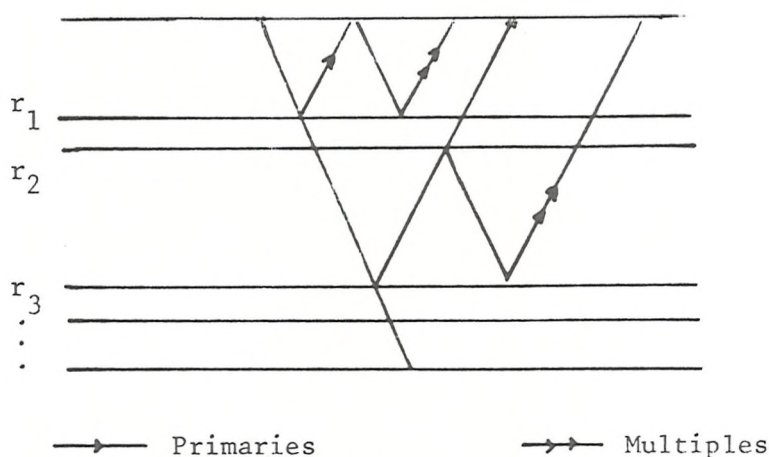


Figure 7.2.1: Reflections from an Ideal Earth

(Reflections drawn at non-normal incidence and only a small subset of possible reflections drawn for clarity).

information. These reverberations (or multiples) render the interpretation of the primary reflections difficult if not impossible, and their removal or attenuation is an important aim of processing. As mentioned above, multiples are particularly strong for some marine work where a hard sea bottom gives rise to a large reflection at the sea bed and the air/sea boundary is an almost perfect reflector. The simplified earth model described above is highly unrealistic for a number of reasons:

(i) Dipping or curved reflectors

As already mentioned, in practice reflectors will generally not be horizontally but may be inclined ('dipped') or curved. This has the immediate effect of negating the normal incidence assumption.

(ii) Attenuation of waves

Apart from the attenuation of amplitude due to transmission losses discussed earlier, there are a number of other sources of attenuation of seismic waves which are not included in the above model:

(a) Spherical divergence

As is well known, a spherical wavefront diminishes in intensity as the inverse square of the radius of the wavefront. A further complication occurs because the earth is not in general a uniform medium and the variations in velocity cause distortion of the wavefront.

(b) Absorption

Absorption results from imperfections in the elastic material and is caused by internal friction within the medium. Absorption causes a progressive loss of seismic amplitudes by a conversion of seismic energy into heat. This loss is known to be frequency selective, causing greater attenuation of higher frequencies than of lower ones. Experiments have demonstrated that in some rock types at least, absorption is proportional to the first power of frequency [59]. It can be shown (e.g., [35]) that this gives an absorption transfer function with frequency response given by

$$H(\omega, T) = e^{\left(-\frac{|\omega|T}{2Q} - i\omega T\right)} \quad (7.2.6)$$

where  $T$  is the travel time from source to observation point, and  $1/Q$  is known as the specific dissipation constant.  $Q$  has experimentally been determined to be independent of frequency, independent of amplitude and relatively independent of temperature, for most situations of interest in reflection seismology.

However, the transfer function of equation (7.2.6) is not physically reasonable since its corresponding time function is acausal and this, in turn, would imply energy travelling at velocities greater than the acoustic velocity of the medium [103]. These difficulties are overcome by using the equivalent minimum phase version of  $H(\omega)$ . This corresponds to including the frequency dependence of velocity (dispersion) in the model [64]. In general, the amplitude of a seismic pulse decays as the higher frequencies are absorbed and also decays as the pulse is lengthened



by dispersion. Dispersion is known to have generally a smaller effect on amplitudes than absorption [42].

### (iii) Noise

Aside from the attenuation effects discussed in the previous section, there are a number of other factors which complicate the interpretation of seismic data and which might be collectively described as noise. As discussed previously, one such source is multiple reflections. Another, for land recorded data, is surface waves. These are waves which propagate in the near surface or 'weathered layer' - a very low velocity layer of earth with a depth varying from 0 - 100 m approximately - when a source is activated within this layer. These surface waves (or ground roll as they are known) constitute one of the main difficulties in recording seismic reflections since they are usually of very large amplitude compared to the reflections. However, as they have a very low frequency characteristic they may be filtered out by using receivers with poor response at these frequencies (see section 7.2.2) or, since they propagate with very low velocities they may be removed by spatial (or velocity) filtering (see section 7.3.4).

In addition to the above, there are background noise sources due to both man-made phenomena (for example, traffic noise) and natural phenomena (for example, microseismic activity or wind action).

### 7.2.2 Sources and receivers

In addition to the problems of transmission through the earth, reflection seismology is further complicated by the effects on the signal of both sources and receivers. Ideally, the source signal should be a sharp impulse in the time domain having a flat frequency response character, though in practice this is difficult to achieve. The sources used vary for land or marine recording. On land a common source is an explosive charge (of varying size) placed in a drilled shot hole some distance (1 - 100 m) below the surface. Explosives give a good impulsive source. However, the resulting waveform is considerably dependent upon the location of the shot in relation to nearby boundaries. Explosive sources

have been largely replaced in marine work because of their harmful environmental effects. There is in fact a further complication in marine seismics which is known as the "bubble effect": if the gas bubble resulting from an explosion is spherical, the water compresses as the bubble expands until a point is reached at which the water pressure exceeds that of the bubble. At this point an implosion occurs and the process is reversed. This expansion and contraction repeats (with decaying amplitude, due to energy loss) and thus gives rise to a complex source signature consisting of a primary pulse followed by a set of secondary bubble pulses. One way of overcoming this problem used in the past was to place the source sufficiently close to the surface so that the first bubble broke surface and destroyed the spherical symmetry. The most commonly used marine seismic source today is the air gun. The air gun uses compressed air which is suddenly released into a chamber whose volume controls the frequency content of the waveform. Several air guns of differing capacities are commonly used together to give an impulse with a wide spectrum.

Air guns, and sources in general, are usually employed in arrays (of up to 100 elements) to give directionality to a source field and, in the case of air guns, to minimise the bubble effects. The arrays are designed using constructive and destructive interference in such a manner as to maximise the near vertical travelling waves whilst minimizing the horizontal waves.

For land work, moving coil geophones are used to record seismic reflections. For frequencies above the resonance (typically 5-7 Hz) these geophones give an output voltage which is approximately proportional to the velocity of the earth's surface. The choice of geophone is, however, usually a compromise because lower resonant geophones have the disadvantage that they are heavier and larger than higher resonant units.

In marine seismic work, streamers of geophone elements are used. Each element is contained in a fluid-filled flexible tube and is designed to give an output voltage which is proportional to the hydrostatic excess pressure caused by the seismic wave. Depth controllers are employed to keep the streamer at the desired depth in the water and acceleration cancelling circuitry is employed to reduce sensitivity to cable movements. Arrays of receivers are commonly employed in a similar fashion to arrays of sources.



### 7.2.3 Data gathering

As far as data gathering is concerned, the only method considered here is the common depth point method (CDP) due to Mayne [58] which is now standard. The basic idea is to improve the signal-to-noise ratio of the section by increasing the coverage of the subsurface. A number of traces pertaining to the same common depth point are obtained by taking shots with source and receiver separation increasing symmetrically about the mid-point (see fig. 7.2.2).

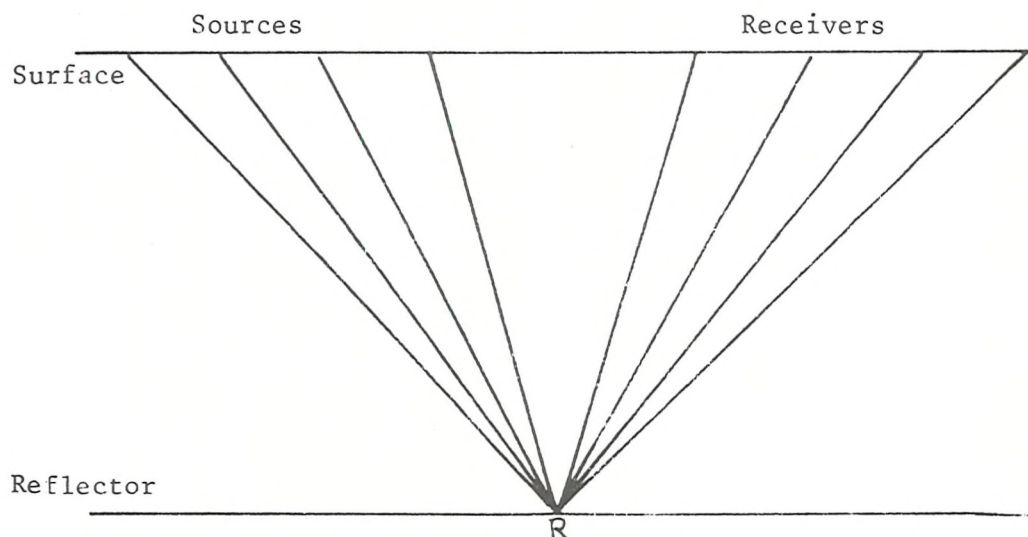


Figure 7.2.2: CDP Data Gathering

Usually 24, 48 or 96 traces are used. The aim is to add together (or stack) the complete set of responses, which in an ideal case with equal SNRs on all traces would give a SNR improvement of  $\sqrt{N}$  (see Chapter 5). Of course, the geometrical effect of increasing the offset between source and receiver is to increase the length of the travel path and thus the travel time. Consequently, the traces in a CDP gather cannot simply be added together without first applying corrections (known as movement corrections) to align corresponding events. These normal movement corrections are a function of velocity and are discussed in detail in section 7.3.3.

A further complication arises from the fact that, if the reflectors are not horizontal (as is usually the case), the common depth point does not correspond to a common reflection point but 'migrates' up the slope

as the offset increases.

It has been demonstrated [46] that this effect increases as the square of the angle of dip. However, complex reflection geometries frequently cause small dispersion of common reflection point locations [93], so that CDP data gathering is generally useful in spite of these problems.

### 7.3 Data Processing

#### 7.3.1 Preprocessing and static corrections

The frequencies of interest in seismology range from a few to a hundred hertz. Accordingly, the data from CDP gathers are anti-alias filtered, and then sampled at intervals of 1, 2 or 4 milliseconds. Normally, the maximum length of data will be 6 seconds, as hydrocarbon accumulations occurring below about 10,000 m (depending on the area) are of little interest due to economic constraints. Six seconds of data is adequate for depths of this order.

There are a number of preliminary corrections which have to be made to the data. Firstly, the data has to be demultiplexed (because the data is initially sampled cyclically over N traces), and then sorted since the order in which shots are made does not correspond to the desired organisation of the data for CDP processing. Secondly, the recording equipment applies time-varying gains to the data to cope with the large dynamic range of the input data over the length of the recording (100 dB in 4 seconds). These changes in gain are removed from the data.

For land data corrections are then made for changes in elevation of source and receiver and for near surface inhomogeneities. These corrections take the form of a time shift or translation which is constant for the entire trace and are thus known as static corrections.

#### 7.3.2 Gain control

Because of the large dynamic range of seismic data it is important to apply some sort of time-varying gain to compensate for the effects of attenuation. The correction should eliminate overall changes in

amplitude but allow local variations to remain. There are two basic approaches to gain control: deterministic and random. The deterministic approach attempts to model the attenuating factor(s) and compensate accordingly. The simplest approach might be to correct for spherical divergence by applying a gain function which linearly increases with time, that is

$$g(t) = t \quad (7.3.1)$$

However, such a correction would only be appropriate for transmission through a simple homogeneous medium. Even if velocity changes could be incorporated into the gain function other problems would arise. For example, in the presence of both primaries and multiples, correct scaling for the primaries would have the effect of over amplifying the multiples [64].

In the statistical approach a form for the gain function is selected, for example,  $a_0 e^{a_1 t}$ ,  $a_0 t e^{a_1 t}$  etc., and the parameters  $a_0$ ,  $a_1$ , etc., are obtained as a best fit from the data (note the data used may be a collection of similar traces). The statistical approach is most commonly used but tends to give poor results in areas of low SNR.

### 7.3.3 Velocity analysis and moveout corrections

As discussed in section 7.2.3 processing of CDP data involves stacking traces obtained with differing source-receiver offsets. Prior to this stacking operation, the data must be corrected to align similar events from traces with increasing offsets. These corrections are known as normal moveout (NMO) corrections. NMO is defined as the increase in reflection time due to an increase in source-receiver offset for a horizontal reflecting interface in a homogeneous medium. NMO corrections are made by computing the extra travel time over that for a zero offset trace and using these values to correct the trace. Simple geometry gives the travel time,  $T_x$ , for a medium characterised by velocity,  $v$ , with a single reflector at depth,  $z$ , and with a horizontal offset,  $x$  (see fig. 7.3.1);

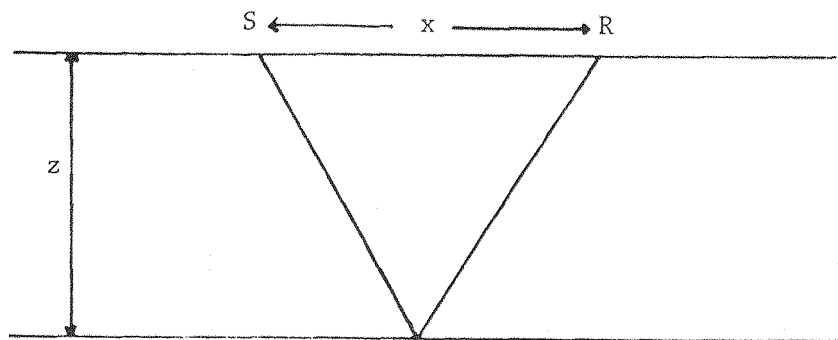


Figure 7.3.1: Simple Reflection Geometry

as:

$$T_x^2 = T_o^2 + \frac{x^2}{v^2} \quad (7.3.2)$$

where

$$T_o = \frac{2z}{v}$$

so that there is a hyperbolic relation between offset and travel time. However, in practice, reflectors are not usually horizontal. For a similar medium but with the reflector inclined at an angle,  $\alpha$ , to the horizontal (see fig. 7.3.2)

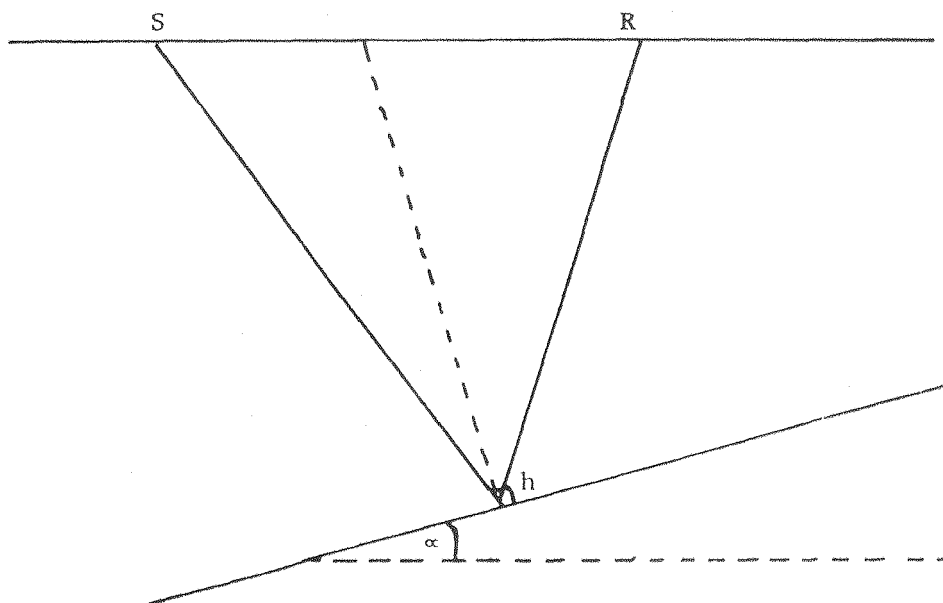


Figure 7.3.2: Effect of Dipping Reflector

the relation is

$$T_x^2 = T_o^2 + \frac{x^2}{(V/\cos \alpha)^2} \quad (7.3.3)$$

(see [5])

where  $T_o$  is the two-way travel time from the surface to the reflector along the normal to the reflector. When the reflectors dip, the common depth points do not generally correspond to a common reflection point - the reflection point migrates along the reflector as the dip increases. For the most common type of reflector - the curved reflector - the situation is even more complex and no equivalent simple formulae exist; often, however, the curvature is small enough to neglect.

In the case where there are  $N$  isotropic homogeneous layers bounded by horizontal reflectors, the travel time for offset  $x$  can be represented by the infinite series

$$T_{x,N}^2 = c_1 + c_2 x^2 + c_3 x^3 + \dots \text{(see [93])} \quad (7.3.4)$$

A hyperbolic approximation analogous to the single layer case results from retention of the first two terms

$$T_{x,N}^2 \approx c_1 + c_2 x^2 \quad (7.3.5)$$

or

$$T_{x,N}^2 = T_{o,N}^2 + \frac{x^2}{v_{rms}^2} \quad (7.3.6)$$

where

$$T_{o,N} = \sum_{k=1}^N \left( \frac{2z_k}{v_k} \right) \quad (7.3.7)$$

and where  $v_k$  is the velocity of the  $k$ 'th layer,  $z_k$  is the depth of the  $k$ 'th layer, and where

$$v_{rms} = \left( \frac{1}{T_{o,N}} \sum_{k=1}^N v_k^2 t_k \right)^{\frac{1}{2}} \quad \text{(see [93])} \quad (7.3.8)$$



Equation (7.3.6) is a good approximation to the movement relation even in areas of complex structures and is the relation used for movement corrections. The data are corrected by the application of (7.3.6) in the form:

$$T_{o,N} = \sqrt{T_{x,N}^2 - \frac{x^2}{v_{rms}^2}} \quad (7.3.9)$$

where  $T_{x,N}$  is the record time.

Now, in addition to the offset  $x$  the rms velocity is also required. However, the rms velocity is an ideal which cannot be obtained; in practice, velocities must be estimated from the data.

Seismic velocities vary considerably from as little as 500 m/s to as high as 7000 m/s and generally increase with depth. Velocities can be estimated by scanning data from a CDP gather for coherence along different hyperbolic trajectories - because of the hyperbolic relation between travel time and offset. The simplest way to check for coherence, and the way which is often used in practice, is to stack the data along a number of separate hyperbolae and select the one which gives the most satisfactory result. Another straightforward approach is to plot the square of arrival time against the square of offset distance for a set of traces. Because of the hyperbolic relation of equation (7.3.6) plotting the square of these quantities maps lines of constant velocity to straight lines, with the velocity given by the gradient. Velocity determination is thus reduced to the problem of picking best straight lines. However, this approach is limited by the interpreter's ability to recognise reflectors.

More sophisticated approaches have been developed. One of the most widely accepted is the velocity spectrum of Taner and Koehler [94]. This is a three-dimensional display of coherence as a function of normal incidence time versus rms velocity. The plot is obtained by measuring the correlation of the data for a range of rms velocities at a fixed normal incidence time, then incrementing the time and repeating the process. Several different correlation measures have been used but the main limitation with this and other similar processes is the large computational requirement.

#### 7.3.4 SNR improvement

One of the main aims of seismic processing is to improve the SNR of the data. However, such improvements are usually observed qualitatively not quantitatively [41]. The improvements sought are visual; clearly, however, visual improvements and SNR improvements are not identical. It is tacitly understood that there is a relation between them but it can happen that improvements in SNR may give little visual improvement and vice versa. In general, SNR varies along a seismic record length. Now, the SNR must be above a certain threshold if the signal is to be visible and below another for the noise to be visible [41]. In many instances, therefore, improvements in SNR may yield visual improvements only in one region of the record where the SNR lies between the two thresholds.

SNR improvements in seismic data are routinely obtained by stacking data from CDP gathers. The conventional N-fold CDP stack consists of a simple sum of the moveout corrected (Normal Incidence) traces. According to the simple theory of signal averaging, such a stack may increase the SNR by up to  $\sqrt{N}$ . The stack also attenuates multiple reflections because these will generally have a lower apparent velocity than the primaries and thus will not be aligned by NMO correction. However, there are several problems with CDP stacking:

(i) NMO corrections induce distortion since different corrections will be applied to the leading and trailing edges of a wavelet so that the result is to apply a nonlinear 'stretching' to the wavelet [23].

(ii) NMO corrections will not usually be sufficiently accurate to give exact alignment of corresponding events.

(iii) The SNR of the large offset traces will usually be lower than that of the corresponding near traces (due to longer travel times).

More sophisticated approaches to stacking, for example, weighted stacks and multi-channel filters, have been developed and are discussed in Chapter 9, where a novel approach based on multi-channel adaptive filtering is presented.

Another approach to SNR improvement is through the rejection of coherent sources of noise on a CDP gather. These noise sources may be caused by, for example, near surface waves. They are characterised by the fact that they have different apparent velocity than the signal -

usually much lower. This coherent noise is attenuated by the CDP stacking process because it does not align correctly. However, it can be more strongly attenuated by two-dimensional filtering. The whole of a CDP gather may be two-dimensional Fourier transformed as:

$$X(k_1, k_2) = \sum_{n=0}^{N-1} \sum_{p=0}^{M-1} x(n, p) e^{-i\left(\frac{2\pi k_1 n}{N} + \frac{2\pi k_2 p}{M}\right)} \quad (7.3.10)$$

where  $N, M$  are the number of samples in time and space and where the units are Hertz and wavenumber with the spatial variable in units of cycles/unit distance.

These transforms have the property that events of constant velocity form straight lines in the  $f$ - $k$  domain with the slope determined by the velocity. Coherent noise can thus be rejected by rejecting regions of the  $f$ - $k$  plane corresponding to unwanted velocities. The simplest approach, known as the 'pie-slice' method, consists of accepting a region of the plane corresponding to the geologically realistic velocities and rejecting the rest. This method has the disadvantage, however, of having a sharply defined region of acceptance which leads to 'ringing' - in an analogous manner to one dimensional processing.

A third approach to SNR enhancement for seismic data is to filter the data with an output energy filter [101] (see Chapter 5). However, referring to that section this may only be used if the amplitude spectrum of the received signal is known, as well as the spectrum of the noise.

### 7.3.5 Deconvolution

Deconvolution accounts for more than 50% of the total computing time used in seismic data processing. There are two distinct forms of deconvolution commonly used in seismic processing, known as spiking and predictive deconvolution, respectively. The aim of spiking deconvolution is to compress the source wavelet into a single spike, hence the name. A simple convolutional model for the seismic response  $x(n)$  is:

$$x(n) = r(n) * s(n) + v(n) \quad (7.3.11)$$



where  $r(n)$  is the sequence of reflectors  
 $s(n)$  is the source wavelet  
and  $v(n)$  is a noise term, see fig. 7.3.3 .

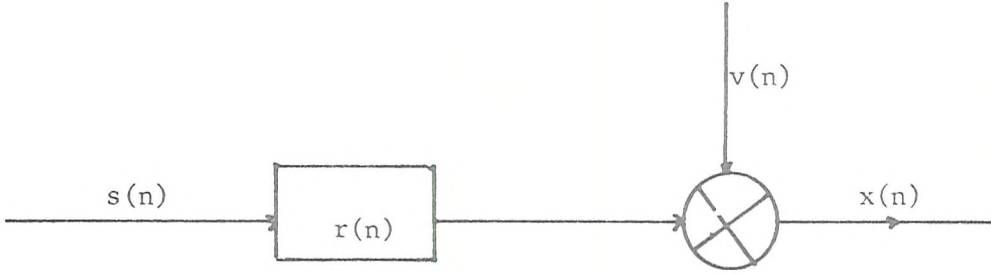


Figure 7.3.3: Convolution Model for Reflection

The source wavelet is not usually a sharp, well-defined pulse (see section 7.2). Spiking deconvolution seeks to correct this by convolving the response with the inverse of  $s(n)$  thus leaving sharp discrete pulses corresponding to the reflectors. Using least-squares methods, the inverse is obtained from the normal equations (see Chapter 3)

$$R_{ss} \underline{f} = \underline{g} \quad (7.3.12)$$

where  $\underline{g}$  is the cross-correlation between the signal  $s(n)$  and a delta function.

In this instance the problem lies with the computation of the correlations since no knowledge of the source signal is generally available. However, from (7.3.11), assuming signal and noise are uncorrelated

$$R_{xx}(m) = R_{rr}(m) * R_{ss}(m) + R_{vv}(m) \quad (7.3.13)$$

Now, if  $r(n)$  and  $v(n)$  are both stationary, purely random sequences, then

$$R_{vv}(m) = k_1 \delta(m), \quad R_{rr}(m) = k_2 \delta(m) \\ (k_1, k_2 \text{ constants})$$

Hence

$$R_{xx}(m) = k_2 R_{ss}(m) + k_1 R_{vv}(m). \quad (7.3.14)$$

Hence  $R_{xx}(m)$  corresponds to a scaled version of  $R_{ss}(m)$  but with added prewhitening (see Chapter 3). Accordingly,  $R_{xx}$  may be used as an estimate of  $R_{ss}$  in the normal equations (7.3.12). The right hand side cross-correlation vector presents no problem, since

$$\underline{g} = [s(0), 0, \dots, 0]^t$$

and although  $s(0)$  is not available an arbitrary (non-zero) value may be used since only the scale will be affected. Note, however, that the delayed version of the least-squares cannot be used since the sequence,  $s(n)$ , would be needed for the right hand side of the equations. There are a number of problems with least-squares spiking deconvolution, the main one being the restrictive nature of the assumptions. The requirement that the reflection sequence should be white is not usually valid and is certainly not so in the presence of multiples. Also, recall from Chapter 3 that the deconvolution will have an all-pass component unless the source is minimum phase. A further problem arises from the usual noise enhancing property of deconvolution (see Chapter 3). Prewhitening helps here but the result may still be a marked degradation in SNR. Other solutions to the SNR problem such as reducing the bandwidth of the inverse or otherwise shaping the wavelet have also been attempted.

The most important restriction is the assumption of time invariance applied to the source signal. A partial solution to this problem is obtained by gating the trace and applying deconvolution to each gate separately. However, as discussed in Chapter 2, this approach has certain limitations and ultimately the only effective solution may be to use adaptive processing. This topic is discussed in Chapter 8, where a novel approach to adaptive deconvolution is also presented.

A second form of deconvolution is used in seismic processing which has the aim of removing (or attenuating) reverberant energy and is known as predictive deconvolution. To consider the application of predictive deconvolution the model of equation (7.3.11) must first be modified to incorporate multiples. This is achieved by replacing the model by:

$$x(n) = r(n) * s(n) * m(n) + v(n) \quad (7.3.15)$$

where  $m(n)$  is the multiple spike train.

For example, in the case of sea bed reverberations (the most common cause of problems), a simple model for  $M(z)$  has the form:

$$M(z) = 1 - r_1 z^{-n_0} + r_1^2 z^{-2n_0} + \dots \quad (7.3.16)$$

where  $r_1$  is magnitude of the reflection coefficient of the first layer and  $n_0$  is the 2-way travel time to the sea bed.

Note also that  $M(z) = 1/(1 + r_1 z^{-n_0})$  and is minimum phase. Reverberation trains for more complex situations can also be obtained and it turns out that the response of an arbitrary system of horizontal layers is also minimum phase [70]. Predictive deconvolution eliminates the effect of the multiples by deconvolving  $m(n)$ . The term predictive arises from the fact that the method works by extracting and removing the predictable component of the response. Now by assumption  $r(n)$  and  $v(n)$  are purely random and thus unpredictable. The multiples, on the other hand, are repetitive and thus highly predictable. These multiples are attenuated by use of a prediction error filter. To obtain the prediction error filter using the least-squares approach a predictive filter is first obtained by replacing the desired signal of the shaping filter by the input, time advanced by  $n_0$  samples. For the normal equations

$$R\mathbf{\underline{f}} = \mathbf{\underline{g}}$$

the cross-correlation vector between input and output,  $\mathbf{\underline{g}}$  becomes

$$g(i) = E\{x(n)x(n + i + n_0)\} = R(i + n_0) \quad (7.3.17)$$

$n_0$  should be set equal to the interval between successive multiples but need only be known approximately, to within the limits

$$\alpha - L < n_0 \leq \alpha \quad (7.3.18)$$

where  $\alpha$  is the true interval and  $L$  is the filter length.

These limits are necessary in order that the peak in the input autocorrelation, which occurs at the multiple interval, should appear in the right hand side of the normal equations. Having obtained the prediction coefficients from the solution of the normal equations, the prediction

error filter is then obtained as:

$$(1, \underbrace{0, 0, \dots, 0}_{n_0 - 1 \text{ zeros}}, -f_{(0)}^{-f_{(1)}}, \dots, -f_{(L-1)}) \quad [80]$$

Of course, the method suffers from the same limitations of time invariance as does spiking deconvolution, and adaptive forms are discussed in Chapter 8. A further problem with the least-squares approach is that the method requires both source and multiple-reflection sequence to be minimum phase [81].

Because of the restrictive nature of the assumptions, using least-squares methods, alternative approaches to seismic deconvolution with the aim of overcoming these restrictions have been developed. Homomorphic deconvolution (see Chapter 3) has been applied to seismic data [105]. Whilst the method has the advantage that the minimum phase assumptions are no longer required, there are a number of difficulties including cepstral aliasing and severe degradation of the method for low SNRs. Attempts have also been made to perform spiking deconvolution based on optimisation of an alternative norm, for example [75, 95]. Apart from overcoming the minimum phase restrictions these methods are designed to produce a more 'spiky' response. However, all of these methods have the disadvantage of being considerably more complex (computationally) than least-squares and none have achieved widespread acceptance. This is probably due to the departure of the real earth from the plane layered model which leads to problems which become more serious as the techniques become more sophisticated.

### 7.3.6 The Processing Sequence

As is clear from the preceding sections, processing of seismic data consists of a complex sequence of distinct operations. There is no universally accepted version of either the elements in the processing sequence or the order in which they should appear. Additionally, the sequence varies according to the area, and of course, whether the data is land or marine. Nevertheless, the major components of the processing which have been discussed in the preceding sections are more or less universally accepted. A typical marine sequence might be:

Demultiplexing  
Sorting  
Gain recovery  
Bandpass filtering  
Predictive deconvolution  
Wiener filtering  
Velocity analysis  
NMO correction  
CDP stacking  
Wiener filtering

For land data this is complicated by the need for static corrections. In addition to this sequence, in recent years finite difference techniques have been used to backward propagate recorded wave fields to compensate for certain physical phenomena (such as non-horizontal layering) which are more or less ignored by the processing [13]. This technique, which is known as migration, is not strictly a signal processing problem, and so will not be considered here.

## CHAPTER 8

### ADAPTIVE DECONVOLUTION OF SEISMIC DATA

#### 8.1 Introduction

In this chapter adaptive approaches to the deconvolution (both spiking and predictive) of seismic data will be considered and a novel approach to adaptive deconvolution will be developed. It will be recalled from Chapter 7 that the need for adaptive deconvolution arises from the non-stationary nature of seismic data which violates the assumptions underlying the conventional stationary approaches.

Some work has been done on adaptive methods for deconvolution for both spiking and predictive deconvolution. This ranges from simple, pragmatic approaches to the problem such as gating the data into smaller sections over which a stationary solution is assumed, to LMS type adaptive solutions, and to more sophisticated solutions involving Kalman filtering.

The chapter begins with a review of these existing techniques (section 8.2). A novel approach to adaptive (spiking) deconvolution of seismic data is also presented (section 8.3). This technique is based on the optimal control method of deconvolution discussed in Chapter 4. It will be recalled from Chapter 4 that the principle advantages of the optimal control approach are that the method can easily be used for both stationary and non-stationary systems, is not dependent on any minimum phase assumptions about the system and is capable of providing effective deconvolution in noisy conditions. A further advantage in seismic spiking deconvolution, as will be seen, is that no assumptions need be made about the statistics of the reflection sequence (in contrast to the usual least-squares approach - see Chapter 7). However, it will also be recalled from Chapter 4 that to apply the optimal control method to deconvolution, a state-space model of the system is required, so that an alternative to the usual, convolutional seismic model is required. Several state-space models of seismic data have been proposed (in conjunction with the Kalman filtering approaches to deconvolution mentioned above) and one of these models is utilised here for the optimal control

approach. The formulation of the model for both stationary and non-stationary cases is discussed. The properties of the method are tested (and contrasted with conventional least-squares) by application to synthetic (both stationary and non-stationary) and field seismic data.

## 8.2 Background and Previous Work

### 8.2.1 Introduction

The stationary approaches to deconvolution discussed in Chapter 7 are limited in practice by the failure of the data to correspond to the required model. The main problems arise (see Chapter 7) due to the assumption of a minimum phase source, the randomness of the reflection sequence and, in particular, the stationarity of the data. Seismic data is often markedly non-stationary and this can cause unsatisfactory results for deconvolution using conventional methods. For example, a least-squares spiking operator derived from an entire trace (which is non-stationary) is, in effect, an average inverse for all of the time-varying wavelets on the trace and as such is not the correct inverse at any point.

A number of attempts to overcome this problem has been made ranging from simple gating of the trace to sophisticated Kalman filtering applications. Some of this work has been directed at 'spiking' deconvolution and some at predictive deconvolution (in the sense of dereverberation). Much, however, is applicable to both forms.

### 8.2.2 Gating the data

The simplest approach to overcoming the problem of non-stationarity in seismic data (and one which is widely practised) is to divide the trace into a number of smaller sections or gates, over each of which the data may be assumed to be approximately stationary. Separate stationary operators are then designed for each gate. This process was discussed in Chapter 2; it has the advantage of simplicity, and it may give satisfactory solutions provided the variation is sufficiently slow.



However, gating can never be more than a partial solution to the problem and it is not applicable to long-period dereverberation.

### 8.2.3 LMS adaptive deconvolution

Several approaches to adaptive deconvolution of seismic data have been proposed which are based on the LMS adaptive algorithm (see Chapter 2) or a variant thereof. A straightforward application of the LMS algorithm to predictive deconvolution is described by Griffiths, Smolka and Trembley [37]. The configuration of the filter is shown in figure 8.2.1. The filter is used as a predictor with the trace as input. The desired signal is provided by a time advanced version of the trace where the advance,  $\alpha$ , is, as usual, set equal (approximately) to the two-way travel time of the multiples. With this configuration the update equation (2.5.5) (see Chapter 2)

$$\underline{f}_{k+1} = \underline{f}_k + \alpha e(k) \underline{x}_k \quad (2.5.5)$$

(where  $\alpha$  is of course subject to the usual stability restrictions) becomes

$$\underline{f}_{k+1} = \underline{f}_k + \alpha [x(k + n_o) - \hat{x}(k + n_o)] \underline{x}_k \quad (8.2.1)$$

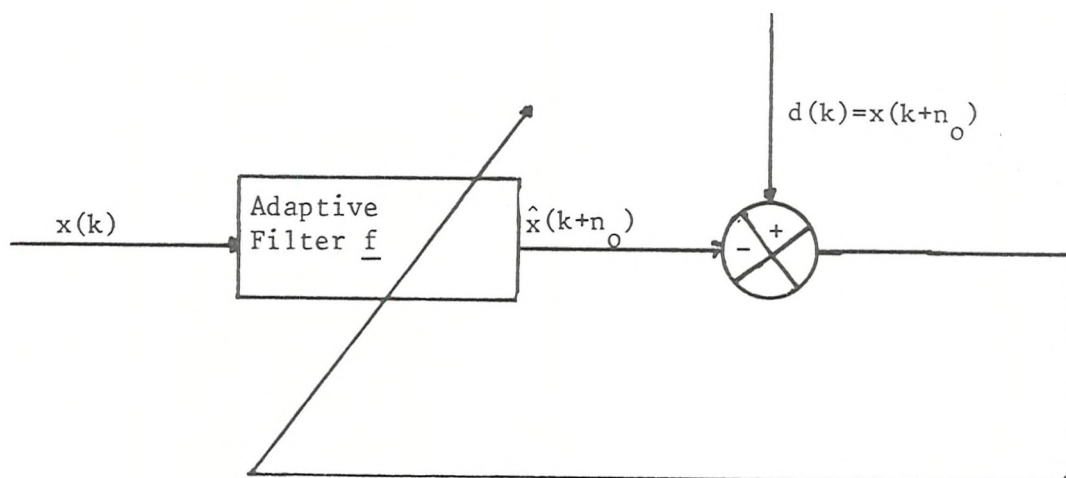


Figure 8.2.1: Adaptive Prediction



To overcome initialisation problems, Griffiths et al [37] use a double operation of the filter. Firstly, starting at the end of the trace with  $\underline{f}_N = 0$ , the processing is performed backwards up the trace, thus allowing the initialisation phase to occur at the end of the data. For this reverse operation the update equation (8.2.1) becomes

$$\underline{f}_{n-1} = \underline{f}_n + \alpha [\underline{x}(k + n_0) - \hat{\underline{x}}(k + n_0)] \underline{x}_n \quad (8.2.2)$$

Then, using the final value obtained from processing backwards as an initial value, the processing is performed in forward time. Initialisation effects are further removed by averaging the results of the forward and backward processing. In their implementation, Griffiths et al use the normalised form for the adaptation constant (see Chapter 2). The technique was demonstrated to work very effectively for a broad range of input parameters. In a study of this method, Hubbard [39] observed that, if the variability in the multiple interval is sufficiently large in relation to the filter length, it may be necessary to vary the predictive gap at different points on the trace. To avoid discontinuities in the data at the changeover points, the filter coefficients can be constrained at these points. However, the influence of these constraints on overall filter behaviour remains unclear. Hubbard conducted fairly extensive trials on both synthetic and field data and concluded that the method generally attenuates sea bottom multiples successfully but may be susceptible to amplitude variations in the input. This point is reinforced by the examples of adaptive filter operation (in a different context) in Chapter 9.

Ristow and Kosbahn [79] suggested a number of further refinements to the method including replacing the adaptation constant  $\alpha$ , by a time-variable parameter  $\alpha(k)$ , which should be a monotonically decreasing function such as  $1/k$ . However, this can only be used with care on non-stationary systems. The same authors also proposed modifying the filter by incorporating a double update procedure. That is, the filter at time  $k$  produces a prediction  $\hat{\underline{x}}(k + n_0) = \underline{x}_k^t \underline{f}_k$ . The filter is updated as usual (with the normalised update equation) but then re-applied at the same point  $k$  to give a second prediction, that is

$$\hat{x}(k + n_o) = \underline{x}_k^t \underline{f}_{k+1}$$

A slightly different approach has been adopted by Wang [108], who has produced a technique for dereverberation. As before, a prediction,  $\hat{x}$ , is made but in this case the prediction has the form

$$\begin{aligned} \hat{x}(k + n_o) &= \sum_{i=0}^{L-1} f_k(i) x(k+i) \\ &= \underline{f}_k^t \underline{x}_k \end{aligned} \quad (8.2.3)$$

where  $\underline{f}_k^t = [f_k(0), f_k(1), \dots, f_k(L-1)]$

and where, in this case,  $\underline{x}_k^t = (x(k), x(k+1), \dots, x(k+L-1))$

For this approach, in contrast to the methods discussed above, the adaptive filter coefficients are assumed to be periodic, thus reducing the number of parameters to be estimated. These periodic coefficients are expanded as a Fourier series, that is,

$$f_k(i) = \sum_{j=0}^{M-1} \{a_j^{(i)} \cos \omega_o jk + b_j^{(i)} \sin j\omega_o k\} \quad (8.2.4)$$

Now substituting in (8.2.3)

$$\hat{x}(k + n_o) = \sum_{i=0}^{L-1} \sum_{j=0}^{M-1} \{a_j^{(i)} \cos \omega_o jk + b_j^{(i)} \sin \omega_o jk\} x(k+i) \quad (8.2.5)$$

which may be written

$$\hat{x}(k + n_o) = \underline{w}^t \underline{x}_k'$$

where  $\underline{x}_k'$  and  $\underline{w}$  are  $L(2M)$  length vectors, given by

$$\underline{x}_k'^t = [\underline{x}_k^t, \underline{x}_k^t \cos \omega_o k, \underline{x}_k^t \sin \omega_o k, \dots, \underline{x}_k^t \cos (M-1)\omega_o k, \underline{x}_k^t \sin (M-1)\omega_o k]$$

$$\underline{w}^t = [a_0^t, b_1^t, \dots, a_{2M-1}^t, b_{2M-1}^t]$$

where  $\underline{a}_i^t = [a_i^{(0)}, a_i^{(1)}, \dots, a_i^{(L-1)}]$

$$\underline{b}_i^t = [b_i^{(0)}, b_i^{(1)}, \dots, b_i^{(L-1)}]$$

The parameters  $\omega_0$  and  $M$  are selected on the basis of the period between successive multiples. Wang suggests that  $2\pi/(M-1)\omega_0$  should be less than the dominant period of the reverberations. The time invariant vector  $\underline{w}$  is then estimated using the normalised form of the LMS algorithm (equation (2.5.48)).

The main disadvantage with this approach would appear to be the assumption of periodicity. Wang justifies this on the grounds that "a large part of the energy in a seismic trace is due to reverberations". In the author's opinion, this assumption is highly dubious since, even in areas of high reverberation, successive multiples will not be periodic due to the effects of transmission through the earth's surface.

#### 8.2.4 Deconvolution using the Kalman filter

Several authors have considered the application of the Kalman filter to seismic deconvolution. These attempts have been exclusively directed at recovery of the reflection sequence. In this context, Kalman methods have a number of potential advantages, since they do not require the phase assumptions of the least-squares approach and, most importantly, they can handle non-stationary systems. However, as will shortly be seen, there are also a number of disadvantages.

As a preliminary to the discussion of these methods, a statement of the Kalman filter equations (in discrete time) will be given. For a system in state form:

$$\begin{aligned}\underline{x}_k &= \phi_{k,k-1} \underline{x}_{k-1} + \underline{\theta}^t \underline{w}_{k-1} \\ \underline{z}_k &= H_k \underline{x}_k + \underline{v}_k\end{aligned}\tag{8.2.6}$$

where  $\underline{x}_k$  is the  $N \times 1$  state vector

$\underline{z}_k$  is the  $M \times 1$  vector of measurements

$\phi_{k,k-1}$  is the state transition matrix

$H_k$  is the measurement matrix

and  $\underline{\theta}$  is a vector arising in the formulation

$\underline{w}_k$  and  $\underline{v}_k$  are the plant and measurement noise, respectively, which are zero-mean, stationary and with

$$E\{\underline{v}_{k-j} \underline{v}_j^t\} = R \delta_{k,j}, \quad E\{\underline{w}_{k-j} \underline{w}_j^t\} = Q_k \delta_{k,j}$$

and  $E\{\underline{v}_{k-j} \underline{w}_j^t\} = 0 \quad \forall \quad k, j.$

The Kalman filter is designed to obtain the optimal state vector  $\hat{\underline{x}}_k$ , which minimises

$$I = E\{(\hat{\underline{x}}_k - \underline{x}_k)^t (\hat{\underline{x}}_k - \underline{x}_k)\} \quad (8.2.7)$$

The equations of the filter, stated without proof are (for example, [8])

(i) Prediction

$$\underline{x}'_k = \phi_{k,k-1} \hat{\underline{x}}_{k-1} \quad (8.2.8)$$

$$P'_k = \phi_{k,k-1} P_{k-1} \phi_{k,k-1}^t + \theta^t Q_k \theta \quad (8.2.9)$$

(ii) Measurement

$$\underline{z}_k = H_k \underline{x}_k + \underline{v}_k \quad (8.2.10)$$

(iii) Optimal estimation

$$\hat{\underline{x}}_k = \underline{x}'_k + G_k [\underline{z}_k - H_k \underline{x}'_k] \quad (8.2.11)$$

$$P_k = P'_k - G_k H_k P'_k \quad (8.2.12)$$

where

$$G_k = P'_k H_k^t [H_k P'_k H_k^t + R_k]^{-1} \quad (8.2.13)$$

is the Kalman gain matrix, and where  $P_k = E\{(\hat{\underline{x}}_k - \underline{x}_k)(\hat{\underline{x}}_k - \underline{x}_k)^t\}.$

The disadvantages of Kalman filtering for deconvolution are immediately apparent. Firstly there is the need to obtain estimates of system parameters, and secondly the computational complexity of these algorithms is far greater than that of conventional methods. The earliest attempt at the application of the Kalman filter to seismic data for spiking deconvolution, is due to Bayless and Brigham [4]. They recast the seismic system in state form. That is, the usual convolutional model of equation (7.3.11) is replaced by:

$$\underline{x}_{k+1} = \phi_{k+1,k} \underline{x}_k + \underline{\theta}^t r(k) \quad (8.2.14)$$

$$z(k) = H \underline{x}_k + v(k)$$

(actually these authors used the continuous form but the discrete equivalent is used here to avoid confusion), where

$z(k)$  is the measured trace

$r(k)$  is the reflection sequence

$\phi_{k+1,k}$  is the (possibly time-varying) wavelet model and the remaining variables are as previously defined.

Now as described above, the Kalman filter is geared to optimal estimation of the state vector  $\underline{x}$ , whereas in spiking deconvolution the aim, given the measurement  $z(k)$ , is to estimate the reflection sequence  $r$ . Bayless and Brigham overcome this by assuming that the reflection sequence is itself the output of a white noise excited shaping filter, which is again cast in state form as

$$\begin{aligned} \underline{x}_{k+1}^{(1)} &= \phi_{k+1,k}^{(1)} \underline{x}_k^{(1)} + \underline{\theta}^{(1)} w_k \\ r(k) &= H^{(1)} \underline{x}_k^{(1)}. \end{aligned} \quad (8.2.15)$$

The output of this system is now the reflection sequence and the two systems can be combined by augmenting the state vector to include both  $\underline{x}_k^{(1)}$  and  $\underline{x}_k$ . The reflectivity sequence can then be obtained directly from the augmented state vector which itself can be estimated using the Kalman filter. A similar approach has been adopted by Crump [16] (in discrete form).

The disadvantage of these methods is that, in addition to the need for a state model of the system and for estimates of the covariance matrices of both plant and measurement noise, they also require estimates of the generating mechanism for the reflection sequence itself. A further disadvantage is that augmenting the order of state increases the already considerable computational burden.

A somewhat different approach, again for spiking deconvolution, has been adopted by Ott and Meder [67]. They used the equivalence of the prediction error filter for unit prediction distance and the inverse filter (mentioned in Chapter 7), to obtain estimates of the reflection sequence direct from the prediction equation of the Kalman filter (equation (8.2.8)). The assumption in this instance is that the state model is as previously described except that the reflection sequence is white. The prediction error filter is obtained simply by subtracting the Kalman prediction  $\underline{x}_k'$  (equation (8.2.8)) from the state estimate  $\hat{\underline{x}}_k$  (though as pointed out by Mendel and Kormylo [61], this gives a vector of errors  $\underline{e}_k = \hat{\underline{x}}_k - \underline{x}_k'$  and it is unclear from Ott and Meder which component to use). One disadvantage of this method as mentioned by the authors and demonstrated by Mendel and Kormylo [61] is that it is very dependent on the SNR of the measurement.

A further approach, the most general to date, is due to Mendel and Kormylo [61]. This method again uses a white input model and obtains optimal (minimum variance) estimates of the reflectivity series. The estimates are obtained by taking conditional expectations on both sides of the state equation (8.2.14), from which it can be shown (see [61]) that

$$\hat{r}(k/k+1) = q\theta^t P^{-1}(k+1/k) \underline{G}(k+1) [z(k+1) - \underline{H}^t \hat{\underline{x}}(k+1/k)] \quad (8.2.16)$$

where  $\hat{r}(k/k+1) = E\{r(k)/z_{k+1}\}$  is the optimal (minimum variance) estimate of  $r(k)$  at  $k+1$  (the single stage smoothed estimate) and where  $q$  is the variance of the plant noise (reflection sequence). From this the authors proceed to obtain the  $j$ 'th stage smoothed estimate ( $\hat{r}(k/k+j)$  referred to as the  $j$ 'th lag estimate) in a recursive manner so that optimal estimates for any desired lag may be computed. The variances associated with these estimates can also be computed recursively

so that the efficiency of any particular estimate can also be gauged. This gives the method considerable generality since optimal estimates can then be computed for a fixed lag  $L$ , or at a fixed point with the lag varying, or over a fixed data interval. The procedure is very expensive computationally, but two modified computational schemes were proposed by Mendel and Kormylo [60], one for fixed point computation and one for a fixed interval. The authors give operations counts for these schemes, those for the multiplications are

$$(N^2 + 2N + 4)L - (N^2 + N) \text{ for the fixed point scheme}$$

and  $(2N^3 + 5N^2 + 4N)M + N$  for the fixed interval,

where  $M$  is the data length (generally  $M \gg N$ ).

A further property of interest is that the single stage estimator of the white reflection sequence is itself white, though this does not extend to the  $L$ -stage scheme. Mendel and Kormylo [61] have compared their scheme with the Ott and Meder prediction error filter described above and found that the variance of the prediction error filter is greater than that of the single stage estimate.

It is worth noting that of all the Kalman filtering methods described in this section only one author (Crump [16]) has made any attempt to apply the process to field seismic data. The remaining authors have preferred to use synthetics of varying complexity. This fact, together with the high computational loads associated with these methods has led to the failure of the Kalman filter to achieve widespread acceptance in the seismic industry, as a method of deconvolution.

### 8.3 Adaptive Deconvolution using Optimal Control

#### 8.3.1 Implementation

In this section a novel method of adaptive deconvolution of seismic data is described. The method is based on the optimal control approach to deconvolution described in Chapter 4. The discrete form of the method is used, the equations, restated here for convenience are as follows:

Given a state space system

$$\begin{aligned}\underline{x}_{k+1} &= \phi_{k+1,k} \underline{x}_k + \underline{\theta} u(k) \\ y(k) &= \underline{c}^t \underline{x}_k\end{aligned}\tag{4.3.4}$$

where the variables are as previously defined, the disturbance  $u(k)$  is estimated by

$$\hat{u}(j) = G_{N-j} - \underline{H}_{N-j}^t \underline{x}_j\tag{4.3.9}$$

where

$$G_{N-j} = \frac{-\underline{\theta}^t (\underline{q} \underline{c} \underline{c}^t + P_{N-j-1}) \phi}{2d_{N-j-1}}\tag{4.3.10}$$

$$\underline{H}_{N-j}^t = \frac{\underline{\theta}^t (\underline{q} \underline{c} \underline{c}^t + P_{N-j-1}) \phi}{d_{N-j-1}}\tag{4.3.11}$$

where

$$d_{N-j-1} = \underline{\theta}^t (\underline{q} \underline{c} \underline{c}^t + P_{N-j-1}) \underline{\theta} + r\tag{4.3.12}$$

$$P_{N-j} = \phi^t (\underline{q} \underline{c} \underline{c}^t + P_{N-j-1}) \phi - d_{N-j-1} \underline{H}_{N-j} \underline{H}_{N-j}^t\tag{4.3.13}$$

$$\text{and } \underline{V}_{N-j} = (\phi^t - \underline{H}_{N-j} \underline{\theta}^t) (-2\underline{q} \underline{c} y(j+1) + \underline{V}_{N-j-1})\tag{4.3.14}$$

with  $P_0 = 0$ ,  $\underline{V}_0 = 0$ .

In order to apply the method to seismic data a state-space model of the data generation mechanism must be formed. The model used is that proposed by Bayless and Brigham [4]. That is, the input is the reflection sequence ( $u(k) = r(k)$ ) and the state transition matrix,  $\phi$ , models the source and the effects of the transmission path. The state-space model can be obtained either from analytic models of the seismic processes or in some cases from the data themselves. The starting point for the formation of the state model is the convolutional description of the seismic response, similar to that given in Chapter 7,

$$y(n) = s(n) * r(n)\tag{8.3.1a}$$

for the noise-free case



where  $s(n)$  is the source signal  
and  $r(n)$  is the reflection sequence.

The effects of noise will be considered later in the context of the noise reduction process proposed in Chapter 4, but the initial development will be made for the noise-free case.

The non-stationary effects of the transmission path may be included by modelling the source  $s(n)$  as a time-varying wavelet  $s(n, n_1)$ , so that

$$y(n) = s(n, n_1) * r(n) \quad (8.3.16)$$

It must be remembered, however, that in reality the source is fixed and it is the transmission path which results in non-stationarity (as a function of distance, see Chapter 7).

Both stationary and non-stationary models are considered here and the formulation of the state-space model will be discussed for both cases.

#### (i) Stationary model

For the stationary case, z-transforming equation (8.3.1a) gives

$$Y(z) = S(z)R(z) \quad (8.3.2)$$

Now, if a pole-zero-model of the source signal can be found with

$$S(z) = \frac{b_0 + b_1 z^{-1} + \dots + b_M z^{-M}}{1 + a_1 z^{-1} + \dots + a_N z^{-N}} = \frac{Y(z)}{R(z)} \quad (8.3.3)$$

Then a state space description can be obtained from this as follows [8] where, for simplicity, it is assumed that the numerator order is less than that of the denominator, though other methods exist to handle the situation where  $M \geq N$ .

Let

$$\frac{W(z)}{R(z)} = \frac{1}{1 + a_1 z^{-1} + \dots + a_N z^{-N}} \quad (8.3.4)$$

Hence

$$Y(z) = (b_0 + b_1 z^{-1} + \dots + b_M z^{-M})W(z) \quad (8.3.5)$$

Now from (8.3.4)

$$w(k) = -a_1 w(k-1) - a_2 w(k-2) - \dots - a_N w(k-N) + r(k)$$

letting

$$\begin{aligned} x_1(k) &= w(k-N+1) = x_2(k-1) \\ x_2(k) &= w(k-N+2) = x_3(k-1) \\ &\vdots \\ x_{N-1}(k) &= w(k-1) = x_N(k-1) \\ x_N(k) &= w(k) \\ &= -a_1 w(k-1) - \dots - a_N w(k-N) + r(k) \end{aligned}$$

or in vector form

$$\underline{x}_k = \phi \underline{x}_{k-1} + \underline{\theta} r(k) \quad (8.3.6)$$

where

$$\underline{x}_k^t = [x_1(k), x_2(k), \dots, x_N(k)]$$

$$\underline{\theta}^t = [0, 0, \dots, 0, 1]$$

$$\phi = \begin{bmatrix} 0 & 1 & 0 & \dots & 0 \\ 0 & 0 & 1 & 0 & \dots & 0 \\ & & & 1 & & \\ & & & & \ddots & \\ & & & & & 1 \\ -a_N & & \dots & & & -a_1 \end{bmatrix}$$

Also, from (8.3.5),

$$\begin{aligned} y(k) &= b_0 w(k) + \dots + b_M w(k-M) \\ &= b_0 x_N(k) + b_1 x_{N-1}(k) + \dots + b_M x_{N-M}(k) \end{aligned}$$

or, in vector form,

$$y(k) = \underline{c}^t \underline{x}_k \quad (8.3.7)$$

where  $\underline{c}^t = [b_0, b_1, \dots, b_M, 0, 0, \dots, 0]$ .

Equations (8.3.6) and (8.3.7) constitute the desired state form. Alternative methods of forming discrete state models exist, for example, Mendel and Kormylo [61] obtain discrete state forms for some typical seismic wavelets starting from continuous time functions. If a pole zero representation of the source is not available as an analytic description (as in many cases), such a form may be obtained numerically from a source signature. The procedure adopted here for this modelling is recursive least-squares parameter estimation [122]. The method will be illustrated in the next section.

## (ii) Non-stationary model

As discussed in an earlier chapter, one of the great strengths of the optimal control formulation is the ease with which non-stationary inputs can be accommodated, provided a non-stationary model can be provided. All that is required is for the state-space model to be modified in the appropriate manner. In the case of seismic data, the transmission path will usually be markedly non-stationary, as discussed in Chapter 7. This non-stationarity may occur as a consequence of absorption which causes frequency dependent attenuation of the propagating waveform. Recall from Chapter 7 that a useful model of this absorption is provided by the minimum phase version of the transfer function:

$$H(\omega, T) = e^{\left(-\frac{|\omega|T}{2Q} - i\omega T\right)} \quad (7.2.6)$$

where  $T$  is the travel time from source to observation point and  $1/Q$  is the specific dissipation, and is assumed constant. It will be recalled from Chapter 7 that this expression relates to absorption of energy travelling through a single homogeneous medium characterised by the specific dissipation constant  $Q$ . In practice, of course, the earth's surface does not correspond to this simple structure. Nevertheless, the constant  $Q$  model can provide a good approximation provided the value of  $Q$  is chosen on an empirical basis to fit the data, rather than on the basis of assumptions about the geology.

Ideally an analytic description of the state-space system would be preferable, based on an equivalent minimum phase version of the transfer function (7.2.6). Unfortunately, the author has found this to be an

intractable problem, so that an alternative numerical approach has been adopted. The equivalent minimum phase version of the transfer function is obtained from the condition that

$$\text{Hilbert Transform } \{\log|H(\omega, T)|\} = \arg\{H(\omega, T)\} \quad (8.3.8)$$

This can be done numerically in a number of ways.

The process is illustrated by the following example with the parameters of equation (7.2.6) selected arbitrarily as  $T = 2$  seconds and  $Q = 25$ . The (discretised) minimum phase version of the transfer function, with these parameters, is shown in fig. 8.3.1.

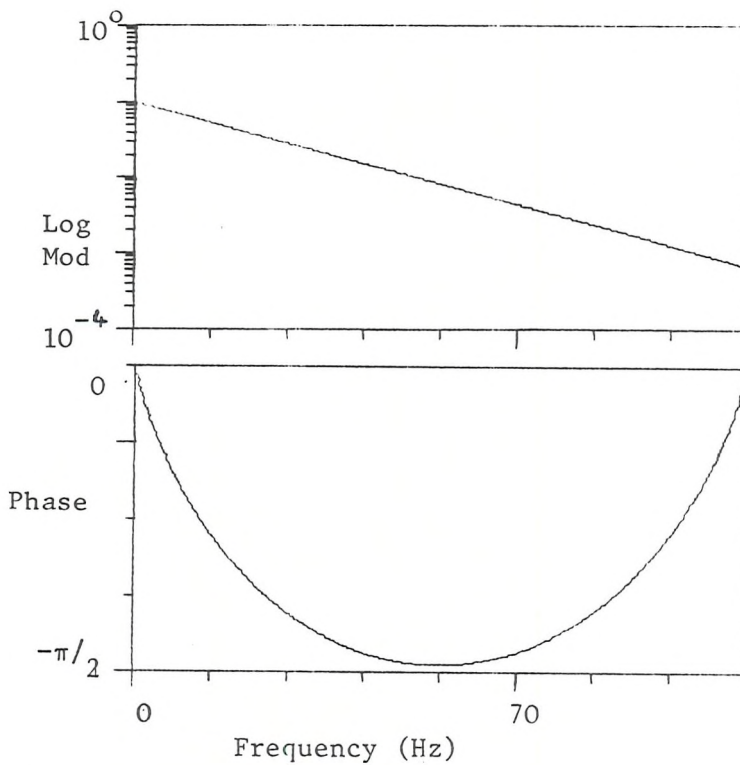


Figure 8.3.1: Modulus and Phase of Equivalent Minimum Phase Version of (7.2.6)

The impulse response function corresponding to this transfer function is shown in fig. 8.3.2. Now, convolution of the response obtained in this way with the assumed source signal produces the wavelet corresponding to  $T = 2$  (fig. 8.3.3(b)), contrast this with the original source (fig. 8.3.3(a)). Finally, the desired pole/zero form corresponding to this time is obtained by a numerical modelling method such as recursive least-squares [122].

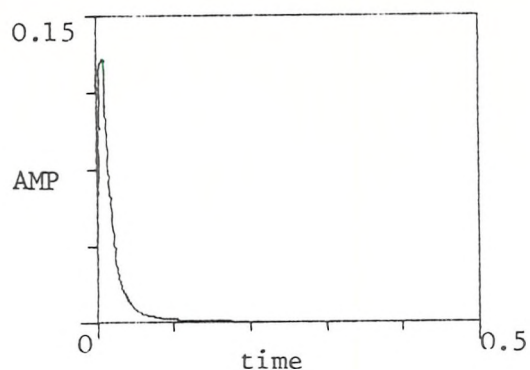


Figure 8.3.2: Impulse Response Corresponding to Transfer function (7.2.6) with  $T=2$ ,  $Q=25$

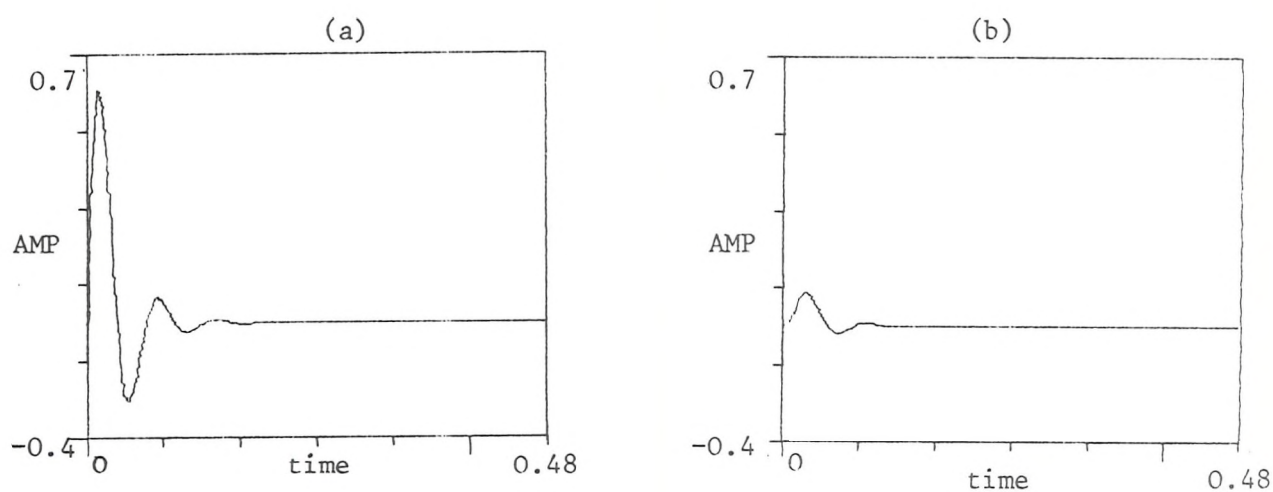


Figure 8.3.3: Source wave and effect of Convolution with Transfer Function of (7.2.6) with  $T=2$ ,  $Q=25$ .

This is a procedure whereby a model in the form of equation (8.3.3) is obtained by performing a least-squares fit on the parameters (poles and zeros). For the purposes of this work the recursive least-squares modelling was performed using existing software on the Data Analysis Centre's PDP 11/50 in the ISVR.



The order of the model may be as large as desired, subject only to computational limitations, though for these reasons it is desirable that the model order should be as small as possible, consistent with giving a good approximation to the waveform.

A time-variant state-space model can be obtained from this method by repeating the procedure for different time points,  $T_i$ ,  $i = 1, \dots, p$ . The parameters of the state-space model are made continuously variable by interpolating between obtained sets of parameters. Any convenient form of interpolation can be used; for simplicity in this case linear interpolation is employed. Note that whilst the values of the parameters are allowed to vary, the order of the model is held constant, thus avoiding problems with the order of the state vector.

### 8.3.2 Discussion

It is interesting to contrast the properties of optimal control deconvolution with those of other methods and in particular the Kalman filtering approaches. Like the Kalman filtering methods, optimal control has the advantage over conventional deconvolution of being able to handle non-stationary systems easily, but has the disadvantage of needing a state-space model. However, the optimal control method has a number of properties which are distinct from those of the Kalman filter. In the first place, in contrast to the Kalman filter, no assumptions about the form of the input sequence (either white, or produced by a white excited shaping filter) need to be made and this is a considerable advantage. Furthermore, with the optimal control method there is no need for estimates of the variances of either plant or measurement noise. The optimal control method also has some advantage in computational terms requiring approximately  $(3N^3/2 + 3N^2)L$  multiplications in contrast to the approximately  $(2N^3 + 5N^2)L$  of the fixed interval estimator of Mendel and Kormylo [60]. However, the optimal control is a fixed interval estimator only and does not have the generality of the Mendel and Kormylo approach in that it cannot be used as a fixed point or a fixed lag estimator. Also the optimal control method is designed for the noise-free case and is thus not optimal in any sense for noisy data. However, it is worth remembering that the optimality of the Kalman filter is related to the accuracy of the estimates of the measurement noise variance, which will often be limited. Also, it will be recalled from Chapter 4, and will again be demonstrated in the simulations of the following section that a powerful though pragmatic method of noise reduction for optimal control is provided by control of the parameters  $q$  and  $r$ .

### 8.3.3 Application to synthetic data

#### (i) Stationary data

The application of the optimal control technique is demonstrated on stationary data using a response obtained by convolving an assumed form for the source with the response obtained from the lattice synthetic described in Appendix XIV. For this example, the synthetic was generated

from a system with just two layers. A sea layer is bounded by a (down-going) reflection coefficient of  $r_1 = -0.6$  with a two-way travel time of 0.4 second. The second layer is characterised by a reflection coefficient of  $r_2 = 0.2$  and a two-way travel time of 0.66 second. The high level of reverberant energy which is generated by these coefficients is designed to show that the white reflection series model is not required for optimal control deconvolution.

As discussed in the previous section there are a number of ways in which a source model may be obtained. For simplicity, in this case the source will be assumed to have the form

$$s(n) = e^{-\lambda n T} \cos(\beta_n T + \phi) \quad (8.3.9)$$

where  $\lambda = 35$ ,  $\beta = 100$  and  $\phi = -\pi/2$ .

This waveform is then convolved with the response obtained from the lattice synthetic. The resulting trace is shown in Fig. 8.3.4(a). The required state-space model for this source is obtained using the techniques described in the previous section. The result is

$$\phi = \begin{bmatrix} 0 & 1 \\ -e^{-2\alpha T} & 2e^{-\alpha T} \cos \beta T \end{bmatrix}, \quad \underline{\theta}^t = (0, 1), \quad \underline{c} = \begin{bmatrix} e^{-\alpha T} \cos(\phi + \beta T) \\ -\cos \phi \end{bmatrix}$$

(with reference to equations (8.3.6) and (8.3.7)).

Application of the optimal control technique to this data with the parameters  $q$  and  $r$  set as 1 and 0.0001 respectively, produces a result (fig. 8.3.4(b)) which is very close to the trace input spike sequence. Note that the fact that the spike sequence is not randomly spaced (due to reverberations) has no influence on the result with this method (in contrast to least-squares).



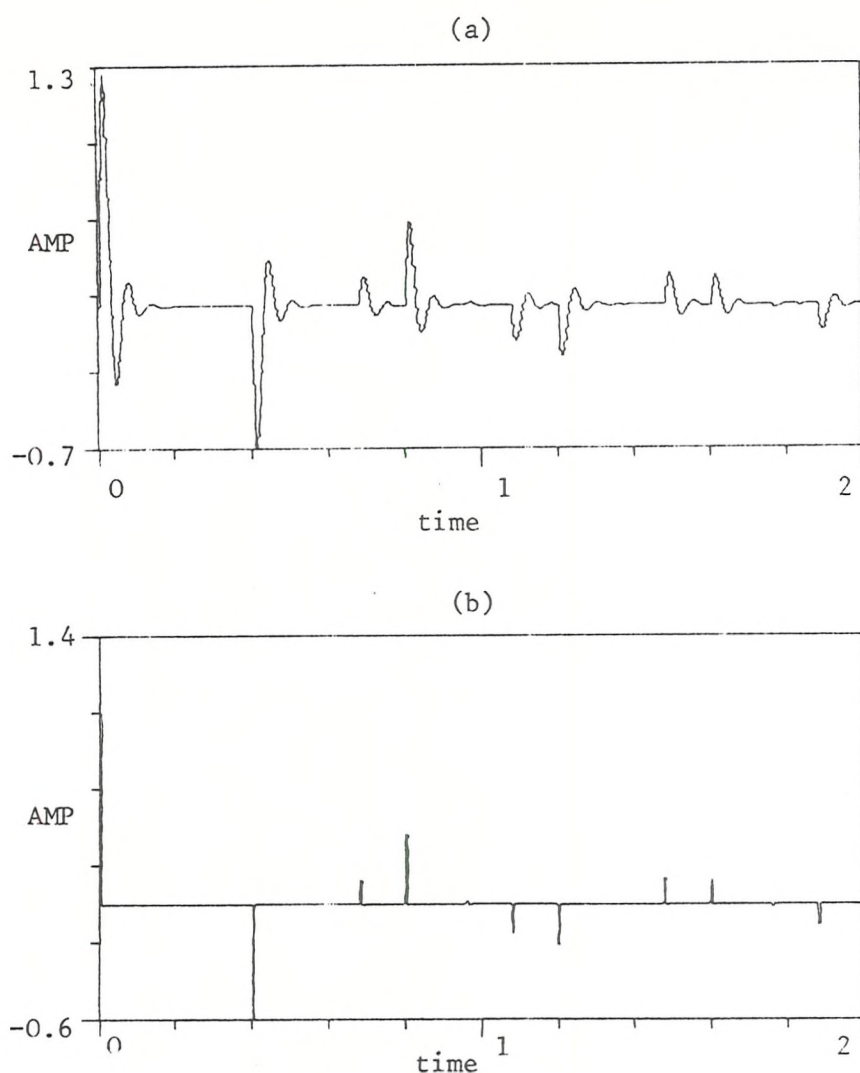


Figure 8.3.4: Lattice Synthetic (a) and optimal control Deconvolution (b)

## (ii) The influence of noise

The influence of additive random noise on the performance is an important factor. Noise enhancement is known to be one of the main problems with the least-squares method (see Chapter 3). This fact is illustrated by adding random noise to the synthetic data of fig. 8.3.4(a) (see fig. 8.3.5(a)). The effect of applying (stationary) least-squares spiking deconvolution (with no pre-whitening) to this data is shown in fig. 8.3.5(b). The deterioration in SNR is obvious. The application of pre-whitening has little effect (fig. 8.3.5(c)), and the results are

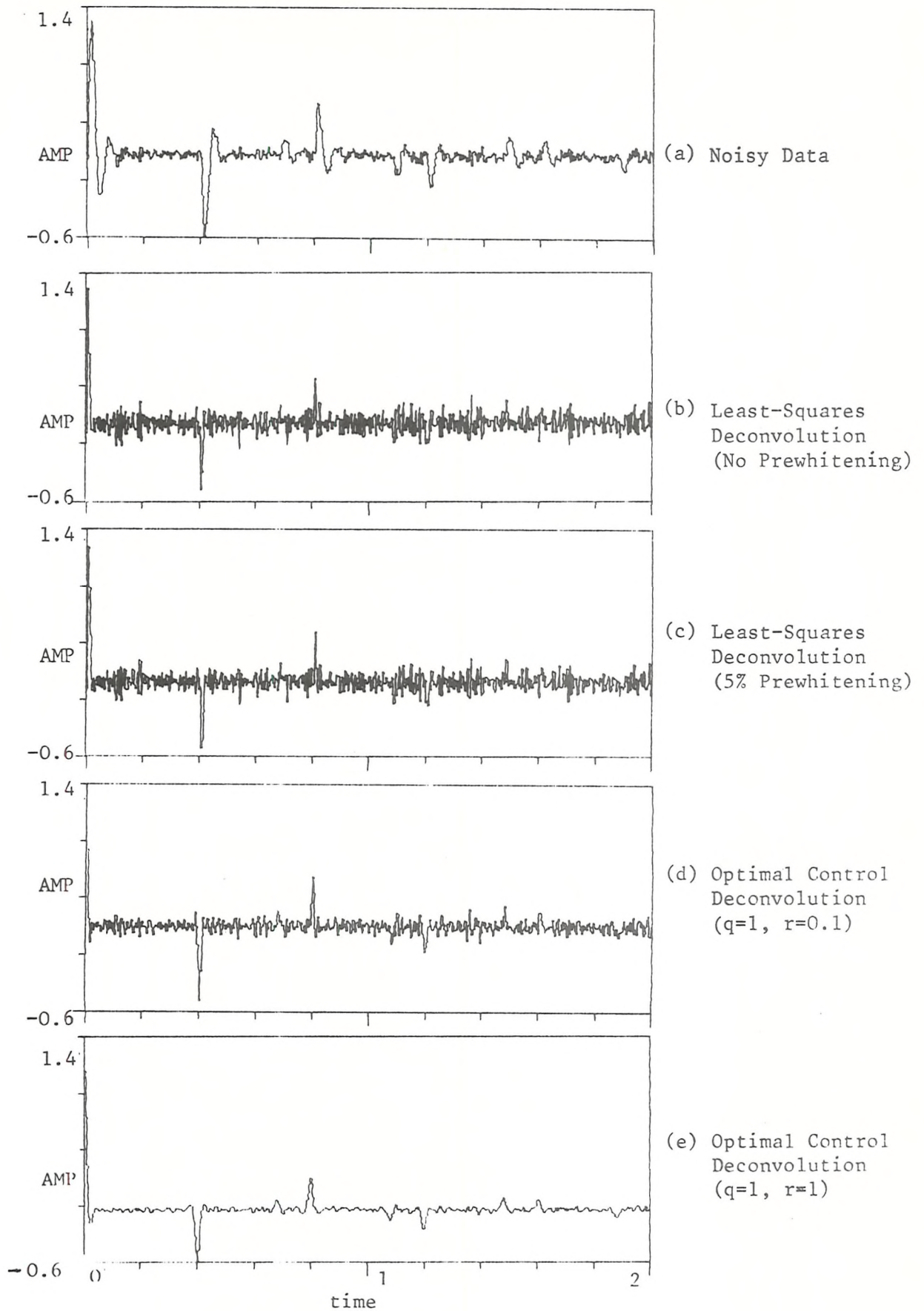


Figure 8.3.5: Deconvolution of Noisy Data by Least-Squares and Optimal Control.

still clearly unsatisfactory. By contrast, the optimal control technique (with  $q = 1$ ,  $r = 0.1$ ) applied to the same data produces the result shown in fig. 8.3.5(d). This is clearly greatly superior to that obtained using conventional least-squares deconvolution. This demonstrates an important property of the optimal control method - that it is robust to the presence of noise. In fact, as discussed in Chapter 4 it is the parameters  $q$  and  $r$  (or more correctly, the ratio  $q/r$ ) which determines the response of the optimal control method, and in particular the nature of the response in the presence of noise. It was shown in Chapter 4 that decreasing the ratio  $q/r$  produces a more smoothed response (and is in fact analogous to a form of pre-whitening). The increased smoothing effect of lowering  $q/r$  is shown in fig. 8.3.5(e) where  $r$  has been increased from 0.1 to 1.

### (iii) Non-stationary data

The application of the optimal control technique is also demonstrated on non-stationary synthetic data. This data was generated using the constant  $Q$  model discussed earlier, as follows.

The minimum phase version of the frequency response corresponding to equation (7.2.6)

$$H(\omega, T) = e^{\left(\frac{-|\omega|T}{2Q} - i\omega T\right)} \quad (7.2.6)$$

was generated for  $T = 0, 1$  and  $2$  seconds,  $Q$  was chosen as  $25$  (see previous section). In each case the equivalent minimum phase version  $H_{eq}(\omega, T)$  was obtained numerically. The source was assumed to have the same form as in the stationary case (eq. (8.3.10)). A time-variable source was then obtained for  $T = 0, 1$  and  $2$  by convolving this response with  $H_{eq}(\omega, T)$  at each point. A model with  $8$  poles and  $8$  zeros was then obtained for each, using a recursive least-squares fit. This was found to be the lowest model order which gave a satisfactory representation of the time-varying wavelet at all points on the trace. Linear interpretation was used between the three sets of parameters to give a continuously time-variable model. This model was driven using the spike series of fig. 8.3.6(a) as input, to create the non-stationary output shown in fig. 8.3.6(b). The non-stationarity is manifested as a progressive loss of the

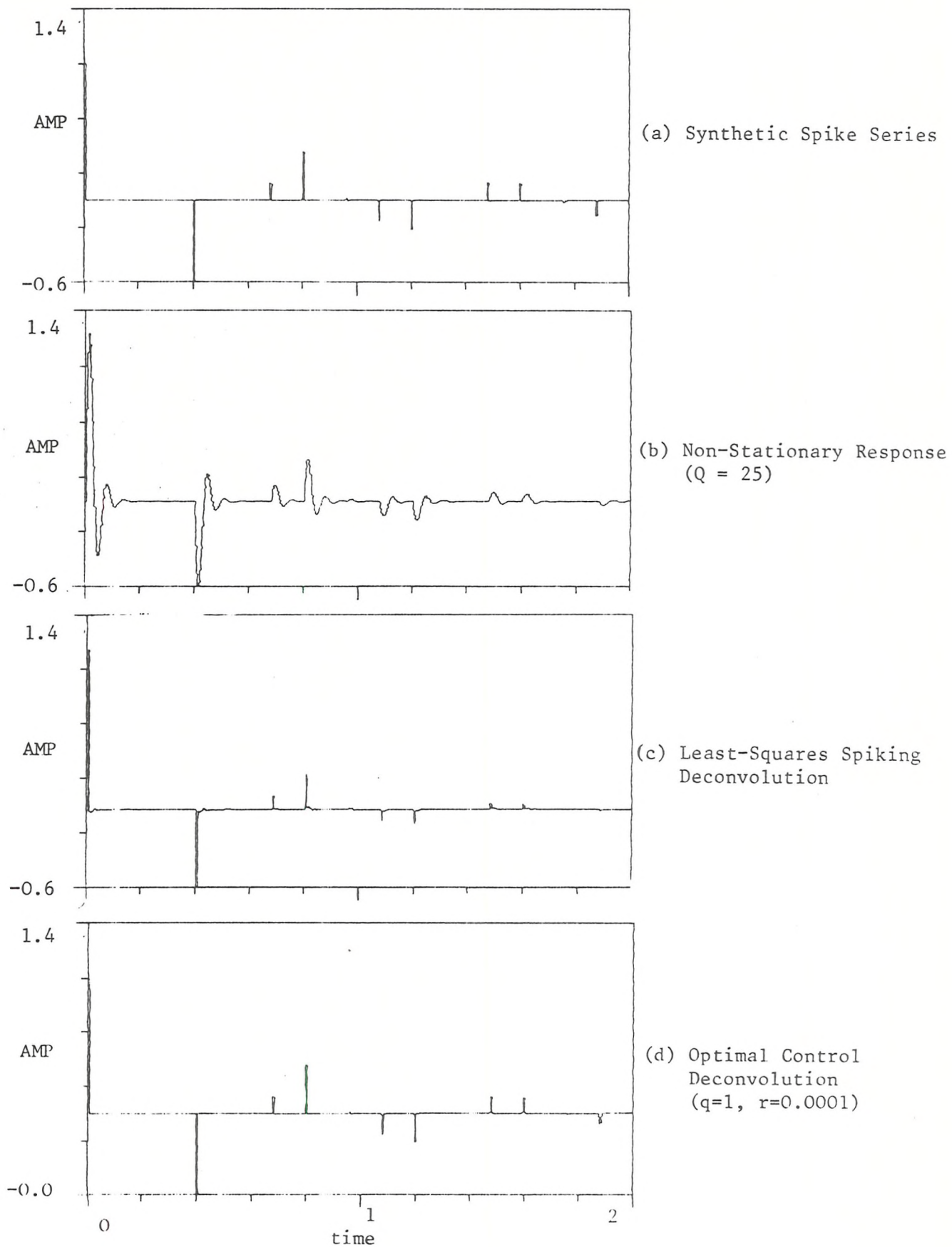


Figure 8.3.6: Least-Squares and Optimal Control Deconvolution of Non-Stationary Synthetic Data.

higher frequency components and broadening of the pulses. An attempt to spike this series using conventional (stationary) least-squares methods is shown in fig. 8.3.6(c). Comparing this with 8.3.6(a) shows the result to be unsatisfactory, particularly for the later reflections. This is due to the fact that the autocorrelation is computed using the whole of the non-stationary trace and is thus 'smeared'. By contrast the optimal control method with  $q = 1$ ,  $r = 0.0001$  (fig. 8.3.6(d)) produces a much closer approximation to the original spike series. Interestingly, the quality of the approximation decreases slightly with time. This is due to the relative influence of the parameters  $q$  and  $r$  discussed in Chapter 4 and formalised in equation (4.4.9).

$$\hat{U}(\omega) = \frac{U(\omega)}{\left[1 + \left(\frac{r}{q}\right) / |H(\omega)|^2\right]} \quad (4.4.9)$$

This equation is for stationary systems though as discussed in Chapter 4, the extension to nonstationary systems is intuitively reasonable. From this equation, in this case, as time progresses the high frequency content of the system  $H$  decreases and so the effect of the constant  $(q/r)$  increases, so that the result becomes more smoothed with time. However, this effect can be reduced by varying  $(q/r)$  in a similar manner to that used for noise reduction.

#### 8.3.4 Application to field seismic data

The application of the optimal control technique to field seismic data is demonstrated using a single trace, displayed in fig. 8.3.7(a), provided by Seismograph Service Ltd. An assumed source wavelet was also provided and used as the basis for the state-space model required. The first 300 milliseconds of data shows the direct signal, reduced in amplitude by gain changes. The first reflection occurs at about 400 milliseconds. A total of 2 seconds of data is displayed and the sample rate used is 250 samples per second.

The effect of attempting to 'spike' this data, using conventional (stationary) least-squares deconvolution is shown in fig. 8.3.7(b). The



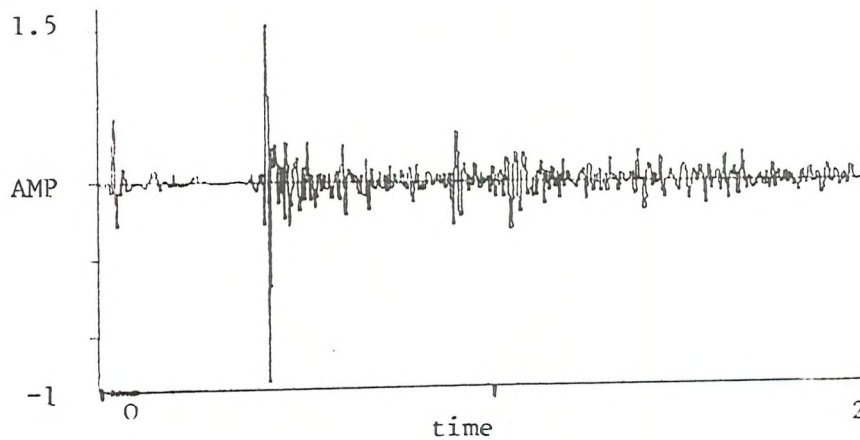
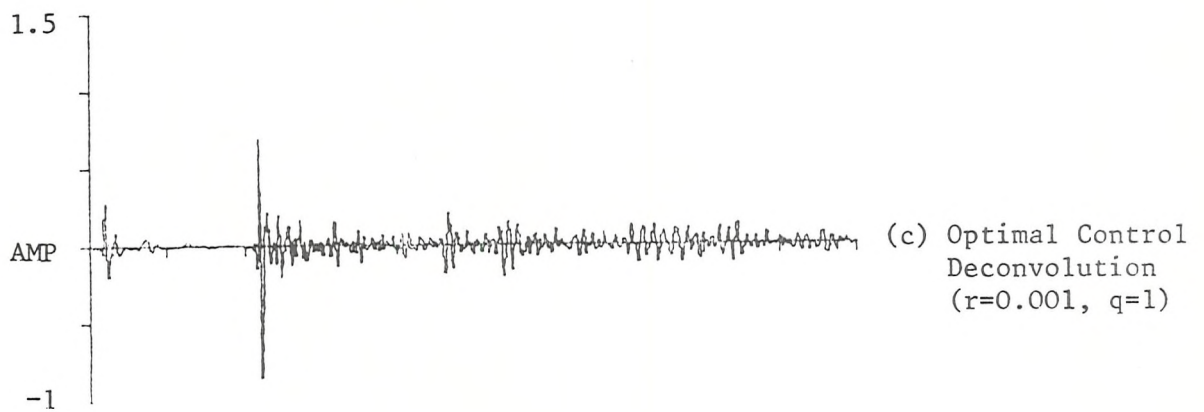
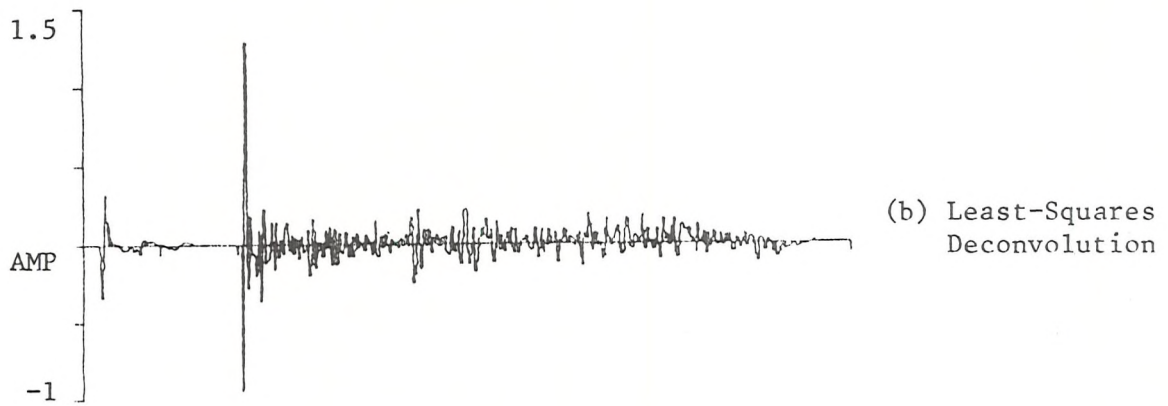
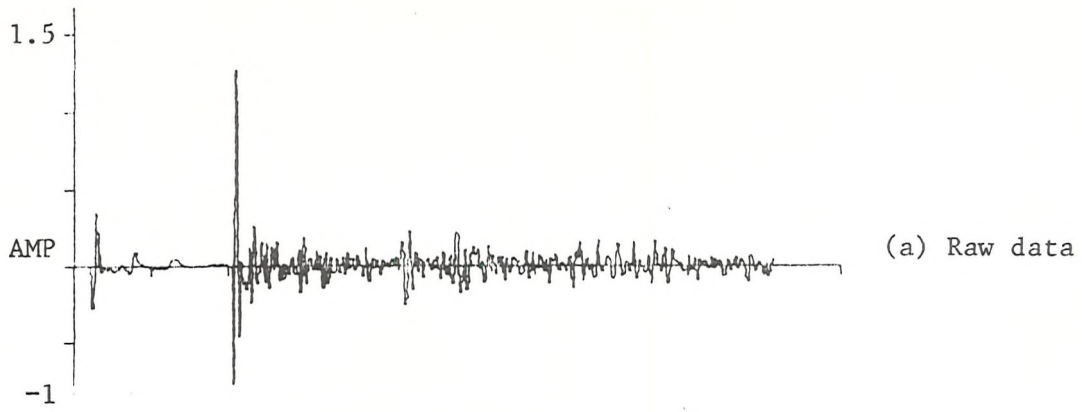


Figure 8.3.7: Application of Optimal Control Deconvolution to Seismic Data

autocorrelation required for the inversion (see Chapter 7) was obtained using the source signature, and the operator was chosen as 100 milliseconds in length (a typical value). The result shows that the process has little effect on the signal, and produces a slight degradation of the SNR. The optimal control method was applied by forming a state-space model from the source signature, using the recursive least-squares approach. The model order was selected as 8 (poles and zeroes). This was found to give a satisfactory description of the source signature. The application of the method with  $r = 0.001$  and  $q = 1$  produces the result of fig. 8.3.7(c). These parameters were found to be about the best, though some improvements were observed over a wide range of  $(q/r)$ . The results for this method are considerably better than for the least-squares, some spiking has occurred and the SNR appears unaffected. The improvements seem to lie mainly in the first half of the data, from the first reflection to about 1.0 second. In the second half of the data, no spiking seems to have taken place. It may be surmised that the reason for this is the effect of transmission through the earth on the source wavelet. That is, in the earlier part of the data the source signature may be a good representation and thus the optimal control performs well, whilst later in the data the source signature is no longer a valid model and so the optimal control method fails to spike the data. An obvious attempt to overcome this is to use the non-stationary constant  $Q$  model employed on the synthetic data of the previous section. The result is shown in fig. 8.3.7(d), with  $Q = 10$ . This shows some slight improvement in the spiking at the lower end of the trace but the result is still unsatisfactory. Furthermore, varying the value chosen for  $Q$  does not appear to improve the situation and the only conclusion which may reasonably be drawn is that for this data the constant  $Q$  attenuation model is not appropriate.

#### 8.4 Conclusions

The method of optimal control described in Chapter 4 provides a novel method for spiking deconvolution of seismic data. The method has the advantage that it is capable of performing adaptive deconvolution for any assumed non-stationarity which can be put in state-space form. Also, in

contrast to most other methods of deconvolution, no assumptions are required about the nature of the reflection sequence or about the phase of the source waveform. Perhaps the most important advantage of the method, demonstrated by the simulations, is the ability to produce effective deconvolution for noisy data, when more conventional methods, particularly least-squares, are unable to do so.

However, the method has a number of disadvantages, including a relatively high computational requirement compared to least-squares, say (though slightly better than Kalman filtering approaches). Perhaps the biggest disadvantage of the technique, in common with the Kalman methods, is the need to obtain a state-space description of the seismic system. Such a model can be obtained either from an available analytic model of the source form, or more usually, from the data themselves by numerical modelling. Similarly, a non-stationary model can be formed by incorporating an available analytic description into the state model for the source, or if no such description is available then a non-stationary description can be obtained by numerical modelling at various points in the data and interpolating between the resulting parameter sets. In this chapter, the widely used 'constant Q' model of attenuation was employed in this way.

Application of the technique to synthetic data shows that the method is a powerful approach to deconvolution for both noisy and non-stationary data. The more limited success obtained in the application of the method to field seismic data demonstrates the main limitation of the method - its dependence on the accuracy of the state-space model. However, even for the case examined with an imprecise model, the method still produces better results than conventional least-squares deconvolution and this indicates that, in spite of this limitation, the method remains a potentially useful approach to seismic deconvolution.



## CHAPTER 9

### ADAPTIVE SIGNAL ENHANCEMENT OF SEISMIC DATA

#### 9.1 Introduction

In this chapter the aim is to demonstrate the approach to SNR enhancement provided by the generalised comb filter (GCF) of Chapter 5. This is achieved using two separate applications to seismic SNR enhancement, one single and one multi-channel.

The general motivation and aims of seismic SNR enhancement were discussed in Chapter 7.

The first SNR enhancement approach considered here (in section 9.2) is based on an entirely novel concept, which can be considered as a development of the GCF, dubbed the predictive stack [15]. The process attempts to enhance the SNR of the seismic response by utilising the reverberant energy. In conventional processing, predictive deconvolution (see Chapter 7) attempts to remove or attenuate reverberant components. Conceptually, at least, this is wasteful since each reverberant component contains coherent signal energy which, if suitably realigned, could be used to enhance the SNR of the trace. Any such realignment is complicated by the fact that successive components are, in general, overlapping and distorted and the interval between successive multiples is only approximately known. The modified GCF or predictive stack provides a method of achieving this realignment.

Of course, most multiples have only small amplitudes and the potential gains would be very small. However, in some areas, notably marine seismic sections recorded in areas having a hard sea-bottom, the reverberant energy may be very high and in these circumstances there are potentially significant gains to be made from the realignment. It is stressed, however, that the aim here is to demonstrate the principle of SNR enhancement by realignment, it is not claimed that the predictive stack is in any sense the optimal approach to the problem.

The second SNR enhancement approach considered (in section 9.3) is again based on the GCF, but in this case is a form of multi-channel operation which is a generalisation of the conventional common depth point

(CDP) stack (Chapter 7). It is well known that the CDP stack is usually a suboptimal way of improving SNR. In general the moveout correction will not be precise, wavelets on successive traces will not be exact replicas (being further distorted by the greater length of passage through the earth) and the SNR varies from trace to trace. Some effort has been directed at this problem, by a number of authors and these attempts are discussed in section 9.3.1. It is demonstrated that the GCF is a powerful technique for improving the SNR of unstacked traces.

Both of these SNR enhancement techniques are applied to synthetic and field seismic data.

## 9.2 SNR Enhancement by Predictive Stack

### 9.2.1 Theory

In this section the idea of SNR enhancement by predictive stack will be developed.

Recall from Chapter 7 that conventional processing makes use of predictive deconvolution to eliminate multiple reflections from a seismic section. As noted before, this is a wasteful process because each multiple component contains energy which is coherent with the primaries and which could be used to improve the SNR of the trace. To see this more clearly consider the idealised earth section of fig. 9.2.1.

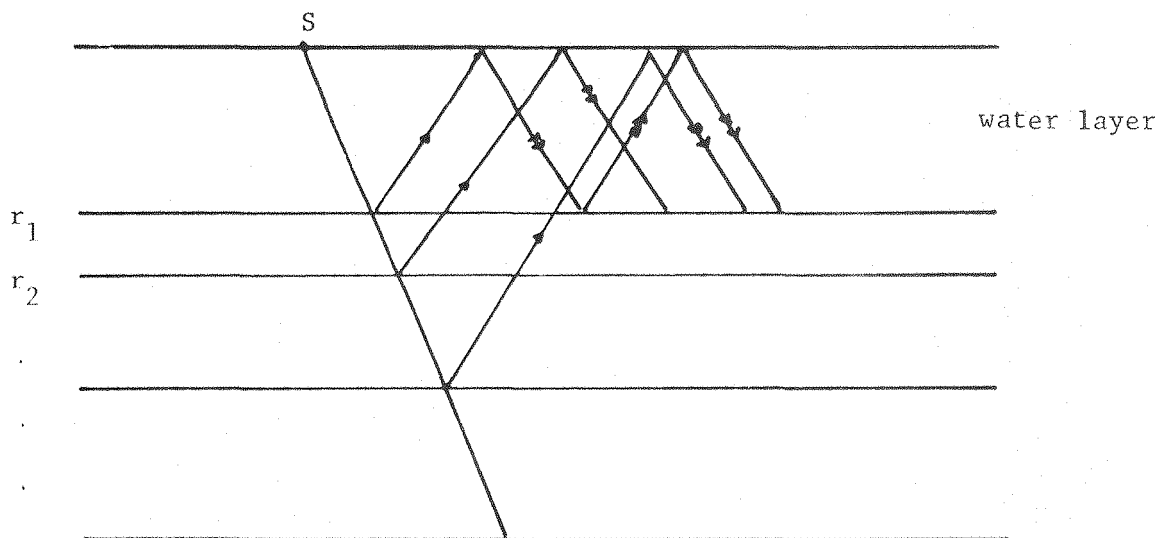


Figure 9.2.1: Idealised Earth Section

The conventional view is that this response consists of a set of primary reflections which are corrupted by the presence of (unwanted) multiple energy, which overlays and interferes with the interpretation of the primaries. An alternative view of the same section would be to interpret each downward reflection at the surface not as a multiple but as a secondary source, albeit delayed, distorted and reduced in amplitude by the passage through the earth. In this interpretation the complete response consists not of primaries and multiples but sets of overlapping primaries. In effect there are  $N$  representations of the same seismic section, though these will be overlapping and distorted. Now, it is known from the theory of Chapter 5, that given  $N$  representations of the same signal it is possible using the generalised comb filter (GCF) to effect improvements in SNR, even if the successive representations are distorted and the noises partially correlated. To apply this procedure to reverberant seismic data is similar to the single channel operation of the filter discussed in Chapter 5. Recall from that chapter that in this mode the GCF operates using  $M$  inputs obtained from different points on a single input signal  $x(n)$ . This signal is assumed to have a pseudo-periodic structure as defined by:

$$x(n) = s(n) + v(n) \quad (5.1.2)$$

$$x(n + kn_0) = h(n, n + kn_0) * s(n) + v(n + n_0) \quad k = 1, 2, \dots$$

where  $v(n)$  is a noise term and is assumed zero mean and stationary,

$h(n, n_1)$  is a slowly time-varying linear system and where  $n_0$  is assumed to be approximately known and approximately constant (see Chapter 5).

In order to relate the seismic response to this form it is necessary to modify the conventional seismic model of equation (7.3.15) (see Chapter 7). The response is now modelled as:

$$x(n) = s(n) + u(n) \quad (9.2.1a)$$

where  $s(n)$  is the signal component due to both primaries and multiples and  $u(n)$  is a noise component which is assumed to be zero mean and stationary. Now, assume the sea bed reverberations recur at intervals  $\alpha$ , say, (which corresponds to the two-way travel time through the water layer).

At  $n + \alpha$  the response is

$$x(n + \alpha) = s(n + \alpha) + u(n + \alpha)$$

but the signal component is itself the sum of two components, namely (i) the component due to the propagation of  $s(n)$  along the multiple transmission path and (ii) the component due to primary arrivals between  $n$  and  $n + \alpha$ , so that

$$x(n + \alpha) = h(n, n + \alpha) * s(n) + d(n + \alpha) + u(n + \alpha) \quad (9.2.1b)$$

The transmission characteristics  $h$  will be referred to as convolutional distortion and the primary arrivals,  $d$ , as additive distortion. In the simplest case, where the transmission path can be characterised entirely by the sea-bottom reflection coefficient,  $h$  is purely a scale factor, so that

$$x(n + \alpha) = r_1 s(n) + d(n + \alpha) + u(n + \alpha)$$

where  $r_1$  is the downgoing reflection coefficient at the sea bed.

In more realistic cases  $h$  represents the effects of earth filtering on the response over the interval and may be regarded as a (slowly) time-varying linear system. Now comparing (9.2.1) with (5.1.2) shows that the seismic model is similar, though not identical to the form needed for the GCF. The distinction lies in the additive distortion term  $d(n + \alpha)$  due to the new primary arrivals in the interval  $n$  to  $n + \alpha$ . However, the generalised averaging theory of Chapter 5 shows that SNR gains can be obtained by averaging signals distorted in this way provided the averaging gain is sufficiently small. Consequently it may be anticipated that the GCF can produce SNR gains for such signals, though the gains will be small if the additive distortion term (primary arrivals) is large. Fortunately, large reflections from subsurface strata are not likely in the areas of high sea-bottom reflection, which are of interest here since the larger the reflections at the sea-bed the less the transmitted energy.

The GCF operates by subdividing the seismic response into  $N$  gates, at intervals approximately equal to  $\alpha$  (see Fig. 9.2.2).

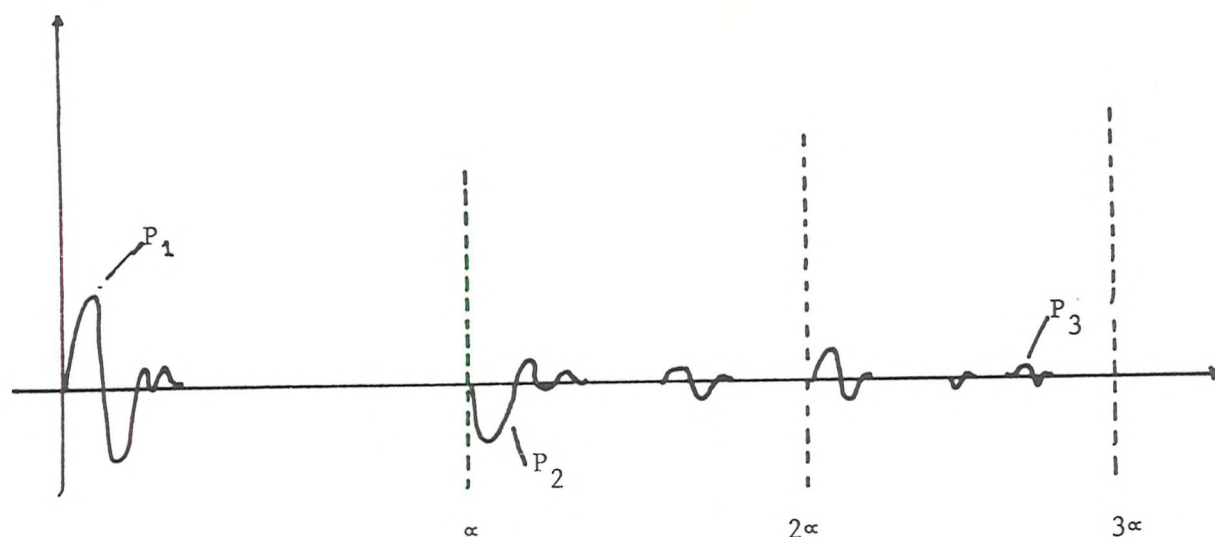


Fig. 9.2.2 - Idealized seismic response, primaries (labelled  $P_i$ ) and sea-bottom multiples.

To ensure that events further down the trace are not enhanced using events farther up the trace, and in contrast to the GCF operation of Chapter 5, the teeth of half of the comb are set to zero so that the comb is one sided (acausal). Of course, the GCF still enhances all events which are coherent from gate to gate (including the multiples). However, the resulting increase in SNR enhances the efficiency of subsequently applied predictive deconvolution (as is seen in the following section).

### 9.2.2 Simulations

#### (i) Synthetic data

The predictive stack method was tested on synthetic data from two sources - one single channel and one multi-channel.

The single channel data was generated using the lattice synthetic form described in Appendix XIV. A simple response was generated with just two reflectors, characterised by downgoing reflection coefficients  $r_1 = -0.6$  and  $r_2 = -0.2$  with two-way travel times of 0.4 and 0.66 seconds, respectively (see Fig. 9.2.3) at a sample rate of 500.

The response generated in this way was convolved with a source wavelet chosen, for simplicity as:

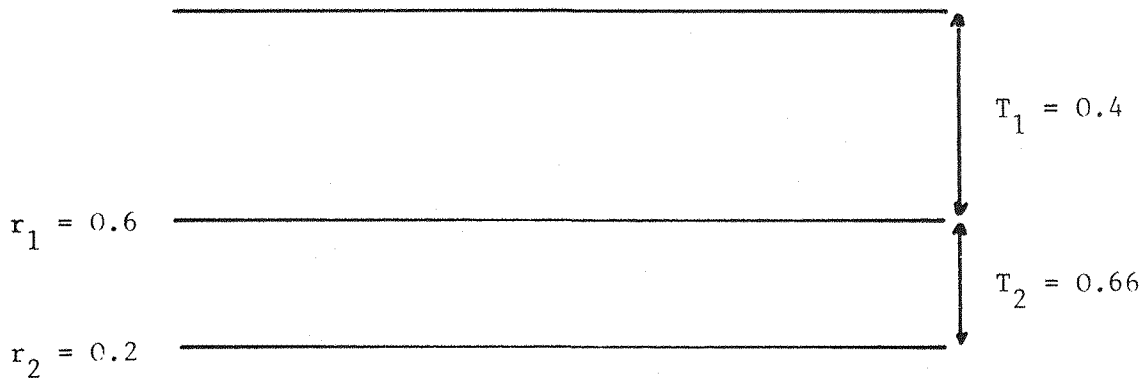


Figure 9.2.3: Idealised Earth (2 layers)

$$e^{-\lambda n} \cos(\omega_0 n t + \phi).$$

The resulting response is shown in fig. 9.2.4(a) with the two primaries marked  $P_1$  and  $P_2$  respectively, all other components of the response are multiples. This simple form of response was chosen to illustrate the principles of the method. The sea-bottom reflection coefficient was chosen as a high value to give a strong reverberant component to the data. The sub-sea bed layer was given an unusually high value to illustrate the capabilities of the method for handling large additive distortional components (see previous section).

The performance of the predictive stack in improving the SNR when the data is corrupted with additive Gaussian white noise was investigated for a range of parameters and input SNR's. The results were evaluated using a performance measure for SNR improvement,  $SNR_I$ , defined by:

$$SNR_I = 10 \log_{10} \left( \frac{\sigma_u^2}{\text{Variance } \{e\}} \right) \quad (9.2.2)$$

where  $\sigma_u^2$  is the variance of the input noise and  $e = \gamma - \hat{\gamma}$  where  
 $\gamma$  is the raw (noise-free) signal  
and  $\hat{\gamma}$  is the enhanced output.



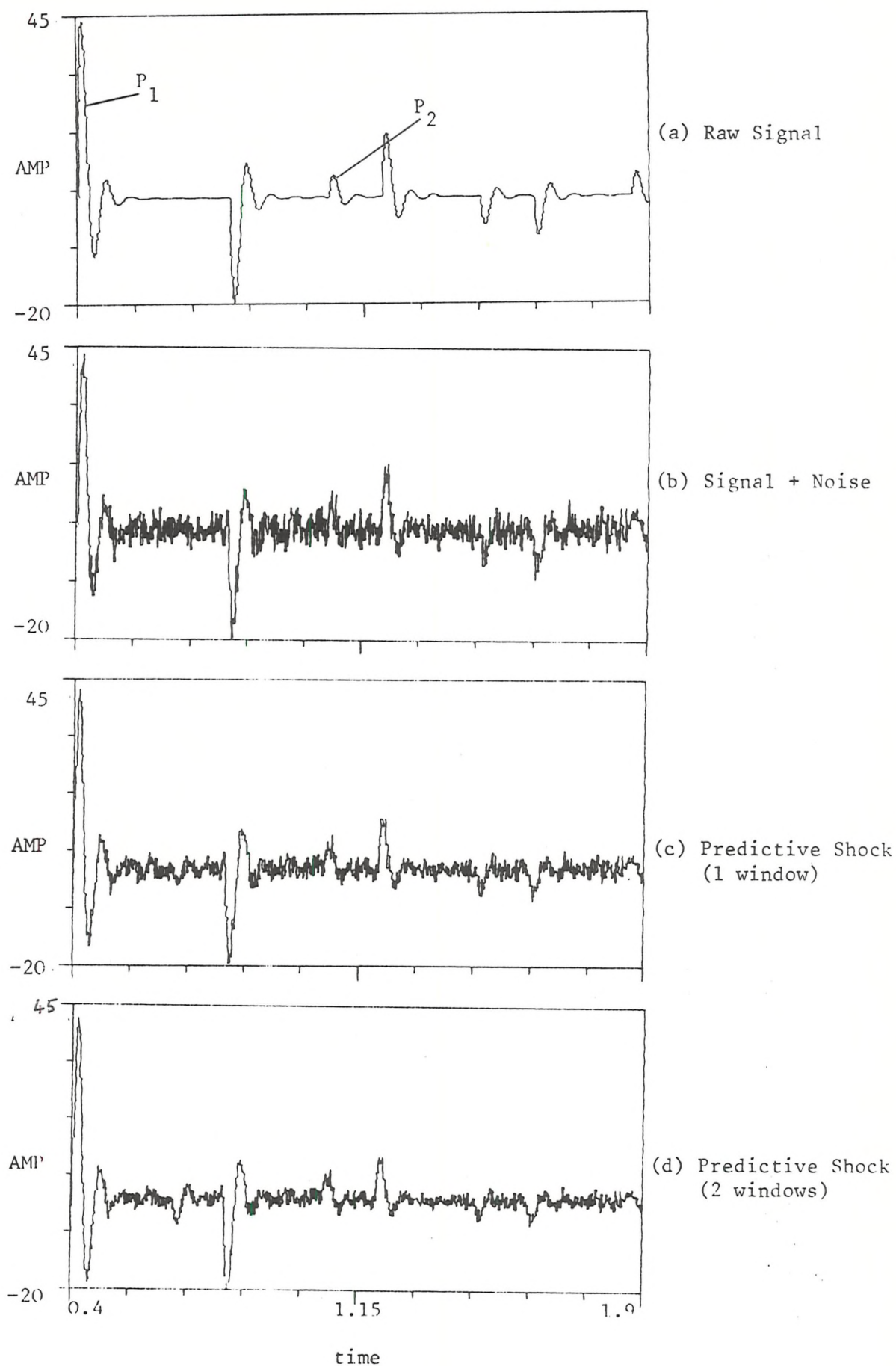


Figure 9.2.4: Application of Prediction Shock Technique

It is recognised that by using an interval measure of SNR gain there is a danger that results may be produced which improve the data in average SNR terms, but are qualitatively unacceptable due to the presence of enhanced distortion at specific points. Care must therefore be taken in interpreting the results.

Throughout the trials the gains on the comb teeth were set equal to one. The first series of results investigates the SNR improvement with a single enhancement frame (1 tooth in the comb) for a fixed input SNR (= 0.78 dB).

Table 9.2.1 shows  $SNR_I$  as a function of adaptation constant  $\alpha$  with the filter length fixed at 20 samples (= 40 ms) whereas in Table 9.2.2  $\alpha$  is fixed and the filter length varies. The results indicate small, but consistent, improvements. Varying the filter would seem to indicate that the results are best for the shortest filter lengths. However, it should be recalled from the LMS theory of Chapter 2 that filters of differing lengths are not strictly comparable at a fixed adaptation rate. All that can be concluded from table 9.2.2 is that the results show improvements consistently over a broad range of filter lengths. A typical example with a filter length of 20 samples and an adaptation constant (normalised) equal to 0.2, is shown in fig. 9.2.4(c). (Fig. 9.2.4(b) shows the noise corrupted signal.) The figure illustrates the SNR improvement indicated in the table but also shows a small residual distortional component at  $t = 0.66$  second, which is predictable from the theory (see previous section). For the above results it was assumed that the interval between successive multiples was exactly known and that the interval between successive teeth was set equal to this interval. The next series of results (table 9.2.3) illustrates the effect on the SNR improvements of inaccuracy in the estimation of multiple intervals. The table shows that, as predicted in the previous section the SNR improvements are maintained, provided  $\alpha < n_0 < \alpha + L$ , where  $\alpha$  is the true interval. Outside this range, improvements cannot be guaranteed. Table 9.2.4 shows the effect of increasing the number of windows (teeth) whilst keeping the other parameters constant. It would appear that for this data at least the optimum number of teeth in the comb is small (= 2). This is consistent with expectations from the theory due to the growth of the distortional component as the number of windows increases. In fact,



Table 9.2.1 (filter length = 20 samples)

Adaptation Constant ( $\alpha$ )	SNR <sub>I</sub> (dB)
0.1	2.41
0.2	2.86
0.3	3.10
0.4	3.29
0.5	3.29

Table 9.2.2 (adaptation constant = 0.3)

Filter length (samples)	SNR <sub>I</sub> (dB)
10	3.40
20	3.10
30	2.98
40	2.61

Table 9.2.3 (filter length = 20 samples, adaptation constant = 0.3)

Prediction distance	SNR <sub>I</sub> (dB)
190	-1.21
200	3.10
205	3.81
210	3.81
220	4.03
225	2.35

Table 9.2.4 (filter length = 20 samples, adaptation constant = 0.3)

Comb 'teeth'	SNR <sub>I</sub> (dB)
1	3.81
2	4.40
3	2.44

Table 9.2.5 (filter length = 20 samples, adaptation constant = 0.3, prediction distance = 200)

SNR of input	SNR <sub>I</sub>
-5.04	6.71
0.78	4.40
8.0	2.21

inspection of a typical response (fig. 9.2.4(d)) shows that even with just two teeth, the distortional component (at 0.66 second) may already be such as to be unacceptable qualitatively even though the SNR gain is greater than for a single window. In the light of this it may be that in general the optimum number of teeth in the comb is just one.

The final series of trials on this data investigated the effect of varying the input SNR (whilst keeping other parameters constant). These results are given in Table 9.2.5. The table indicates that the results improve as the SNR diminishes and conversely. This is because the effect of a constant level of distortion reduces as the SNR is decreased. Of course, it follows that if the SNR is sufficiently high, the method may produce no increase in SNR, or actually degrade the data.

The method was also tested on synthetic data generated from a second model. This data was generated using the multi-channel model described in Appendix XIV. This represents a far more complex model than the lattice data - including the effects of spherical divergence, ghosts, array effects and changes in reflection coefficient with angle. The model is assumed to consist of two layers - the sea layer characterised by acoustic velocity of  $1500 \text{ ms}^{-1}$  and bounded by a downgoing reflection coefficient  $r_1 = -0.7$ , and a second layer with velocity  $3000 \text{ ms}^{-1}$  and reflection coefficient  $r_2 = 0.2$ .

A twenty trace response generated in this way with horizontal offset increasing by increments of 100 m is then convolved with a source model, which for simplicity is identical to that for the previous example. The resulting section is shown in fig. 9.2.5. This data was corrupted by the addition of Gaussian white noise of variance 0.01623. The resulting SNR varies from trace to trace as the amplitude of the signal components is lower on far traces (see fig. 9.2.6). Application of the signal enhancement method, with a typical (though not necessarily optimal) set of parameters, produces the result shown in fig. 9.2.7. The results show a clear improvement in SNR over the unprocessed section, with no obvious distortion components present.

The effect of applying (adaptive) predictive deconvolution (on the lines suggested by Griffiths et al [37], to the enhanced data is shown in fig. 9.2.8.

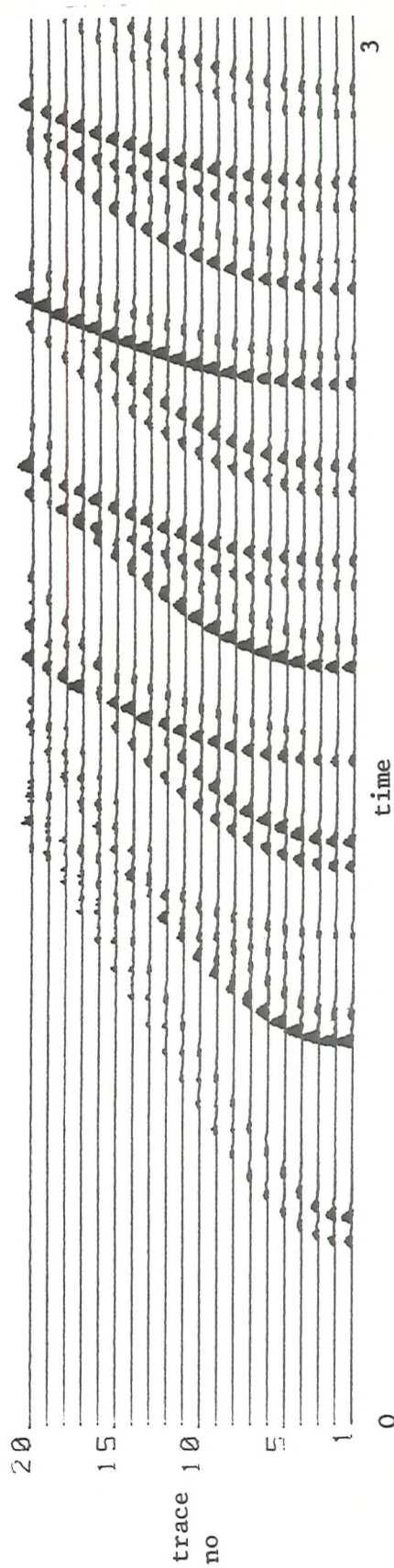


Figure 9.2.5: 20 Trace Synthetic CDP Section

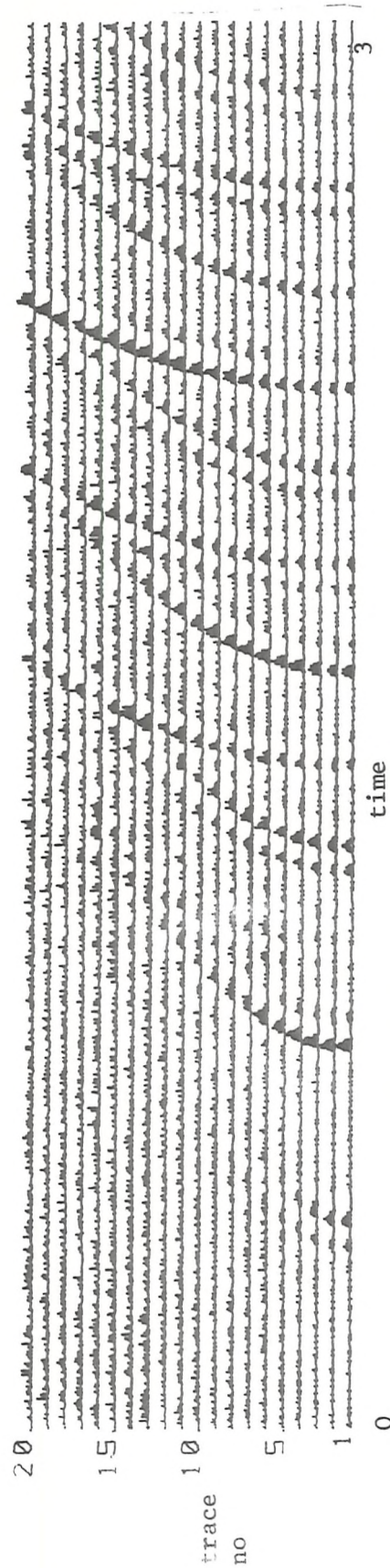


Figure 9.2.6: 20 Trace Synthetic Corrupted by Gaussian white noise



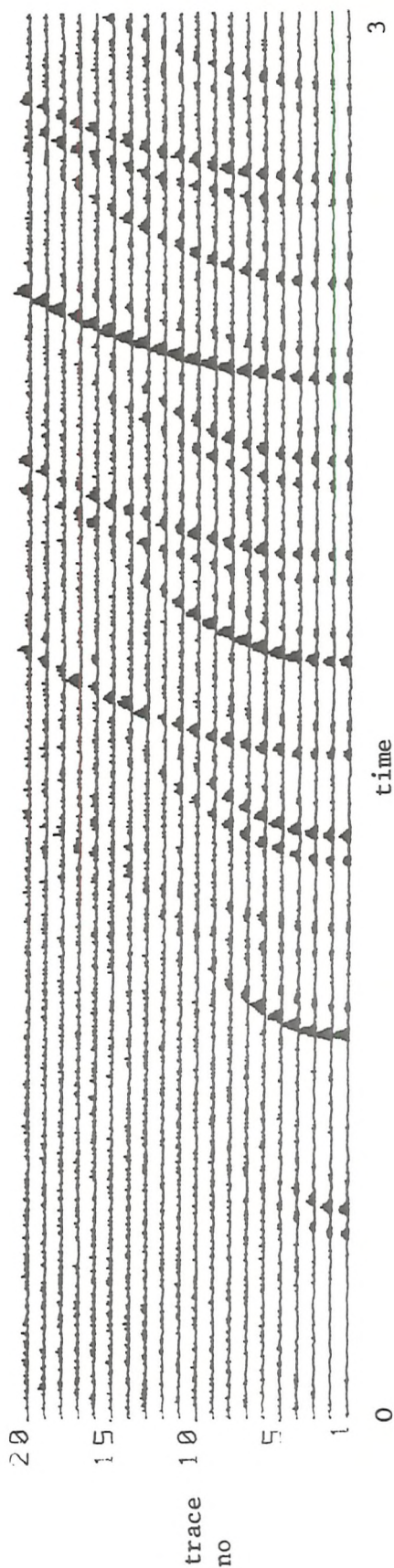


Figure 9.2.7: Predictive Stack Applied to Noisy Data

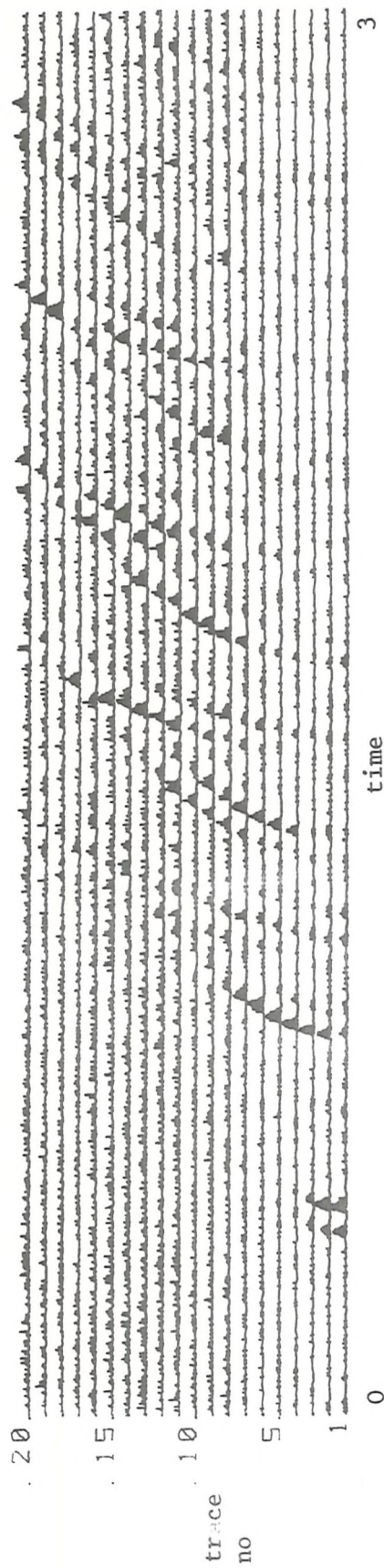


Figure 9.2.8: Adaptive Predictive Deconvolution Applied to Enhanced Data

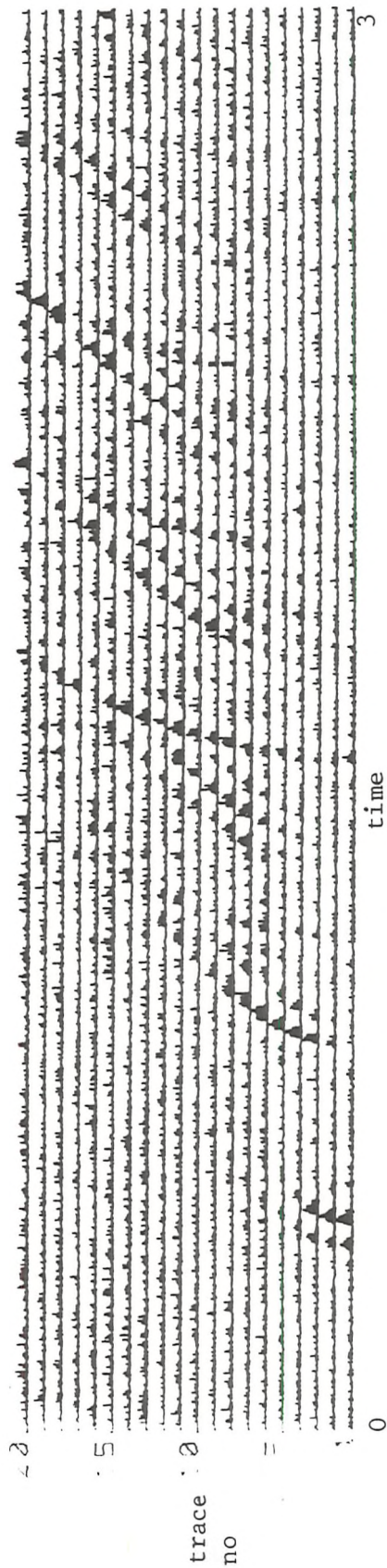


Figure 9.2.9: Adaptive Predictive Deconvolution Applied to the Unprocessed data



The results may not appear very impressive but comparison with the application of the same adaptive deconvolution to the unprocessed data, using similar parameters (fig. 9.2.9) shows that performing the predictive stack prior to deconvolution gives a markedly superior final SNR.

(ii) Field data

The predictive stack method was tested on a section of field seismic data provided by Seismograph Service Ltd. The data consists of a 48-fold CDP gather of offshore Norwegian data (to which a preliminary gain correction has been applied), see fig. 9.2.10(a). The data is characterised by relatively few primary events and a high level of sea-bed reverberation which recurs at approximately 700 ms intervals. Another feature of interest is the presence of coherent noise across the gather between approximately 3.5 and 3.0 seconds. A total of 5.0 seconds of data is displayed at a sample rate of 250.

Figures 9.2.10(b) and (c) show the effect of applying the predictive stack with the parameters chosen, typically, as  $n_0 = 800$  ms, filter length = 140 ms and adaptation constant = 0.01. Figure 9.2.10(b) shows the backward prediction alone and fig. 9.2.10(c) shows the effect of stacking the results. It is clear that the process has failed to achieve the desired objective. The reasons for this will be considered shortly; however, it is worth noting that the failure is only partial, from about 2.0 seconds onwards the method appears to work to some extent. In fig. 9.2.10(b) after 2.0 seconds only the coherent events appear to be predicted (though with low amplitude) and in fig. 9.2.10(c) the stacked output, this has led to some strengthening of coherent events in this region. The real failure of the method occurs from 0 to 2 seconds, and the reason for this is the failure of the adaptive filter to respond sufficiently quickly to changes in the data. This is caused partly by the relatively lengthy seismic wavelet (140 ms) requiring a long operator and thus producing a sluggish response. However, the main cause of the problems is the rapid and considerable changes in amplitude in the data. Such problems were also noted as potential pitfalls in a report, on adaptive deconvolution, by Hubbard [39] (see also Chapter 8). In fact a fairly sophisticated normalisation procedure for the algorithm has been adopted, involving a constrained running power computation, with the constraints indexed to both trace number and time. However, this has not proved sufficient to overcome the problems.



(a)

(b)

(c)

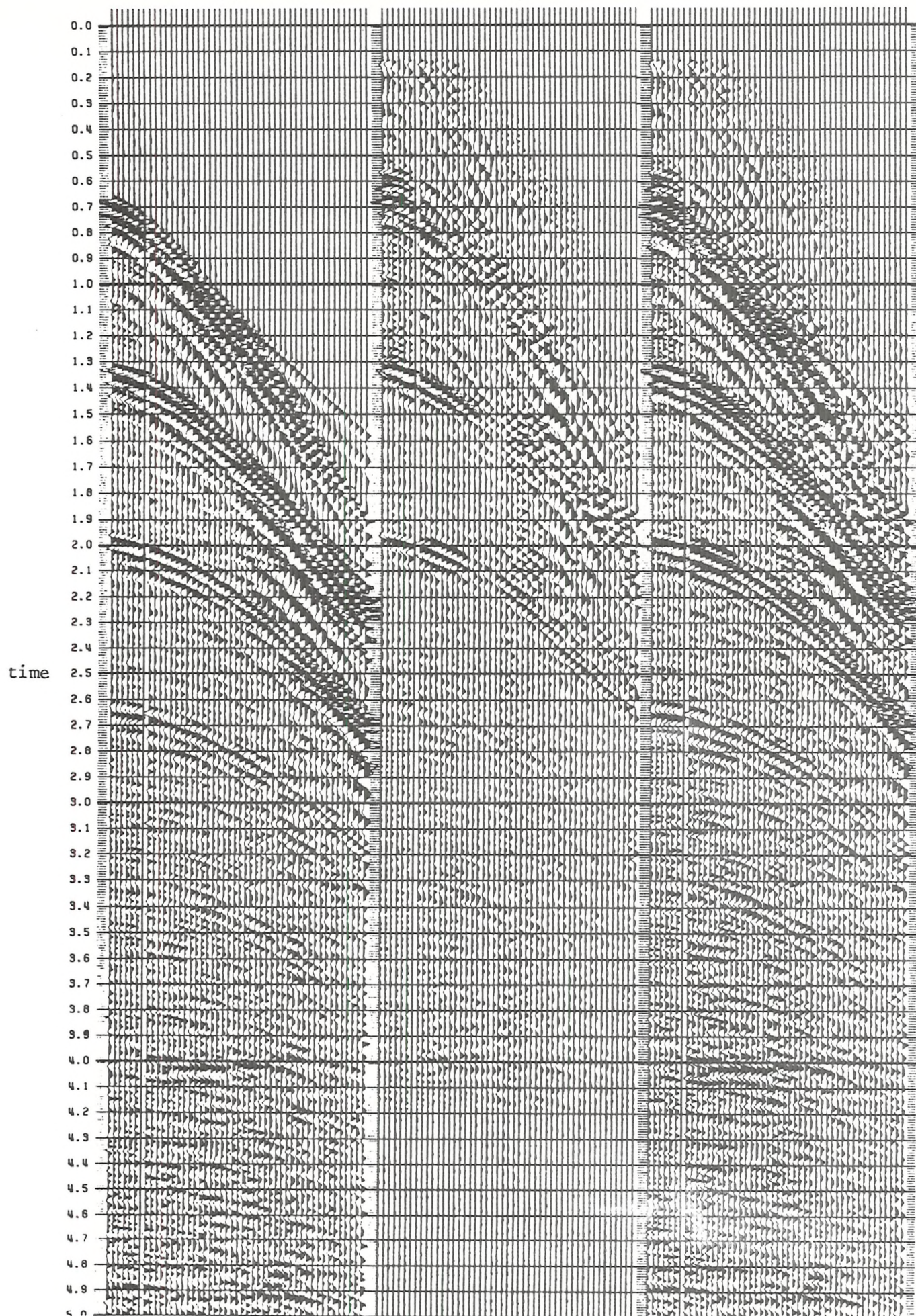


Figure 9.2.10: Application of Predictive Stack to Field Seismic



### 9.3 SNR Enhancement of Multi-Channel Seismic Data by Generalised Comb Filtering

#### 9.3.1 Background and previous work

In this section a second approach to SNR enhancement of seismic data is developed. This method is also based on the generalised comb filter (GCF) of Chapter 5. However, in contrast to the predictive stack method of the previous section the approach here is multi-channel. The idea is to replace the conventional CDP stacking procedure by a form of generalized comb filtering operation.

It is well known that the conventional CDP stack is suboptimal in the sense that it does not maximise the SNR of the stacked data. There are a number of reasons for this; the movement corrections are not normally exact (because of both inexact velocity estimates and the effects of digitisation). Also, corresponding wavelets on successive traces will not be exact replicas because (i) they have travelled unequal distances through the earth along different paths, and more significantly, (ii) they have been distorted by the effects of NMO correction. Finally, the SNR of the data varies from trace to trace, again due to signals from far offset traces having travelled further. Some efforts to improve on standard CDP stacking have been made, the most straightforward of which involves replacing the simple averaging of conventional CDP stacking with a weighted average, that is the moveout corrections are computed as usual, but the usual stack equation

$$\bar{x}(j) = \frac{1}{M} \sum_{i=1}^M x^{(i)}(j) \quad (9.3.1)$$

is replaced by

$$y(j) = \sum_{i=1}^M w(i)x^{(i)}(j) \quad (9.3.2)$$

where  $x^{(i)}$ ,  $i = 1, \dots, M$  are the corrected input traces.

The weights  $w(i)$  are chosen with the objective of maximising the output SNR as in Chapter 5, no signal shaping is attempted. The optimum weights are dependent on the corresponding SNR's (assuming these are known) and are obtained by minimising the output noise power whilst constraining the signal power to be constant. The straight stack is found to be



optimum when the SNR's are constant, but this will not normally be the case. White [110] concluded, however, that in practice, because of imprecise knowledge of the input trace SNR, optimum stacks are unlikely to perform as well as straight stacks.

A more sophisticated approach involves the use of a multi-channel Wiener filter; the earliest such approach was due to Schneider et al [83], but a more general form has been adopted by Galbraith and Wiggins [30]. In this approach the input data are filtered as in fig. 9.3.1, which shows a three

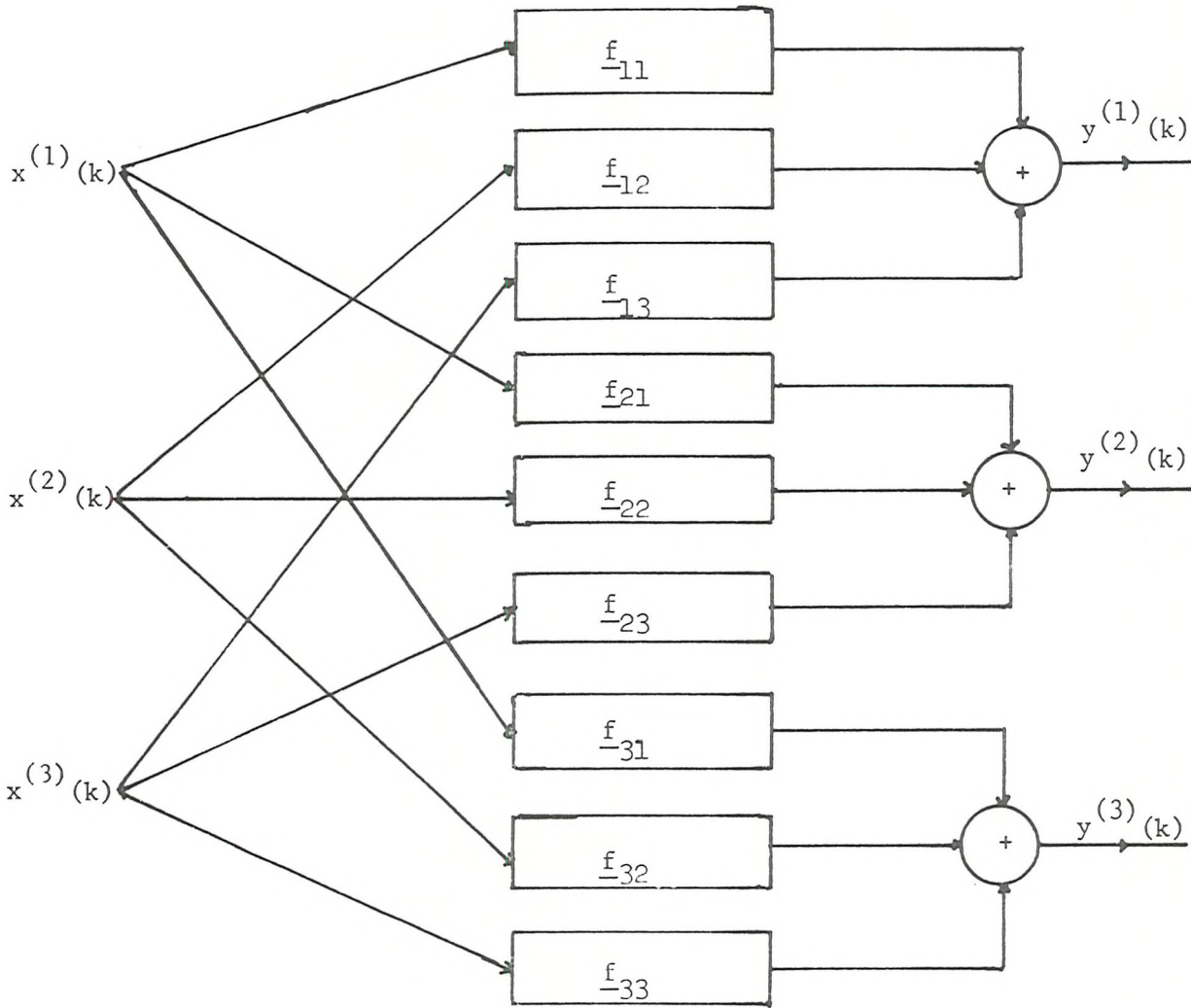


Figure 9.3.1: Multichannel Filter Structure (3 Channels)

channel set for simplicity. The filters  $f_{ij}$  are designed in such a manner as to minimise the difference between a set of desired outputs and the actual outputs. The derivation of the filters [30] follows similar

lines to that of the single-channel Wiener filter (see Chapter 2) and leads to a set of multi-channel normal equations:

$$\sum_i \sum_k f_{ij}(k) R_{ip}(\ell - k) = G_{qp}(\ell) \quad (9.3.3)$$

where  $f_{ij}$  is the filter between traces  $i$  and  $j$ , as in fig. 9.3.1 and  $R_{ip}$  is the autocorrelation between input traces and  $G_{qp}$  is the cross-correlation between input and desired output. In Galbraith and Wiggins' scheme the auto- and cross-correlations are computed not from seismic traces but from idealised models of signal and noise. The models are as follows. The  $i$ 'th input trace is

$$x^{(i)}(n) = s^{(i)}(n) + v^{(i)}(n) \quad (9.3.4)$$

where  $s^{(i)}$  is the signal input and  $v^{(i)}$  is noise (both correlated and uncorrelated) and where  $s$  and  $v$  are uncorrelated. The desired signal is

$$d^{(i)}(n) = s^{(i)}(n). \quad (9.3.5)$$

Any form of input can be incorporated but a model of signal and noise is required. The signal (and noise) regions for each channel are defined by relative moveout. The signal velocity is assumed uniformly distributed within a given interval but once specified on two channels is then defined for all channels. Some flexibility is given by allowing some tolerance or 'chatter' in the arrival times. The cross-correlation between traces becomes the expected value of the signal with itself, with a random delay. The delay is the sum of three independent uniform random variables, the moveout, and the 'chatter' on both traces.

Galbraith and Wiggins applied their filter to the problem of horizontal (CDP) stacking, by applying the method as in fig. 9.3.1, then stacking the resulting outputs. They used synthetic data and concluded that such multi-channel stacking filters offer considerable advantages over standard techniques.

A still more sophisticated approach has been provided by Sengbush and Foster [84]. These authors again used a multi-channel Wiener filter where the model of the data used was

$$x^{(i)}(n) = s(n) + u(n) + v_i(n) \quad (9.3.5.)$$

where  $s(n)$  is the signal shape,  $u(n)$  is coherent noise and  $v^{(i)}(n)$  is the incoherent noise on trace  $i$ .

The signal and coherent noise are assumed to have identical shapes from trace to trace. The moveouts of both the signal and coherent noise are specified by probability density functions which may be of any form. In contrast to the method of Galbraith and Wiggins [30] the power spectra of the signal and noise (needed to complete the autocorrelations) may be either modelled or estimated directly from the data. In a further refinement to the Galbraith and Wiggins approach, Ozdemir [68] divides the section into time gates to allow variation in the moveout window at different record times. This is to allow for the changes which occur in the moveouts associated with given velocities along the trace length, and which in the former approach meant that pass and reject windows would overlap. Cassano and Rocca [10] have developed a frequency domain implementation of the Galbraith and Wiggins method, which they report, is more stable than the corresponding time domain implementation.

In a different approach to the problem, known as the full gradient projection method [9], the stacking is performed using an adaptive filter. Beginning with the NMO corrected traces  $x^{(i)}(j)$ , the conventional stacked trace,  $\bar{x}(j)$ , given by equation (9.3.1) is subtracted from each input trace in turn. Now provided the signal components are identical on each channel the residual contains noise alone. This trace is then filtered and subtracted from the stacked trace to give the final output:

$$\hat{x}(j) = \bar{x}(j) - \sum_i \sum_k f^{(i)}(k) [\bar{x}(j-k) - x^{(i)}(j-k)] \quad (9.3.6)$$

where  $f_j^{(i)}$  is the  $j$ 'th update of the filter associated with the  $i$ 'th input.

The adaptive filter is updated according to

$$\underline{f}_j^{(i)} = \underline{f}_{j-1}^{(i)} + \alpha \hat{x}(j-1) (\bar{x}(j-1) - x^{(i)}(j-1)) \quad (9.3.7)$$

but additionally the filter coefficients are constrained to satisfy

$$\sum_i \underline{f}_j^{(i)}(k) = \delta_{jk} \quad (9.3.8)$$

This constraint requires events which arrive simultaneously to be passed without distortion.

The idea is that the filter will cancel the noise in the stacked trace and leave the signal component. In this respect the method is similar to adaptive noise cancelling with  $\bar{x}$  interpreted as primary and  $(\bar{x} - x^{(i)})$  as reference (see fig. 9.3.2); see also Chapter 6. Like ANC, the method

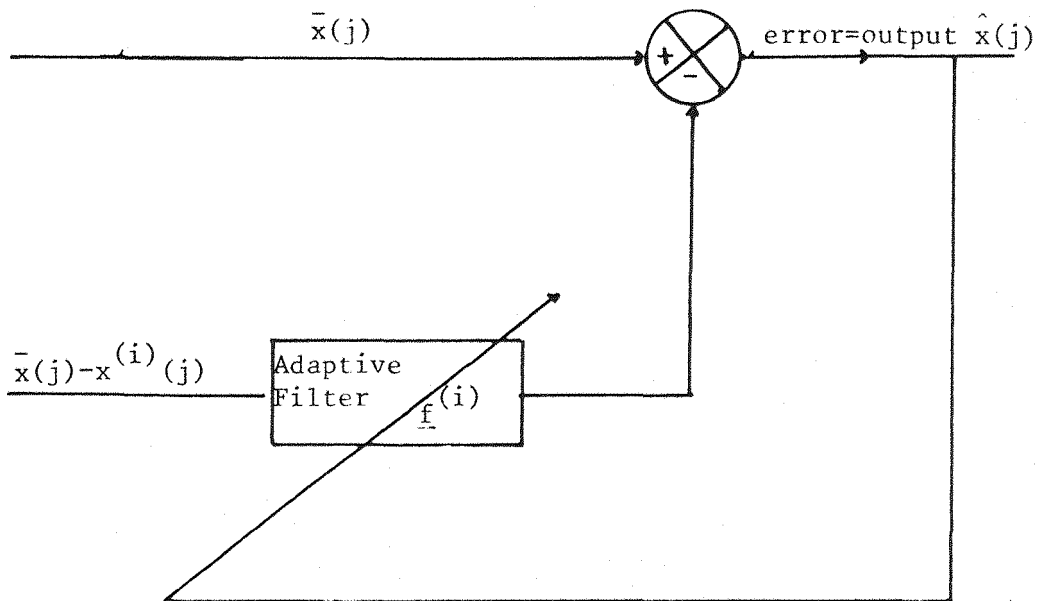


Figure 9.3.2: Full Gradient Projection Method Interpreted as Adaptive Noise Cancellation.

attempts to cancel the noise using the correlation between the interferences in the primary and reference traces. However, if the signal components are not identical on each channel, then the reference input will contain residual signal components and strong signal cancellation will occur. It

is hard to see how this cannot be a major disadvantage of the method since for NMO corrected traces the identical signals assumption will not generally be even approximately correct [23]. However, Laster [45] reports good results with this technique.

### 9.3.2 Generalised comb filtering approach

Although many of the approaches of the previous section have the potential to give improved performance over the conventional CDP stack there are still problems associated with each. In the case of the weighted stack, ignorance about input SNR's makes selection of the gains at best imprecise. The more sophisticated Wiener filtering approaches have potentially greater gains, but are restricted by the stationary nature of the solution and in some cases by the idealised models of signal and noise on which they are based. For instance, many of the methods rely on identical signal components on each channel, but this assumption cannot be justified on data which has had NMO corrections applied.

Some of these problems are overcome by the full gradient projection method of Burg et al [9]. However, this method also uses the identical signal model and may suffer from problems of signal cancellation, particularly if the moveout correction applied to the data prior to processing is inexact. This latter point can be a problem for any technique which uses NMO corrected data.

By contrast, the technique proposed here is based on the GCF described in Chapter 5. The process is designed to attenuate events which are either uncorrelated or which are correlated but fall outside a specified velocity window. The operation is similar to the multi-channel form described in Chapter 5, where the inputs are provided by M traces from a CDP gather (before NMO correction). The method is not designed to replace the usual CDP stack, but is supplementary to it. The operation can in fact be performed after stack but in these circumstances there are some dangers. The filter has a tendency to enhance horizontal coherence (in fact, it is designed to do that). On post stack data this may cause smearing over small discontinuities in the data. This is known as 'mixing' [11]. Henceforth for the purposes of this discussion it will be assumed that the method is applied to data before stacking.

An advantage of the technique is that the adaptive nature of the solution should cater for variations in the data structure. Unlike the adaptive scheme of Burg et al [9] the method does not involve dangers of signal cancellation. Also in contrast to that approach the method does not rely on data which is NMO corrected and is thus not dependent on the accuracy of such corrections. Also the signals are not required to be identical on all channels, but merely to satisfy the model of equation (5.4.4)

$$\begin{aligned} x^{(i)}(n) &= s(n) + v^{(i)}(n) \\ x^{(i+k)}(n) &= h^{(k)}(n) * s(n) + v^{(i+k)}(n) \end{aligned} \tag{5.4.4}$$

where  $h^{(k)}(n)$  is a slowly time-varying linear system and  $s(n)$  and  $v^{(i)}(n)$  are the signal and noise components respectively for the  $i$ 'th channel.

That is, where it is assumed that the signal on any channel can be related to the signal on other channels via a linear system. This is a far less restrictive assumption than the identical signals model.

As mentioned above, the filter effectively enhances events which are coherent and lie within a velocity window determined by the filter position and length. To illustrate the relation between these parameters and the velocity window, consider the action of a single 'tooth' in the GCF. Assume that the filter corresponding to this 'tooth' is aimed at enhancing a trace from a CDP gather with offset  $X + \Delta X$ , using a trace with offset  $X$ . Now, the normal movemout,  $\Delta T$ , say, between the two traces corresponding to an event with a normal incidence travel time  $T_0$ , with RMS velocity  $V$  (see fig. 9.3.3) is approximately determined by the relation

$$\Delta T = T_{X+\Delta X} - T_X \tag{9.3.9}$$

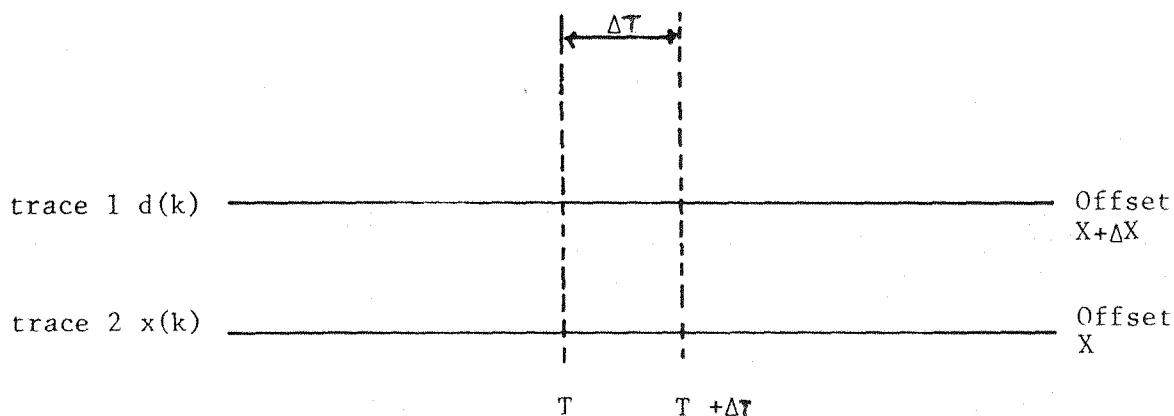


Figure 9.3.3: Moveout Relations on Traces at Offset  $x$  and  $X+\Delta X$

$$\text{where } T_X^2 \approx T_o^2 + \frac{X^2}{V_{\text{RMS}}^2} \quad (7.3.6)$$

(see Chapter 7)

$$T_{X+\Delta X}^2 \approx T_o^2 + \frac{(X + \Delta X)^2}{V_{\text{RMS}}^2} \quad (9.3.10)$$

Substituting (7.3.6) and (9.3.10) in (9.3.9) and rearranging gives

$$\Delta T = \left( T_X^2 + \frac{(2X + \Delta X)\Delta X}{V_{\text{RMS}}^2} \right)^{\frac{1}{2}} - T_X \quad (9.3.11)$$

Now the action of the filter is to enhance events on  $d$  at a point  $k$ , say, using data from  $x(k)$  to  $x(k - L + 1)$  where  $L$  is the filter length, this is because the filter is designed to minimise

$$\left( d(k) - \sum_{i=0}^{L-1} f(i)x(k-i) \right)^2.$$

It follows that in the case above the spike at  $T_{X+\Delta X}$  on trace 1 will only be enhanced using the spike at  $T_X$  on trace 2 if  $\Delta T < L \cdot \left( \frac{1}{f_s} \right)$ , where  $f_s$  is the sample rate. That is, if the gap is no greater than the length of the filter.



Hence from equation (9.3.11) the event will not be enhanced unless the RMS velocity is such that

$$L > f_s \left[ \left( T_X^2 + \frac{(2X + \Delta X)\Delta X}{v_{RMS}^2} \right)^{\frac{1}{2}} - T_X \right] \quad (9.3.12)$$

which shows the relation between RMS velocity and filter length. The window of accepted velocities (those for which events are enhanced) is obtained by rearrangement of (9.3.12) as those for which

$$v_{RMS}^2 > \frac{(2X + \Delta X)\Delta X}{\left(\frac{L}{f_s}\right)^2 + 2T_X\left(\frac{L}{f_s}\right)} \quad (9.3.13)$$

The filter length  $L$  can be computed from (9.3.12) in such a way as to enhance events which occur at physically reasonable velocities. There are a number of points which arise from this:

(i) The filter length corresponding to a fixed velocity  $V$  varies with time, so that the length of the filter must be varied at different points along the trace. However, the processing is usually performed backwards to ensure the learning curve occurs at the bottom of the data and the filter length corresponding to a particular velocity is shortest at the end of the trace. So the processing proceeds backwards starting with the shortest filter length, and points are simply added to the filter as this becomes necessary. Each new filter coefficient starts from  $f(i) = 0$ , so that to allow some period for initialisation each new coefficient is incorporated slightly before it is required by equation (9.3.12).

(ii) Equation (9.3.13) shows that the filter enhances events with arbitrarily high velocities. In practice, seismic velocities should have a finite limit. This limit is incorporated into the formulation by applying a shift to the data. The shift should be such that

$$d(k) \rightarrow d(k - n_s)$$

where  $n_s$  is determined as in (9.3.12) as

$$n_s = f_s \left[ \left( T_X^2 + \frac{(2X + \Delta X)\Delta X}{V_{\max}^2} \right)^{\frac{1}{2}} - T_X \right] \quad (9.3.14)$$

where  $V_{\max}$  is the maximum desired acceptance velocity. This change is itself time-varying and care should be taken to minimise the number of changes made to avoid creating discontinuities in the data.

However, it should be noted in assigning such a limit that dipping reflectors give rise to events with an increased apparent velocity (see Chapter 7).

(iii) There are limits to the resolution of this velocity filtering caused by the sampled nature of the data. This is particularly prevalent on traces corresponding to small offsets where a single sample may span a large range of velocities. In contrast, on traces with large offsets (or large gaps between traces) the filter lengths required may be considerable. In such circumstances it is essential that a finite limit is put on the maximum velocity as described above.

(iv) The velocity relations given here are for a filter enhancing a trace with positive moveout (from  $X$  to  $X + \Delta X$ ). The relations for enhancement with negative moveout are similar, the only distinction being that the data is shifted prior to the enhancement.

(v) It is clear that since no part of the acceptance region is given greater weight than another, the filter effectively assumes the signal velocities are uniformly distributed within this region (see previous section).

### 9.3.3 Simulations

#### (i) Synthetic data

The multi-channel stacking procedure was tested initially using synthetic data generated from the multi-channel synthetic described in Appendix XIV. The parameters of the data are identical to those described in section 9.2,

used to demonstrate the predictive stack method. This data is shown in fig. 9.2.5 in raw form and in fig. 9.2.6 corrupted by additive Gaussian white noise of variance 0.01623 (see section 9.2 for details). Application of the GCF technique with typical (though not optimal) parameters, and just 3 teeth, produces the result shown in fig. 9.3.4. The improvement in SNR is obvious by comparison with fig. 9.2.6 and no distortion is apparent. Application of the method with the same parameters but with 5 teeth produces the result shown in fig. 9.3.5. Again, the improvement is apparent and the results appear more successful than those of fig. 9.3.4. In order to quantify the gains obtained in relation to the parameters chosen a number of tests were performed using a single trace to measure the SNR improvements. The trace chosen was selected (arbitrarily) as trace no. 4 from the section of figure 9.2.6. The SNR improvements obtained are measured using the same measure ( $SNR_I$  of equation (9.2.2)) used in the evaluation of the predictive stack (though the results are not directly comparable because different sets of data were used). Indeed, whilst it may be tempting to compare the results obtained from the two SNR enhancement techniques proposed in this chapter, this temptation should be resisted as they are different techniques applicable to quite different classes of data.

The effect of varying the number of teeth is shown in table 9.3.1 which gives  $SNR_I$  versus numbers of teeth. It would appear from this that the signal-to-noise improvement is greatest when there are 5 teeth. This is in line with what might be expected - the gains to be obtained by increasing the number of averages are counterbalanced by the decrease in correlation between traces which are further apart. Table 9.3.2 shows the effect of varying the filter length whilst keeping the remaining parameters constant (5 teeth, adaptation constant = 0.1) and Table 9.3.3 shows the influence of varying adaptation constant with filter length fixed at 20 samples and 5 teeth in the comb. Both these tables indicate the useful property that the method gives SNR gains consistently for a broad range of parameters. The results in general would appear to suggest that the method is capable of producing between about 5 and 7.5 dB improvement in SNR (for this class of data at least). Though all of these figures tend to underestimate the improvement somewhat due to the difficulties in

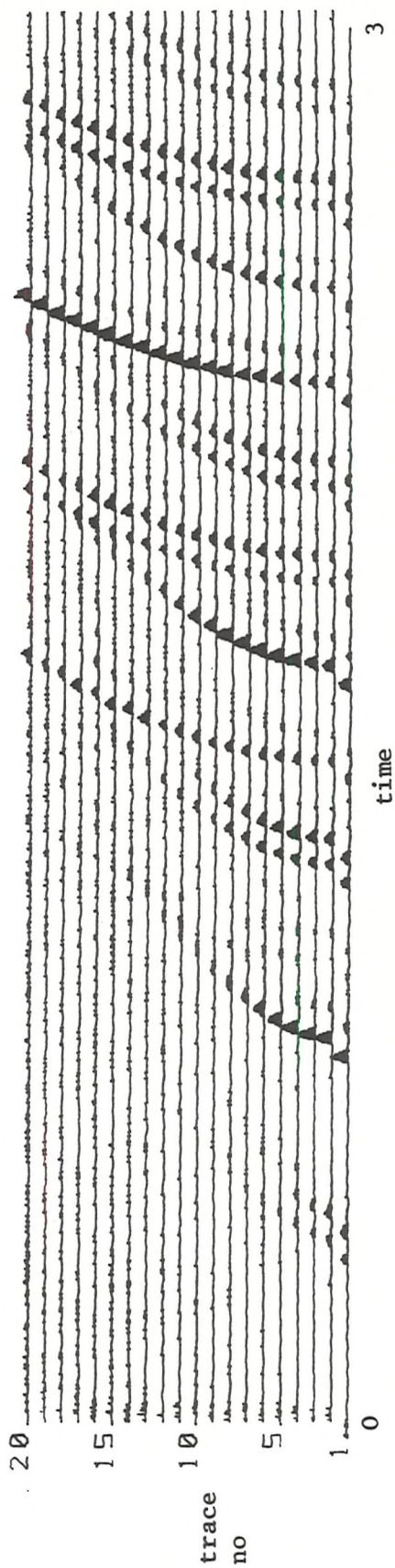


Figure 9.3.4: Application of Multi-channel Enhancement Technique to Noisy Synthetic (3 teeth)

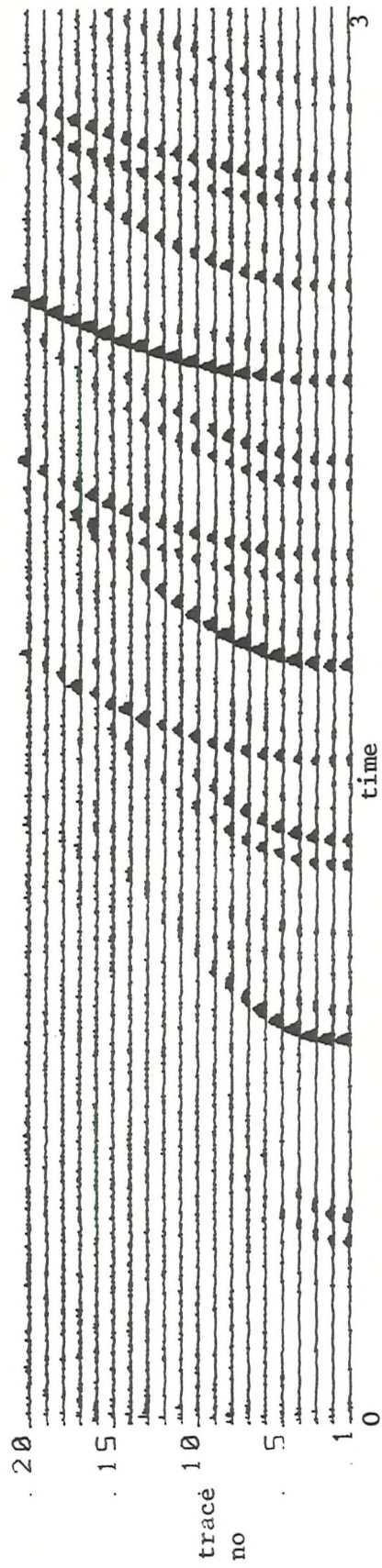


Figure 9.3.5: Application of Multi-channel Enhancement Technique to Noisy Synthetic (5 teeth)

Table 9.3.1 (adaptation constant = 0.1, filter length = 20)

Comb 'teeth'	SNR <sub>I</sub> (dB)
3	5.27
5	6.32
7	5.98

Table 9.3.2 (5 teeth, adaptation constant = 0.1)

Filter length (samples)	SNR <sub>I</sub> (dB)
10	7.46
20	6.32
30	5.28
40	4.95

Table 9.3.3 (5 teeth, filter length = 20)

Adaptation constant	SNR <sub>I</sub>
0.1	6.32
0.2	6.88
0.3	7.01
0.4	6.57

scaling the output for the computation of  $SNR_I$  in equation (9.2.2).

(ii) Field data

The multi-channel stacking procedure was applied to the same 48 trace CDP gather used for the predictive stack and discussed in section 9.2. Figure 9.3.6(a) shows the raw data after a preliminary gain correction has been applied. Figure 9.3.6(b) shows the effect of applying the multi-channel stacking procedure to this data. The algorithm is implemented in a normalised form, where the adaptation constant is scaled by the power computed from a moving window (see Chapter 2). As discussed in section 9.2, this scaling goes some way to countering the wide variability in the power level which is evident in the input data. It seems clear that some overall improvement has occurred. This improvement is particularly marked at greater arrival times, where the SNR is lower (and where SNR improvements are most necessary). The velocity window (for enhancement) was defined as  $V_{min} = 0$ ,  $V_{max} = 10,000 \text{ ms}^{-1}$ . Note that the coherent noise which occurs on the data between approximately 3.0 and 3.5 seconds has not been enhanced by the process, demonstrating the ability of the method to enhance only events within the specified velocity window. The parameters chosen (filter length 120 ms, adaptation constant = 0.1 (notionally)) are typical, though not necessarily optimal for the procedure. The robustness of the method is illustrated in fig. 9.3.6(c) which shows the same process applied with the adaptation constant modified to 0.5 and as is clear, the results are relatively unaffected by the change of parameters.

It would appear that the wide variations in input power do not affect the SNR enhancement technique as much as the predictive stack. This may well be partly because the algorithm is inherently stronger than the predictive stack, but also the method works laterally across the CDP gather, where changes in power are less sudden. Whereas the predictive stack works vertically along the trace (with a predictive gap).



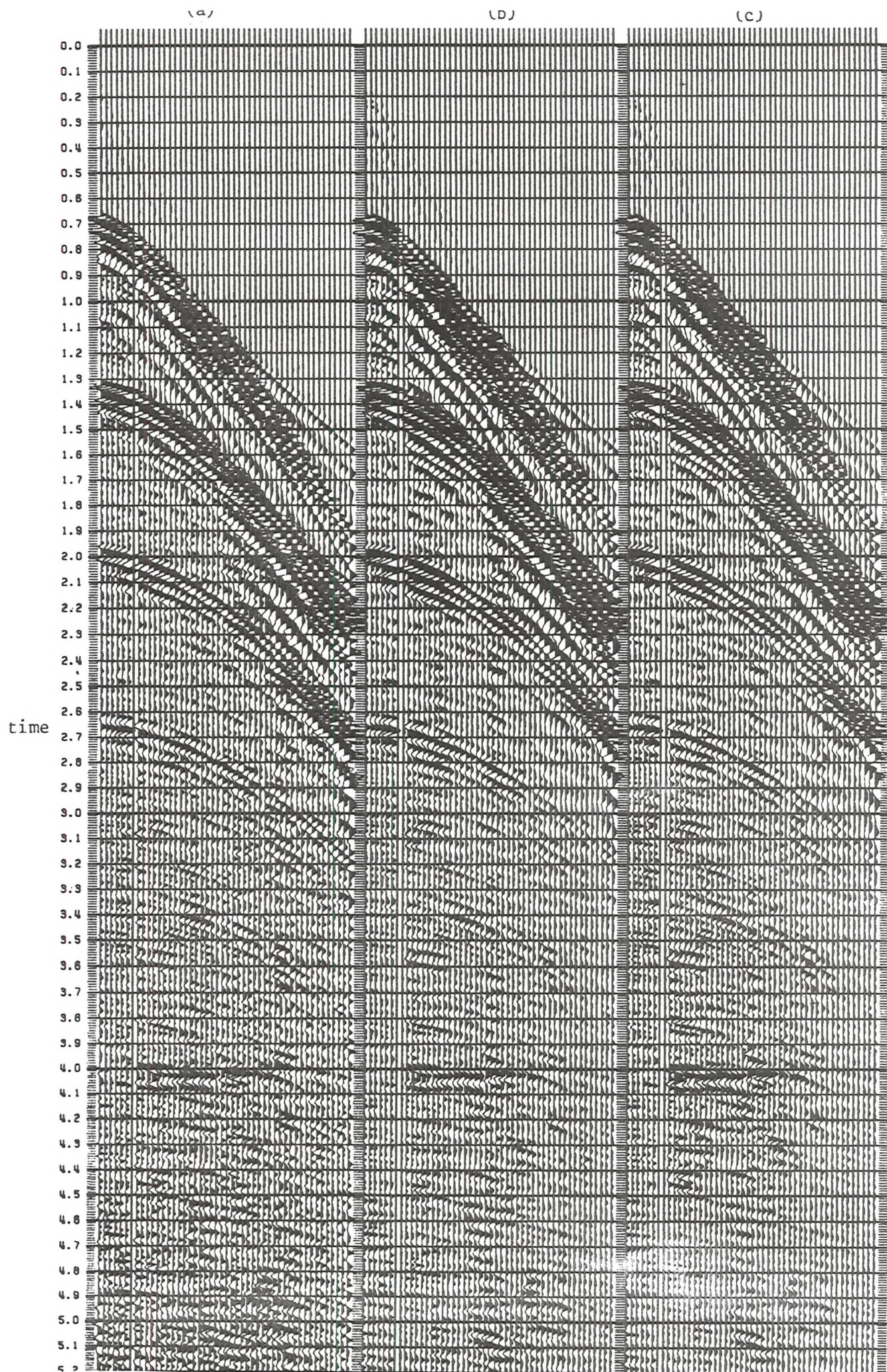


Figure 9.3.6: Application of Multi-Channel Enhancement Technique to Field Seismic Data



#### 9.4 Conclusions

In this chapter two novel techniques for SNR enhancement of seismic data have been proposed and tested. Both methods are applications of the generalised comb filter developed in Chapter 5 and it has been demonstrated here that two distinct classes of seismic data can be approximately modelled in the form required for the GCF. In the first case, referred to as the predictive stack, the method applies to highly reverberant data. It has been seen that this data can be modelled as a set of slowly time-varying waveforms recurring at intervals determined by the two-way travel time of the reverberant layer, embedded in noise and with an additive distortion component due to primary arrivals. A modified version of the GCF is applied, which is acausal, thus avoiding enhancing multiples purely at the expense of primaries. The technique has been demonstrated on both synthetic and field data. The synthetic results (on two classes of synthetic data) produced improvements in SNR for a wide range of input parameters. The gains were small ( $< 5$  dB) but were, nevertheless, clearly visible on the resulting section. Of course, the method enhances all coherent on the trace, primaries and multiples, but this serves to improve the performance of predictive deconvolution applied after the enhancement. For the field data the results were not successful, some improvements were noted in some areas of the data but the overall effect did not produce the desired SNR improvements. The main reason for this failure was identified as the rapid variations in power level which occur on the data and have the effect of destabilising the adaptive algorithm.

It seems likely that this is a problem which will recur in most field seismic data. Consequently this will result in the method having only limited value for field seismic data, unless some way can be found to make the algorithm more robust to changes in amplitude.

The second SNR enhancement algorithm is applicable to M-fold CDP data. In this case the signal component on any channel is assumed to be related to that on any other channel via a time-varying linear system. Uncorrelated noise is also assumed present. It has been seen that for such data the GCF is able to reject uncorrelated noise as well as noise which is correlated but falls outside a selected velocity window (as defined by the normal

moveout of the CDP traces). This technique has also been tested on both synthetic and field data. On the synthetic data the method produced SNR improvements from 5 to 7.5 dB for a wide range of parameters, but the improvements were again clearly visible. On field data, too, the method appears to produce some SNR improvements with the improvements apparently inversely proportional to the input SNR. The ability of the method to penalise coherent noise was also successfully demonstrated on field data.

## CHAPTER 10

### CONCLUSIONS AND RECOMMENDATIONS

This thesis has attempted to demonstrate the value of adaptive approaches to problems of deconvolution and signal enhancement. This has been achieved by extending the theoretical understanding of such algorithms, by creating novel configurations, and through a number of applications, particularly in reflection seismology.

Adaptive processes have been divided essentially into two classes - modelled and empirical. The thesis has demonstrated the power of both these approaches by concentrating mainly on one algorithm of each class. In the case of the modelled approach the technique chosen is the optimal control method of deconvolution, whilst the empirical approach has been developed via the LMS algorithm. Neither of these techniques is new, but in both cases the theory has been rationalised and extended, various configurations have been introduced and new applications have been explored.

Specifically, the theory of the LMS algorithm has been extended both for broadband (Chapter 2) and narrowband inputs (Chapter 6). For broadband inputs, a description of the response of the algorithm for non-stationary inputs has been obtained, whilst for narrowband inputs a generalised form was developed which gives a better description of the response for most inputs. The theory for the optimal control method has been extended to include the important problem of noise reduction in deconvolution (Chapter 4). Novel configurations were obtained for the LMS filter both as a generalised comb filter (Chapter 5) and as a sparse adaptive filter (Chapter 6). In both cases the theory of these formulations was examined and developed in terms of the theory discussed above. The optimal control method was redeveloped in discrete time. In addition to the main application to seismic data a number of other secondary applications were also included. The optimal control method was applied to the problem of deconvolution of velocity meter signals (Chapter 4). The results were very successful with near perfect deconvolution for the noise-free case and good results for noisy data. The LMS algorithm was applied to speech enhancement in two separate ways. Firstly the generalised comb filter

was applied to the enhancement of voiced speech corrupted by additive noise (Chapter 5) and improvements in SNR were obtained. Secondly the sparse adaptive filter was applied to the enhancement of speech signals corrupted by multiple interfering tones (Chapter 6), again with successful results. A further application to physical systems was provided by the comparative study of two deconvolution techniques in Chapter 3.

The main application of the thesis, however, is to seismic data. Here both LMS and optimal control techniques were again demonstrated. The optimal control method was applied to the deconvolution of seismic data (for both stationary and non-stationary cases). The results were again successful. The LMS algorithm was applied to the enhancement of seismic data, through the generalised comb filter, in two separate ways. Firstly, the method was employed in a single channel capacity to highly reverberant data. The results in this case were less successful with SNR improvements being achieved for synthetic data, but poor results being obtained for field data. In the second application the method was employed in a multi-channel capacity to enhance the data, improvements in SNR were again obtained. In general the application of these techniques to seismic data was somewhat less successful than for other applications and this is probably a reflection of the inherent complexity of, and difficulties involved in, modelling seismic data.

Overall, the work has demonstrated the strengths and limitations of both approaches. The modelled approach has the advantages of generality, including, in particular, the potential ability to deal with non-stationarity, and increased precision. Against that, however, there is the important disadvantage of the need to form a model. Also modelled approaches may be unattractive computationally both in terms of the computational load and, possibly, the need to perform computations in an acausal manner.

The empirical approach, by contrast, has the advantages of requiring minimal a priori information, and may be computationally attractive - with a potential for real-time solutions. Against this, however, these methods are less effective at dealing with non-stationarity due to their propensity to create spurious noise (misadjustment). The applications have demonstrated that whilst adaptive techniques are a powerful approach they cannot be applied indiscriminately. It is important to utilise any available information whilst ensuring that the method is consistent with the

data. It is clear that the work performed in this thesis has demonstrated the power of adaptive approaches to deconvolution and signal enhancement. It is possible from this to identify a number of specific areas where further development would be advantageous. As far as enhancement is concerned there are a number of possible further applications of the generalised comb filter. Two particular applications worthy of consideration are EEG signals, and signals encountered in machinery health monitoring. It would also be of interest (though not strictly relevant to the objective of SNR enhancement) to establish the subjective effects of generalised comb filter application to speech.

Other opportunities for further work have been created by the development of the sparse adaptive filter. In particular, much work remains to be done on the development of the two-point frequency response tracker (Appendix XIII). A further possibility is the use of a bank of sparse two-point filters as a short-time spectrum analyser - though this remains entirely speculative.

As far as deconvolution is concerned, as stated above, the main limitation with the optimal control approach is the need to form a state-space model. Whilst for some areas, notably aerospace and defence applications, the formulation of such models is well developed, in others it is not. In particular, in reflection seismology little effort has been applied to such problems and there is a clear need for work to be done on the formulation of state-space models of the reflection process before the advantages of the optimal control technique can be fully exploited.

## REFERENCES

1. J.B.Allen and D.A.Berkely, "Image method for efficiently simulating small-room acoustics", Journal Acoustic Society of America V65, pp 943-950, 1979.
2. T.M.Apostol, "Mathematical Analysis", Addison-Wesley, 1960
3. M.Athens and P.L.Falb, "Optimal Control", McGraw-Hill Book Co., 1966
4. J.W.Bayless and E.O.Brigham, "Application of the Kalman Filter to Continuous Signal Restoration", Geophysics, V35, pp2-23, 1970
5. A.J.Berkhout, "Minimum Phase in Sampled Signal Theory", Ph.D. Thesis, Koninklyke Shell Exploration and Production Laboratory, Rijswijk, Netherlands
6. N.J.Bershad, P.L.Feintuch, F.Reed and B.Fisher, "LMS Adaptive Line Enhancer Response to a Chirp in Noise", IEEE Transactions on Acoustics, speech and signal processing, V 28, 1980.
7. R.Bitmead and B.D.O.Anderson, "Performance of Adaptive Estimation Algorithms in Dependent Random Environments" IEEE Transactions on Automatic Control, V25,pp 788-793, 1980
8. S.M.Bozic, "Digital and Kalman Filtering", Arnold, 1979
9. J.P.Burg, A.Booker and R.Holyer, "Adaptive Filtering of Seismic Array Data", Advanced Array Research, Special Report No.1, Texas Instruments, 1967
10. E.Cassano and F.Rocca, "Multichannel Linear Filters for Optimal Rejection of Multiple Reflections", Geophysics V38, pp 1053-1061, 1973
11. E.Cassano and F.Rocca, "After-Stack Multichannel Filters Without Mixing Effects", Geophysical Prospecting "V22, pp 330-344, 1974
12. D.Childers and A.Durling, "Digital Filtering and Signal Processing", West Publishing Co., 1975
13. J.F.Claerbout, "Fundamentals of Geophysical Data Processing", McGraw-Hill, 1976
14. P.M.Clarkson and J.K.Hammond, "Deconvolution" in Applications of Time Series Analysis, ISVR Short Course Notes, 1981
15. P.M.Clarkson and J.K.Hammond, "Improvement of the Signal to Noise Ratio of Seismic Traces by Re-Alignment of Reverberant Energy", Proceedings of the 1981 IEEE International Conference on Acoustics, Speech and Signal Processing
16. N.D.Crump, "A Kolman Filter Approach to the Deconvolution of Seismic Signals", Geophysics V39 pp 1-13, 1974
17. T.P.Daniell, "Adaptive Estimation with Mutually Correlated Training Sequences", IEEE Transactions on Systems Science and Cybernetics, V6 pp12-19, 1970
18. L.Davisson, "Steady-State Error in Adaptive Mean-Square Minimisation", IEEE Transactions on Information Theory, V16, pp 382-385, 1970

19. M.Dentino, J.McCool and B.Widrow, "Adaptive Filtering in the Frequency Domain", Proceedings of the IEEE, V66, pp 1658-1659, 1978
20. N. De-Voogt. "Wavelet Shaping and Noise Reduction", Geophysical Prospecting, V22, pp 354-369, 1974
21. E.J.Douze, "Prediction Error Filters, White Noise and Orthogonal Components", Geophysical Prospecting, V19, pp 253-264, 1971
22. H.Drucker, "Speech Processing in a High Ambient Noise Environment", IEEE Transactions on Audio Electroacoustics V16, pp 165-168, 1968
23. J.W.Dunkin and F.K.Levin, "Effect of Normal Moveout on a Seismic Pulse", Geophysics V38, pp 635-642, 1973
24. J.Durbin, "Efficient Estimation of Parameters in Moving-Average Models", Biometrika, V46, Parts 1 and 2, 1959
25. P.L.Feintuch, "An Adaptive Percussive LMS Filter", Proceedings of the IEEE, pp 1622-1624, V64, 1976
26. E.Ferrara, "Fast Implementation of LMS Adaptive Filters", IEEE Transactions on Acoustics, Speech and Signal Processing V28, 1980
27. E.Fererara and B.Widrow, "Multichannel Adaptive Filtering for Signal Enhancement", IEEE Transactions on Acoustics, Speech and Signal Processing V29, pp 766-780 , 1981
28. W.T.Ford, "Optimum Mixed Delay Spiking Filters", Geophysics, V43, pp 125-132, 1978
29. R.H.Frazier et al, "Enhancement of Speech by Adaptive Filtering", Proceedings of the IEEE International Conference on Acoustics, Speech and Signal Processing, 1978
30. J.N.Galbraith and R.A.Wiggins, "Characteristics of Optimum Stacking Filters", Geophysics, V33, pp36-48, 1968
31. A.Gersho, "Adaptive Equalisation of Highly Dispersive Channels for Data Communication", Bell System Technical Journal, V48, pp55-70, 1969
32. R.D.Gitlin and F.,R.Magee, "Self-Orthogonalising Adaptive Equalisation Algorithms", IEEE Transactions on Communications, V25, pp666-672, 1977
33. J.R.Glover, "Adaptive Noise Cancelling Applied to Sinusoidal Interferences", IEEE Transactions on Acoustics, Speech and Signal Processing, V25, pp 484-491, 1977
34. J.R.Glover, "High Order Algorithms for Adaptive Filters", IEEE Transactions on Communications V27, pp 216-221, 1979
35. J.Goodwin, "Earth Filtering", Seismograph Service Ltd., Research Report
36. L.J.Griffiths, "Rapid Measurement of Digital Instantaneous Frequency", IEEE Transactions Acoustics, Speech, and Signal Processing, V23, pp207-221, 1975



37. L.J.Griffiths, F.R.Smolka and L.D.Trembley, "Adaptive Deconvolution: A New Technique for Processing Time-Varying Seismic Data", Geophysics, V42, pp 742-759, 1977
38. J.K.Hammond, P.M.Clarkson and J.J.Langford, "The Application of Optimal Control Techniques to the Deconvolution of Velocity Meter Signals", Mechanique, Materiaux Electricite pp 389-391, 1982
39. T.P.Hubbard "Adaptive Deconvolution", Seismograph Service Ltd. Research Report, R66
40. F.Itakura and S.Saito, "Digital Filtering Techniques for Speech Analysis and Synthesis", 7th International Congress on Acoustics, Budapest, 1971, Paper 25-C-1
41. A.Junger, "Signal-to-Noise Ratio and Record Quality", Geophysics, V29, pp922-925, 1964
42. A. Kalinin, S.A.Azimi, and V.V.Kalinin, "Estimate of Phase-Velocity Dispersion in Absorbing Media", IZVESTIA, Earth Physics, 1967, pp78-83
43. J.R.Kim and L.D.Davisson, "Adaptive Linear Estimation for Stationary M-Dependent Processes", IEEE Transactions on Information Theory, V21, pp23-31, 1975
44. M.G.Larimore, J.R.Treichler and C.R.Johnson, "Sharf: An Algorithm for Adapting IIR Digital Filter" IEEE Transactions on Acoustics, Speech and Signal Processing, V28, pp428-440, 1980
45. S.J.Laster, "Adaptive Processing of Seismic Data" in Applied Time Series Analysis, D.F.Findley (ED), Academic Press, 1978
46. F.Levin, "Apparent Velocity for Dipping Interface Reflections", Geophysics, V36, pp510-516
47. N. Levinson, "The Wiener RMS Error Criterion in Filter Design and Prediction", Journal of Mathematical Physics, V25, 1947
48. J.S.Lim and A.V.Oppenheim, "All-Pole Modelling of Degraded Speech", IEEE Transactions on Acoustics, Speech and Signal Processing V26, pp197-210, 1978
49. J.S.Lim, A.V.Oppenheim and L.D.Braida, "Evaluation of an Adaptive Comb Filtering Method for Enhancing Speech Degraded by White Noise Addition" IEEE Transactions on Acoustics, Speech and Signal Processing, V26, pp354-358, 1978
50. J.S.Lim, "Evaluation of a Correlation Subtraction method for Enhancing Speech Degraded by Additive White Noise", IEEE Transactions on Acoustics, Speech and Signal Processing, V26, pp471-472, 1978
51. J.S.Lim and A.V.Oppenheim, "Enhancement and Bandwidth Compression of Noisy Speech", Proceedings of the IEEE, V67, pp1586-1604, 1979
52. C.F.Lorenzo, "Variable Sweep Rate Testing: A Technique to Improve the Quality and Acquisition of Frequency Response and Vibration Data", 'NASA Technical Note TN D-7022, 1970'

53. J.Makhoul, "Linear Prediction: A Tutorial Review", Proceedings of the IEEE V63, pp561-581, 1975
54. J. Makhoul, "A Class of All-Zero Lattice Digital Filters: Properties and Applications", IEEE Transactions on Acoustics, Speech and Signal Processing, V26, pp304-314, 1978
55. D.W.March, "A Review of Signal Processing in Geophysics", MSc Thesis, Polytechnic of Central London, 1979
56. J.D.Markel and A.H.Gray, "Roundoff Noise Characteristics of a Class of Orthogonal Polynomial Structures", IEEE Transactions on Acoustics, Speech and Signal Processing, V23, pp473-486, 1975
57. J.D.Markel and A.H.Gray, "Linear Prediction of Speech", New York, Springer-Verlag, 1976
58. W.Mayne, "Common Reflection Point Horizontal Stacking Techniques", Geophysics, V27, pp927-938, 1962
59. F.McDonal et al, "Attenuation of Shear and Compressional Waves in Pierre Shale", Geophysics V23, pp421-439, 1959
60. J.M.Mendel and J.Kormylo, "New Fast Optimal White-Noise Estimates for Deconvolution", IEEE Transactions on Geoscience Electronics, VGE-15, pp32-41, 1977
61. J.M.Mendel and J.Kormylo, "Single-Channel White-Noise Estimators for Deconvolution", Geophysics, V43, pp102-124, 1978
62. J.M.Mendel, N.E.Nahi and M.Chan, "Synthetic Seismograms using the State Space Approach", Geophysics, V44 pp880-895, 1979
63. J. Moorjopoulos, P.M.Clarkson and J.K.Hammond, "A Comparative Study of Least-Squares and Homomorphic Techniques for the Inversion of Mixed Phase Signals", Proceedings of the 1982 IEEE International Conference on Acoustics, Speech and Signal Processing, 1982
64. R.F.O'Doherty and N.A.Anstey, "Reflections on Amplitudes", Geophysical Prospecting, V19, pp430-458, 1971
65. A.V.Oppenheim and R.W.Schafer, "Digital Signal Processing", Prentice Hall, 1975
66. A.V.Oppenheim, G.E.Kopec and J.M.Tribolet, "Signal Analysis by Homomorphic Prediction", IEEE Transactions on Acoustics, Speech and Signal Processing, V24, pp327-333, 1976
67. N.Ott and H.G.Meder, "The Kalman Filter as a Prediction Error Filter", Geophysical Prospecting, V20, pp549-560, 1972
68. H.Ozdemir, "Optimum Hyperbolic Moveout Filters with Applications to Seismic Data", Geophysical Prospecting, V29, pp702-714, 1981
69. A.Papoulis, "Signal Analysis", McGraw-Hill Book Co. 1977
70. K.L.Peacock and S.Treitel, "Predictive Deconvolution : Theory and Practise", Geophysics, V34, pp155-169, 1969

71. A.Pervozvanskii, "Random Processes in Non-Linear Control Systems", Academic Press, 1965
72. E.Plotkin, "Non-Linear Filter for Rejection of an Unknown Frequency Sine Wave Interference in an 'ASK' system", International Journal of Acoustics, V43, pp577-583, 1977
73. E.Plotkin, "Using Linear Prediction to Design a Function Elimination Filter to Reject Sinusoidal Interference", IEEE Transactions on Acoustics, Speech and Signal Processing, V27, 1979, pp501-505
74. E.Plotkin and D.Wulich, "A Comparative Study of Two Adaptive Algorithms for Suppression of a Narrow-Band Interface", Signal Processing, V4, pp35-44, 1982
75. A.Postic, J. Fourmann and J. Claerbout, "Parsimonious Deconvolution", Proceedings of the 50th Annual Meeting of the SEG, Houston, Texas, 1980
76. J.Proakis, "Channel Identification for High Speed Digital Communications, IEEE Transactions on Automatic Control, V19, 1974
77. L.R.Rabiner and B.Gold, "Theory and Application of Digital Signal Processing", Prentice-Hall, 1975
78. J.T.Rickard and J.R.Zeidler, "Second Order Output Statistics of the Adaptive Line Enhancer", IEEE Transactions on Acoustics, Speech and Signal Processing, V27, pp31-39, 1979
79. D.Ristow and B.Kosbahn, "Time-Varying Prediction Filtering by Means of Updating", Geophysical Prospecting, V27, pp40-61, 1979
80. E.A.Robinson, "Multichannel Z Transforms and Minimum Delay", Geophysics, V31, pp482-500, 1966
81. E.A.Robinson, "Statistical Communication and Detection with Special Reference to Radar and Seismic Signals", Griffin, 1967
82. M.R.Sambur, "Adaptive Noise Cancelling for Speech Signals", IEEE Transactions on Acoustics, Speech and Signal Processing, V26, pp419-423, 1978
83. W.Schneider, E.R.Prince, and B.F.Giles, "A New Data-Processing Technique for Multiple Attenuation Exploiting Differential Normal Moveout", Geophysics, V30, pp348-362, 1965
84. R.Sengbush and M.R.Foster, "Optimum Multichannel Velocity Filters", Geophysics V33, pp11-35, 1968
85. S.Senmoto and D.G.Childers, "Signal Resolution via Digital Inverse Filtering", IEEE Transactions on Aerospace and Electronic Systems, V8, pp633-640, 1972
86. K.D.Senne, "Adaptive Linear Discrete Time Estimation", PhD dissertation, Stanford University, 1968
87. M.J.Shensa, "Non-Wiener Solutions of the Adaptive Noise Canceller with a Noisy Reference", IEEE Transactions on Acoustics, Speech and Signal Processing, V28, pp468-473, 1980

88. U.C.Shields, "Separation of Added Speech Signals by Digital Comb Filtering", S.M. Thesis, M.I.T., 1970
89. M.T.Silva and E.A.Robinson, "Deconvolution of Geophysical Time Series in the Exploration for Oil and Natural Gas", Elsevier, 1979
90. S.M.Simpson, "Recursive Schemes for Normal Equations of Toeplitz Form".Scientific Report No.7, ARPA Project-Vela-Uniform, M.I.T., 1963
91. M.Sondhi, "An Adaptive Echo-Canceller", Bell. System Technical Journal, V46, pp497-511, 1967
92. H.W.Sorenson, "Parameter Estimation Principles and Problems", Dekker, 1980
93. M.Taner, E.Cook and N.Neidell, "Limitations of the Reflection Seismic Method: Lessons from Computer Simulations", Geophysics, V20, pp551-573, 1956
94. M.Taner and F.Koehler, "Velocity Spectra - Digital Computer Derivation and Applications of Velocity Functions", Geophysics V34, pp859-881, 1969
95. H.Taylor, S.Banks and J.McCoy, "Deconvolution with the  $L_1$  Norm", Geophysics, V44, pp39-52, 1979
96. G.Thomas, "Deconvolution and Linear Tracking Problems", Signal Processing, V2, 1980
97. G.Thomas, "Reconstitution de Signaux Deformes par un Systeme Lineaire", PhD Thesis, L'Universite Claude Bernard de Lyon, 1981
98. J.R.Treichler, "Transient and Convergent Behaviour of the Adaptive Line Enhancer", IEEE Transactions on Acoustics, Speech and Signal Processing, V27, pp53-62, 1979
99. J.R.Treichler, "Response of the Adaptive Line Enhancer to Chirped and Doppler-Shifted Sinusoids", IEEE Transactions on Acoustics, Speech and Signal Processing, V28, pp343-348, 1980
100. S.Treitel and E.A.Robinson, "The Design of High Resolution Digital Filters", IEEE Transactions on Geoscience Electronics, V4, 1966, pp25-38
101. S.Treitel and E.A.Robinson, "Optimum Digital Filters for Signal-to-Noise Ratio Enhancement", Geophysics, V34, pp248-291, 1969
102. S.Treitel and R.J.Wang, "The determination of Digital Wiener Filters from an Ill-Conditioned System of Normal Equations", Geophysical Prospecting, V24, pp317-327, 1976
103. A.W.Trorey, "Theoretical Seismograms with Frequency and Depth Dependent Absorbtion", Geophysics, V27, pp766-785, 1962
104. D.W.Tufts, "Adaptive Line Enhancement and Spectrum Analysis", Proceedings of the IEEE (letters) V65, pp169-170, 1977
105. T.J.Ulrych, "Application of Homomorphic Deconvolution to Seismology", Geophysics, V36, pp650-660, 1971

106. R.J.Wang, "The Determination of Optimum Gate Lengths for Two-Varying Wiener Filtering", Geophysics V36, pp683-695, 1969
107. R.J.Wang and S.Treitel, "The Determination of Digital Wiener Filters by Means of Gradient Methods", Geophysics, V38, pp310-326, 1973
108. R.J.Wang, "Adaptive Predictive Deconvolution of Seismic Data", Geophysical Prospecting V25, pp 342-381, 1977
109. K.H.Waters, "Reflection Seismology", Wiley, 1978
110. R.E.White, "The Performance of Optimum Stacking Filters in Suppressing Uncorrelated Noise", Geophysical Prospecting, V25, pp165-178, 1977
111. S.A.White, "An Adaptive Recursive Digital Filter", Proceedings of the 9th Asilomar Conference on Circuits, Systems and Computers, 1975
112. D.M.Wiberg, "State-Space and Linear Systems", McGraw-Hill Book Co., 1971
113. B.Widrow and M.E.Hoff, "Adaptive Switching Circuits" in 1960 Wescon Convention Record pt.4, pp 96-140
114. B.Widrow "Adaptive Filter I: Fundamentals", Stanford Electronics Labs., Stanford, California SEL-66-126, 1966
115. B.Widrow et al, "Adaptive Antenna Systems" Proceedings of the IEEE, V55, pp2143-2159, 1967
116. B.Widrow, "Adaptive Filters" in Aspects of Network and System Theory, R.Kalman and N.De Claris (Eds), New York: Holt, Rinehart and Winston, pp563-587, 1971
117. B.Widrow et al, "Adaptive Noise Cancellation : Principles and Applications", Proceedings of the IEEE,. pp1691-1717, 1975
118. B.Widrow and J.McCool, "A Comparison of Adaptive Algorithms based on the Methods of Steepest Descent and Random Search", IEEE Transactins on Antennas and Propagation, V24, pp615-637, 1976
119. B.Widrow et al, "Stationary and Non-Stationary Learning Characteristics of the LMS Adaptive Filter", Proceedings of the IEEE, V64, pp1151-1162, 1976
120. R.A.Wiggins and E.A.Robinson, "Recursive Solution to the Multichannel Filtering Problem", Journal of Geophysical Research, V70, pp1885-1891, 1965
121. L.C.Wood and S.Treitel, "Seismic Signal Processing", Proceedings of the IEEE, V63, pp649-661, 1975
122. P.Young, "A Recursive Approach to Time Series Analysis", Bulletin of the Institute of Mathematics and it's Applications", V10, pp209-223
123. J.R.Zeidler et al, "Adaptive Enhancement of Multiple Sinusoids in Uncorrelated Noise", IEEE Transactions on Acoustics, Speech and Signal Processing, V26, pp240-254, 1978

## APPENDIX I

As discussed in section 2.2, the solution for the causal, finite least-squares filter reduces to the solution of a set of linear algebraic equations of order  $L$ . Classical techniques for the solution of such a set require  $O(L^3/3)$  operations and  $O(L^2)$  storage (see, for example, [53]). However, it is possible to take advantage of the special structure of the coefficient matrix to reduce the computational burden. For the autocovariance method the symmetry of the matrix admits the use of the Choleski factorisation which reduces computation by a factor of 2 (for example, [53]).

For the autocorrelation method more substantial gains are possible using an algorithm devised by Levinson [47] which utilises the Toeplitz structure of the autocorrelation matrix to reduce the computation to approximately  $2L^2$  with a reduced storage requirement. A simplified description of the Levinson recursion will now be given since the results will be needed in Appendix VII. This description is similar to that given by Robinson [81].

The Levinson recursion is an algorithm for the solution of a set of linear algebraic equations of the form

$$R\underline{f} = \underline{g}$$

where  $R$  is a positive definite, symmetric, Toeplitz matrix, and  $\underline{f}$  and  $\underline{g}$  are vectors.

Levinson gave the algorithm for real, single-channel processes, but it can be adapted to complex or multi-channel time series [120].

The recursion begins with the trivial solution to the scalar system

$$r_o f_o^{(0)} = g_o \quad (I.1)$$

(Note that in this appendix, all elements of vectors are denoted with subscripts for brevity )

and proceeds by incrementing the order at each step, up to the full  $L \times L$  system. A single step from  $m$  to  $m + 1$  will be considered, where  $m = 2$  (this can easily be generalised).

Denote

$$\begin{bmatrix} r_0 & r_1 & r_2 \\ r_1 & r_0 & r_1 \\ r_2 & r_1 & r_0 \end{bmatrix} \quad \text{by } R_2$$

and

$$\begin{bmatrix} r_0 & r_1 & r_2 & r_3 \\ r_1 & r_0 & r_1 & r_2 \\ r_2 & r_1 & r_0 & r_1 \\ r_3 & r_2 & r_1 & r_0 \end{bmatrix} \quad \text{by } R_3$$

Assume from the previous step the filter coefficients  $f_0^{(2)}$ ,  $f_1^{(2)}$  and  $f_2^{(2)}$  have been computed, where

$$R_2 \begin{bmatrix} f_0^{(2)} & f_1^{(2)} & f_2^{(2)} \end{bmatrix}^T = \begin{bmatrix} g_0 & g_1 & g_2 \end{bmatrix}^T \quad (\text{I.2})$$

Assume, further, that the values  $a_0^{(2)}$ ,  $a_1^{(2)}$ ,  $a_2^{(2)}$  and  $\alpha_2$  have also been computed, where

$$R_2 \begin{bmatrix} a_0^{(2)} & a_1^{(2)} & a_2^{(2)} \end{bmatrix}^T = \begin{bmatrix} \alpha_2 & 0 & 0 \end{bmatrix}^T. \quad (\text{I.3})$$

The system (I.2) is extended as:

$$R_3 \begin{bmatrix} f_0^{(2)} & f_1^{(2)} & f_2^{(2)} & 0 \end{bmatrix}^T = \begin{bmatrix} g_0 & g_1 & g_2 & \gamma_2 \end{bmatrix}^T \quad (\text{I.4})$$

where  $\gamma_2$  is computed from:

$$\gamma_2 = r_3 f_0^{(2)} + r_2 f_1^{(2)} + r_1 f_2^{(2)}. \quad (\text{I.5})$$

The auxiliary system (I.3) is also extended as:

$$R_3 \begin{bmatrix} a_0^{(2)} & a_1^{(2)} & a_2^{(2)} & 0 \end{bmatrix}^T = \begin{bmatrix} \alpha_2 & 0 & 0 & \beta_2 \end{bmatrix}^T \quad (\text{I.6})$$

where

$$\beta_2 = r_3 a_0^{(2)} + r_2 a_1^{(2)} + r_1 a_2^{(2)}. \quad (\text{I.7})$$



The structure of the autocorrelation matrix is such that the system (I.6) may be reversed as:

$$R_3 \begin{bmatrix} 0, a_2^{(2)}, a_1^{(2)}, a_0^{(2)} \end{bmatrix}^T = \begin{bmatrix} \beta_2, 0, 0, \alpha_2 \end{bmatrix}^T. \quad (I.8)$$

Then multiplying (I.8) by a constant  $\kappa_2$  and subtracting from (I.6), where  $\kappa_2$  is determined so that the resulting system has only one non-zero element on the right-hand-side, that is

$$R_3 \begin{bmatrix} a_0^{(2)} \\ a_1^{(2)} \\ a_2^{(2)} \\ 0 \end{bmatrix} - \kappa_2 \begin{bmatrix} 0 \\ a_2^{(2)} \\ a_1^{(2)} \\ a_0^{(2)} \end{bmatrix} = \begin{bmatrix} \alpha_2 \\ 0 \\ 0 \\ \beta_2 \end{bmatrix} - \kappa_2 \begin{bmatrix} \beta_2 \\ 0 \\ 0 \\ \alpha_2 \end{bmatrix} \quad (I.9)$$

$$\text{where } \kappa_2 = \beta_2 / \alpha_2 \quad (I.10)$$

$$\text{gives } R_3 \begin{bmatrix} a_0^{(3)}, a_1^{(3)}, a_2^{(3)}, a_3^{(3)} \end{bmatrix}^T = \begin{bmatrix} \alpha_3, 0, 0, 0 \end{bmatrix}^T \quad (I.11)$$

$$\text{where } \alpha_3 = \alpha_2 - \kappa_2 \beta_2$$

$$\begin{aligned} a_0^{(3)} &= a_0^{(2)} \\ a_1^{(3)} &= a_1^{(2)} - \kappa_2 a_2^{(2)} \\ a_2^{(3)} &= a_2^{(2)} - \kappa_2 a_1^{(2)} \\ a_3^{(3)} &= -\kappa_2 a_0^{(2)} \end{aligned} \quad (I.12)$$

Now (I.11) may be reversed:

$$R_3 \begin{bmatrix} a_3^{(3)}, a_2^{(3)}, a_1^{(3)}, a_0^{(3)} \end{bmatrix}^T = \begin{bmatrix} 0, 0, 0, \alpha_3 \end{bmatrix}^T. \quad (I.13)$$

Subtracting some multiple  $q_2$ , say, of (I.13) from (I.4), where  $q_2$  is selected so that

$$\gamma_2 - q_2 \alpha_3 = \beta_3, \quad (I.14)$$

then

$$q_2 = \frac{\gamma_2 - g_3}{\alpha_3} \quad (I.15)$$

so that

$$R_3 \left\{ \begin{bmatrix} f_o^{(2)} \\ f_1^{(2)} \\ f_2^{(2)} \\ 0 \end{bmatrix} - q_2 \begin{bmatrix} a_3^{(3)} \\ a_2^{(3)} \\ a_1^{(3)} \\ a_o^{(3)} \end{bmatrix} \right\} = \left\{ \begin{bmatrix} g_o \\ g_1 \\ g_2 \\ \gamma_2 \end{bmatrix} - q_2 \begin{bmatrix} 0 \\ 0 \\ 0 \\ \alpha_3 \end{bmatrix} \right\} \quad (I.16)$$

and hence

$$R_3 [f_o^{(3)}, f_1^{(3)}, f_2^{(3)}, f_3^{(3)}]^T = [g_o, g_1, g_2, g_3]^T \quad (I.17)$$

where

$$\begin{aligned} f_o^{(3)} &= f_o^{(2)} - q_2 a_3^{(3)} \\ f_1^{(3)} &= f_1^{(2)} - q_2 a_2^{(3)} \\ f_2^{(3)} &= f_2^{(2)} - q_2 a_1^{(3)} \\ f_3^{(3)} &= -q_2 a_o^{(3)} \end{aligned} \quad (I.18)$$

Hence, all the variables required for the next step have been computed. It remains only to specify initial conditions for the algorithm.

Now

$$r_o f_o^{(0)} = g_o \quad (I.1)$$

Therefore  $f_o^{(0)} = g_o / r_o$

$$r_o a_o^{(0)} = \alpha_o$$

$a_o^{(0)}$  is selected arbitrarily (non-zero),  $a_o^{(0)} = 1$  is a common choice.

## APPENDIX II

In contrast to many iterative techniques convergence to the fixed least-squares solution (for stationary inputs) can be established for the method of steepest descent. A number of proofs exist, e.g., [92, 114]; a novel version is presented below.

Recall from section 2.2 that the error energy associated with a least-squares criterion for any filter  $\underline{f}$  is

$$I(\underline{f}) = R_{dd}(0) + \underline{f}^t R \underline{f} - 2 \underline{f}^t \underline{g} \quad (2.2.8)$$

Now the steepest descent update equation is

$$\underline{f}_{j+1} = \underline{f}_j + \alpha(\underline{g} - R \underline{f}_j) \quad (2.4.4)$$

The error energy associated with  $\underline{f}_j$  is

$$I(\underline{f}_j) = R_{dd}(0) + \underline{f}_j^t R \underline{f}_j - 2 \underline{f}_j^t \underline{g} \quad (II.1)$$

and with  $\underline{f}_{j+1}$

$$I(\underline{f}_{j+1}) = R_{dd}(0) + \underline{f}_{j+1}^t R \underline{f}_{j+1} - 2 \underline{f}_{j+1}^t \underline{g} \quad (II.2)$$

Subtracting (II.2) from (II.1)

$$I(\underline{f}_j) - I(\underline{f}_{j+1}) = 2(\underline{f}_{j+1} - \underline{f}_j)^t \underline{g} + \underline{f}_j^t R \underline{f}_j - \underline{f}_{j+1}^t R \underline{f}_{j+1}$$

Using (2.4.4)

$$\begin{aligned} I(\underline{f}_j) - I(\underline{f}_{j+1}) &= 2\alpha(\underline{g} - R \underline{f}_j)^t \underline{g} + \underline{f}_j^t R \underline{f}_j - \underline{f}_j^t R \underline{f}_j \\ &\quad - 2\alpha(\underline{g} - R \underline{f}_j)^t R \underline{f}_j - \alpha^2(\underline{g} - R \underline{f}_j)^t R (\underline{g} - R \underline{f}_j) \end{aligned}$$

$$I(\underline{f}_j) - I(\underline{f}_{j+1}) = \alpha(\underline{g} - R \underline{f}_j)^t [2I - \alpha R] (\underline{g} - R \underline{f}_j) \quad (II.3)$$

Now (II.3) is a quadratic form so that

$$I(\underline{f}_j) - I(\underline{f}_{j+1}) > 0 \quad \text{iff} \quad \alpha > 0$$

and provided  $[2I - \alpha R]$  is positive definite.

Now  $R$  is a correlation matrix and may be assumed positive definite and symmetric. Consequently its eigenvalues are real and positive. Now if  $\lambda_1, \dots, \lambda_L$  are the eigenvalues of  $R$  then  $(2 - \alpha\lambda_1), \dots, (2 - \alpha\lambda_L)$  are the eigenvalues of  $(2I - \alpha R)$ . The matrix  $[2I - \alpha R]$  is positive definite if

$$2 - \alpha\lambda_i > 0 \quad \forall \quad i$$

$$\text{that is if } 0 < \alpha < \frac{2}{\lambda_{\max}}. \quad (\text{II.4})$$

Hence, if this condition holds,

$$I(\underline{f}_j) > I(\underline{f}_{j+1}). \quad (\text{II.5})$$

It has been demonstrated that successive iterations of steepest descent reduce the error energy and this is sufficient for

$$\lim_{j \rightarrow \infty} I(\underline{f}_j) \rightarrow I(\underline{f}^*)$$

so that since  $I(\underline{f}^*)$  is unique

$$\lim_{j \rightarrow \infty} \underline{f}_j \rightarrow \underline{f}^* \quad (\text{II.6})$$

### APPENDIX III

Widrow [114] has demonstrated that, for the LMS algorithm defined by  $\underline{f}_{j+1} = \underline{f}_j + \alpha e(j) \underline{x}_j$  if  $\underline{x}_j, \underline{x}_{j+i}$  are uncorrelated  $\forall i \neq 0$ , where  $x(j)$  is a stationary process, then

$$\lim_{j \rightarrow \infty} E\{\underline{f}_j\} \rightarrow \underline{f}^*.$$

#### Proof

The following is a simple proof beginning from equation (2.5.16) which is very similar to that of Widrow [116]

$$\underline{v}_{j+1} = (I - \alpha R) \underline{v}_j + \alpha \underline{N}_j \quad (2.5.16)$$

so that

$$E\{\underline{v}_{j+1}\} = (I - \alpha R)E\{\underline{v}_j\} + \alpha E\{\underline{N}_j\} \quad (III.1)$$

where from equation (2.5.19)

$$E\{\underline{N}_j\} = RE\{\underline{f}_j\} - E\{\underline{x}_j \underline{x}_j^t E(\underline{f}_j / \underline{x}_j \underline{x}_j^t)\} \quad (2.5.19)$$

Now  $\underline{f}_j$  is dependent solely on  $\underline{x}_{j-1}, \underline{x}_{j-2}, \dots, \underline{x}_0, d_{j-1}, \dots, d_0$  and by assumption  $\underline{x}_j \underline{x}_{j+i}$  are uncorrelated. So that

$$E\{\underline{f}_j / \underline{x}_j \underline{x}_j^t\} = E\{\underline{f}_j\}$$

and hence  $E\{\underline{x}_j \underline{x}_j^t E(\underline{f}_j / \underline{x}_j \underline{x}_j^t)\} = RE\{\underline{f}_j\}$

Therefore  $E\{\underline{N}_j\} = 0.$

Hence from (III.1)

$$E\{\underline{v}_{j+1}\} = (I - \alpha R)E\{\underline{v}_j\} \quad (III.2)$$

Now  $R$  may be factorised as

$$R = Q\Lambda Q^t \quad (III.3)$$

where  $Q$  is the orthonormal matrix of eigenvectors and  $\Lambda$  is the spectral matrix (diagonal matrix of eigenvalues).

$$\text{Defining } \underline{v}_j' = Q^t \underline{v}_j \quad (\text{III.4})$$

then from (III.2)

$$E\{\underline{v}_{j+1}'\} = (I - \alpha\Lambda)E\{\underline{v}_j'\} \quad (\text{III.5})$$

or

$$E\{\underline{v}_j'\} = (I - \alpha\Lambda)^j E\{\underline{v}_0'\}. \quad (\text{III.6})$$

Now (III.6) is a set of decoupled equations so that

$$E\{v_j'(i)\} = (1 - \alpha\lambda_i)^j E\{v_0'(i)\} \quad (\text{III.7})$$

where  $\lambda_i$  is the  $i$ 'th eigenvalue of  $R$ . Hence

$$\lim_{j \rightarrow \infty} E\{v_j'(i)\} \rightarrow 0 \text{ if } |1 - \alpha\lambda_i| < 1$$

or

$$0 < \alpha < \frac{2}{\lambda_i}.$$

Hence convergence is attained  $\forall i$  if

$$0 < \alpha < \frac{2}{\lambda_{\max}}. \quad (\text{III.8})$$

## APPENDIX IV

### Lemma

If  $(1 - a_n) \leq 1, \forall n$  except at most at a finite number of places, and  $|(1 - a_n)| < L < \infty \forall n$  with  $a_n \geq 0$  and  $\sum_{n=0}^{\infty} a_n \rightarrow \infty$ , then

$$\prod_{n=0}^{\infty} (1 - a_n) \rightarrow 0.$$

### Proof

The above Lemma is a slight generalisation of a result due to Wang [108] and the proof follows similar lines. Beginning with the following theorem - stated without proof [2].

### Theorem

If  $a_n \geq 0 \forall n$ ,  $\prod_{n=0}^{\infty} (1 - a_n)$  converges iff  $\sum_{n=0}^{\infty} a_n$  converges.

Conversely, if  $a_n \geq 0 \forall n$  then  $\prod_{n=0}^{\infty} (1 - a_n)$  diverges to 0 or  $\infty$  iff  $\sum_{n=0}^{\infty} a_n \rightarrow \infty$ .

Now if  $(1 - a_n) \leq 1 \forall n$  except at a finite number of places and is bounded  $\forall n$  then

$$\left| \prod_{n=0}^{\infty} (1 - a_n) \right| \leq m < \infty$$

and hence

$$\prod_{n=0}^{\infty} (1 - a_n) \rightarrow 0 \text{ if } \sum_{n=0}^{\infty} a_n \rightarrow \infty$$

which completes the proof.



## APPENDIX V

In this Appendix an expression is obtained for the zero delay infinite causal least-squares inverse filter. This result is well known and is included only as background for the result in the following Appendix. The proof given follows that of Papoulis [69].

The starting point is the normal equations (2.2.3 )

$$\sum_{k=0}^{\infty} R(m-k)f(k) = g(m) \quad m \geq 0 \quad (2.2.3b)$$

$$\begin{aligned} \text{with} \quad g(m) &= h(0) \quad m = 0 \\ &= 0 \quad m > 0. \end{aligned} \quad (V.1)$$

$$\text{Now let} \quad y(m) = g(m) - \sum_{k=0}^{\infty} R(m-k)f(k). \quad (V.2)$$

Then from (2.2.3(b)) it is sufficient to find two sequences  $y$  and  $f$ , such that

$$\begin{aligned} y(m) &= 0, \quad m \geq 0 \\ f(k) &= 0 \quad k < 0 \end{aligned} \quad (V.3)$$

$z$ -transforming (V.2) gives

$$Y(z) = G(z) - R(z)F(z) \quad (V.4)$$

where the condition (V.3) becomes:

$$\begin{aligned} Y(z) &\text{analytic for } |z| < 1 \\ F(z) &\text{analytic for } |z| > 1 \quad (\text{e.g., [65]}) \end{aligned} \quad (V.5)$$

For convenience, let  $H(z)$  have the rational form (3.2.3), then

$$R(z) = H(z)H(1/z) \quad (3.3.5)$$

$$= \frac{\prod_{i=1}^k (1 - a_i z^{-1}) \prod_{i=k+1}^N (1 - a_i z^{-1}) \prod_{i=1}^k (1 - a_i z) \prod_{i=k+1}^N (1 - a_i z)}{\prod_{j=1}^M (1 - b_j z^{-1}) \prod_{j=1}^M (1 - b_j z)} \quad (V.6)$$

where the  $a_i$ 's and  $b_i$ 's are as previously defined. This equation may be rewritten as

$$R(z) = H_{eq_{min}}(z) H_{eq_{min}}(1/z), \quad (V.7)$$

where

$$H_{eq_{min}}(z) = \frac{\prod_{i=1}^k (1 - a_i z^{-1}) \prod_{i=k+1}^N (1 - a_i z)}{\prod_{j=1}^M (1 - b_j z^{-1})} \quad (V.8)$$

$H_{eq_{min}}(z)$  has all its poles and zeros within the unit circle and it is known as the equivalent minimum phase version of  $H(z)$ .

It follows that  $H_{eq_{min}}(z)$  and its inverse are analytic for  $|z| > 1$ , and conversely,  $H_{eq_{min}}(z^{-1})$  and its inverse are analytic for  $|z| < 1$ .

Now combining (V.4) and (V.7) gives

$$Y(z) = G(z) - H_{eq_{min}}(z) H_{eq_{min}}\left(\frac{1}{z}\right) F(z) \quad (V.9)$$

Now, form

$$\frac{G(z)}{H_{eq_{min}}\left(\frac{1}{z}\right)} = B^+(z) + B^-(z) \quad (V.10)$$

where  $B^+(z)$  is analytic for  $|z| > 1$  and  $B^-(z)$  is analytic for  $|z| < 1$ .  $z$ -transforming (V.1) gives

$$G(z) = h(0) \quad (V.11)$$

and hence

$$\frac{G(z)}{H_{eq_{min}}\left(\frac{1}{z}\right)} = C + B^-(z) \quad (V.12)$$

then the desired filter is given by

$$F(z) = B^+(z)/H_{eq_{min}}(z) \quad (V.13)$$

Hence

$$F(z) = \frac{C}{H_{eq_{min}}(z)} \quad (V.14)$$

That this solution does indeed satisfy the conditions (V.3) can easily be verified by substituting (V.13) and (V.12) into (V.9).

## APPENDIX VI

In this Appendix an expression is obtained for the infinite causal least-squares inverse filter with delay, in terms of the input system  $H$ . From this expression, two further results which have previously been obtained by Ford [28] using a somewhat different approach are rederived.

The approach used is similar to that of the previous appendix. Starting from the normal equations (2.2.3a) with

$$\begin{aligned} g(m) &= h(k - m) & m \geq 0 \\ &= 0 & m < 0 \end{aligned} \quad (\text{VI.1})$$

and letting

$$y(m) = g(m) - \sum_{\ell=0}^{\infty} R(m - \ell) f_k(\ell) \quad (\text{VI.2})$$

$z$ -transforming gives

$$Y(z) = G(z) - R(z)F_k(z) \quad (\text{VI.3})$$

As before, it is sufficient to find two sequences,  $y$  and  $f_k$ , such that

$$\begin{aligned} Y(z) &\text{ is analytic for } |z| < 1 \\ F_k(z) &\text{ is analytic for } |z| > 1 \end{aligned} \quad (\text{VI.4})$$

For convenience  $H(z)$  is again restricted to the rational form (3.2.3). Then factorising  $R(z)$  into

$$R(z) = H_{\text{eq}_{\min}}(z) H_{\text{eq}_{\min}}(z^{-1}) \quad (\text{VI.5})$$

where  $H_{\text{eq}_{\min}}$  is given by (3.3.8).

Hence

$$Y(z) = G(z) - H_{\text{eq}_{\min}}(z) H_{\text{eq}_{\min}}(z^{-1}) F_k(z) \quad (\text{VI.6})$$

forming

$$\frac{G(z)}{H_{\text{eq}_{\min}}(z^{-1})} = B^+(z) + B^-(z) \quad (\text{VI.7})$$

such that  $B^+(z)$  is analytic for  $|z| > 1$  and  $B^-(z)$  is analytic for  $|z| < 1$ .

The desired filter is given by:

$$F_k(z) = \frac{B^+(z)}{H_{eq_{min}}(z)} \quad (VI.8)$$

and it follows that this solution satisfies the required conditions since

(a)  $F_k(z)$  is analytic for  $|z| > 1$

(b) Substitution of (VI.8) and (VI.7) into (VI.6) yields:

$$Y(z) = H_{eq_{min}}(z^{-1})B^-(z) \quad (VI.9)$$

which is clearly analytic for  $|z| < 1$ .

In order to obtain further insight into  $F_k(z)$  it is necessary to examine the structure of  $B^+(z)$ . Now

$$G(z) = \sum_{m=0}^{\infty} h(k-m)z^{-m} \quad \text{from (VI.1))}$$

Therefore,

$$G(z) = (h(k) + h(k-1)z^{-1} + \dots + h(0)z^{-k})$$

Now  $H_{eq_{min}}(z^{-1})$  has a purely acausal inverse which may be written as:

$$\frac{1}{H_{eq_{min}}(z^{-1})} = (\alpha_0 + \alpha_1 z + \dots) \quad (VI.10)$$

Hence

$$\frac{G(z)}{H_{eq_{min}}(z^{-1})} = (h(k) + h(k-1)z^{-1} + \dots + h(0)z^{-k}) \cdot (\alpha_0 + \alpha_1 z + \dots) \quad (VI.11)$$

Consider now

$$G^+(z) = \sum_{m=-\infty}^{\infty} h(k-m)z^{-m} = z^{-k} H(z^{-1}) \quad (VI.12)$$

$$= (\dots + h(k+1)z + h(k) + h(k-1)z^{-1} + \dots + h(0)z^{-k})$$

so that

$$\frac{G'(z)}{H_{eq_{min}}(z^{-1})} = (\dots + h(k+1)z + \dots + h(0)z^{-k})(\alpha_0 + \alpha_1 z + \dots) \quad (VI.13)$$

However,

$$\frac{G'(z)}{H_{eq_{min}}(z^{-1})}$$

may also be written, using (VI.12), as

$$\frac{G'(z)}{H_{eq_{min}}(z^{-1})} = \frac{\prod_{j=1}^M (1 - b_j z) z^{-k} \prod_{i=1}^k (1 - a_i z) \prod_{i=k+1}^N (1 - a_i z)}{\prod_{i=1}^k (1 - a_i z) \prod_{i=k+1}^N (1 - a_i z^{-1}) \prod_{j=1}^M (1 - b_j z)} \quad (VI.14)$$

Cancelling gives

$$\frac{G'(z)}{H_{eq_{min}}(z^{-1})} = z^{-k} \frac{\prod_{i=k+1}^N (1 - a_i z)}{\prod_{i=k+1}^N (1 - a_i z^{-1})} \quad (VI.15)$$

$$= z^{-k} H_{AP}(z^{-1}) \quad (VI.16)$$

Now the aim is to obtain  $B^+(z)$  from:

$$\frac{G(z)}{H_{eq_{min}}(z^{-1})} = B^+(z) + B^-(z)$$

but comparing (VI.11) and (VI.13) it is clear that the causal components of these equations are identical, that is,

$$\frac{G'(z)}{H_{eq_{min}}(z^{-1})} = B^+(z) + B'^-(z) \quad (VI.17)$$

$$\text{Now } H_{ap}(z) = h_{ap}(0) + h_{ap}(1)z^{-1} + \dots \text{ is causal} \quad (VI.18)$$

Hence  $H_{ap}(z^{-1}) = h_{ap}(0) + h_{ap}(1)z + \dots$  is acausal.

Hence from (VI.16) and (VI.17)

$$\begin{aligned} B^+(z) + B'^-(z) &= z^{-k} H_{ap}(z^{-1}) \\ &= h_{ap}(0)z^{-k} + h_{ap}(1)z^{-k+1} + \dots + h_{ap}(k) \\ &\quad + h_{ap}(k+1)z + \dots \end{aligned} \quad (VI.19)$$

Hence

$$B^+(z) = h_{ap}(0)z^{-k} + \dots + h_{ap}(k) \quad (VI.20)$$

and hence from (VI.8)

$$F_k(z) = \frac{h_{ap}(0)z^{-k} + h_{ap}(1)z^{-k+1} + \dots + h_{ap}(k)}{H_{eq\_min}(z)} \quad (VI.21)$$

which is the desired expression for  $F_k(z)$ .

Using this expression it will now be demonstrated that:

(i) the infinite causal least-squares filter perfectly spikes  $H(z)$  if the output is sufficiently delayed;

(ii) the performance (defined mathematically in section 3.3.3) is a monotonically non-decreasing function of  $k$ .

The starting point is the filter output:

$$\begin{aligned} X_k(z) &= F_k(z)H(z) \\ &= \frac{(h_{ap}(0)z^{-k} + h_{ap}(1)z^{-k+1} + \dots + h_{ap}(k))}{H_{eq\_min}(z)} H(z) \end{aligned}$$

but

$$\frac{H(z)}{H_{eq\_min}(z)} = \frac{\prod_{i=1}^k (1 - a_i z^{-1}) \prod_{i=k+1}^N (1 - a_i z^{-1}) \prod_{i=1}^M (1 - b_i z^{-1})}{\prod_{i=1}^M (1 - b_i z^{-1}) \prod_{i=1}^k (1 - a_i z^{-1}) \prod_{i=k+1}^N (1 - a_i z)}$$



Therefore

$$\frac{H(z)}{H_{eq_{min}}(z)} = \frac{\prod_{i=k+1}^N (1 - a_i z^{-1})}{\prod_{i=k+1}^M (1 - a_i z)} = H_{AP}(z) \quad (VI.23)$$

Hence,

$$X_k(z) = (h_{ap}(0)z^{-k} + \dots + h_{ap}(k))H_{AP}(z)$$

$$X_k(z) = \left( \sum_{i=0}^k h_{ap}(i) z^{-k+i} \right) H_{AP}(z) \quad (VI.24)$$

Now

$$\begin{aligned} x_k(k) &= \text{coefficient of } z^{-k} \text{ in } X_k(z) \\ &= \text{coefficient of } z^{-k} \text{ in } \left( \sum_{i=0}^k h_{ap}(i) z^{-k+i} \right) \left( \sum_{j=0}^{\infty} h_{ap}(j) z^{-j} \right) \end{aligned}$$

$$\text{Hence } x_k(k) = \sum_{i=0}^k h_{ap}^2(i) \quad (VI.25)$$

Now, as shown in section 3.3.3, the error energy  $I$  is given by:

$$I_k = 1 - x_k(k) \quad (3.3.19)$$

which is, therefore:

$$= 1 - \sum_{i=0}^k h_{ap}^2(i) \quad (VI.26)$$

Using the definition of performance (3.3.25),

$$P_k = 1 - I_k = \sum_{i=0}^k h_{ap}^2(i) \quad (VI.27)$$

Now

$$P_{k+1} = \sum_{i=0}^{k+1} h_{ap}^2(i) \quad (VI.28)$$

Hence,

$$P_{k+1} - P_k = h_{ap}^2(k+1) \geq 0 \quad (VI.29)$$

which demonstrates the first result.

Also

$$\lim_{k \rightarrow \infty} P_k = \lim_{k \rightarrow \infty} \sum_{i=0}^k h_{ap}^2(i) \rightarrow 1$$

since  $h_{ap}$  is all pass, which demonstrates the second result.

## APPENDIX VII

In this Appendix a simplified description of the sideways recursion due to Simpson [90] will be given. Only real, single-channel processes are considered.

The aim is to solve a set of  $(N + 1)$  equations of the form

$$R\mathbf{f}_{-k} = \mathbf{g}_k; \quad k = 1, 2, \dots, M \quad (\text{VII.1})$$

where in each case  $\mathbf{g}_{k+1}$  is obtained from  $\mathbf{g}_k$ , by shifting all the elements one position and incorporating a single new element, that is, if

$$\mathbf{g}_k = (g_0, g_1, \dots, g_N)^t, \text{ say}$$

then 
$$\mathbf{g}_{k+1} = (g_{-1}, g_0, \dots, g_{N-1})^t$$

In all cases the coefficient matrix,  $R$ , remains unchanged.

Note that in this Appendix, all elements of vectors are denoted with subscripts for brevity.

The Simpson recursion proceeds by firstly solving the system

$$R\mathbf{f} = \mathbf{g}$$

for the zero delay solution, using the Levinson recursion discussed in Appendix I. The solution for delays  $k = 1, 2, \dots, M$  are then computed sequentially. The process may be illustrated by considering a single step. This may be formulated as follows:

Given the coefficients  $(f_0, f_1, \dots, f_N)^t = \mathbf{f}$  from the Levinson recursion in the system

$$R[f_0, f_1, \dots, f_N]^T = [g_0, g_1, \dots, g_N]^T \quad (\text{VII.2})$$

and the associated auxiliary coefficients  $a_i$ :

$$R[a_0, a_1, \dots, a_N]^T = [\alpha_N, 0, \dots, 0]^T \quad (\text{VII.3})$$

where  $a_0^{(i)} = 1$   $i$  (see Appendix I) the aim is to obtain coefficients

$\underline{f}' = [f'_0, f'_1, \dots, f'_N]^T$  such that

$$R[f'_0, f'_1, \dots, f'_N]^T = [g_{-1}, g_0, g_1, \dots, g_{N-1}]^T. \quad (\text{VII.4})$$

The solution is obtained as follows. Firstly, reverse the system (VII.3)

$$R[a_N, a_{N-1}, \dots, a_0]^T = [0, 0, \dots, 0, \alpha_N]^T \quad (\text{VII.5})$$

then shifting the  $a_i$

$$\begin{bmatrix} r_0 & r_1 & r_2 & \dots & r_N \\ r_1 & r_0 & r_1 & & \\ & r_1 & r_0 & & \\ \vdots & & & & \\ r_N & & & & r_0 \end{bmatrix} \begin{bmatrix} 0 \\ a_N \\ a_{N-1} \\ \vdots \\ a_1 \end{bmatrix} = \begin{bmatrix} \gamma_1 \\ 0 - r_N a_0 \\ 0 - r_{N-1} a_0 \\ \vdots \\ 0 - r_1 a_0 \end{bmatrix} \quad (\text{VII.6})$$

where  $\gamma_1 = r_1 a_N + r_2 a_{N-1} + \dots + r_N a_1$ .

Also, shifting (VII.2)

$$\begin{bmatrix} r_0 & r_1 & \dots & r_N \\ r_1 & r_0 & r_1 & \\ & & & r_1 \\ r_N & \dots & r_1 & r_0 \end{bmatrix} \begin{bmatrix} 0 \\ f_0 \\ f_1 \\ \vdots \\ f_{N-1} \end{bmatrix} = \begin{bmatrix} \gamma_2 \\ g_0 - r_N f_N \\ g_1 - r_{N-1} f_N \\ \vdots \\ g_{N-1} - r_1 f_N \end{bmatrix} \quad (\text{VII.7})$$

$\gamma_2 = r_1 f_0 + r_2 f_1 + \dots + r_N f_{N-1}$ .

Remembering that  $a_0 = 1$ , subtract  $f_N$  times (VII.6) from (VII.7) to obtain

$$\begin{bmatrix} r_0 & r_1 & \dots & r_N \\ r_1 & r_0 & r_1 & \\ & & & r_1 \\ r_N & \dots & r_1 & r_0 \end{bmatrix} \begin{bmatrix} 0 \\ f_0 - f_N a_N \\ f_1 - f_N a_{N-1} \\ f_{N-1} - f_N a_1 \end{bmatrix} = \begin{bmatrix} \gamma_3 \\ g_0 \\ g_1 \\ \vdots \\ g_{N-1} \end{bmatrix} \quad (\text{VII.8})$$

where

$$\gamma_3 = \gamma_2 - f_N \gamma_1.$$

Finally, combining (VII.3) and (VII.8) as:

$$\begin{bmatrix} r_0 & r_1 & \dots & r_N \\ r_1 & r_0 & r_1 & \\ & & & r_1 \\ r_N & \dots & r_1 & r_0 \end{bmatrix} \left\{ \begin{bmatrix} 0 \\ f_0 - f_N a_N \\ f_1 - f_N a_{N-1} \\ f_{N-1} - f_N a_1 \end{bmatrix} + k \begin{bmatrix} a_0 \\ a_1 \\ a_N \end{bmatrix} \right\} = \begin{bmatrix} \gamma_3 \\ g_0 \\ g_{N-1} \end{bmatrix} + k \begin{bmatrix} \alpha_N \\ 0 \\ 0 \\ 0 \end{bmatrix} \quad (\text{VII.9})$$

and selecting  $k$  such that

$$\gamma_3 + k \alpha_N = g_{-1}$$

the result follows with

$$\begin{aligned} f'_0 &= k a_0 \\ f'_1 &= f_0 - f_N a_N + k a_1 \\ &\vdots \\ f'_N &= f_{N-1} - f_N a_1 + k a_N \end{aligned} \quad (\text{VII.10})$$

This procedure may be implemented recursively to compute new filters for any desired delay (or more generally for any desired right hand side).

## APPENDIX VIII

The form of the filter which is obtained here is analogous to the results stated in Chapter 2, however, in this instance the concern is with signals which have a mixed random and deterministic form.

The aim is to approximate the adaptive signal enhancement scheme of Section 5.4.2, by an unconstrained Wiener filter. Accordingly, the infinite filter  $f(n)$  which minimises

$$I = \sum_{n=-\infty}^{\infty} \left( x(n + kn_0) - \sum_{i=-\infty}^{\infty} f(i)x(n-i) \right)^2 \quad (\text{VIII.1})$$

is sought.

Let  $x(n + kn_0) = x_1(n)$  and  $v(n + kn_0) = v_1(n)$ , so that

$$\begin{aligned} x(n) &= s(n) + v(n) \\ x_1(n) &= h(n, n + kn_0) * s(n) + v_1(n) \end{aligned} \quad (\text{from equ. 5.1.2})$$

The solution, obtained by differentiating and equating to zero is obtained from:

$$\sum_{n=-\infty}^{\infty} x_1(n) x(n-j) = \sum_{n=-\infty}^{\infty} \sum_{i=-\infty}^{\infty} f(i)x(n-i)x(n-j) \quad (\text{VIII.2})$$

(see Chapter 2)

Assuming

$$\sum_{n=-\infty}^{\infty} V(n)s(n-i) \rightarrow 0 \text{ etc.}$$

then

$$\begin{aligned} R_{vv_1}(j) &+ \sum_{n=-\infty}^{\infty} s(n-j) [h(n + kn_0) * s(n)] \\ &= \sum_{i=-\infty}^{\infty} f(i) \left[ R_{vv}(i-j) + \sum_{n=-\infty}^{\infty} s(n-i)s(n-j) \right] \end{aligned} \quad (\text{VIII.3})$$

$z$  transforming this gives:

$$R_{vv_1}(z) + |S(z)|^2 H(z) = F(z) [R_{vv}(z) + |S(z)|^2]$$



and hence

$$F(z) = \frac{R_{vv1}(z) + H(z)|S(z)|^2}{R_{vv}(z) + |S(z)|^2} \quad (\text{VIII.4})$$

Now:

$$R_{yy}(z) = |F(z)|^2 R_{xx}(z) \quad (\text{VIII.5})$$

where

$$R_{xx}(z) = |S(z)|^2 + R_{vv}(z) \quad (\text{VIII.6})$$

$$\text{and so } R_{yy}(z) = \frac{|R_{vv1}(z) + H(z)|S(z)|^2|^2}{R_{vv}(z) + |S(z)|^2} \quad (\text{VIII.7})$$

If  $E\{v(n)v(n + kn_0)\} = 0$ , a better approximation to the finite filter performance is obtained by setting  $R_{vv1}(z) = 0$  (although this is not correct).

This gives

$$F(z) = \frac{H(z)}{1 + \frac{R_{vv}(z)}{|S(z)|^2}} \quad (\text{VIII.8})$$

and

$$R_{yy}(z) = \frac{|H(z)|^2 |S(z)|^2}{1 + \frac{R_{vv}(z)}{|S(z)|^2}} \quad (\text{VIII.9})$$

Define SNR density for the signal  $x(n) = s(n) + v(n)$  by

$$\rho_x(z) = \frac{|S(z)|^2}{R_{vv}(z)} \quad (\text{VIII.10})$$

Now (VIII.9) may be rewritten as

$$R_{yy}(z) = |H(z)|^2 |S(z)|^2 - \frac{R_{vv}(z) |H(z)|^2}{1 + \frac{R_{vv}(z)}{|S(z)|^2}} \quad (\text{VIII.11})$$

so that

$$\rho_y(z) = \frac{|H(z)|^2 |S(z)|^2}{\left( \frac{R_{vv}(z) |H(z)|^2}{1 + \frac{R_{vv}(z)}{|S(z)|^2}} \right)} \quad (\text{VIII.12})$$

which, upon rearranging may be written as:

$$\rho_y(z) = \frac{R_{xx}(z)}{R_{vv}(z)} \quad (\text{VIII.13})$$



## APPENDIX IX

In this appendix some results will be obtained for signal averaging of signals of the form:

$$\begin{aligned} y_0(n) &= s(n) + u_0(n) \\ y_1(n) &= \alpha s(n) + d(n) + u_1(n) \end{aligned} \quad (\text{IX.1})$$

$$\text{where } E\{u_0(n)u_0(n)\} = E\{u_1(n)u_1(n)\} = \sigma_u^2$$

$$\text{and } E\{u_0(n)u_1(n)\} = k\sigma_u^2 \quad 0 \leq k < 1 \quad \text{say, taking } \alpha > 0 \text{ for convenience.}$$

$$\begin{aligned} \text{Firstly, forming } y(n) &= \frac{1}{(1+\alpha)} \{y_0(n) + y_1(n)\} \\ &= s(n) + \frac{1}{(1+\alpha)} \{d(n) + u_0(n) + u_1(n)\} \end{aligned} \quad (\text{IX.2})$$

$$\begin{aligned} \text{Now, bias } \{y(n)\} &= E\{y(n) - x(n)\} \\ &= \frac{d(n)}{(1+\alpha)} \end{aligned} \quad (\text{IX.3})$$

$$\text{Also Variance } \{y(n)\} = \frac{2\sigma_u^2}{(1+\alpha)^2} (1+k) \quad (\text{IX.4})$$

from equation (5.2.2)

$$(\text{SNR}_y) = \frac{|s(n)|}{(\text{mean square error } y(n))^{\frac{1}{2}}}$$

$$\text{but mean square error}\{y(n)\} = \text{bias}^2(y(n)) + \text{Variance}(y(n))$$

Hence

$$(\text{SNR}_y) = \frac{|s(n)|}{(\text{Bias}^2 y(n) + \text{Variance } y(n))^{\frac{1}{2}}} \quad (\text{IX.5})$$

and hence

$$(\text{SNR}_y) = \frac{|s(n)| (1 + \alpha)}{\{d^2(n) + 2\sigma_u^2 (1+k)\}^{\frac{1}{2}}} \quad (\text{IX.6})$$

Therefore, the ratio of output SNR to input is

$$\frac{(\text{SNR}_y)}{(\text{SNR}_{y_o})} = \frac{(1+\alpha)\sigma_u}{\{d^2(n) + 2\sigma_u^2 (1+k)\}^{\frac{1}{2}}} \quad (\text{IX.7})$$

which is  $>1$  if  $(1+\alpha)^2 \sigma_u^2 > (d^2(n) + 2\sigma_u^2 + 2k\sigma_u^2)$

or rearranging

$$\frac{(\text{SNR}_y)}{(\text{SNR}_{y_o})} > 1 \quad \text{if} \quad \alpha > \left(2(1+k) + \frac{d^2(n)}{\sigma_u^2}\right)^{\frac{1}{2}} - 1 \quad (\text{IX.8})$$

If, however, a gain  $G$  is introduced, so that

$$y(n) = \frac{1}{(1+G\alpha)} \{y_o(n) + Gy_1(n)\} \quad \text{then}$$

$$y(n) = s(n) + \frac{1}{(1+G\alpha)} \{u_o(n) + GU_1(n) + Gd(n)\} \quad (\text{IX.9})$$

$$\text{Hence bias } \{y(n)\} = \frac{Gd(n)}{(1+G\alpha)} \quad (\text{IX.10})$$

$$\text{and Variance } \{y(n)\} = \frac{1}{(1+G\alpha)^2} \{ (1+G^2)\sigma_u^2 + 2Gk\sigma_u^2 \} \quad (\text{IX.11})$$

Hence

$$(\text{SNR}_y) = \frac{(1+G\alpha) s(n)}{(G^2 d^2(n) + (1+G^2+2Gk)\sigma_u^2)^{\frac{1}{2}}} \quad (\text{IX.12})$$

and

$$\frac{(\text{SNR}_y)}{(\text{SNR}_{y_o})} = \frac{(1+G\alpha) \sigma_u}{\{G^2 d^2(n) + (1+G^2+2Gk)\sigma_u^2\}^{\frac{1}{2}}} \quad (\text{IX.13})$$

Furthermore the value of the gain can be optimised by differentiating this expression and equating to zero, which yields, upon rearrangement:

$$G_{\text{opt}} = \frac{(\alpha-k)}{\frac{d^2(n)}{\sigma_u^2} + (1-k\alpha)} \quad (\text{IX.14})$$

Substituting (IX.14) into (IX.13) yields:

$$\left( \frac{\text{SNR}_y}{\text{SNR}_{y_o}} \right)_{\text{opt}} = \frac{\frac{d^2(n)}{\sigma_u^2} + 1 + \alpha^2 - 2\alpha k}{\{ (\alpha^2 - k^2) \left( \frac{d^2(n)}{\sigma_u^2} + 1 \right) - 2(\alpha - k)k^2\alpha + \left( \frac{d^2(n)}{\sigma_u^2} + (1 - k\alpha) \right)^2 \}^{\frac{1}{2}}}$$

(IX.15)

Upon simplification:

$$\left( \frac{\text{SNR}_y}{\text{SNR}_{y_o}} \right)_{\text{opt}} > 1 \quad \text{if} \quad \alpha^2 + \frac{d^2(n)}{\sigma_u^2} + 1 - 2k\alpha > 0$$

or

$$\alpha(\alpha - k) + \frac{d^2(n)}{\sigma_u^2} > (\alpha k - 1)$$

but  $\alpha k < 1$

Hence

$$\left( \frac{\text{SNR}_y}{\text{SNR}_{y_o}} \right)_{\text{opt}} > 1 \quad \text{if} \quad \alpha > k$$

## APPENDIX X

### 1. Approximate Transfer Function (Single Interfering Sinusoid)

The following result has previously been obtained by Widrow et al [2] (by an erroneous derivation) and by Glover [1], who gives a correct proof. An alternative, novel derivation is given here. Given a primary input which contains, in addition to the desired signal, a single interfering tone of frequency  $\omega_0$ , and given a noise-free reference input, the filter output is

$$y_k = \underline{f}_k^t \underline{x}_k \quad (X.1)$$

and the update equation is

$$\underline{f}_k = \underline{f}_{k-1} + \alpha e(k-1) \underline{x}_{k-1}; \quad k = 1, 2, \dots \quad (X.2)$$

(see Chapter 2)

assuming  $\underline{f}_0 \equiv 0$ , for simplicity, then by repeated substitution

$$y(k) = \alpha \sum_{i=0}^{K-1} e(i) \underline{x}_k^t \underline{x}_i \quad K \geq 1 \quad (X.3)$$

$$\text{Now } \underline{x}_k = \begin{bmatrix} A \cos(\omega_0 kT + \phi) \\ A \cos(\omega_0 (k-1)T + \phi) \\ \vdots \\ A \cos(\omega_0 (k-L+1)T + \phi) \end{bmatrix}$$

Hence

$$\begin{aligned} \underline{x}_k^t \underline{x}_i &= \sum_{j=0}^{L-1} A^2 \cos[\omega_0 (k-j)T + \phi] \cos[\omega_0 (i-j)T + \phi] \\ &= \frac{LA^2}{2} \cos[\omega_0 (i-k)T] + \frac{A^2}{2} \sum_{j=0}^{L-1} \cos[\omega_0 (-i-k+2j)T - 2\phi] \end{aligned} \quad (X.4)$$

Now if

$$L = \frac{N\pi}{\omega_0 T} \quad N = 1, 2, \dots$$

that is  $L$  is an integer multiple of  $\pi$  samples, then

$$\sum_{j=0}^{L-1} \cos[\omega_0(-i - k + 2j)T - 2\phi] = 0 \quad (X.5)$$

In any case, the influence of the second term in (X.4) decreases with L and assuming it may be neglected

$$x_k^t x_{-1} = \frac{LA^2}{2} \cos[\omega_0(i - k)T] \quad (X.6)$$

and hence substituting (X.6) in (X.3) gives

$$y(k) = \frac{\alpha LA^2}{2} \sum_{i=0}^{K-1} e(i) \cos[\omega_0(k - i)T] \quad K \geq 1 \quad (X.7)$$

which is the convolution of the error sequence with the cosine wave. Taking the z-transform of (X.7) gives

$$Y(z) = \frac{\alpha LA^2}{2} \left[ \frac{z^{-1} \cos \omega_0 T - z^{-2}}{1 - 2z^{-1} \cos \omega_0 T + z^{-2}} \right] E(z) \quad (X.8)$$

Also

$$D(z) = E(z) + Y(z) \quad (X.9)$$

and combining yields

$$H(z) = \frac{E(z)}{D(z)} = \frac{z^{-2} - 2z^{-1} \cos \omega_0 T + 1}{(1 - \frac{\alpha LA^2}{2})z^{-2} + (\frac{\alpha LA^2}{2} - 2)z^{-1} \cos \omega_0 T + 1} \quad (X.10)$$

## 2. Pole-Zero Structure of the Transfer Function

From equation (X.10) the zeros of the transfer function are given by  $z^{-2} - 2z^{-1} \cos \omega_0 T + 1 = 0$ , which gives

$$z_0 = e^{\pm i\omega_0 T} \quad (X.11)$$

The poles are obtained from

$$(1 - \frac{\alpha LA^2}{2})z^{-2} + (\frac{\alpha LA^2}{2} - 2)z^{-1} \cos \omega_0 T + 1 = 0$$

Neglecting  $\alpha^2$  this gives

$$z_p = (1 - \frac{\alpha LA^2}{4}) e^{+i\omega_o T} \quad (X.12)$$

### 3. Time Domain Characteristics

The time domain (convergence) properties of the system are investigated by examining the response to a primary input consisting of a pure sine wave

$$d(k) = B \cos(\omega_o kT + \psi) \quad (X.13)$$

then

$$D(z) = B \left[ \frac{\cos \psi - z^{-1} \cos(\omega_o T - \psi)}{z^{-2} - 2z^{-1} \cos \omega_o T + 1} \right] \quad (X.14)$$

Hence, from (X.10) and assuming the pole structure of (X.12)

$$E(z) = \frac{B(\cos \psi - z^{-1} \cos(\omega_o T - \psi))}{(1 - (1 - \frac{\alpha LA^2}{4}) e^{i\omega_o T} z^{-1})(1 - (1 - \frac{\alpha LA^2}{4}) e^{-i\omega_o T} z^{-1})} \quad (X.15)$$

This expression may be inverse transformed by firstly partial fractioning.

After some tedious algebra the result is obtained as

$$e(k) = (1 - \frac{\alpha LA^2}{4})^k C \cos(\omega_o kT - \xi) \quad K \geq 1 \quad (X.16)$$

where

$$C = \frac{B}{1 - \cos 2\psi} \left[ (1 - \frac{\alpha LA^2}{4}) \cos^2 \psi \sin^4 2\omega_o T + (1 - \frac{\alpha LA^2}{4}) \cos^2 \psi \sin^2 2\omega_o T \right. \\ \left. + 4(1 - \frac{\alpha LA^2}{4})^{-1} \cos^2(\omega_o T - \psi) \sin^2 \omega_o T - 4 \cos \psi \sin 2\omega_o T \sin \omega_o T \cos(\omega_o T - \psi) \right]^{\frac{1}{2}}$$

and

$$\xi = \tan^{-1} \left( \frac{2 \cos(\omega_o T - \psi) \sin \omega_o T - (1 - \frac{\alpha LA^2}{4}) \cos \psi \sin 2\omega_o T}{-(1 - \frac{\alpha LA^2}{4}) \cos \psi \sin^2 \omega_o T} \right) \quad (X.18)$$

From (X.16)

$$\lim_{k \rightarrow \infty} e(k) \rightarrow 0 \quad \text{iff} \quad \left| 1 - \frac{\alpha LA^2}{4} \right| < 1$$

that is, if

$$0 < \frac{\alpha LA^2}{4} < 2$$

However, the assumptions made above mean that the expression for  $e(k)$  is only valid for  $\alpha LA^2/4 \ll 2$ .

It is also possible to compute the number of samples required for the error to fall from its first peak value to  $1/M$  times this level.

At the peaks

$$e(k) = C' \left( 1 - \frac{\alpha LA^2}{4} \right)^k \quad (\text{X.19})$$

If the first peak occurs at  $k = L_1$ , then the required peak,  $k = L_2$ , say, is obtained from

$$\frac{C' \left( 1 - \frac{\alpha LA^2}{4} \right)^{L_1}}{C' \left( 1 - \frac{\alpha LA^2}{4} \right)^{L_2}} = M$$

which gives

$$(L_2 - L_1) = \frac{-\log_{10} M}{\log \left( 1 - \frac{\alpha LA^2}{4} \right)} \quad (\text{X.20})$$

Time constant  $T$  may also be defined as:

$$T = \frac{(L_2 - L_1)}{\text{Sample Rate}}$$

Hence

$$T = \frac{-\log_{10} M}{(\text{Sample rate}) \log \left( 1 - \frac{\alpha LA^2}{4} \right)} \quad (\text{X.21})$$



Finally in this section, the differences in adaptation constant required to produce similar convergence rates (as defined by T), for differing values of L and A are considered. From equation (X.20) with  $L_1$  and  $L_2$  weights and amplitudes A and B, to have equal convergence rates, the requirement is that

$$\frac{-\log_{10} M}{\log_{10} \left(1 - \frac{\alpha_1 L_1 A^2}{4}\right)} = \frac{-\log_{10} M}{\log_{10} \left(1 - \frac{\alpha_2 L_2 B^2}{4}\right)}$$

Hence

$$\alpha_2 = \left(\frac{L_1 A^2}{L_2 B^2}\right) \alpha_1 \quad (X.22)$$

In particular, for a fixed number of weights, L, to have equal convergence with amplitudes A and B, the adaptation constant must vary as the inverse square of the amplitudes. That is

$$\alpha_2 = \left(\frac{A^2}{B^2}\right) \alpha_1 \quad (X.23)$$

#### 4. Approximate Transfer Function (Multiple Interfering Sinusoids)

The multiple interfering sinusoidal case is now considered. For simplicity the number of interferences is limited to two, but the results can easily be generalised.

The reference input is

$$\underline{x}_n = \begin{bmatrix} A_0 \cos(\omega_0 kT + \phi_0) + A_1 \cos(\omega_1 kT + \phi_1) \\ A_0 \cos(\omega_0 (k-1)T + \phi_0) + A_1 \cos(\omega_1 (k-1)T + \phi_1) \\ \vdots \\ A_0 \cos(\omega_0 (k - (L-1))T + \phi_0) + A_1 \cos(\omega_1 (k - (L-1))T + \phi_1) \end{bmatrix}$$

Hence

$$\begin{aligned}
 x_k^t x_i = & \sum_{j=0}^{L-1} A_o^2 \cos[\omega_o(k-j)T + \phi_o] \cos[\omega_o(i-j)T + \phi_o] \\
 & + \sum_{j=0}^{L-1} A_1^2 \cos[\omega_1(k-j)T + \phi_1] \cos[\omega_1(i-j)T + \phi_1] \\
 & + \sum_{j=0}^{L-1} A_o A_1 \cos[\omega_o(k-j)T + \phi_o] \cos[\omega_1(i-j)T + \phi_1] \\
 & + \sum_{j=0}^{L-1} A_o A_1 \cos[\omega_1(k-j)T + \phi_1] \cos[\omega_o(i-j)T + \phi_o] \quad (X.24)
 \end{aligned}$$

The first two terms have the same form as for the single interfering sinusoid (see equation (X.4)). Consider the third term

$$\sum_{j=0}^{L-1} A_o A_1 \cos[\omega_o(k-j)T + \phi_o] \cos[\omega_1(i-j)T + \phi_1]$$

This can be expressed as

$$\begin{aligned}
 & \frac{A_o A_1}{2} \cos[\omega_o kT + \omega_1 iT + (\phi_o + \phi_1)] \sum_{j=0}^{L-1} \cos[(\omega_o + \omega_1)jT] \\
 & + \frac{A_o A_1}{2} \sin[\omega_o kT + \omega_1 iT + (\phi_o + \phi_1)] \sum_{j=0}^{L-1} \sin[(\omega_o + \omega_1)jT] \\
 & + \frac{A_o A_1}{2} \cos[\omega_o kT - \omega_1 iT + (\phi_o - \phi_1)] \sum_{j=0}^{L-1} \cos[(\omega_1 - \omega_o)jT] \\
 & - \frac{A_o A_1}{2} \sin[\omega_o kT - \omega_1 iT + (\phi_o - \phi_1)] \sum_{j=0}^{L-1} \sin[(\omega_1 - \omega_o)jT] \quad (X.25)
 \end{aligned}$$

These terms can only be identically zero if  $L$  is an integer multiple of  $2\pi$  samples at both the sum and difference frequencies. However, if  $L$  is sufficiently large these terms become negligible compared with those proportional to  $L$  (from the first two terms of (X.24)).

If it is assumed that these terms are negligible and similarly those of the fourth term of (X.24) then

$$\underline{x}_k^t \underline{x}_i = \frac{LA_o^2}{2} \cos \omega_o(i-k)T + \frac{LA_1^2}{2} \cos \omega_1(i-k)T \quad (X.26)$$

and hence using equation (X.3)

$$y(k) = \sum_{i=0}^{K-1} e(i) \left( \frac{LA_o^2}{2} \cos[\omega_o(i-k)T] + \frac{LA_1^2}{2} \cos[\omega_1(i-k)T] \right) \quad (X.27)$$

z-transforming this equation gives

$$Y(z) = \frac{\alpha LA_o^2}{2} \left[ \frac{z^{-1} \cos \omega_o T - z^{-2}}{1 - 2z^{-1} \cos \omega_o T + z^{-2}} \right] + \frac{\alpha LA_1^2}{2} \left[ \frac{z^{-1} \cos \omega_1 T - z^{-2}}{1 - 2z^{-1} \cos \omega_1 T + z^{-2}} \right] \quad (X.28)$$

Finally, using (X.9)

$$H(z) = \frac{E(z)}{D(z)} = \left[ \frac{(z^{-2} - 2z^{-1} \cos \omega_o T + 1)(z^{-2} - 2z^{-1} \cos \omega_1 T + 1)}{(1 - 2z^{-1} \cos \omega_o T + z^{-2})(1 - 2z^{-1} \cos \omega_1 T + z^{-2}) + \frac{\alpha LA_o^2}{2} (z^{-1} \cos \omega_o T - z^{-2}) \cdot (z^{-2} - 2z^{-1} \cos \omega_1 T + 1) + \frac{\alpha LA_1^2}{2} (z^{-1} \cos \omega_o T - z^{-2}) \cdot (1 - 2z^{-1} \cos \omega_o T + z^{-2})} \right] \quad (X.29)$$

Hence the transfer function has zeroes at  $z = e^{\frac{+i\omega_o T}{2}}$  and at  $z = e^{\frac{+i\omega_1 T}{2}}$ .

Neglecting  $O(\alpha^2)$  the poles of the transfer function are given by

$$z = \left( 1 - \frac{\alpha LA_o^2}{4} \right) e^{\frac{+i\omega_o T}{2}}$$

and

$$z = \left( 1 - \frac{\alpha LA_1^2}{4} \right) e^{\frac{+i\omega_1 T}{2}}$$

## APPENDIX XI

In this Appendix those properties of the adaptive noise cancellation system which are not included in the appropriate transfer functions of Appendix X are investigated. The starting point is the transfer function response developed in the manner adopted by Glover.

Let  $f_{k+1}(i)$  denote the  $i$ 'th component of the filter response at time  $k + 1$ . Then

$$f_{k+1}(i) = f_k(i) + \alpha e(k)x(k-i) \quad (\text{XI.1})$$

(see Chapter 2)

$z$ -transforming gives

$$zF_i(z) = F_i(z) + \alpha z\{e(k)x(k-i)\}$$

or

$$F_i(z) = \alpha U(z)z\{e(k)x(k-i)\} \quad (\text{XI.2})$$

where

$$U(z) = 1/(z-1).$$

Considering, initially, a single sinusoidal interference and assuming, for simplicity, that the phase angle at  $x(k)$  is zero, that is

$$x(k-i) = A \cos [\omega_0(k-i)T]$$

or

$$= A \cos [\omega_0 kT - \phi_i]$$

where  $\phi_i = \omega_0 iT$ .

Hence

$$z\{e(k)x(k-i)\} = \frac{A}{2} e^{i\phi_i} z\{e(k)e^{i\omega_0 kT}\} + \frac{A}{2} e^{-i\phi_i} z\{e(k)e^{-i\omega_0 kT}\}$$

or

$$z\{e(k)x(k-i)\} = \frac{A}{2} \left[ e^{i\phi_i} \mathcal{E}(ze^{-i\omega_0 T}) + e^{-i\phi_i} \mathcal{E}(ze^{i\omega_0 T}) \right]$$

(XI.3)

Combining (XI.2) and (XI.3) gives

$$F(z) = \frac{\alpha}{(z-1)} \frac{A}{2} \left[ e^{i\phi_i} \mathcal{E}(ze^{-i\omega_0 T}) + e^{-i\phi_i} \mathcal{E}(ze^{i\omega_0 T}) \right] \quad (\text{XI.4})$$

Similarly,

$$\begin{aligned} Y_i(z) &= z \{ f_k(i) x(k-i) \} \\ &= \frac{A}{2} \left[ e^{i\phi_i} F(ze^{-i\omega_0 T}) + e^{-i\phi_i} F(ze^{i\omega_0 T}) \right] \end{aligned}$$

and hence, using (XI.4)

$$\begin{aligned} Y_i(z) &= \frac{A^2}{4} \alpha \left[ U(ze^{-i\omega_0 T}) + U(ze^{i\omega_0 T}) \right] \mathcal{E}(z) \\ &\quad + \frac{A^2}{4} \alpha \left[ e^{i2\phi_i} U(ze^{-i\omega_0 T}) \mathcal{E}(ze^{-2i\omega_0 T}) \right] \\ &\quad + \frac{A^2}{4} \alpha \left[ e^{-i2\phi_i} U(ze^{i\omega_0 T}) \mathcal{E}(ze^{2i\omega_0 T}) \right] \end{aligned} \quad (\text{XI.5})$$

Now

$$Y(z) = \sum_{i=0}^{L-1} Y_i(z)$$

and using  $Y(z) = D(z) - (z)$  gives

$$\begin{aligned} D(z) &= \left[ 1 + \alpha L \frac{A^2}{4} (U(ze^{-i\omega_0 T}) + U(ze^{i\omega_0 T})) \right] \mathcal{E}(z) \\ &\quad + \frac{A^2}{4} \alpha \left( \sum_{i=0}^{L-1} e^{i2\phi_i} \right) U(ze^{-i\omega_0 T}) \mathcal{E}(ze^{-2i\omega_0 T}) + \frac{A^2}{4} \alpha \left( \sum_{i=0}^{L-1} e^{-i2\phi_i} \right) U(ze^{i\omega_0 T}) \mathcal{E}(ze^{2i\omega_0 T}) \end{aligned} \quad (\text{XI.6})$$

At this point Glover assumes the last two terms are negligible which leads to the transfer function of (X.10). Here, however, the concern is to quantify these extra effects. Now, from (XI.6)

$$D(z) = R(z) \mathcal{E}(z) + G_1(z) \mathcal{E}(ze^{-i2\omega_0 T}) + G_2(z) \mathcal{E}(ze^{i2\omega_0 T}) \quad (\text{XI.7})$$



where

$$R(z) = \frac{(1 - \frac{\alpha LA^2}{2})z^{-2} + 2(\frac{\alpha LA^2}{4} - 1)\cos\omega_0 T z^{-1} + 1}{(1 - e^{-i\omega_0 T} z^{-1})(1 - e^{i\omega_0 T} z^{-1})} = \frac{1}{H(z)}$$

$$G_1(z) = \frac{\alpha A^2}{4} \left( \sum_{i=0}^{L-1} e^{i2\phi_i} \right) U(z e^{-i\omega_0 T})$$

$$G_2(z) = \frac{\alpha A^2}{4} \left( \sum_{i=0}^{L-1} e^{-i2\phi_i} \right) U(z e^{i\omega_0 T})$$

From (XI.7) it follows that

$$D(z e^{i2\omega_0 T}) = R(z e^{i2\omega_0 T}) \zeta(z e^{i2\omega_0 T}) + G_1(z e^{i2\omega_0 T}) \xi(z) + G_2(z e^{2i\omega_0 T}) \xi(z e^{4i\omega_0 T}) \quad (XI.8)$$

and

$$D(z e^{-i2\omega_0 T}) = R(z e^{-i2\omega_0 T}) \zeta(z e^{-i2\omega_0 T}) + G_1(z e^{-2i\omega_0 T}) \xi(z e^{-4i\omega_0 T}) + G_2(z e^{-2i\omega_0 T}) \xi(z) \quad (XI.9)$$

Hence

$$\begin{aligned} \frac{G_2(z) D(z e^{i2\omega_0 T})}{R(z e^{i2\omega_0 T})} &= G_2(z) \xi(z e^{i2\omega_0 T}) + \frac{G_2(z) G_1(z e^{i2\omega_0 T}) \xi(z)}{R(z e^{i2\omega_0 T})} \\ &\quad + \frac{G_2(z) G_2(z e^{i2\omega_0 T}) \xi(z e^{4\omega_0 T})}{R(z e^{i2\omega_0 T})} \end{aligned} \quad (XI.10)$$

and

$$\begin{aligned} \frac{G_1(z) D(z e^{-i2\omega_0 T})}{R(z e^{-i2\omega_0 T})} &= G_1(z) \xi(z e^{-i2\omega_0 T}) + \frac{G_1(z) G_1(z e^{-i2\omega_0 T}) \xi(z e^{-4\omega_0 T})}{R(z e^{-i2\omega_0 T})} \\ &\quad + \frac{G_1(z) G_2(z e^{-2i\omega_0 T}) \xi(z)}{R(z e^{-i2\omega_0 T})} \end{aligned} \quad (XI.11)$$

Subtracting (XI.10) and (XI.11) from (XI.7) and neglecting second order terms gives

$$\frac{D(z) - \frac{G_1(z)D(ze^{-2i\omega_0 T})}{R(ze^{-2i\omega_0 T})} - \frac{G_2(z)D(ze^{2i\omega_0 T})}{R(ze^{2i\omega_0 T})}}{R(ze^{-2i\omega_0 T})} = R(z)\Sigma(z) \quad (XI.12)$$

Note that at first glance it may not seem reasonable to neglect these terms since some contain uncanceled poles on the unit circle. However, the resulting response also contains such poles and these are always an order of magnitude greater since they are  $O(\alpha)$  rather than  $O(\alpha^2)$ .

Now (XI.12) may be written as

$$\Sigma(z) = H(z) \left[ D(z) - G(z)H(ze^{-2i\omega_0 T})D(ze^{-2i\omega_0 T}) - G_2(z)H(ze^{2i\omega_0 T})D(ze^{2i\omega_0 T}) \right] \quad (XI.13)$$

where  $H(z)$  is the linear time invariant transfer function given by (X.10).

### Multiple Sinusoid Reference

The case of multiple sinusoidal interferences in the reference is now considered where for simplicity the number of sinusoids  $M$  is restricted to 2 so that  $x(k-i) = A_0 \cos(\omega_0 kT - \phi_{1i}) + A_1 \cos(\omega_1 kT - \phi_{2i})$ . Using the same approach applied above and (by direct analogy with equation (XI.5))

$$\begin{aligned} Y_i(z) = & \Sigma(z) \left[ \frac{A_0^2}{4} \alpha [U(ze^{-i\omega_0 T}) + U(ze^{i\omega_0 T})] + \frac{A_1^2}{4} \alpha [U(ze^{-i\omega_1 T}) + U(ze^{i\omega_1 T})] \right] \\ & + \frac{A_0^2}{4} \alpha [e^{i2\phi_{1i}} U(ze^{-i\omega_0 T}) \Sigma(ze^{-2i\omega_0 T})] + \frac{A_0^2}{4} \alpha [e^{-i2\phi_{1i}} U(ze^{i\omega_0 T}) \Sigma(ze^{2i\omega_0 T})] \\ & + \frac{A_1^2}{4} \alpha [e^{i2\phi_{2i}} U(ze^{-i\omega_1 T}) \Sigma(ze^{-2i\omega_1 T})] + \frac{A_1^2}{4} \alpha [e^{-i2\phi_{2i}} U(ze^{i\omega_1 T}) \Sigma(ze^{2i\omega_1 T})] \\ & + \frac{A_0 A_1}{4} \alpha [U(ze^{-i\omega_0 T}) e^{i(\phi_{1i} + \phi_{2i})} + U(ze^{-i\omega_1 T}) e^{i(\phi_{2i} + \phi_{1i})}] \Sigma(ze^{-i(\omega_0 + \omega_1)T}) \end{aligned}$$



$$\begin{aligned}
& + \frac{A_0 A_1}{4} \alpha \left[ U(z e^{-i\omega_0 T}) e^{-i(\phi_{1i} + \phi_{2i})} + U(z e^{i\omega_1 T}) e^{-i(\phi_{2i} + \phi_{1i})} \right] \xi(z e^{i(\omega_0 + \omega_1) T}) \\
& + \frac{A_0 A_1}{4} \alpha \left[ U(z e^{-i\omega_0 T}) e^{i(\phi_{1i} - \phi_{2i})} + U(z e^{i\omega_1 T}) e^{i(\phi_{1i} - \phi_{2i})} \right] \xi(z e^{-i\omega_0 T + i\omega_1 T}) \\
& + \frac{A_0 A_1}{4} \alpha \left[ U(z e^{i\omega_0 T}) e^{i(\phi_{2i} - \phi_{1i})} + U(z e^{-i\omega_1 T}) e^{i(\phi_{2i} - \phi_{1i})} \right] \xi(z e^{i(\omega_1 T - \omega_0 T)})
\end{aligned}$$

(XI.14)

Again, using  $Y(z) = D(z) - \xi(z)$  and  $Y(z) = \sum_{i=0}^{L-1} Y_i(z)$ , rearranging and neglecting second order terms gives

$$\begin{aligned}
\xi(z) = H(z) \left[ D(z) + G_1(z) H(z e^{-i2\omega_0 T}) D(z e^{-i2\omega_0 T}) + G_2(z) H(z e^{i2\omega_0 T}) D(z e^{i2\omega_0 T}) \right. \\
+ G_3(z) H(z e^{-2i\omega_1 T}) D(z e^{-2i\omega_1 T}) + G_4(z) H(z e^{i2\omega_1 T}) D(z e^{i2\omega_1 T}) \\
+ G_5(z) H(z e^{i(\omega_1 - \omega_0) T}) D(z e^{i(\omega_1 - \omega_0) T}) + G_6(z) H(z e^{i(\omega_0 - \omega_1) T}) D(z e^{i(\omega_0 - \omega_1) T}) \\
\left. + G_7(z) H(z e^{i(\omega_0 + \omega_1) T}) D(z e^{i(\omega_1 + \omega_0) T}) + G_8(z) H(z e^{-i(\omega_0 + \omega_1) T}) D(z e^{-i(\omega_1 + \omega_0) T}) \right]
\end{aligned}$$

(XI.15)

where

$$G_1(z) = \frac{-A_0^2 \alpha}{4} \left( \sum_{i=0}^{L-1} e^{2i\phi_{1i}} \right) U(z e^{-i\omega_0 T}) \quad (XI.16)$$

$$G_2(z) = \frac{-A_0^2 \alpha}{4} \left( \sum_{i=0}^{L-1} e^{-2i\phi_{1i}} \right) U(z e^{i\omega_0 T}) \quad (XI.17)$$

$$G_3(z) = \frac{-A_1^2 \alpha}{4} \left( \sum_{i=0}^{L-1} e^{2i\phi_{2i}} \right) U(z e^{-i\omega_1 T}) \quad (XI.18)$$

$$G_4(z) = \frac{-A_1^2 \alpha}{4} \left( \sum_{i=0}^{L-1} e^{-2i\phi_{2i}} \right) U(z e^{i\omega_1 T}) \quad (XI.19)$$

$$G_5(z) = -\frac{A_0 A_1 \alpha}{4} \left( \sum_{i=0}^{L-1} e^{i(\phi_{1i} - \phi_{2i})} \right) \left[ U(z e^{-i\omega_0 T}) + U(z e^{i\omega_1 T}) \right] \quad (XI.20)$$

$$G_6(z) = -\frac{A_0 A_1 \alpha}{4} \left( \sum_{i=0}^{L-1} e^{i(\phi_{2i} - \phi_{0i})} \right) \left[ U(z e^{i\omega_0 T}) + U(z e^{-i\omega_1 T}) \right] \quad (XI.21)$$

$$G_7(z) = -\frac{A_0 A_1 \alpha}{4} \left( \sum_{i=0}^{L-1} e^{-i(\phi_{1i} + \phi_{2i})} \right) \left[ U(z e^{i\omega_0 T}) + U(z e^{i\omega_1 T}) \right] \quad (XI.22)$$

$$G_8(z) = -\frac{A_0 A_1 \alpha}{4} \left( \sum_{i=0}^{L-1} e^{i(\phi_{0i} + \phi_{2i})} \right) \left[ U(z e^{-i\omega_0 T}) + U(z e^{-i\omega_1 T}) \right] \quad (XI.23)$$

and where  $H(z)$  is the two sine wave reference approximate transfer function given by (X.29).

### Examples

We now consider the response obtained for a single sine reference using equation (XI.13), for two simple examples.

$$(a) \text{ Reference} = A \cos(\omega_0 kT + \phi) \quad d(k) = B \cos(\omega_0 kT + \psi)$$

$z$ -transforming  $d(k)$  and substituting in (XI.13) gives

$$\xi(z) = [T_1(z) + T_2(z) + T_3(z)] H(z) \quad (XI.24)$$

where

$$H(z) = \left[ \frac{(1 - z^{-1} e^{i\omega_0 T})(1 - z^{-1} e^{i\omega_0 T})}{(r e^{i\omega_0 T} z^{-1} - 1)(r e^{-i\omega_0 T} z^{-1} - 1)} \right], \quad r = \left(1 - \frac{\alpha L A^2}{4}\right)$$

is the usual transfer function, and where

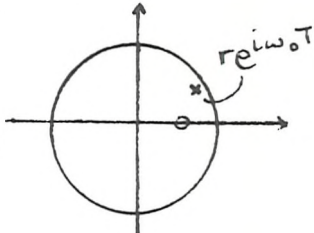
$$T_1(z) = \frac{B(1 - z^{-1} \cos \omega_0 T)}{(r e^{i\omega_0 T} z^{-1} - 1)(r e^{-i\omega_0 T} z^{-1} - 1)} \quad (XI.25)$$

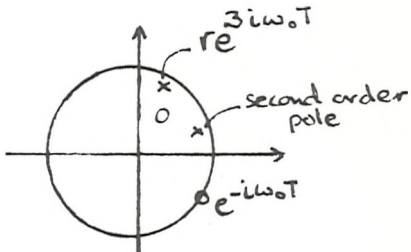
$$T_2(z) = \frac{B(1 - z^{-1} e^{2i\omega_0 T} \cos \omega_0 T)M}{(r e^{3i\omega_0 T} z^{-1} - 1)(r e^{i\omega_0 T} - 1)(1 - z^{-1} e^{i\omega_0 T})} \quad (XI.26)$$

$$T_3(z) = \frac{B(1-z^{-1}e^{-2i\omega_0 T} \cos \omega_0 T) M^*}{(re^{-i\omega_0 T} z^{-1} - 1)(re^{-3i\omega_0 T} z^{-1} - 1)} \quad (\text{XI.27})$$

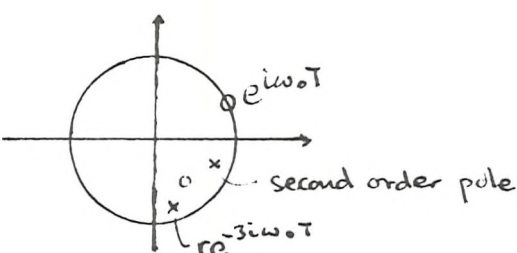
$$M = -\frac{\alpha A^2}{4} \left( \sum_{i=0}^{L-1} e^{i2\phi_i} \right)$$

Hence

$$T_1(z)H(z) = \frac{B(1-z^{-1} \cos \omega_0 T)}{(re^{i\omega_0 T} z^{-1} - 1)(re^{-i\omega_0 T} z^{-1} - 1)} \Rightarrow$$


$$T_2(z)H(z) = \frac{B(1-z^{-1}e^{2i\omega_0 T} \cos \omega_0 T) M(1-z^{-1}e^{-i\omega_0 T})}{(re^{3i\omega_0 T} z^{-1} - 1)(re^{i\omega_0 T} z^{-1} - 1)(re^{-i\omega_0 T} z^{-1} - 1)} \Rightarrow$$


$$T_3(z)H(z) = \frac{B(1-z^{-1}e^{-2i\omega_0 T} \cos \omega_0 T) M^*(1-z^{-1}e^{i\omega_0 T})}{(re^{-3i\omega_0 T} z^{-1} - 1)(re^{-i\omega_0 T} - 1)^2(re^{i\omega_0 T} z^{-1} - 1)}$$

$$\Rightarrow$$


Hence, the main influence of the nonlinear terms is to introduce a pole at  $re^{3i\omega_0 T}$ . Note also the second order pole at  $re^{i\omega_0 T}$ . The relative magnitude of the three components of the response is determined by  $M$ .

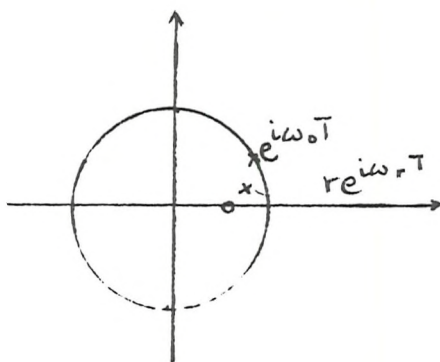
---

(b) Reference =  $A \cos(\omega_0 kT + \phi)$ ,  $d(k) = B_0 \cos(\omega_0 kT) + B_1 \cos(\omega_r kT)$

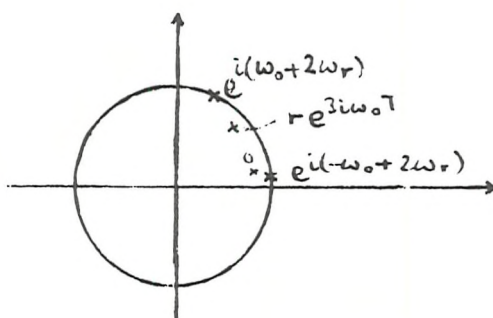
---

In a similar manner to the above

$$D(z)H(z)$$

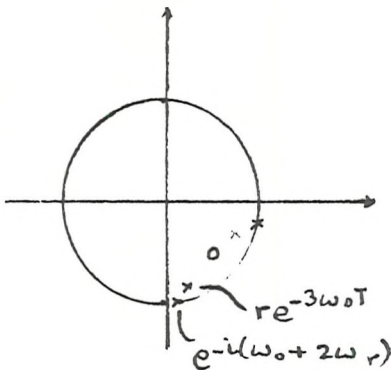


$$G_1(z)H(z) e^{i2\omega_0 T} D(z e^{i2\omega_0 T}) H(z)$$



and finally,

$$G_2(z)H(z)e^{-2i\omega_o T}D(z)e^{-2i\omega_o T}H(z)$$





## APPENDIX XII

In this Appendix the behaviour of the sparse filter for multitone cancellation is examined. The transfer function representation is particularly inappropriate in this case. Instead the response is analysed in terms of the generalised equation in Appendix XI.

Beginning with the LMS update equation

$$\underline{f}_{k+1} = \underline{f}_k + \alpha e(k) \underline{x}_k \quad (\text{XII.1})$$

for the sparse filter the  $i$ 'th coefficient is then

$$f_{k+1}(i) = f_k(i) + \alpha e(k) x(k - n_i) \quad (\text{XII.2})$$

Starting with equation (XII.2) and proceeding in an identical manner to Appendix XI produces

$$\begin{aligned} E(z) = H(z) \big[ & D(z) - G_1(z) H(z e^{-2i\omega_o T}) D(z e^{-2i\omega_o T}) - G_2(z) H(z e^{i2\omega_o T}) D(z e^{i2\omega_o T}) \\ & - G_3(z) H(z e^{-2i\omega_1 T}) D(z e^{-2i\omega_1 T}) - G_4(z) H(z e^{-i2\omega_1 T}) D(z e^{-2i\omega_1 T}) \\ & - G_5(z) H(z e^{i(\omega_1 - \omega_o) T}) D(z e^{i(\omega_1 - \omega_o) T}) - G_6(z) H(z e^{i(\omega_o - \omega_1) T}) D(z e^{i(\omega_o - \omega_1) T}) \\ & - G_7(z) H(z e^{i(\omega_o + \omega_1) T}) D(z e^{i(\omega_o + \omega_1) T}) - G_8(z) H(z e^{-i(\omega_o + \omega_1) T}) D(z e^{-i(\omega_o + \omega_1) T}) \big] \end{aligned} \quad (\text{XII.3})$$

which is identical to the form for the conventional ANC given by (XI.15) but where the  $G_i(z)$  of equations (XI.16)-(XI.23) are replaced by

$$G_1(z) = \frac{\Lambda^2 \alpha}{4} \left( \sum_{j=0}^{M-1} e^{i2\theta_1 j} \right) U(z e^{-i\omega_o T}) \quad (\text{XII.4})$$

$$G_2(z) = \frac{\Lambda^2 \alpha}{4} \left( \sum_{j=0}^{M-1} e^{-i2\theta_1 j} \right) U(z e^{i\omega_o T}) \quad (\text{XII.5})$$

$$G_3(z) = \frac{A_1^2 \alpha}{4} \left( \sum_{j=0}^{M-1} e^{i2\theta_{1j} 2j} \right) U(z e^{-i\omega_1 T}) \quad (\text{XII.6})$$

$$G_4(z) = \frac{A_1^2 \alpha}{4} \left( \sum_{j=0}^{M-1} e^{-i2\theta_{1j} 2j} \right) U(z e^{i\omega_1 T}) \quad (\text{XII.7})$$

$$G_5(z) = \frac{A_o A_1 \alpha}{4} \left( \sum_{j=0}^{M-1} e^{i(\theta_{1j} - \theta_{2j})} \right) [U(z e^{-i\omega_o T}) + U(z e^{i\omega_1 T})] \quad (\text{XII.8})$$

$$G_6 = \frac{A_o A_1 \alpha}{4} \left( \sum_{j=0}^{M-1} e^{i(\theta_{2j} - \theta_{1j})} \right) [U(z e^{i\omega_o T}) + U(z e^{-i\omega_1 T})] \quad (\text{XII.9})$$

$$G_7(z) = \frac{A_o A_1 \alpha}{4} \left( \sum_{j=0}^{M-1} e^{-i(\theta_{1j} + \theta_{2j})} \right) [U(z e^{i\omega_o T}) + U(z e^{i\omega_1 T})] \quad (\text{XII.10})$$

$$G_8(z) = \frac{A_o A_1 \alpha}{4} \left( \sum_{j=0}^{M-1} e^{i(\theta_{1j} + \theta_{2j})} \right) [U(z e^{-i\omega_o T}) + U(z e^{-i\omega_1 T})] \quad (\text{XII.11})$$

where  $H(z)$ ,  $U(z)$ ,  $A_i$  and  $\alpha$  are as previously defined and

$$\theta_{1i} = \omega_o n_i T, \quad \theta_{2i} = \omega_1 n_i T \quad (\text{XII.12})$$

In the simplest (multitone) case where  $M = 2$  and where it is assumed that each coefficient has a delay equal to  $\pi/2$ , samples at the corresponding frequency, that is:

$$\theta_{10} = 0, \quad \theta_{21} = 0 \quad (\text{XII.13})$$

so that (XII.4)-(XII.12) become:

$$G_1(z) = \frac{A_o^2 \alpha}{4} (e^{i2\omega_o n_1 T}) U(z e^{-i\omega_o T}) \quad (\text{XII.14})$$

$$G_2(z) = \frac{A_o^2 \alpha}{4} (e^{-i2\omega_o n_1 T}) U(z e^{i\omega_o T}) \quad (\text{XII.15})$$



$$G_3(z) = \frac{A_1^2 \alpha}{4} (e^{i2\omega_1 n_o T} U(z e^{-i\omega_1 T})) \quad (\text{XII.16})$$

$$G_4(z) = \frac{A_1^2 \alpha}{4} (e^{-i2\omega_1 n_o T} U(z e^{i\omega_1 T})) \quad (\text{XII.17})$$

$$G_5(z) = \frac{A_o A_1 \alpha}{4} (1 + i e^{-i\omega_1 n_o T} - i e^{i\omega_o n_1 T}) \quad (\text{XII.18})$$

$$G_6(z) = \frac{A_o A_1 \alpha}{4} (1 - i e^{i\omega_1 n_o T} + i e^{-i\omega_o n_1 T}) \quad (\text{XII.19})$$

$$G_7(z) = \frac{A_o A_1 \alpha}{4} (1 - i e^{-i\omega_o n_1 T} - i e^{-i\omega_1 n_o T}) \quad (\text{XII.20})$$

$$G_8(z) = \frac{A_o A_1 \alpha}{4} (1 + i e^{i\omega_o n_1 T} + i e^{i\omega_1 n_o T}) \quad (\text{XII.21})$$

## APPENDIX XIII

### Introduction

In this section a novel application of the two point sparse adaptive filter is developed in the area of frequency response determination by swept sine testing.

In the form of testing considered, a linear sweep is input to the system under investigation,  $H$ , and the response is measured. In the usual formulation the response is then obtained by heterodyning and low pass filtering the output.

### 2 point Filter Approach

In the approach to slow sweep testing proposed here the conventional system is replaced with that shown in figure XIII.1. Assume initially that a fixed sinusoid of frequency  $\omega_0$  provides the reference input to such a system and the output of the system under investigation,  $H$ , provides the primary input. Now, by the results of section 6.4, the filter output will effectively cancel the system output, that is  $e(n) \rightarrow 0$  (in steady state)

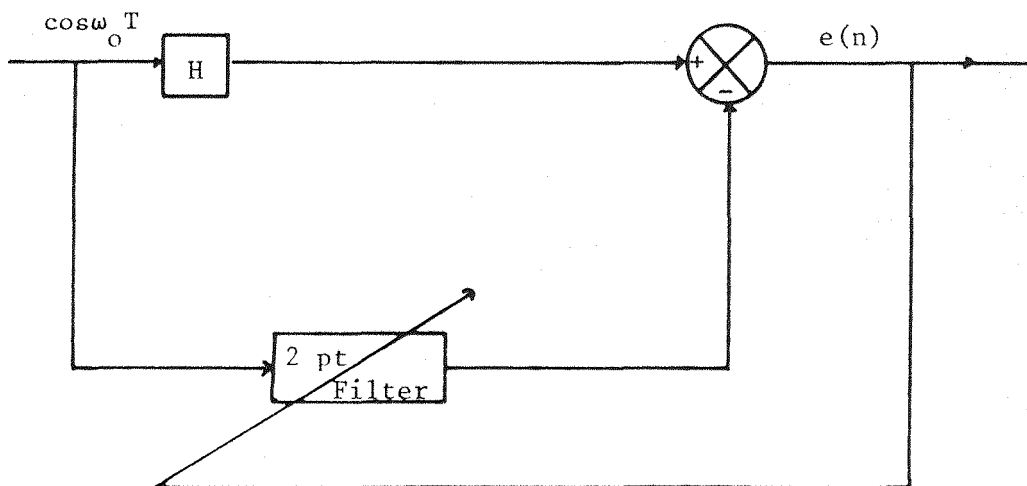


Figure XII.1: Slow Sweep testing with the 2 point Adaptive Filter.

or

$$f_0(n) \cos \omega_0 nT + f_1(n) \cos \omega_0 (n - n_0)T = A \cos(\omega_0 nT - \phi) \quad (\text{XIII.1})$$

Both sides of this equation may be expanded separately:

$$\begin{aligned} \text{RHS:} \quad & A \cos(\omega_0 nT - \phi) \\ & = A [\cos \omega_0 nT \cos \phi + \sin \omega_0 nT \sin \phi] \end{aligned} \quad (\text{XIII.2})$$

$$\begin{aligned} \text{LHS:} \quad & f_0(n) \cos \omega_0 nT + f_1(n) \cos \omega_0 (n - n_0)T \\ & = f_0(n) \cos \omega_0 nT + f_1(n) [\cos \omega_0 nT \cos \omega_0 n_0 T \\ & \quad + \sin \omega_0 n_0 T \sin \omega_0 nT] \end{aligned} \quad (\text{XIII.3})$$

Equating (XIII.2) and (XIII.3) gives

$$\cos \omega_0 nT: \quad A \cos \phi = f_0(n) + f_1(n) \cos \omega_0 n_0 T \quad (\text{XIII.4})$$

$$\sin \omega_0 nT: \quad A \sin \phi = f_1(n) \sin \omega_0 n_0 T \quad (\text{XIII.5})$$

Hence, using (XIII.4) and (XIII.5)

$$A = [f_0^2(n) + f_1^2(n) + f_0(n)f_1(n)\sin 2\omega_0 n_0 T] \quad (\text{XIII.6})$$

and

$$\phi = \tan^{-1} \left( \frac{f_1(n) \sin \omega_0 n_0 T}{f_0(n) + f_1(n) \cos \omega_0 n_0 T} \right) \quad (\text{XIII.7})$$

To test the frequency response of the system H the frequency of the input sinusoid is slowly swept over a pre-determined range. Now the results of the previous section are only valid for the case of a sinusoid with fixed frequency.

## Simulations

The following simulations were performed using a second order system of the form:

$$X(s) = \frac{1}{s^2 + 2\xi\omega_0 s + \omega_0^2} \quad (\text{XIII.8})$$

$\omega_0$  was set  $\approx 35$  Hz and two values of  $\xi$  were used. In both cases the system was tested with a swept sine input from 10 to 60 Hz at 5 Hz/second.

### (a) $\xi = 0.1$

Figure XIII.2 shows the true response (crosses) together with the responses obtained using the 2 point filter with adaptation rates = 0.05, 0.1 and 0.5. As can be seen, increasing the adaptation rate increases the accuracy of the response.

### (b) $\xi = 0.01$

Figure XIII.3 shows the same results when  $\xi = 0.01$ . It is clear that the results are much less accurate in this case. However, comparing error curves for differing sweep rates shows that it is not the mobility of the algorithm to track the sweep but a basic problem of this form of slow sweep testing, as discussed above.

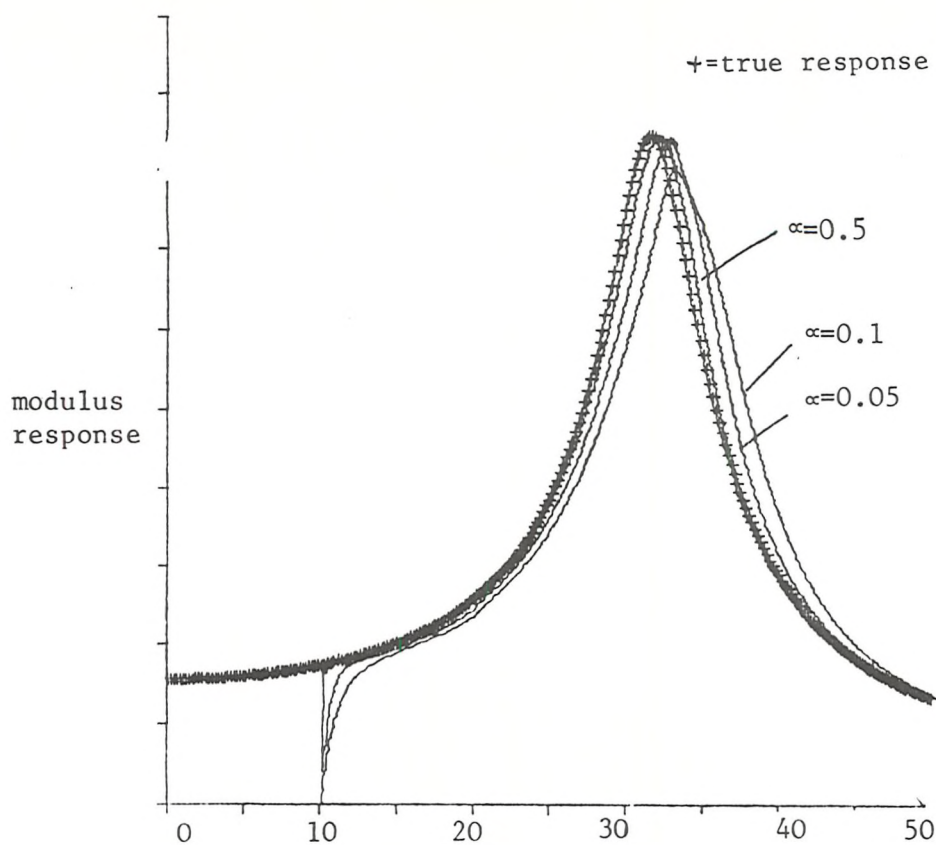


Figure XIII.2: True Frequency Response and Recovered Approximations ( $\xi=0.1$ )

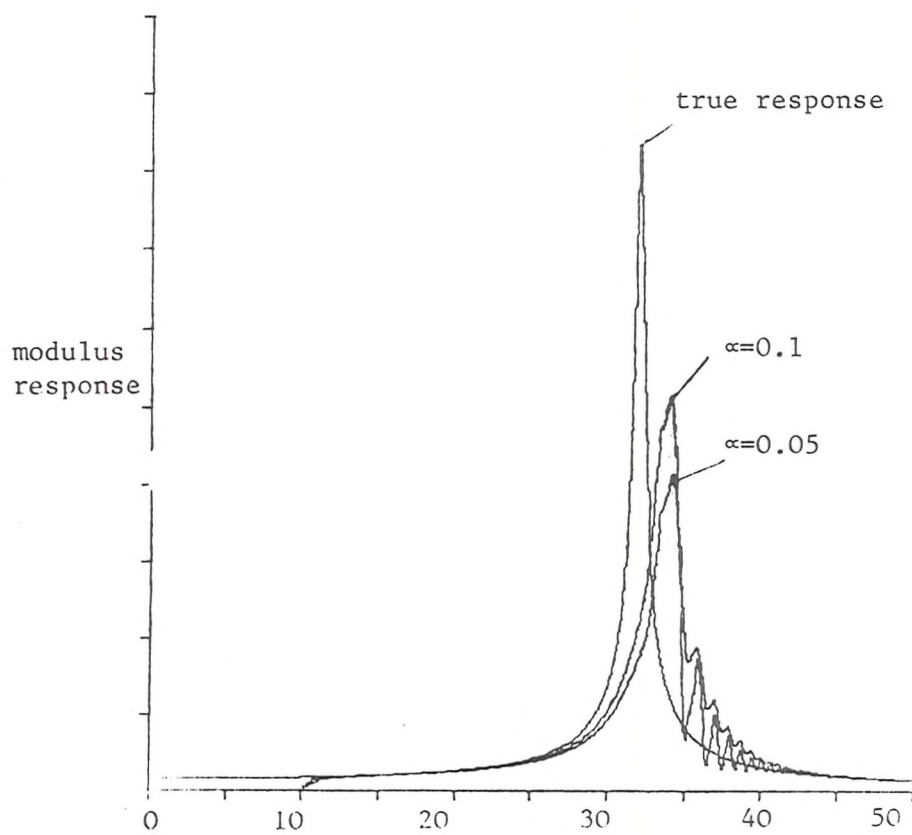


Figure XIII.3: True Frequency Response and Recovered Approximations ( $\xi=0.01$ )

## APPENDIX XIV

To provide a test bed for the novel approaches to seismic deconvolution and signal enhancement discussed in Chapters 8 and 9, synthetic seismic data based on models of the earth's response has been generated. Two such models were used.

### 1. Lattice synthetic

The simpler of the two synthetic forms is for single channel normal incidence marine data from an earth consisting of  $N$  horizontal, homogeneous layers, characterised by travel times  $n_i$  with downgoing reflection coefficients  $r_i$ , bounded by a sea layer with perfect reflection at the air/sea interface. No losses are included.

A number of authors have used similar models and the generating equations for this synthetic can easily be obtained by considering fig. XIV.1.

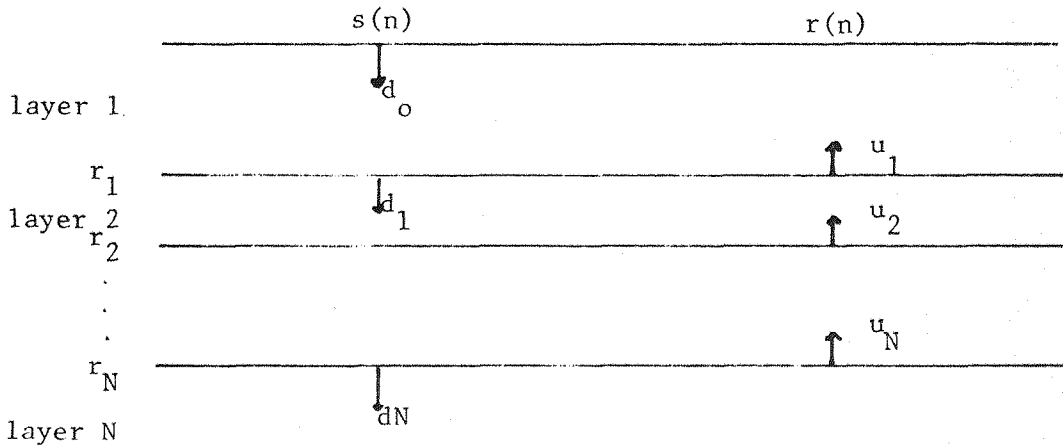


Figure XIV: Idealised Earth System

Let the amplitude of the upward bound wave into layer  $i$  be  $u_i$  and the downward bound from layer  $i$  be  $d_i$  (see fig. XIV.1). If layer  $i$  is bounded below by an interface with downgoing reflection coefficient  $r_i$  (strictly  $r_{i,i+1}$  in terms of equation (7.2.1) but abbreviated for simplicity) and if the downgoing transmission is  $t_i = (1 - r_i)$  so that the upward is  $t_i' = (1 + r_i)$ ; then by inspection, from the diagram:

$$d_i(n) = t_i d_{i-1}(n - n_i) - r_i u_{i+1}(n - n_{i+1}) \quad (\text{XIV.1})$$

$$u_i(n) = r_i d_{i-1}(n - n_i) + t_i' u_{i+1}(n - n_{i+1}) \quad (\text{XIV.2})$$

and at the surface

$$d_o(n) = s(n) + u_1(n - n_1) \quad (\text{XIV.3})$$

$$R(n) = u_1(n - n_1) \quad (\text{XIV.4})$$

and  $r_{N+1} = 0$ .

Similar equations have been used by Mendel to obtain a state-space form for the synthetic. The same author also considers the slightly more complex case arising when source and receiver are not at the surface but within the surface layer.

The synthetic can be generated using the equations in the above form but it is interesting to lump the two-way transmission  $= 1 - r_i^2$  on to the upward travelling energy and have the downward energy free from transmission loss. Again referring to fig. XIV.1, the equations may be written down as:

$$d_i'(n) = d_{i-1}'(n - n_i) - r_i u_{i+1}'(n - n_{i+1}) \quad (\text{XIV.5})$$

$$u_i'(n) = r_i d_{i-1}'(n - n_i) + (1 - r_i^2) u_{i+1}'(n - n_{i+1}) \quad (\text{XIV.6})$$

where the ' are used to distinguish the variables from the previous.

Rearranging (XIV.5) gives

$$d_{i-1}'(n - n_i) = d_i'(n) + r_i u_{i+1}'(n - n_{i+1}) \quad (\text{XIV.7})$$

and substituting in (XIV.6) gives

$$u_i'(n) = r_i d_i'(n) + u_{i+1}'(n - n_{i+1}) \quad (\text{XIV.8})$$

Equations (XIV.5) and (XIV.8) may be depicted as in fig. XIV.2,

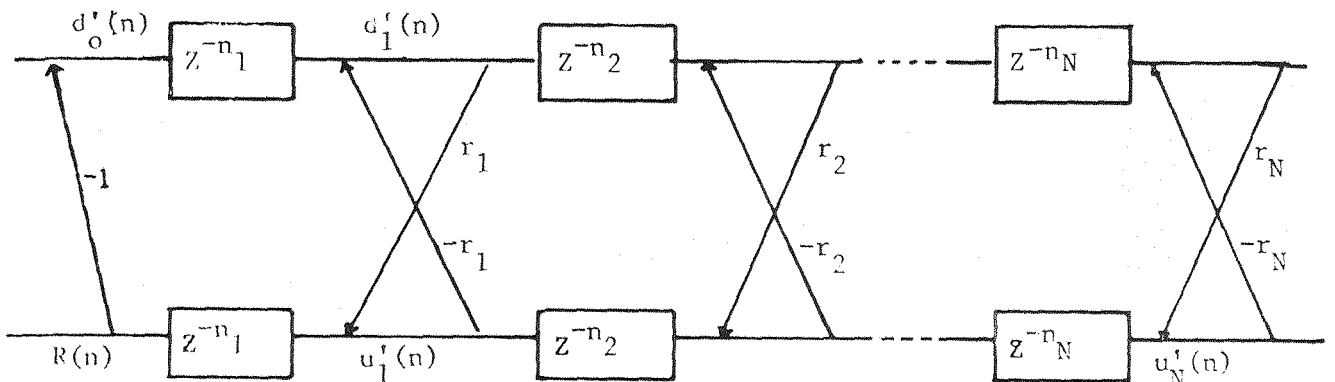


Figure XIV.2: Lattice Form For Synthetic



which is the lattice form discussed briefly in Chapter 3. The response  $R(n)$  is identical to that for the previous form, though at subsurface points the downward variables are different. The program works by computing the response (all primaries and multiples) to a single pulse. This response is then convolved with a source signal and noise added if required.

## 2. Multi-channel synthetic

The second synthetic used was developed by T.P. Hubbard of Seismograph Service Ltd. This synthetic generates a complete CDP gather for a two-layered system with horizontal reflectors, generating both the primaries and all sea-bottom multiples. The program also models the effects of spherical divergence, source and receiver ghosts, array effects and even changes in reflection coefficient with angle of incidence. The models used were as follows:

- (a) Spherical divergence: corrected for energy delay as  $T^2$ .
- (b) Ghosts: Source and receiver assumed at equal depths of 6 m. Three ghosts are generated, two corresponding to single reflections from the surface at the source or receiver (negative in sign). The third ghost corresponds to a reflection from the surface at both the source and receiver (positive in sign).
- (c) Array effects: The source array is assumed to cover 20 m and the receiver array 50 m. Nine combinations of travel distances are included (see fig. XIV.3).
- (d) Changes in reflection coefficient with angle: 9 tabulated values are used (from  $0^\circ$  to  $90^\circ$ ) with linear interpolation.

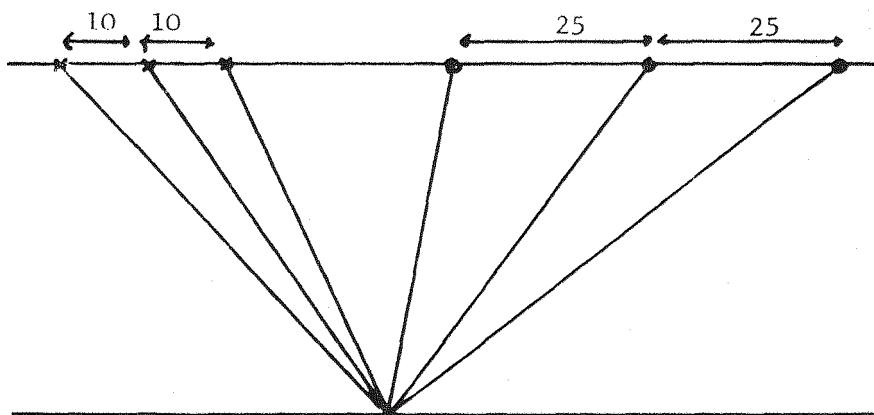


Figure XIV.3: Possible Distance Combinations for Source and Receiver Arrays.

The program again gives an output which is the response to a unit spike which is then convolved with a source wavelet.